Variation in fitness and infection phenotype among strains of *Borrelia burgdorferi* emerging in Canada

A thesis submitted to the
College of Graduate and Postdoctoral Studies
in partial fulfilment of the requirements for the
Degree of Doctor of Philosophy
in the department of Veterinary Microbiology
University of Saskatchewan

By
CHRISTOPHER B. ZINCK

Permission to use post-graduate thesis

In presenting this thesis in partial fulfillment of the requirements for a post-graduate degree from the University of Saskatchewan, the author agrees that the Libraries of this University may make it freely available for inspection. I further agree that permission for copying of this thesis/dissertation in any manner, in whole or in part, for scholarly purposes may be granted by the professor or professors who supervised my thesis/dissertation work or, in their absence, by the Head of the Department or the Dean of the College in which my thesis work was done. It is understood that any copying or publication or use of this thesis/dissertation or parts thereof for financial gain shall not be allowed without my written permission. It is also understood that due recognition shall be given to me and to the University of Saskatchewan in any scholarly use which may be made of any material in my thesis/dissertation.

Requests for permission to copy or to make other uses of materials in this thesis/dissertation in whole or part should be addressed to:

Head of the Department of Veterinary Microbiology University of Saskatchewan

Saskatoon, Saskatchewan S7N 5B4

Canada

OR

Dean

College of Graduate and Postdoctoral Studies, University of Saskatchewan

116 Thorvaldson Building, 110 Science Place

Saskatoon, Saskatchewan S7N 5C9 Canada

Abstract

Evolutionary virulence theory is life history theory for pathogens that explains why pathogen-induced damage (virulence) to the host is adaptive. Virulence theory examines the relationships between three pathogen life history traits: within-host replication and pathogen abundance in host tissues, pathogen transmission, and the damage caused to the host by the pathogen (virulence). Pathogen abundance in host tissues is positively correlated with pathogen transmission to new hosts. Higher pathogen abundance in host tissues also leads to higher levels of host exploitation, which should increase the pathogen-induced mortality rate or virulence. Thus, there is a positive relationship between virulence and transmission, which represents a life history trade-off for the pathogen. By increasing its exploitation of the host, the pathogen obtains the benefit of more current transmission at the cost of a shorter duration of infection. If the relationship between virulence and transmission is one of diminishing returns, natural selection should favour the evolution of an an optimal value of virulence to maximize lifetime transmission. In summary, virulence theory allows us to understand the selective pressures influencing the evolution of pathogen life history traits.

Borrelia burgdorferi is a tick-borne spirochete bacterium that causes Lyme borreliosis, the most common tick-borne disease in the Northern Hemisphere. In North America, *B. burgdorferi* is commonly vectored by the black-legged tick *Ixodes scapularis*, which acquires the infection from competent reservoir hosts. *Borrelia burgdorferi* is comprised of genetically distinct strains. These strains coexist in the same tick and vertebrate host populations at different frequencies and are variable in their life history traits.

For this study, we investigated the relationships between the three canonical pathogen life history traits of pathogen abundance in host tissues, transmission, and virulence among 11 strains

of *B. burgdorferi*. Mice (male and female *Mus musculus* C3H/HeJ) were experimentally infected by tick bite with 1 of the 11 strains. To measure lifetime host-to-tick transmission, mice were infested with *I. scapularis* larval ticks at days 30, 60, and 90 post-infection (PI). To track the spirochete population in the host over time, the spirochete load was estimated in ear biopsies at days 29, 59, and 89 PI using qPCR. The mouse serum IgG antibody response against B. burgdorferi was measured at days 28 and 97 PI. Mice were euthanized at day 97 PI and necropsy tissues (left ear, right ear, ventral skin, tibiotarsal joint, heart, bladder, and kidney) were tested for their spirochete loads by qPCR. Over the course of the infection, weight gain and ankle swelling were measured as possible virulence phenotypes. Mouse necropsy tissues (kidney, ventral skin, tibiotarsal joint, and heart) were also prepared for histopathology.

As expected, we found significant variation among the 11 *B. burgdorferi* strains in each of the three life history traits. As predicted by evolutionary virulence theory, we found a significant positive relationship between spirochete load in the mouse tissues and lifetime host-to-tick transmission. Our lab-based estimates of mouse tissue spirochete load and lifetime host-to-tick transmission were also significantly positively related to the frequencies of these strains in natural populations of *I. scapularis* ticks. Our study suggests a simple mechanism where strains that reach a greater abundance in the tissues of their host have greater transmission to feeding ticks and are therefore more common in nature. We did not find a relationship between virulence and the other pathogen life history traits. Instead, we found that the host immune response was positively related to our ankle swelling measure of virulence.

Finally, this experimental infection study used both male and female C3H/HeJ mice. To the best of our knowledge, we report here the first finding of a sex-specific difference in the abundance of *B. burgdorferi* in the tissues of a rodent host. This sex-specific difference was also

found for transmission, where ticks that fed on male mice were more likely to be infected than ticks that fed on female mice. Females had a significantly stronger antibody response to *B. burgdorferi*, which is consistent with known sex-specific differences in immune responses. Interestingly, female mice had higher levels of carditis compared to male mice suggesting that the immune response rather than heart spirochete loads were responsible for this sex-specific difference in pathology.

Acknowledgements

There is an old proverb, “it takes a village to raise a child”. I think this can be adapted to say it takes a village, or scientific community, to make a PhD. I would firstly like to thank my supervisor Dr. Maarten Voordouw for giving me this opportunity, and for helping me not just in the project and writing, but in developing professional skills and becoming a more well-rounded researcher. I think the best example of his support is when he would come in on the weekend to check the animals so the grad student could stay home. I would also like to thank my committee members Dr. J, Hill, Dr. N. Chilton, and Dr. S. Detmer, as well as my committee chair Dr. V. Misra for their support and input on this project.

I am extremely grateful for the wonderful people I have had the opportunity to work with in this lab, and who have helped me immensely with my work. I would like to thank Prasobh Thampy, Eva Marie-Uhlemann, Georgia Hurry, Alexandra Aiello, and Cody Koloski.

This project required the work of many people to complete. I would like to think Dr. S. Detmer and Dr. P. Zvionow for their help with necropsies and histopathology. I would also like to thank the WCVM animal care unit for their support and care of my mice.

I would like to thank the entire department of Veterinary Microbiology. Help and support was always eagerly given by the people in this department. I would especially like to thank Linda and Lana, who in addition to always being there to help, were also always there for friendship and a nice chat.

I am incredibly grateful for the continued support I get from my family, and especially my mother who has supported my education even when it meant moving further and further away. A PhD project and a global pandemic are not a good mix, but I want to thank my partner Carly, and her family, for taking care of me and getting me out for fresh air from time to time.

Table of Contents

List of Tables

List of Figures

1 Introduction and Literature Review

1.1 *Borrelia*

1.1.1 *Borrelia* genospecies

The genus *Borrelia* contains multiple zoonotic species of bacteria with a global distribution. *Borrelia* are spirochetal bacteria similar to *Treponema* and *Leptospira*, but the pathogenic species are vector transmitted. Within the genus, there are two groupings that functionally divide *Borrelia* species, they are categorized as either Lyme borreliosis (LB) *Borrelia* or relapsing fever (RF) *Borrelia* (Adeolu & Gupta, 2014). As the names imply, these two groups of *Borrelia* cause different diseases in human patients. RF *Borrelia* are mostly vectored by soft bodied (Argasid) ticks common in more tropical areas, whereas LB *Borrelia* are exclusively vectored by hard bodied (Ixodid) ticks found mostly in the temperate areas of the Northern hemisphere (Piesman & Gern, 2004; Wang et al., 2014). Currently, there are more than 20 named species of both LB and RF *Borrelia* (Stanek & Reiter, 2011; Wang et al., 2014).

The LB group of *Borrelia* is also known as the *Borrelia burgdorferi* sensu lato (sl) complex, named after the first identified member, *B. burgdorferi* sensu stricto (herein: *B. burgdorferi*). In the LB group, there are at least 5 species known to cause disease in humans, (Stanek & Reiter, 2011; Wang et al., 2014). The three most prevalent species are *B. burgdorferi, B. afzelii,* and *B. garinii.* All three species are present in Europe, however *B. burgdorferi* is the only one present in North America (Margos et al., 2011; Steere et al., 2004). There are other *Borrelia* species in North America including RF *Borrelia* (Barbour et al., 2009) but most human cases of LB are caused by *B. burgdorferi* (Schotthoefer & Frost, 2015). The existence of multiple closely related species in the *B. burgdorferi* sl complex has made it a model system for the evolutionary ecology of zoonotic pathogens. While there are important differences among

Borrelia species in genetics, life history, and pathology, especially in regions where multiple species co-occur, equally important is the variation among strains within a single species.

1.1.2 *Borrelia burgdorferi* strains and classification

Many pathogen species are also comprised of strains, or distinct sub-species groups. Strains of *B. burgdorferi* sl do not occur at the same frequencies in nature. There are high and low frequency strains, or common and rare strains (Durand et al., 2017; Ogden et al., 2011; Råberg et al., 2017; Travinsky et al., 2010). In endemic areas, the frequencies of these strains are consistent over time (Durand et al., 2017; Råberg et al., 2017). A 9-year field study on *B. afzelii* in small mammal hosts found that strains differed dramatically in frequency, but these frequencies remained stable over time (Råberg et al., 2017). Similarly, an 11-year study on *B. afzelii* in *I. ricinus* ticks also found that strains differed dramatically in frequency, but these frequencies remained stable over time (Durand et al., 2017). Differences among strains are the driver for subclassification and it is equally important to understand what criteria are used to differentiate strains.

The term strain is heavily context dependent. In the context of pathogens, strains are often defined by their phenotype or by characteristics of importance to humans such as antibiotic resistance. Earlier diagnostic methods for important human pathogens, such as *Streptococcus pneumoniae* and *Salmonella enterica*, used the specificity of the host antibody response to delineate strains of the bacteria into serovars or serotypes. This approach can be diagnostically beneficial but is not always linked to pathogen phenotypes of interest (Achtman et al., 2012; Forbes et al., 2008). Modern molecular techniques use genome sequencing to classify strains

based on the conserved core genome that defines the species, but without the use of accessory genes like those found on plasmids (Enright & Spratt, 1999; Segerman, 2012).

Comparison of genetic, serologic, or phenotypic traits among isolates of *B. burgdorferi* has shown that there are numerous distinct strains regardless of the method of strain classification (Bunikis, Garpmo, et al., 2004; Earnhart et al., 2005; Wormser et al., 1999). Methods of strain classification are also used to distinguish among species of *Borrelia burgdorferi* sensu lato (Baranton, Postic, et al., 1992; Canica et al., 1993; G. Margos et al., 2013). *B. burgdorferi* has a highly segmented genome, with one of the highest plasmid complements of any characterized bacterium (Stewart et al., 2005). The segmented genome adds complexity to strain typing as the plasmid content includes genes critical for the basic function of *B. burgdorferi* sl. For example, circular plasmid 26 (cp26) contains the *ospC* gene, which encodes outer surface protein C (OspC) (Sadziene et al., 1993), which is a membrane bound surface protein expressed in the early stages of host invasion. The OspC protein is highly variable and generates a type-specific antibody response within the host which has made it a diagnostic marker, and a framework for defining strains of *B. burgdorferi* sl for decades (Brisson & Dykhuizen, 2004; Durand et al., 2017; Hellgren et al., 2011; Jauris-Heipke et al., 1995; Råberg et al., 2017; Strandh & Råberg, 2015; Theisen et al., 1993).

With the onset of sequencing technologies there have been multiple efforts to classify and subdivide the *B. burgdorferi* sl genospecies into strains. Early methods mostly relied on single polymorphic loci (e.g., *ospC* and the *rrs-rrlA* and *rrfA-rrlB* ribosomal spacer system) (Dolan et al., 2004; Jolley et al., 2018; Margos et al., 2008). A multi-locus sequence typing (MLST) system for *B. burgdorferi* sl strains was developed in 2008 (Margos et al., 2008). In this MLST system, strains are defined based on the sequence of eight conserved housekeeping genes found

on the linear chromosome; it does not include any plasmid encoded genes. Each of the eight housekeeping genes has numerous unique alleles that can differ at a single nucleotide and each unique sequence of 8 alleles is assigned a unique MLST number. This classification system is purely genetic and allows for easy inference of strain relatedness (Enright & Spratt, 1999; Margos et al., 2008; Urwin & Maiden, 2003). It also results in there being hundreds of strains. MLST types and their location of origin are tracked in a public database (Jolley et al., 2018; Margos et al., 2015). This data has been used to show that eastern and western North America have different populations of strains (Hoen et al., 2009), and where *B. burgdorferi* (sensu stricto) may have originated (Castillo-Ramírez et al., 2016). As whole genome sequencing becomes more accessible, there is the potential to combine both chromosomal and plasmid targeted methods (Casjens et al., 2017; Tyler et al., 2018).

The major benefit of a single locus system over MLST is in mixed strain infections. Sequencing a single locus can differentiate multiple strains in a mixed infection, but when the separate sequences of 8 loci have to be concatenated, mixed infections cannot be resolved by conventional sequencing (Wang et al., 2014). As whole genome sequencing becomes more common this is less of an issue, but a single locus classification system remains a useful tool especially when variation at that locus is contributing to strain differentiation directly like *ospC*.

The different classification methods of *B. burgdorferi* strains can make a review of the topic difficult where the exact definition can vary on a per study basis. With studies that only report *ospC* types, there is no way to reconcile those with the current MLST strain definitions. Despite this, there are underlying universal truths that brought about the desire to create the strain classifications in the first place. Within *B. burgdorferi*, there is a great amount of phenotypic variation. Strains, regardless of definition, have been shown to differ in their clinical

presentation of disease. Strains also differ in important life history traits like their tissue abundance and transmission rates which will be discussed below.

1.1.3 Public health impacts of *Borrelia burgdorferi*

Borrelia burgdorferi sensu lato are zoonotic pathogens, meaning they can be transmitted to humans. The discovery of *B. burgdorferi* and identification of it as a zoonotic agent occurred because of an apparent outbreak of arthritis around Old Lyme Connecticut (Steere et al., 1977). Species of the *Borrelia burgdorferi* sensu lato complex are the causative agent of Lyme borreliosis (LB) in humans. Currently, LB is the most common tick-borne disease in Europe and North America (Steere et al., 2016). The true impact of LB and number of infections is complicated by the nature of the infection, diagnostic complexities, and even sociopolitical controversy. In the USA, the annual incidence of LB is ~30,000 – 40,000 cases per year (Schwartz et al., 2017). The potential number of cases has been estimated at 10-fold higher than reported numbers (Nelson et al., 2015). In the USA, reporting of LB by medical doctors is voluntary and reporting practices vary at the state level (Schwartz et al., 2017). In Canada, the annual incidence of LB has increased from 144 cases in 2009 to 3,147 cases in 2021 (Public Health Agency of Canada, 2023). One study suggested that LB is similarly underreported in Canada, but this is under contention (Lloyd & Hawkins, 2018; Ogden et al., 2019). In addition, there appears to be regional differences in the ability for serological testing to detect infections (Ogden et al., 2017). This may be explained by strain differences in *B. burgdorferi* (Schmid-Hempel, 2009).

The probability of transmission from infected ticks to humans is surprisingly low. Such studies rely on comparing the known infection level in the wild tick population against the

number of reported cases of human LB after a tick bite. Early probability estimates of human infection risk from a tick bite in an endemic area ranged from 0.012 to 0.025 (Agre & Schwartz, 1993; Costello et al., 1989; Falco & Fish, 1988; Magid et al., 1992; Shapiro et al., 1992). The tick infection levels ranged from 0.14 to 0.39 which suggests that only a fraction of infected ticks feeding on humans successfully transmit, assuming there are no biases in encounter rates (Anderson et al., 1983; Magnarelli et al., 1984).

When a human is infected with *B. burgdorferi*, the first clinical manifestation is erythema migrans, a rash around the site of the tick bite that does not occur in all patients (Feder et al., 1993; Steere et al., 2003). Early clinical symptoms of LB mimic viral infections with fever, fatigue, headaches, and muscle and joint pain (Steere et al., 1983; Wormser, 2006). If left untreated, the disease can progress into a debilitating and sometimes fatal multi-systemic infection (Aucott et al., 2013; Aucott et al., 2012; Cameron, 2007; Dattwyler et al., 1997; Marcus et al., 1985; Muehlenbachs et al., 2016; Shadick et al., 1994). As discussed above, *B. burgdorferi* sl disseminates heterogeneously through the host. While the symptoms can vary by patient and strain factors, there is commonly cardiac, joint, and neurological involvement. *Borrelia* genospecies are also associated with different clinical symptoms. The three main agents of human infection in North America and Europe all follow a pattern of early dissemination at the tick bite, followed by dissemination and chronic manifestations (Stanek & Reiter, 2011). *B. burgdorferi* is strongly associated with joint pain, *B. garinii* with neuroborreliosis (a central nervous system disorder), and *B. afzelii* is associated with acrodermatitis chronica atrophicans (inflammatory wasting of the skin) (Balmelli & Piffaretti, 1995; Canica et al., 1993; Strle & Stanek, 2009).

The non-specific nature of symptoms adds to the complexity of diagnosis. In most patients, LB in early dissemination is treatable with a short course of antibiotics (Choo-Kang et al., 2010; Wormser, 2006; Wormser et al., 2006). There is a subset of LB patients that do not respond to antibiotics and that remain ill for many months or even years after the original antibiotic treatment (Hunfeld et al., 2005; Marques et al., 2014; Middelveen et al., 2018; Priem et al., 1998). This post-treatment illness is often referred to as post-treatment Lyme disease syndrome (PTLDS). Lyme borreliosis, the disease caused by species of the *B. burgdorferi* sensu lato complex, is a disease that is highly variable making it difficult to diagnose, it also has the potential to resist treatment and be debilitating to the patient. With the current trend of increasing cases in North America, this trend is likely to continue and further the impact of LB.

1.1.4 *Borrelia burgdorferi* in North America

In North America, *B. burgdorferi* is the primary agent of LB (Gasmi et al., 2017). *Borrelia burgdorferi* is capable of infecting a wide range of vertebrate hosts (LoGiudice et al., 2003). *Borrelia burgdorferi* sl genospecies are vectored through the bite of ticks in the genus *Ixodes* (Kurtenbach et al., 2006). In North America, the two tick species that transmit *B. burgdorferi* are the black-legged tick *Ixodes scapularis* and the western black-legged tick *Ixodes pacificus*, which are located east and west of the Rocky Mountains (Sperling & Sperling, 2009). In basic terms, the vector is differentiated from the host by being the agent that facilitates transmission through its actions (i.e., feeding) where a host may just harbor the pathogen.

In Canada, the incidence of LB has increased dramatically in the human population over the last 30 years (Gasmi et al., 2017; Ogden et al., 2009). The main explanation for the emergence of LB in Canada is the northward expansion of the geographic range of *I. scapularis*.

The introduction of *B. burgdorferi* into a new area requires competent vertebrate hosts and a population of competent tick vectors. The northern edge of the *I. scapularis* range is within Canada, so much of the tick populations are recently established (Leo et al., 2017). As changing environmental factors (i.e., climate change increasing average temperatures) increase the suitable habitat for *I. scapularis*, this will in turn expand the range of *B. burgdorferi* (Lieske & Lloyd, 2018; Nicholas H. Ogden et al., 2008; Sonenshine, 2018).

Birds can carry live ticks and their tick-borne pathogens into new areas, and bird migration is a key contributor to the geographic expansion of *I. scapularis* populations in Canada (Leo et al., 2017; N. H. Ogden et al., 2008; Talbot et al., 2020). Assuming there are suitable environmental conditions for tick survival, and competent hosts where the ticks are deposited, *B. burgdorferi* can be introduced with the arrival of ticks into an area. In contrast, within the LB-endemic areas of the northeastern and midwestern United States, there is clear evidence of *I. scapularis* population structure suggesting that these two populations have little mixing (Humphrey et al., 2010). This same population structure is not found in *B. burgdorferi* suggesting that it does not have the same barriers in place, i.e., without the movement of ticks, there is still movement of *B. burgdorferi* throughout regions of the United States (Humphrey et al., 2010). It is the movement and dispersal of both the tick vector and the vertebrate host that contribute to the geographic expansion of *B. burgdorferi* and LB in North America.

1.1.5 Vector transmission

1.1.5.1 Vector competence for *Borrelia burgdorferi*

A competent vector is an organism capable of acquiring a pathogen and effectively transmitting that pathogen to another host. The first competent vector identified for *Borrelia*

burgdorferi was the black-legged tick *Ixodes scapularis* (previously: *Ixodes dammini*), one of multiple endemic hard-bodied tick species in North America. To properly understand the risk of Lyme disease, studies were done to assess the vector competence of other hard-bodied tick species. In North America, the western black-legged tick *Ixodes pacificus* was found to be a competent vector, whereas other common tick species, such as the American dog tick *Dermacentor variabilis* and the Lonestar tick *Amblyomma americanum* were not (Burgdorfer, 1984; Mather & Mather, 1990; Piesman, 1993; Piesman et al., 1997; Piesman & Sinsky, 1988).

In Europe, the two *Borrelia* genospecies that cause most human cases of Lyme borreliosis are *B. afzelii* and *B. garinii*. These two genospecies share the same tick vector, the castor bean tick or sheep tick, *Ixodes ricinus*, but they differ in their reservoir hosts. *Borrelia afzelii* is found in small mammals (rodents and insectivores), whereas *B. garinii* is found in birds (Durand et al., 2015; Gern, 2008). *Ixodes ricinus* is also a competent vector of *B. burgdorferi* sensu stricto (Dolan et al., 1998; Gern et al., 1993). In North America, *I. scapularis* and *I. pacificus* have been tested for their ability to vector other *Borrelia* genospecies (Eisen, 2020). In experimental infection trials, *I. scapularis* has been shown to readily acquire *B. bissetti, B. mayonii, B. afzelii,* and *B. garinii* (Dolan et al., 2016; Dolan et al., 1998; Sanders & Oliver, 1995). While less commonly researched, *I. pacificus* has been shown to acquire *B. bissetti* (Eisen et al., 2003). In general, it is well established that *Ixodes* ticks are competent vectors for members of the *Borrelia* genospecies, even when those borreliae do not co-occur with the tick vector (i.e., *I. scapularis* acquiring *B. afzelii*). To date, there is not much evidence that the genetics of the tick influence the fitness of different *B. burgdorferi* strains.

1.1.5.2 Vector life cycle and the transmission of *Borrelia burgdorferi*

Ticks of the genus *Ixodes* are blood feeding ectoparasites that have 4 developmental stages: egg, larva, nymph, and adult. Larvae and nymphs require a blood meal to moult into the next stage, nymphs and adult ticks, respectively. Adult female ticks take a third blood meal to provide nourishment for reproduction; adult male ticks do not blood feed (Radolf et al., 2012; Sperling & Sperling, 2009). Ticks acquire *B. burgdorferi* when they take a blood meal from an infected host. There is no transovarial (vertical) transmission of *B. burgdorferi* so eggs hatch into uninfected larvae (Rollend et al., 2013). Larvae acquire the infection after feeding on an infected host and moult into infected nymphs; transstadial transmission refers to the maintenance of the spirochete population across the larva-to-nymph moult. Infected nymphs over winter and are responsible for transmitting the spirochetes to the naïve reservoir hosts the following year. Larvae and nymphs feed on the same types of vertebrate reservoir species which facilitates horizontal transmission of *B. burgdorferi* between tick generations (Figure 1.1, Kurtenbach et al., 2006). A reservoir is a host that is readily infected by and maintains the pathogen for subsequent transmission. Adult *I. scapularis* will preferentially target larger hosts such as white-tailed deer or humans (Bouchard et al., 2013; Madhav et al., 2009).

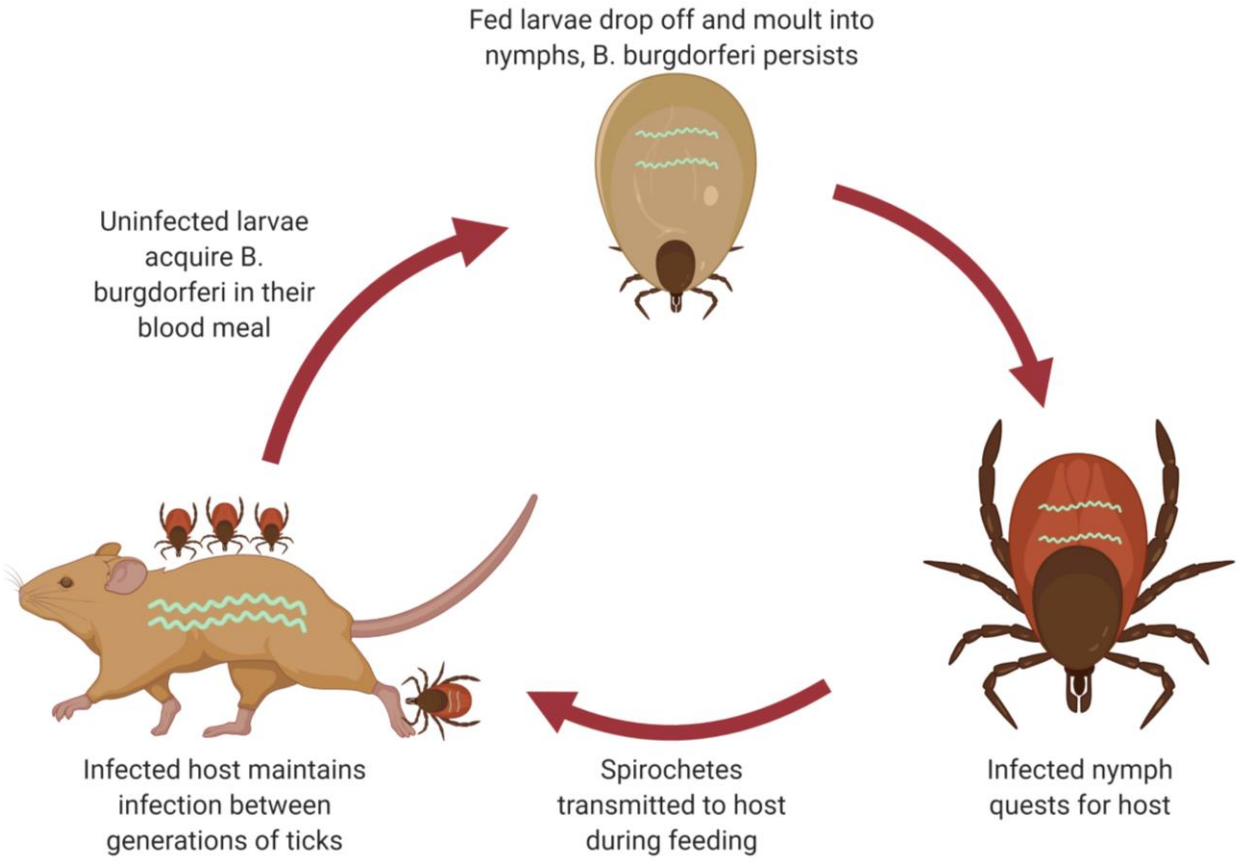

Figure 1.1 The basic maintenance cycle of *Borrelia burgdorferi* involves a vertebrate reservoir host, and the larval and nymphal life stages of the *Ixodes scapularis* tick vector.

The life cycle of *Ixodes* ticks can take 2 or more years with the 3 stages from different cohorts all co-occurring in the same year. In North America, the season phenology (activity patterns) of larvae and nymphs is important for the epidemiology of *B. burgdorferi*. Nymphs quest (search) for hosts in the spring and early summer, and the larvae quest for hosts from spring to late summer depending on the region. This seasonal activity pattern ensures that reservoir hosts are infected by nymphs before they are fed upon by larvae (Sperling & Sperling, 2009). As the larval and nymphal blood meals generally happen in consecutive summers, *B. burgdorferi* overwinters in the unfed nymph (and potentially also in unfed adult ticks). In North America, *Ixodes scapularis* has a wide geographic range from southern Canada to Florida and

the details of its lifecycle vary considerably among geographic locations. In the southern United States, *I. scapularis* exhibits different temporal feeding patterns brought on by the warmer year-round climate which in turn alters the typical transmission cycle associated with *B. burgdorferi* (Diuk-Wasser et al., 2006; Gatewood et al., 2009).

1.1.5.3 Host-to-tick transmission

In a vector-host cycle there are typically two transmission steps: from vector to host, and from host to vector. For *B. burgdorferi*, we refer to these as tick-to-host, and host-to-tick transmission (HTT). In the common transmission cycle, a tick acquires *B. burgdorferi* during its larval bloodmeal, and will not take in any other nutrients until its nymphal bloodmeal where it is then also passing on the infection to the susceptible host. Despite the actual transmission occurring in the larval stage, transmission is most commonly measured in nymphs.

To measure HTT in an experimental study, infected hosts are infested with naïve larval ticks that are left to feed to repletion. These ticks are left to moult into nymphs prior to testing their infection status and determining HTT. The detection of *B. burgdorferi* in the larvae is more difficult than in the nymph. The larvae is engorged with mammalian blood which can inhibit DNA amplification (Schrader et al., 2012; Sidstedt et al., 2018). Additionally, the absolute quantity of spirochetes in a replete larvae is lower than a moulted nymph. Studies on *B. burgdorferi* in *I. scapularis* and on *B. afzelii* in *I. ricinus* suggest that the mean spirochete load in an engorged larval tick following drop off is a few hundred spirochetes (de Silva & Fikrig, 1995; Genné et al., 2019; Jacquet et al., 2017; Piesman et al., 1990; Pospisilova et al., 2019). The engorged larva takes 4 to 6 weeks to moult into a nymph and during this time the spirochete population increases dramatically and reaches a peak after the larva-to-nymph moult (de Silva & Fikrig, 1995; Piesman et al., 1990; Pospisilova et al., 2019). Finally, measuring transmission in

the nymph rather than the larvae includes the probability of transstadial (i.e., across tick life stages) transmission. The nymph is the important stage for the epidemiology of *B. burgdorferi*, so it is advantageous to have the measure of transmission taken in that life stage (Eisen, 2020).

In reservoir hosts, transmission of *B. burgdorferi* generally increases after infection to a peak at 4-5 weeks, before gradually declining to a lower plateau (Derdáková et al., 2004; Donahue et al., 1987; Hanincova et al., 2008; Jacquet et al., 2016; Lindsay et al., 1997). While OspC is the *B. burgdorferi* protein associated with invasion of the host, outer surface protein A (OspA) is upregulated for invasion of the tick (Srivastava & De Silva, 2008; Yang et al., 2004). *B. burgdorferi* is not actively circulating or present in the blood stream after initial dissemination (see section 1.1.6.2). How does *B. burgdorferi* get to the site of tick feeding in the host tissues and achieve transmission to feeding larval ticks?

When a tick feeds, it creates a fluid-filled space in the skin of the host (Bockenstedt et al., 2014; Richter et al., 2013). *Borrelia* from the infected host enters this space and in some instances actively moves toward the hypostome to be acquired by the tick (Bockenstedt et al., 2014). Tick salivary extract, and tick salivary protein Salp12 have been shown using *in vitro* experiments to be chemoattractants for *B. burgdorferi* (Murfin et al., 2019; Van Gundy et al., 2021). The question of where these spirochetes that infect the larval tick come from within the host remains. With *B. afzelii* there are multiple studies suggesting that the spirochete population in the skin is critical for transmission (Bernard et al., 2020; Genné et al., 2021; Grillon et al., 2017; Jacquet et al., 2015; Råberg, 2012). This makes intuitive sense as the spirochete population in the skin is already at or near the site of tick feeding. With *B. burgdorferi*, there is no evidence linking abundance in the skin to transmission. However, the general consensus for *B. burgdorferi*

is that the spirochete population in the skin is important for host-to-tick transmission and that spirochetes in internal organs probably do not contribute to transmission (Tsao, 2009).

1.1.5.4 Tick-to-host transmission

The second transmission in the life cycle of *B. burgdorferi* is tick-to-host transmission. In the context of human health this would mark the beginning of an infection or exposure to *B. burgdorferi*. It is important to understand that ticks derive all of their nutrients from their blood meals. Following the larva-to-nymph moult, the spirochete population persists in the tick midgut where it declines over time until the nymphal blood meal (de Silva & Fikrig, 1995; Genné et al., 2019; Jacquet et al., 2017; Piesman et al., 1990; Pospisilova et al., 2019; Soares et al., 2006). The nymphal blood meal triggers a host of gene expression changes within the bacterium and a rapid increase in growth (Anguita et al., 2003). The *B. burgdorferi* present in the tick midgut express OspA, which allows the spirochete to bind itself to the midgut endothelium (Dunham-Ems et al., 2009). Expression of OspA declines while expression of OspC increases, a hallmark of the changes made by the spirochete in preparation for the mammalian host environment (Dunham-Ems et al., 2009; Srivastava & De Silva, 2008). *Borrelia burgdorferi* exits the midgut and transits to the tick salivary glands where it can then invade the host (Dunham-Ems et al., 2009; Pal et al., 2004).

The time required for *B. burgdorferi* to enter the host after an *I. scapularis* tick begins feeding is variable but does not occur immediately. Transmission is unlikely to occur before 24 hours of tick feeding and attachment (des Vignes et al., 2001; Eisen, 2018; Hojgaard et al., 2008). The probability of transmission increases the longer the tick remains attached and feeding. Measuring the probability of nymph-to-host transmission of a *B. burgdorferi* strain

requires feeding single putatively infected nymphs on mice and determining the percentage of mice that become infected following this challenge (des Vignes et al., 2001). A major limitation is that the infection status of a nymph cannot be known before using it to challenge a mouse. For strains that have low infection prevalence in the challenge nymphs, this means that many mice will be challenged with uninfected nymphal ticks. One study that challenged hosts with 3 putatively infected ticks found significant differences in both nymph-to-host transmission and HTT among strains of *B. afzelii* (Tonetti et al., 2015). Interestingly, this study found that the strains with the greatest HTT had the greatest nymph to host transmission (Tonetti et al., 2015). A study of tick-to-host transmission using two strains of *B. burgdorferi* did not find significant differences in their transmission when using single ticks to infect hosts (des Vignes et al., 2001). This study also prematurely removed the ticks rather than allowing them to feed to repletion. Generally, studies of tick-to-host transmission show that tested strains of *B. burgdorferi* sl have a >50% probability of transmission to a host, though challenge with multiple ticks can increase these estimates (Belli et al., 2017; des Vignes et al., 2001; Goddard et al., 2015; Jacobs et al., 2003; Piesman & Sinsky, 1988).

1.1.6 Wildlife hosts

1.1.6.1 Reservoir competence for *Borrelia burgdorferi*

A reservoir competent host is a host that is readily infected by the pathogen, and when fed on by the vector has a high probability of transmission. One of the key determinants to reservoir competence is the duration of infection as this would define the window of transmission. As discussed in section 1.1.5.2, larval and nymphal *Ixodes* ticks of different generations feed concurrently (Kurtenbach et al., 2006). Rodent reservoirs of *B. burgdorferi* and

B. afzelii can transmit these pathogens to feeding ticks for months and even years, potentially contributing to multiple tick feeding seasons (Donahue et al., 1987; Gern et al., 1994).

The main tick vectors of *B. burgdorferi* sl are generalist feeders. In North America, *I. scapularis* and *I. pacificus*, and in Europe, *I. ricinus* and *I. persulcatus* readily feed on a wide variety of hosts (Kurtenbach et al., 2006). Not all these hosts contribute to the spread of *Borrelia*. Two important vertebrate reservoirs for the immature stages of *I. scapularis* and for *B. burgdorferi* are the white-footed mouse *Peromyscus leucopus* and the closely related deer mouse *Peromyscus maniculatus* (Barbour, 2017; Donahue et al., 1987; Fiset et al., 2015; Rand et al., 1993). Experimental studies have shown that other species of rodents and shrews are competent reservoir species for both immature *I. scapularis* ticks and *B. burgdorferi* (Ginsberg et al., 2005; LoGiudice et al., 2003; Markowski et al., 1998; Salkeld et al., 2008). Nymphs and adult *I. scapularis* ticks regularly parasitize deer and mesocarnivores, such as raccoons, skunks, and opossums. These species are less competent (or fully incompetent) hosts for *B. burgdorferi*; infected animals have little or no host-to-tick transmission (LoGiudice et al., 2003; Telford et al., 1988). Instead, these vertebrate hosts contribute to the maintenance of *I. scapularis* populations but not to the transmission of *B. burgdorferi*.

1.1.6.2 *Borrelia* propagation within the host

Previously, we had discussed the transmission of *B. burgdorferi* sl from the host (see section 1.1.5.3), and into the host (see section 1.1.5.4). Here we will focus on *B. burgdorferi* within the host, its distribution and the negative effects it can cause.

When *B. burgdorferi* is first introduced into the host, initial dissemination is mediated by outer surface protein C (OspC) upregulation and aided in early immune evasion by tick salivary

proteins (Anguita et al., 2002; Kern et al., 2011). As few as 100 spirochetes could be delivered by a feeding tick to infect a host (Kern et al., 2011). When infected ticks take a blood meal, *B. burgdorferi* is released into the host as the tick regurgitates excess liquid. The first tissue colonized is the skin (Bernard et al., 2020). Immediately after feeding there is a localized concentration of *B. burgdorferi* present in the skin around the tick bite, this can cause the diagnostic erythema migrans rash in some human patients (Feder et al., 1993; Steere et al., 2003). After growth in the skin, *B. burgdorferi* will enter the vasculature to disseminate through the host (Moriarty et al., 2008). *B. burgdorferi* levels in the blood peak at 10 days post tick feeding (Dolan et al., 2004), and it does not persist in the blood but will disseminate into tissues. There is no definitive pattern in tissue colonization which contributes to the random progression of symptoms (Caine & Coburn, 2015; Lee et al., 2010; Moriarty et al., 2008).

Dissemination to distal tissues is what causes the severe symptoms of Lyme borreliosis in susceptible hosts. The timeline of tissue colonization in the *Mus musculus* C3H/He mice is summarized in Table 1.1. In the closely related species *B. afzelii*, infection and abundance in the skin is important for transmission (Bernard et al., 2020; Genné et al., 2021; Grillon et al., 2017; Råberg, 2012; Tsao, 2009). There is no evidence to suggest this is also true for *B. burgdorferi* (Bernard et al., 2020), but this is reasonable to assume due to the limited evidence of *B. burgdorferi* in the blood after initial dissemination. The spirochetes that disseminate to internal organs (bladder, heart, joints) may never achieve transmission to the host (Tsao, 2009). *Borrelia burgdorferi* persists in the heart and decorin-rich tissues like joints as a protective niche from the host immune response (Hill et al., 2021; Liang, Brown, et al., 2004).

Table 1.1 The detection of *B. burgdorferi* in various tissues in C3H mice. The method of detection, infection source (i.e., needle or tick) and inoculum size, and earliest detection time in that study are shown.

Tissue	Detection method	Infection source[a]	Timing	Source
Joint	Culture	IP (10^6)	4 weeks PI	(Barthold et al., 1990)
Ear	Culture, PCR	ID (10^4)	2 weeks PI	(Barthold et al., 1991)
Kidney, spleen	Culture	ID (10^4)	1 week PI	(Barthold et al., 1991)
Heart	Culture, PCR	ID (10^4)	2 weeks PI	(Armstrong et al., 1992)
Ear, kidney, spleen	Culture	ID (10^4)	2 weeks PI	(Barthold et al., 1992)
Ear, kidney, spleen	Culture	IP (10^7)	4 weeks PI	(Barthold et al., 1993)
Bladder, brain, liver	Culture	IP (10^7)	1 year PI	(Barthold et al., 1993)
Ear, heart, joint, spleen	PCR	ID (2*10^5)	1 week PI	(Yang et al., 1994)
Bladder, brain, kidney, liver, lymph node	PCR	ID (2*10^5)	3 weeks PI	(Yang et al., 1994)
Uterus	PCR	ID (2*10^5)	5 weeks PI	(Yang et al., 1994)
Bladder, heart, joint	PCR	*I. scapularis*	6 weeks PI	(Zeidner et al., 2001)
Bladder, brain, ear, heart, joint, spleen	Culture, PCR	ID (10^4)	2 weeks PI	(Wang et al., 2001)
Bladder, brain, ear, heart, joint, spleen	Culture	ID (10^4)	3 weeks PI	(Wang et al., 2002)
Skin (of injection site)	Culture	ID (10^4)	4 days PI	(Wang et al., 2002)
Bladder, heart	PCR	*I. scapularis*	8 weeks PI	(Dolan et al., 2004)

[a] ID = intradermal inoculation; IP = intraperitoneal inoculation

1.2 Pathogen evolution

The most basic definition of evolution is a change in allele frequency in a population. Novel alleles that confer some benefit adaptive to the organism become more common in the population and may eventually replace other alleles. Fundamental to evolution is genetic variation, without which no evolution can occur (Hershberg, 2015). The ultimate source of genetic variation is mutation, which results in the creation of new genes and/or new alleles. In

organisms with sexual reproduction, independent segregation of chromosomes and crossing over during meiosis are an important source of genetic variation. Bacteria, which do not have sexual reproduction, can acquire new genes via transformation (uptake of DNA from the environment), transduction (bacteriophage-mediated transfer of DNA), and conjugation (plasmid exchange). The Darwinian theory of evolution explains how natural selection influences the fate of new mutations (Darwin, 1859). Deleterious or bad mutations reduce the fitness of the organism and are less likely to be passed on to subsequent generations. Advantageous or good mutations increase fitness and are positively selected for (Loewe & Hill, 2010). The cost or benefit of a new mutation can depend on the environment and genetic background of the organism. In the Galapagos Finches, Darwin observed how different instances of positive selection occurred to allow multiple closely related species to coexist and exploit different ecological niches effectively (Darwin, 1859).

Evolution also applies to pathogens and parasites. The evolution of a pathogen is inherently tied to its hosts (Anderson & May, 1982). Pathogens (or parasites) live in an intimate relationship with a host organism. The pathogen exploits the host resources for its own benefit, which results in harm or damage to the host, which we recognize as infectious disease. Other organisms, such as symbionts or commensal species, also live in a close relationship with their host, but they have a positive effect or no effect on host fitness. Thus, a key feature of a pathogen or parasite is that they reduce the fitness (survival and reproduction) of their host organism. Evolutionary biologists use the term ‘virulence’ to refer to this negative effect of the parasite on host fitness (Anderson & May, 1982; Musser, 1996).

The life cycle of pathogens contains a paradox. The pathogen uses the host resources to grow and multiply, but this exploitation can kill the host, which would also kill the pathogen.

Early models on the evolution of pathogens focused on this apparent paradox. How does pathogen virulence persist when becoming commensal (i.e., not damaging or killing the host) would improve survival of both the host and the pathogen (Anderson & May, 1982; Baalen & Sabelis, 1995; Ebert & Bull, 2003)? Consider *Staphylococcus aureus*. In 20-30% of the global population, this bacterium is a commensal part of the human microbiome (Jenkins et al., 2015). It is also a leading cause of hospital acquired infection deaths (Cheung et al., 2021; Jenkins et al., 2015). The avirulent *S. aureus* persists in the human population yet in some cases, the bacterium causes serious infections of the skin or respiratory system, possibly killing its host. Thus, the basic argument against virulence is that the pathogen destroys its own environment (i.e., the host). However, the observation that the parasitic lifestyle is common in nature suggests that a life history strategy that damages or kills the host is adaptive.

1.2.1 Virulence – transmission theory

Evolutionary virulence theory was developed to explain the evolution and persistence of pathogen virulence. Theoretical models of virulence evolution typically define virulence as the additive parasite-induced host mortality rate (Anderson & May, 1982). In empirical studies where it is often difficult to measure host mortality, virulence can refer to any pathogen-induced reduction in host fitness (Alizon et al., 2009). Prior to the development of evolutionary virulence theory, the conventional view was that all pathogens (and parasites) should evolve towards avirulence (i.e., not harming the host) over time (Alizon et al., 2009; Visher et al., 2021). This avirulence hypothesis suggested that virulence occurred whenever pathogens colonized new host species, but over time the pathogen would evolve to reduce doing damage to its host. The fundamental concepts for the evolution of pathogen virulence come from the previously

mentioned paradox: pathogens exploit host resources to achieve transmission, but this host exploitation results in virulence that damages or kills the host and thereby ends the infection. For this reason, there must be some advantage or purpose to virulence to explain its persistence and magnitude. Virulence is a trait that varies among pathogen species and among pathogen strains (De Roode et al., 2005; De Roode et al., 2008; May & Nowak, 1995). However, empirical evidence for evolutionary virulence theory is generally based on comparing strains of the same pathogen species that differ in their virulence but that are otherwise very similar.

Anderson and May (1982) were the first to use theoretical models to show that pathogen virulence is adaptive (and can evolve in the pathogen population) if this trait is linked to pathogen transmission success. A pathogen must infect new hosts. To do this, the pathogen must replicate in the relevant tissues of the infected host to reach a density or abundance where transmission is possible and highly probable. The virulence-transmission trade-off (VTT) hypothesis states that virulence is a necessary by-product of replication and transmission to complete the life cycle (Anderson & May, 1982). This theory is well illustrated by malaria parasites of the genus *Plasmodium*. High abundance of malaria parasites (merozoites) in the blood of the vertebrate host increases the abundance of gametocytes, which are the transmissible stage that are acquired by *Anopheles* mosquitoes during the blood meal. The merozoites grow inside erythrocytes (red blood cells) and cause their destruction, which releases more parasites that continue the cycle of invading other erythrocytes. A high abundance of malaria parasites in the blood results in more severe anemia and more severe malaria symptoms, which can result in host death (Mackinnon & Read, 1999, 2004; Marsh & Snow, 1997). Thus, high parasitemia (parasite density in host blood) is good for parasite transmission but bad for host health and the duration of the infection (Mackinnon & Read, 1999). Another example is the viral pathogen

HIV-1, which is sexually transmitted between human hosts. In the absence of treatment, infection with HIV-1 results in an asymptomatic phase that can last for years followed by the onset of acquired immunodeficiency syndrome (AIDS) when transmission is strongly reduced because patients are too ill to engage in sexual activity. Thus, the duration of the asymptomatic phase represents the transmission window of HIV-1. A higher viral titre in the blood of infected humans increases the likelihood of transmission during the asymptomatic phase of infection. High viral titres also result in an earlier onset of AIDS (i.e., pathogen virulence) and a shorter duration of asymptomatic infection (Fraser et al., 2007). Higher viral titres increase transmission up to an optimal point after which, the reduced asymptomatic period reduces lifetime transmission.

As described in the examples of malaria and HIV-1, increasing abundance leads to increasing transmission at the cost of increasing virulence. Theoretical models show that if the relationship between virulence and transmission were linear or exponential, then natural selection would result in the evolution of infinite pathogen virulence. For this reason, models of virulence evolution typically assume that the relationship between virulence and transmission has a concave shape where increasing virulence produces diminishing returns on transmission. As pathogen transmission cannot exceed 100%, it seems intuitive that there must be some pathogen abundance in the host tissues at which there is little or no improvement in pathogen transmission. Once this maximum pathogen tissue abundance is reached, any further selection for increased virulence will not increase pathogen transmission success.

The main conclusion of the VTT hypothesis is that an intermediate level of host exploitation and hence virulence leads to the highest lifetime pathogen fitness. Virulence has an optimal value, where increasing or decreasing it from that point leads to a reduction in lifetime

transmission success (Anderson & May, 1982; Bull, 1994; De Roode et al., 2008). Higher virulence than this optimal value would increase current transmission but would decrease the lifespan of the infection (Mackinnon et al., 2008) and hence future opportunities of transmission. Conversely, lower virulence than this optimal value would increase the lifespan of the infection (i.e., by delaying host death) but it would decrease probability of transmission. The studies of HIV-1 and malaria as well as others have shown selection favors intermediate virulence where the balance allows for optimum transmission (Bonneaud et al., 2020; De Roode et al., 2008; Fraser et al., 2007; Jensen et al., 2006; Mackinnon & Read, 2004).

Virulence-transmission theory is a foundational theory of pathogen evolution. The central points are that there is an expected positive relationship between transmission and in-host pathogen replication or abundance, and that virulence is related as a trade-off that constrains selection for increasing abundance and transmission. This theory provides a framework to explain the existence of virulence, and to determine the relative fitness of pathogen strains based on their replication (or abundance) in host tissues, virulence, and transmission.

1.2.2 Immune-mediated selection and antigenic differentiation

Immune-mediated selection is a theory of pathogen evolution centered on the selective pressures of the host immune response on pathogens (Bockenstedt et al., 1997; Li et al., 2012; Lipsitch & O'Hagan, 2007; Weedall & Conway, 2010). The interaction between pathogens and host immune responses is a broad topic and will be discussed more in section 1.2.5. Here we will focus on how the host immune response is a source of selective pressure that can drive pathogen strain diversification. In addition to theory, this section will summarize studies of immune-mediated selection and the evidence for it in *B. burgdorferi* sensu lato.

1.2.2.1 Pathogens have immunodominant antigens that dominate the host antibody response

Pathogens may contain many antigens that induce an antibody response in the vertebrate host, but not all antigens are created equal. Immunodominant antigens are those pathogen proteins that dominate the host antibody response (Conway & Polley, 2002; Gupta & Anderson, 1999). These immunodominant antigens are often expressed on the surface of the pathogen and are critical for establishment of infection. An effective host antibody response against such immunodominant antigens can prevent infection and represents an existential threat to pathogen fitness. The host antibody response therefore represents a strong force of selection that causes the pathogen genes underlying these immunodominant antigens to diversify over time. This immune-mediated selection is a major explanation as to why many pathogen populations consist of antigenically distinct strains (i.e., serovars or serotypes) that induce strain-specific immunity. Examples of such highly polymorphic immunodominant antigens include the outer membrane protein PorA of the bacterium *Neisseria meningitidis* (Gupta et al., 1996), major surface protein-2 (Msp2) of the tick-borne bacterium *Anaplasma marginale* (Futse et al., 2008), and the merozoite surface proteins of malaria parasites (Fairlie-Clarke et al., 2013; Futse et al., 2008). One outcome of immune-mediated selection is the proliferation of antigenically distinct strains that infect the same host species.

In *B. burgdorferi* sensu lato, outer surface protein C (OspC) is an immunodominant antigen that has diversified in response to the host antibody response. When *B. burgdorferi* initially invades a vertebrate host, the *ospC* gene is upregulated (Grimm et al., 2004). OspC is involved in the early stages of animal infection and is also important in dissemination through the host (Kenedy et al., 2012; Skare et al., 2016). Vertebrates develop a strong antibody response

against the highly polymorphic OspC protein (Dressler et al., 1993). Alleles of the *ospC* gene are classified into *ospC* major groups (oMGs) that are clearly defined by sequence homology (Attie et al., 2007; Barbour & Travinsky, 2010; Wang et al., 1999). Critically, these oMGs or *ospC* types are characterized by a highly strain-specific antibody response. Immunization with a particular recombinant OspC protein will protect against strains carrying that oMG but not against strains carrying other oMGs (Jacquet et al., 2015; Preac-Mursic et al., 1992; Probert et al., 1997; Probert & LeFebvre, 1994). Due to the absence of cross-reactive antibody responses, hosts can be sequentially infected with strains carrying different oMGs (Derdáková et al., 2004; Rogovskyy & Bankhead, 2014; Rynkiewicz et al., 2017). If there is no difference in function among these oMGs, then each strain carrying a different oMG would have equal success in a naïve susceptible host, all else being equal.

1.2.2.2 Negative frequency-dependent selection

Theoretical studies have shown that immune-mediated selection on immunodominant antigens is important for influencing pathogen population structure (Gupta & Anderson, 1999; Gupta et al., 1998; Gupta et al., 1996). Field studies have shown that tick populations and vertebrate host populations often contain substantial diversity of *ospC* alleles at small spatial scales (Brisson & Dykhuizen, 2004; Hellgren et al., 2011; Qiu et al., 2002; Qiu et al., 1997; Wang et al., 1999). An important question is what factors or processes maintain these relatively high levels of *ospC* strain diversity in nature. Numerous studies have suggested that negative frequency-dependent selection (NFDS) on the OspC antigen of *B. burgdorferi* sensu lato pathogens determines their strain population structure (Haven et al., 2011; Qiu et al., 2002; Qiu et al., 2004; Wang et al., 1999).

NFDS is when genotypes or variants that are rare have a selective advantage over those genotypes or variants that are common. NFDS is a fitness penalty that targets the most common strains, and that gives a selective benefit to rare strains. NFDS maintains strain diversity because it increases the frequency of rare genotypes and decreases the frequency of common genotypes. The exact mechanism that allows the host immune system to target the more common strain is not always clear, but there are two potential mechanisms by which this can occur in *B. burgdorferi* sl pathogens.

In LB-endemic areas where the density of infected nymphs is high, vertebrate reservoir hosts are repeatedly bitten by infected nymphs over the same transmission season. Reservoir hosts are more likely to repeatedly encounter those *B. burgdorferi* strains that are most common in the cohort of nymphal ticks that are questing that year. If recurring exposure to the same strain via nymphal tick bite is analogous to repeated vaccination, hosts will develop stronger antibody responses against common strains compared to rare strains (Wang et al., 1999). If stronger antibody responses reduce the spirochete abundance in the host tissues, which in turn reduces HTT, there is an opportunity for NFDS to select against *ospC* major groups (oMGs) that are common in the pathogen population. However, given that *B. burgdorferi* establishes chronic infections in the reservoir host (Donahue et al., 1987; Gern et al., 1994), it remains unknown whether additional tick bites would really enhance the host antibody response against common strains (Brisson et al., 2012; Donahue et al., 1987; Gern et al., 1994).

The second mechanism by which NFDS can maintain strain diversity is the transfer of maternal antibodies from infected female reservoir hosts to their offspring. Maternal antibodies protect offspring during their initial development before their own system is capable of protection (Niewiesk & Gans, 2014). The host antibody response to *B. burgdorferi* sl is unusual;

the same antibodies that fail to clear the pathogen from the infected host can, upon passive transfer, protect naïve hosts from infectious challenge (Mbow et al., 1999). This passive transfer of antibodies occurs when females infected with *B. burgdorferi* transmit maternal antibodies to their offspring. The importance of maternal antibodies was shown in an experimental infection study using *B. afzelii* and an important reservoir host, the bank vole *Myodes glareolus* (Gomez-Chamorro, Heinrich, et al., 2019). Female bank voles that were uninfected or infected with *B. afzelii* were mated to produce offspring. Offspring born to infected mothers contained maternal antibodies against *B. afzelii*, whereas offspring born to uninfected mothers did not. All offspring were subsequently challenged with either the maternal strain or a different strain. Offspring from uninfected mothers were susceptible to both strains. Offspring from infected mothers were protected against the maternal strain and susceptible to the different strain (Gomez-Chamorro, Heinrich, et al., 2019). The offspring from infected mothers had a strong IgG antibody response against the oMG of the maternal strain. Transfer of maternal antibodies from infected mothers to their offspring could result in NFDS and maintain strain diversity as follows. At the start of the *B. burgdorferi* sl transmission season, females are more likely to encounter the oMGs that have a higher frequency in the questing nymphs. Females infected with common strains transmit maternal antibodies to their offspring that would protect the latter from infection to these common strains. In contrast, the offspring would still be susceptible to the less common strains in the nymphs that had not been encountered by the mothers (or that had been encountered less frequently). In North America, *I. scapularis* nymphs quest during the early spring and summer when rodent reservoirs are mating and reproducing. Thus, the transfer of the maternal antibodies from mothers to offspring coincides with the time that nymphs are inoculating their *B. burgdorferi* strains into the rodent reservoir population (Kurtenbach et al., 2006).

Epidemiological models that incorporate this seasonal exposure of mothers and their offspring to a fixed strain structure in the questing nymphs and the mother-offspring transfer of protective but strain-specific maternal antibodies are required to determine whether these phenomena could maintain strain diversity of *B. burgdorferi* sl pathogens in nature.

1.2.2.3 Immune-mediated selection and linkage disequilibrium

Immune-mediated selection on immunodominant antigens can result in linkage disequilibrium in the pathogen genome (Gupta & Anderson, 1999; Gupta et al., 1998; Gupta et al., 1996). Linkage disequilibrium is the non-random association of alleles when there is no physical (i.e., distance on a chromosome) link. It is difficult for two strains that have the same immunodominant variant but that are genetically distinct at other loci to co-exist in the same host population. The reason is because as one strain becomes more common, a large fraction of the host population will carry antibodies against the shared immunodominant variant, which will prevent the less common strain carrying the same immunodominant variant from establishing infection in the host population. As one strain becomes more common, selection against all other strains carrying the same immunodominant variant becomes stronger and extinction of these less common strains becomes more likely. Note that this is an example of positive frequency-dependent selection where common strains have a selective advantage over rare strains. In *B. burgdorferi*, immune-mediated selection on the OspC antigen is expected to result in linkage disequilibrium between the cp26 plasmid on which the *ospC* gene is located and the rest of the genome. Numerous studies have found a strong association between *ospC* on cp26 and various other genes located on other genetic elements across strains at small geographic scales (Attie et al., 2007; Bunikis, Garpmo, et al., 2004; Hellgren et al., 2011; Qiu et al., 2004). Across the entire

distribution of *B. burgdorferi*, there are differences in the associations between *ospC* and other genetic elements (Barbour & Travinsky, 2010; Qiu et al., 2004), because this selection only occurs where strains co-occur, allowing for regional variation in the specific associations.

Pathogen evolution is strongly influenced by the immune response of the host and the selective pressures it creates. With *B. burgdorferi*, immune-mediated selection has likely contributed to the maintenance of a diverse and abundant population of antigenically distinct strains. Importantly, this is not mutually exclusive from any other theory for pathogen evolution, rather focusing on a critical external factor for pathogens. The antigenically distinct strains of *B. burgdorferi* may have fitness differences that would be investigated in their in-host abundance, transmission, and virulence.

1.2.3 Co-infection and competition effects

Basic evolutionary virulence theory determines the optimal level of virulence for a single pathogen strain. This model does not consider how co-infections and competition between strains will influence the evolution of the optimal level of virulence (Baalen & Sabelis, 1995; Ebert & Bull, 2003). When two or more closely related species or strains occupy the same ecological niche then competition is likely. Mixed infections or co-infections all refer to the situation where the host is infected with different pathogen species or with multiple strains of the same species. For human pathogens that consist of multiple strains, mixed infections (here referred to as co-infections) are common in human hosts (Balmer & Tanner, 2011).

Competition can be broadly classified as scramble competition over limited host resources and apparent competition mediated by the host immune system. Scramble competition over limited host resources tends to select for virulent strains over avirulent ones. This is because

virulent strains with faster replication obtain a greater share of host resources and will have greater transmission compared to avirulent strains. This phenomenon has been demonstrated in multiple systems (Bashey et al., 2011; Ben-Ami et al., 2008; De Roode et al., 2005). Under scramble competition, the virulent strain has a competitive advantage because early death of the host has an even greater negative impact on the avirulent strains, which may not have achieved any transmission. In summary, co-infection and scramble competition over limited resources shift the evolutionary optimum towards fast-growing strains with higher virulence.

Apparent competition or indirect competition refers to immune-mediated competition between strains (Schmid-Hempel, 2009). Here the antibody response against one strain can interfere with the performance of another strain. This phenomenon can be very important when hosts are repeatedly infected by different strains, in other words a sequential co-infection rather than a simultaneous co-infection. In a sequential co-infection, the primary resident strain is present in the host prior to the arrival of a secondary invading strain. One theory suggests that higher virulence should allow invading strains to displace resident strains by inducing a greater immune response (Brown et al., 2008). What has been demonstrated in experimental infections, is that the host immune response incurred by the resident strain represents a barrier that must be overcome by the invading strain, and that virulent strains are better at overcoming this barrier than avirulent strains (Fleming-Davies et al., 2018; Mackinnon et al., 2008; Råberg et al., 2006). In a host population where the prevalence of infection is high, increased virulence over the expected would be necessary to allow for transmission and replication within the host.

In systems with multiple strains, there will be naïve uninfected hosts and infected hosts that have developed an immune response (i.e., primed hosts) (Alizon et al., 2013). Theoretical models of vaccination have found that vaccines that reduce pathogen abundance in the host

tissues but that do not block transmission will favour the evolution of pathogen virulence (Barclay et al., 2012; Gandon et al., 2001; Mackinnon et al., 2008; Read et al., 2015). In these models, virulent strains are better able to overcome the antibody response in vaccinated hosts. Marek's disease in chickens provides evidence of how vaccines that do not block transmission can result in the evolution of highly virulent pathogens (Read et al., 2015).

The immune response generated by a previous infection of a conspecific strain can have the same effect as incomplete immunity by vaccination. In a study of *Mycoplasma gallisepticum* in finches, prior infection led to increased levels of virulence in the circulating strains (Fleming-Davies et al., 2018). Further, the higher the virulence of the primary resident strain, the greater its inhibition of the secondary invading strains. In this system, co-infections lead to higher levels of virulence to overcome the greater cost of infecting previously infected hosts.

Competitive interactions between pathogen strains can only occur if the strains co-occur in the same host or vector (Alizon & Lion, 2011). For *B. burgdorferi* sl pathogens, multi-strain infections or co-infections are common in both the vertebrate host and the tick vector (Balmer & Tanner, 2011; Brisson & Dykhuizen, 2004; Devevey et al., 2015; Perkins et al., 2003; Qiu et al., 2002; Swanson & Norris, 2008). In a population of *I. scapularis* in an endemic area of the northeastern United States, 50% of ticks tested were co-infected with multiple strains of *B. burgdorferi* (Wang et al., 1999). Despite the common occurrence of co-infections of *B. burgdorferi* sl strains in vertebrate hosts, there are few experimental studies that have investigated inter-strain competition (Derdáková et al., 2004; Devevey et al., 2015; Genné et al., 2021; Rogovskyy & Bankhead, 2014; Rynkiewicz et al., 2017). The study by Devevey et al. (2015) needle inoculated their mice to generate infections and found a strain-independent priority effect in sequential co-infections. Needle inoculations can alter infection dynamics and influence

results (Gern et al., 1993; Roehrig et al., 1992; Sertour et al., 2018). Three of the studies investigated competition in sequential co-infections using tick challenges or tissue transplants (Derdáková et al., 2004; Rogovskyy & Bankhead, 2014; Rynkiewicz et al., 2017). In each case, both the resident and invading strain were capable of transmitting, however strains had asymmetric effects of competition. In a comparison of *B. burgdorferi* strains in homologous and heterologous infections of *P. leucopus*, only one strain had reduced transmission from competition (Rynkiewicz et al., 2017). In single infections these two strains showed similar transmission, but in co-infections the strain that was able to maintain its transmission would be selected for. Studies of competition in *B. afzelii* using simultaneous co-infections found strain-specific effects in the host as well as in the tick (Genné et al., 2021; Genné et al., 2018; Genné et al., 2019). These studies again show an asymmetric effect of inter-strain competition where one strain has both reduced abundance in the host and tick, and reduced transmission resulting from competition.

1.2.4 Multiple niche polymorphism hypothesis of strain diversity

One of the fundamental drivers of speciation is that different environments (i.e., different ecological niches) select for different genotypes. In the case of a pathogen, different host species represent different ecological niches. An example is the avian influenza virus, which consists of multiple strains. The avian influenza (AI) virus originated as a pathogen of birds. Some AI strains with key mutations have been able to cross the species barrier (spillover) and infect other animals like humans and pigs (Chauhan & Gordon, 2021). These strains have in effect colonized a new ecological niche where they no longer compete with AI strains that are restricted to the original avian hosts. Once pathogen strains become specialized on different host species, they are

less likely to encounter each other, and the potential for genetic exchange between them decreases. Adaptive evolution will result in further host-strain specialization and in continued genetic divergence between strains. Eventually, the pathogen strains in different vertebrate hosts might be so genetically different from each other that they are considered separate pathogen species.

We had previously discussed how the *B. burgorferi* sensu lato complex consists of different genospecies. Some of these genospecies are associated with different hosts. For example, *B. afzelii* and *B. bavariensis* are found in small mammals such as rodents and shrews, whereas *B. garinii* and *B. valaisiana* are found in birds (Hanincová, Schafer, et al., 2003; Hanincová, Taragelova, et al., 2003; Kurtenbach et al., 2001; Gabriele Margos et al., 2013). Interestingly, while *B. burgdorferi* is predominantly associated with small rodent species, some birds are also competent competent reservoir hosts (LoGiudice et al., 2003; Richter et al., 2000a, 2000b). *Borrelia burgdorferi* has a wide range of competent vertebrate hosts that may explain the diversity of strains.

1.2.4.1 Host adaptations as a mechanism for strain diversification

The multiple niche polymorphism (MNP) hypothesis is another explanation of how strains of *B. burgdorferi* were generated and how these strains can co-exist in nature (Brisson et al., 2012; Brisson & Dykhuizen, 2004). In North America, field studies have found *B. burgdorferi* in a wide variety of vertebrate hosts including the white-footed mouse, chipmunks, grey squirrels, shrews, and birds (Brisson & Dykhuizen, 2004; Hanincová et al., 2006; LoGiudice et al., 2003; Mechai et al., 2016; Richter et al., 2000a; Vuong et al., 2014). The MNP hypothesis states that different strains of *B. burgdorferi* are adapted to and specialized on

different vertebrate host species (Brisson & Dykhuizen, 2004; Hanincová et al., 2006; Mechai et al., 2016; Vuong et al., 2014). Each host species differs in its immune system that favors a different pathogen strain. Host species also differ in their tick burdens, where larger hosts can carry and thus potentially transmit to more ticks than smaller hosts (LoGiudice et al., 2003). Under the MNP hypothesis, the frequency of each strain depends on the number of ticks fed by each species (a function of the species abundance and tick burden). All else being equal, strains that are specialized on the high abundance, high tick burden species will be more common (i.e., have higher frequency in the *B. burgdorferi* population).

Studies on the MNP hypothesis investigate whether there are associations between *B. burgdorferi* strains and vertebrate host species. In statistical terms, these studies are testing whether the interaction between *B. burgdorferi* strain and host species has a significant effect on the presence and/or spirochete abundance of strains in the host tissues (Råberg et al., 2017) and/or on the transmission to feeding ticks. There are studies that found these host-strain associations (Brisson & Dykhuizen, 2004; Mechai et al., 2016) and studies that have not (Hanincová et al., 2006; Råberg et al., 2017; Vuong et al., 2014). Most MNP studies investigate the strain diversity in field-captured and naturally infected hosts. The major limitation of these studies is that they do not control for differences in exposure to different strains (Brisson & Dykhuizen, 2004; Hanincová et al., 2006; Mechai et al., 2016; Vuong et al., 2014). Experimental infection studies suggest that most *B. burgdorferi* strains can establish persistent infections in the white-footed mouse (*Peromyscus leucopus*), as well as the laboratory model house mouse (*Mus musculus*) (Baum et al., 2012; Hanincova et al., 2008; Wang et al., 2002; Zinck et al., 2022). Brisson et al. (2004) who developed the MNP hypothesis to explain the diversity of *B. burgdorferi* strains (based on *ospC* major group, oMG) in the eastern United States, suggested

that most strains could infect most vertebrate hosts, but that strains differed in their HTT success among vertebrate host species. For example, strains carrying oMG B were found in 38.6% and 20.0% of the larvae that had fed upon infected *P. leucopus* and *Blarina brevicauda* (short-tailed shrew), respectively. In contrast, strains carrying oMG E were found in 30.0% and 46.2% of the larvae from *P. leucopus* and *B. brevicauda*, respectively (Brisson & Dykhuizen, 2004). As both strains had appreciable HTT in both host species, these differences could be reconciled if strains are not solely constrained to the host they are specialized to, but rather that they are at the maximum fitness within this host. It is important to point out that these field-captured animals were naturally coinfected with different combinations of *B. burgdorferi* strains, and as discussed above inter-strain competition can influence the strain-specific HTT.

1.2.4.2 Contribution of MNP to strain diversification

A recent modelling study showed that antigenic differentiation (through immune-mediated selection and negative frequency dependence, NFDS) and MNP can both contribute to the maintenance of strain diversity in nature (Adams et al., 2021). MNP states that different *ospC* types (and thus strains) are adapted to different vertebrate host species and that different hosts are different niches. Immune-mediated selection states that the *ospC* types have diversified to avoid cross-reactive antibody responses within the same set of vertebrate host species, and that each *ospC* type has its own unique immunological niche. These two explanations are not mutually exclusive, though the existence of OspC-specific antibody responses is strong evidence for the importance of immune-mediated selection in shaping the strain structure of *B. burgdorferi* in nature (Barbour & Travinsky, 2010).

We point out that evidence that demonstrates a significant additive effect of host species on the tissue infection prevalence and/or tissue spirochete abundance of all strains does not provide evidence for MNP because all strains are similarly affected. For example, field studies have shown that bank voles (*Myodes glareolus*) have higher abundance of *B. afzelii* in their tissues and higher transmission to feeding *I. ricinus* ticks compared to yellow-necked mice (*Apodemus flavicollis*) (Råberg, 2012; Råberg et al., 2017; Zhong et al., 2019). This result shows that host species influences pathogen fitness, but this is not evidence for MNP because all strains are affected in the same way (Råberg et al., 2017). Similarly, an experimental infection that tested all combinations of two *B. burgdorferi* strains and two host species found that the strain with higher HTT in *M. musculus* C3H mice also had higher HTT in *P. leucopus* (Hanincova et al., 2008). In summary, immune-mediated selection and MNP are two alternative and not mutually exclusive explanations for the creation of the strain diversity of *B. burgdorferi* sl pathogens and for the persistence of this strain diversity in nature.

1.2.5 Influence of the host on pathogen phenotypes

1.2.5.1 Host immune response to infection

A throughline of measuring pathogen traits and understanding the evolutionary forces that shape pathogen populations is the effect of the host. The pathogen causes damage to the host which we refer to as virulence, but the host has an immune system that can defend against pathogens. Detailed coverage of the mechanisms of the immune system against infection is beyond the scope of this review. This section will focus on how the host immune response influences the pathogen life history traits of interest.

The vertebrate immune system consists of two branches: innate and adaptive. The innate branch provides an immediate but non-specific response to pathogens (Janeway et al., 2001). The innate immune system includes macrophages and dendritic cells that use their Toll-like receptors to recognize pathogens. It also includes the complement system that is believed to be responsible for mediating the vertebrate host specificity of some *Borrelia* genospecies (Kurtenbach et al., 2002). The adaptive branch of the immune system is based on antigen recognition and 'memory' of past infections through antibodies and T cell receptors produced by B and T lymphocytes (Flajnik & Kasahara, 2010; Janeway et al., 2001). As discussed above, host antibody responses drive antigenic differentiation, NFDS, and the strain structure of pathogen populations. The effectiveness of these systems is highly variable within a single host species, and within a single host temporally. Comparing *B. burgdorferi* infection between immunocompetent and immunocompromised mice shows that the host immune response can reduce the abundance of spirochetes in the host tissues (Barthold et al., 2006; Bockenstedt et al., 2021; Liang, Brown, et al., 2004; Liang et al., 2020; Rahman et al., 2016; Tschirren et al., 2013; Zhi et al., 2018). Variation in immunocompetence can confound studies of pathogen evolutionary theory by generating relationships between abundance and host immune status, rather than the pathogen genetic background (Mackinnon & Read, 2004).

An important example of how the host immune response shapes pathogen life history traits is immunopathology. Immunopathology is infection-associated damage that is caused by the host immune response rather than pathogen abundance in the host tissues (Graham et al., 2005). A lot of infection-related damage is caused in some part by the host immune response. Examples of immunopathology include lung damage from influenza, pulmonary edema from tuberculosis, and arthritis and carditis from LB; all this pathology is exacerbated by a functional immune response

(Bekker et al., 2000; Graham et al., 2005; Hussell et al., 2001; McKisic et al., 2000; Xu et al., 2004). The host immune response impacts virulence in two ways: it reduces pathogen abundance in the host tissues and thereby the burden of infection, but it can also contribute to the infection-associated damage.

1.2.5.2 Host sex

In the previous section, we discussed how the host immune response can influence pathogen life history traits. Host sex is another important host factor that alters the host immune response within mammalian species. Here we use sex in its specific biological definition where males (XY) and females (XX) are defined by chromosomal differences. There has been a longstanding bias in research towards the study of males and the assumption that any results found are equally applicable to females (Beery & Zucker, 2011).

In the host immune response to infection, the general trend is that females mount a stronger antibody response and are therefore less susceptible than males (Billingham, 1986; Klein & Flanagan, 2016; Schuurs & Verheul, 1990; Zuk & McKean, 1996). Females tend to show greater antibody production compared to males (Butterworth et al., 1967; Schuurs & Verheul, 1990). The mechanisms controlling these sex-specific differences are not fully understood, though sex hormones are likely to play a role (Furman et al., 2014; Klein, 2000; Klein, 2004; Klein & Flanagan, 2016; Trigunaite et al., 2015). Host sex via its effect on the host immune system will also influence pathogen phenotypes. If males have a reduced immune response, this should lead to greater presence and abundance of the pathogen in the tissues of male hosts compared to female hosts. If there is a direct relationship between pathogen abundance in the host tissues and virulence, males are expected to exhibit more virulence

compared to females. In contrast, if virulence is largely driven by host immune responses (i.e., immunopathology), then females are expected to exhibit more virulence compared to males. In summary, host sex and the relative importance of pathogen tissue abundance versus immunopathology can result in sex-specific patterns of pathogen abundance, virulence, and transmission.

1.3 Application of evolutionary theory to *Borrelia*

One of the limitations to evolutionary virulence theory is that theoretical modelling studies far outnumber the empirical evidence to confirm these models (Acevedo et al., 2019). Thus, more studies are needed that demonstrate the relationships between the 3 canonical life history traits of pathogen replication (or abundance in host tissues), virulence, and transmission. Empirical studies should remember that evolutionary virulence theory assumes that variation in these three life history traits has a genetic component in the pathogen population. To ensure that the variance and covariance in these life history traits has a genetic basis in the pathogen population (and is therefore subject to virulence evolution), these traits should be compared across pathogen strains in a common host environment (Schmid-Hempel, 2009). Host factors such as age, sex, immune status, nutritional status, and so on should be carefully controlled or included as factors in the experimental design. Relationships between abundance, transmission, and virulence can exist across factors other than pathogen strains (Mackinnon & Read, 2004). For example, measuring replication, virulence, and transmission of the same pathogen in naïve hosts versus immunized hosts would undoubtedly show the expected positive relationships

between abundance, virulence, and transmission, but this result would provide no evidence for the existence of life history trade-offs in the pathogen population.

Among strains of *B. burgdorferi*, there is consistent evidence of strain-specific differences in the three life history traits (Baum et al., 2012; Brisson & Dykhuizen, 2004; Derdáková et al., 2004; Dolan et al., 2004; Rynkiewicz et al., 2017; Wang et al., 2002; Wang et al., 2001; Zeidner et al., 2001). This evidence proves that there is some genetic component to the variance in replication, transmission, and virulence.

Three previous studies have related transmission to the abundance of *Borrelia* in host tissues (Genné et al., 2021; Jacquet et al., 2015; Råberg, 2012). The study by Råberg (2012) found a positive relationship between *B. afzelii* abundance in ear biopsies of field-captured rodents and the transmission to *I. ricinus* ticks that had naturally attached to the rodents. The study by Jacquet et al. (2015) found a similar relationship for spirochete density in ear biopsies and transmission in experimental infections with one strain of *B. afzelii* in BALB/c mice. Finally, the study by Genné et al. (2021) had co-infected BALB/c mice with two strains of *B. afzelii* and found that strain-specific abundances were positively related to strain-specific transmission. These studies are not without limitations. Using wild caught rodents that were naturally infected means there are many uncontrolled factors that could drive the relationship (e.g., host age, age of infection, *B. afzelii* strain). In the study by Jacquet et al. (2015), variation in tissue abundance and transmission must be due to unknown host factors because all the mice were infected with the same strain. The study by Genné et al. (2021) used co-infection and competition among strains to generate variation in tissue abundance and transmission. In summary, there is evidence that spirochete abundance in host tissues influences host-to-tick transmission, but there is no evidence to these two traits covary across *B. burgdorferi* strains.

Four studies examined the relationship between virulence and tissue abundance in *B. burgdorferi* (Dolan et al., 2004; Wang et al., 2002; Wang et al., 2001; Zeidner et al., 2001). The studies by Wang et al. (2001, 2002) needle inoculated C3H/HeJ *M. musculus* mice with different strains of *B. burgdorferi*. They found strains caused different severities of lesions in the colonized tissues, and that this was positively related to the abundance of *B. burgdorferi* within those tissues (Wang et al., 2002). In contrast, the studies by Zeidner et al. (2001) and Dolan et al. (2004) used tick challenges to infect their mice, and while they found differences in abundance and virulence between strains of *B. burgdorferi*, they did not find a relationship between the two traits. In summary, there is no conclusive evidence that a relationship between virulence and abundance exists for strains of *B. burgdorferi*.

A limitation of experimental infection studies and the measurement of pathogen life history traits in the lab is that the relevance of such measures to the natural world remains unknown. The value of our estimates of these strain-specific life history traits increases if we can relate them to measures of strain fitness in nature. As we mentioned previously, numerous studies have shown that natural *B. burgdorferi* populations have strain structure and that the frequencies of these strains represent an estimate of their fitness. All else being equal, common strains with higher frequencies have higher fitness compared to rare strains with low frequencies. Strain frequencies in nature are typically measured in wild *Ixodes* tick populations, just like experimental measures of HTT. We therefore expect that strains with higher HTT in the lab will have a higher frequency in wild tick populations. This expectation assumes that the performance of the strains in a host model is representative of the most important reservoir hosts in nature. This relationship can be used to prove whether experimental estimates of pathogen traits are representative of what is occurring in nature. An experimental infection study with various

strains of *B. afzelii* in *M. musculus* BALB/c mice estimated three types of transmission: host-to-tick, tick-to-host, and co-feeding (Tonetti et al., 2015). A subsequent study combined these transmission components to estimate the reproduction number (R_0) for each strain (Durand et al., 2017). This study found that *B. afzelii* strains with the highest R_0 were also the most common in nature (Durand et al., 2017). Similarly, an experimental infection with field-collected strains of *B. burgdorferi* in *P. leucopus* found that the strains that had higher frequencies in wild *I. scapularis* populations established higher abundance in the mouse tissues (Baum et al., 2012). Thus, there is some evidence that laboratory measures of strain-specific fitness are relevant to the strain structure in nature.

To date, there are no studies of *B. burgdorferi* that have investigated all three life history traits, replication, transmission, and virulence across a large set of strains. Within *B. burgdorferi* and the closely related *B. afzelii*, there are studies that investigate abundance and virulence, or abundance and transmission. In *B. afzelii*, a positive relationship between the abundance of the spirochete in the host tissues and its transmission to feeding ticks has been repeatedly shown (Genné et al., 2021; Jacquet et al., 2015; Råberg, 2012). Studies on *B. burgdorferi* have shown that strains that reached higher abundance in the host tissues also had greater virulence as measured by ankle swelling (Derdáková et al., 2004; Wang et al., 2002; Wang et al., 2001). This result does agree with evolutionary virulence theory, but more recent studies that compared abundance and virulence using naturally infected (via tick bite) mice did not find this relationship (Dolan et al., 2004; Zeidner et al., 2001). In summary, a study that investigates the relationships among the life history traits among a large set of *B. burgdorferi* strains would be a welcome addition to the literature.

Objectives

This purpose of this study is to investigate the variation among life history traits in strains of *B. burgdorferi*. This work has three main objectives.

Objective 1: quantify the variation among strains of *B. burgdorferi*. The traits investigated include the bacterial abundance in host tissues (Chapter 2), lifetime host-to-tick transmission (Chapter 3), and the damage caused to the host (Chapter 4).

Objective 2: Test whether basic virulence theory applies to *B. burgdorferi*, which predicts that across strains there should be positive relationships among these three canonical life history traits.

Objective 3: Test whether our strain-specific estimates of lifetime fitness are predictive of the frequencies of these strains in the field.

With the discovery of a sex-specific effect on *B. burgdorferi* infection, an additional objective apart from pathogen evolutionary theory is to investigate the effect of host sex on the three canonical life pathogen life history traits.

2 *Borrelia burgdorferi* strain and host sex influence pathogen prevalence and abundance in the tissues of a laboratory rodent host

Zinck, C. B., Thampy, P. R., Rego, R. O. M., Brisson, D., Ogden, N. H., & Voordouw, M. (2022). *Borrelia burgdorferi* strain and host sex influence pathogen prevalence and abundance in the tissues of a laboratory rodent host. Molecular Ecology. https://doi.org/10.1111/mec.16694

Authors' contributions
MJV, CZ, DB, and NO designed the study. ROMR performed the plasmid content analysis on the strains of *B. burgdorferi*. CZ and PRT executed the study. CZ performed all the molecular work. CZ conducted all the statistical analyses of the data. CZ and MJV wrote the manuscript. All authors read and approved the final version of the manuscript.

This work has been reformatted from its final published version to conform to document standards. In addition, Table 2.2 was added to this version where it was only present in the supplementary materials (Table S28) in the final published version. No other alterations have been made.

Acknowledgements
The authors would like to thank Dr. Susan Detmer and Dr. Pini Zvionow for their assistance in necropsy and tissue collection. We would like to thank Georgia Hurry, Alexandra Foley-Eby, and the staff of the WCVM animal care unit for their assistance with the experimental infection study. We would like to thank Dr. Robbin Lindsay and Antonia DiBernardo for kindly providing us with the strains of *B. burgdorferi* that were used in this study, and for their advice on how to culture these strains. We would like to thank Helena Rohackova for technical assistance in determining the plasmid content of the *B. burgdorferi* strains.

2.1 Transition Statement

To determine the relationships among the life history traits of *B. burgdorferi*, independent analyses of the life history traits must be done. This chapter focuses on pathogen abundance in the host tissues, one of the three canonical life history traits of evolutionary virulence theory. Here we describe in detail the model host choice, experimental design, and validation of our *B. burgdorferi* detection methods. We investigated whether *B. burgdorferi* strains differ in their tissue tropism (i.e., some strains prefer certain host tissues) and whether host sex influenced the presence and abundance of *B. burgdorferi* in the host tissues. The mouse tissue spirochete loads presented in this chapter lay the foundation for investigating relationships among pathogen life history traits and determining whether our estimates are meaningful to the natural system.

2.2 Abstract

Experimental infections with different pathogen strains give insight into pathogen life history traits. The purpose of our study was to compare variation in tissue infection prevalence and spirochete abundance among strains of *B. burgdorferi* in a rodent host (*Mus musculus*, C3H/HeJ). Male and female mice were experimentally infected via tick bite with one of 12 strains. Ear tissue biopsies were taken at days 29, 59, and 89 post-infection (PI), and 7 tissues were collected at necropsy. The presence and abundance of spirochetes in the mouse tissues were measured by qPCR. To determine the frequencies of our strains in nature, their MLSTs were matched to published datasets.

For the infected mice, 56.6% of the tissues were infected with *B. burgdorferi*. The mean spirochete load in the mouse necropsy tissues varied 4.8-fold between the strains with the lowest and highest values. The mean spirochete load in the ear tissue biopsies decreased rapidly over time for some strains. The percentage of infected tissues in male mice (65.4%) was significantly higher compared to female mice (50.5%). The mean spirochete load in the 7 tissues was 1.5x higher in male mice compared to female mice; this male bias was 15.3x higher in the ventral skin. Across the 11 strains, the mean spirochete loads in the infected mouse tissues were positively correlated with the strain-specific frequencies in their tick vector populations. Our study suggests that laboratory-based estimates of pathogen abundance in host tissues can predict the strain composition of this important tick-borne pathogen in nature.

2.3 Introduction

Many pathogen species are comprised of multiple genetically distinct strains. Pathogen strains often differ in fundamental life history traits such as abundance in host tissues, host immune response stimulation, virulence, and transmission (Balmer & Tanner, 2011; Cobey, 2014; De Roode et al., 2008; Forbes et al., 2008). Evolutionary theory suggests that there are trade-offs between pathogen transmission and virulence (Acevedo et al., 2019; Anderson & May, 1982), which are often mediated by pathogen abundance in host tissues (De Roode et al., 2008; Massad, 1987). Pathogen strains with higher abundance in host tissues have a higher probability of transmission, but they also consume more host resources resulting in higher virulence compared to strains with lower abundance in host tissues (Schmid-Hempel, 2021). Thus, to fully understand the variation in pathogen life history traits, it is crucial to study the strain-specific variation in pathogen abundance within host tissues.

Pathogen life history traits are also impacted by host factors, such as host sex. In vertebrate hosts, females tend to have a stronger immune response than males (Klein & Flanagan, 2016), and the underlying mechanism is the greater abundance of immunosuppressive androgens (e.g., testosterone) in males (Hughes & Randolph, 2001; Klein, 2004; Trigunaite et al., 2015). These sex-specific differences in immunocompetence predict that pathogens will have higher abundance in the tissues of male hosts compared to female hosts.

Lyme borreliosis (LB) is the most common vector-borne disease in Europe and North America (Steere et al., 2016). This disease is caused by spirochete bacteria belonging to the *Borrelia burgdorferi* sensu lato (sl) complex, which includes more than 20 genospecies (Margos et al., 2011; Stanek & Reiter, 2011). The three genospecies responsible for most of the disease burden are *B. afzelii* and *B. garinii* in Europe, and *B. burgdorferi* sensu stricto (hereafter *B.*

burgdorferi) in North America. These *Borrelia* genospecies are transmitted among vertebrate reservoir hosts (e.g., rodents and birds) primarily by the immature stages (larvae and nymphs) of Ixodid ticks (Kurtenbach et al., 2006; Piesman & Gern, 2004). The most important tick vectors in eastern North America and western Europe are *Ixodes scapularis* and *I. ricinus*, respectively.

In nature, populations of each *B. burgdorferi* sl genospecies consist of multiple strains (Brisson & Dykhuizen, 2004; Durand et al., 2017; Margos et al., 2012; Ogden et al., 2015; Ogden et al., 2011; Råberg et al., 2017; Wang et al., 1999). Previous studies have shown that strains of the same genospecies (e.g., *B. burgdorferi* and *B. afzelii*) differ in their spirochete abundance in host tissues (Baum et al., 2012; Genné et al., 2021; Jacquet et al., 2015; Wang et al., 2002; Wang et al., 2001) and in their transmission from infected hosts to immature ticks (hereafter host-to-tick transmission) (Brisson & Dykhuizen, 2004; Derdáková et al., 2004; Genné et al., 2018; Genné et al., 2019; Jacquet et al., 2016; Rynkiewicz et al., 2017; Tonetti et al., 2015). Other studies have found that infection phenotypes from experimental studies, such as spirochete abundance in host tissues and host-to-tick transmission success, are predictive of the strain frequencies observed in nature (Baum et al., 2012; Durand et al., 2017). Thus, investigating the phenotypes of these strains in a controlled laboratory setting may help us understand which strains are dominant in areas where LB is endemic and which strains will spread in areas where LB is emerging.

B. burgdorferi sl genospecies have a wide tissue tropism and invade a variety of organs including the skin, joints, bladder, and heart (Belli et al., 2017; Wooten & Weis, 2001; Zhong et al., 2019). Studies on *B. afzelii* and *I. ricinus* suggest that the skin is the critical source for the host-to-tick transmission of this pathogen (Genné et al., 2021; Jacquet et al., 2015; Råberg, 2012). Studies on *B. burgdorferi* have suggested that colonization of internal organs with a large

proportion of connective tissue (e.g., joints) represents an immune evasion strategy that facilitates persistent infections (Embers et al., 2004; Liang, Brown, et al., 2004; Lin et al., 2020). Importantly, *B. burgdorferi* sl genospecies do not persist in the host blood stream, although they do use the blood to disseminate from the tick bite site to organs and tissues (Hyde, 2017; Shih et al., 1992; Wang et al., 2001). Tissue tropism can vary among strains (Baum et al., 2012; Brisson et al., 2011), and may influence strain-specific fitness in nature.

This manuscript is part of a larger study that investigated strain-specific variation in important pathogen life history traits including pathogen tissue abundance, virulence, and host-to-tick transmission. Male and female *Mus musculus* mice were experimentally infected via nymphal tick bite with 12 different strains of *B. burgdorferi*. Here we explore differences in tissue tropism and tissue spirochete burden. We predict that strains will differ in their prevalence and abundance in the necropsy tissues of the rodent host (i.e., strain-specific tissue tropism). Given possible impacts of testosterone on immunity in adult male mice (e.g., Hughes & Randolph, 2001), we predict that the percentage of infected tissues and the tissue spirochete abundance will be higher in male mice compared to female mice. Finally, we predict that strains that establish a higher prevalence and/or abundance in mouse tissues will have higher frequency in nature.

2.4 Materials & Methods

2.4.1 *B. burgdorferi*, *I. scapularis* ticks, and C3H/HeJ mice

Twelve low passage strains of *B. burgdorferi* used in this study came from the isolate collection of the Public Health Agency of Canada (PHAC). The isolates were obtained from *I. scapularis* ticks collected during field surveillance in Canada and were cultured on semi-solid

agar to obtain single strain colonies. These clones were sequenced using whole genome sequencing (Tyler et al., 2018) and are hereafter referred to as strains. The 12 strains were selected based on their MLST type, *ospC* type, and region of origin (Midwestern Canada; n = 7, Eastern Canada; n = 5) (Table 2.1). These two regions were included because previous work has shown substantial differences in strain diversity between Midwestern Canada and Eastern Canada (Margos et al., 2012; Mechai et al., 2015; Ogden et al., 2011). Priority was given to maximizing the MLST diversity of the strains and representing the two regions equally. In addition, *B. burgdorferi* contains numerous linear and circular plasmids that contain the critical virulence factors that allow this tick-borne pathogen to complete its lifecycle (Casjens et al., 2017; Casjens et al., 2012; Grimm et al., 2005; Stewart et al., 2005). Each strain was therefore tested for the presence of plasmids necessary to complete a natural life cycle (see Appendix A Section 1). All *B. burgdorferi* strains contained the plasmids necessary for establishing a persistent infection in the rodent host (see Appendix A Section 1).

Laboratory reared specific pathogen-free *I. scapularis* larvae were obtained from the National Tick Research and Education Resource at Oklahoma State University. This colony is regularly outbred with wild *I. scapularis* to prevent inbreeding and screened for multiple tick-borne pathogens including *B. burgdorferi*.

Specific pathogen-free *Mus musculus* C3H/HeJ mice purchased from The Jackson Laboratory were used as the reservoir host in this study. This mouse strain was selected for its well-documented manifestations of arthritis and cardiac abnormalities following *B. burgdorferi* infection, which are useful measures of the capacity of strains to cause pathology (Barthold et al., 1990; Wang et al., 2002; Wang et al., 2001; Yang et al., 1994). This mouse strain has also been used in previous studies comparing infection phenotypes of different *B. burgdorferi* strains

(Dolan et al., 2004; Wang et al., 2002; Wang et al., 2001). The use of mice and all procedures in this study were reviewed and approved by the Animal Research Ethics Board at the University of Saskatchewan (permit number 20190012).

2.4.2 Creation of I. scapularis nymphs infected with each of the 12 strains

The *I. scapularis* nymphs infected with one of the 12 strains were created as follows. All strains were cultured in BSK-H media at 37 ºC for 9-14 days growth. Mice (C3H/HeJ, n = 2-4) were needle-inoculated with a single strain ($10^4 – 10^5$ spirochetes) and infested with naïve *I. scapularis* larvae at 2-4 weeks post-infection (PI). Larvae were maintained in humidity chambers and allowed to moult into nymphs. A random subset of 10 nymphs per mouse were tested for their *B. burgdorferi* infection status using qPCR. All strains were present in 80-100% of nymphs tested. Uninfected control nymphs were generated by feeding naïve *I. scapularis* larvae on uninfected C3H/HeJ mice. These nymphs were used for the nymphal infestations to infect the mice with the *B. burgdorferi* strains (see below). To minimize plasmid loss during culture, the *B. burgdorferi* strains had undergone only 4 passages from the time of isolation from field-collected *I. scapularis* ticks to needle inoculation into our mice.

2.4.3 Experimental infection of mice with strains of *B. burgdorferi* via tick bite

Previous studies have shown that the mode of infection, tick bite versus needle inoculation, can influence the infection phenotype (Gern et al., 1993; Roehrig et al., 1992; Sertour et al., 2018). For this reason, all the mice used in this study were infected via the bite of an infected nymph to reproduce a natural infection rather than a needle inoculation. A total of 120 specific-pathogen-free C3H/HeJ mice (60 male, 60 female) aged 6-8 weeks were used in this

study. For all 12 strains, 8 mice (4 male, 4 female) were used for a total of 96 mice in the infected group, with an additional 24 (12 male, 12 female) uninfected control mice. To manage the workload, the experiment was run in two orthogonal temporal blocks (A and B; separated by ~6 months; each block contained 48 infected mice and 12 uninfected control mice). At 6-8 weeks, experimental mice were infested with 3 *I. scapularis* nymphs putatively infected with the strain of interest (see Appendix A Section 2), whereas control mice were infested with 3 uninfected nymphs. To confirm the infectious challenge for each mouse, engorged nymphs were recovered and tested for infection using qPCR targeting the *23s rRNA* gene of *B. burgdorferi* (see below and Appendix A Section 2).

Another objective of this study was to compare transmission of the 12 *B. burgdorferi* strains from infected mice to *I. scapularis* ticks over the first 90 days of the infection. For this reason, mice were infested with 50-100 naïve *I. scapularis* larval ticks at days 30, 60, and 90 post-infection (PI). The host-to-tick transmission data of the 12 different *B. burgdorferi* strains will not be discussed in this manuscript. However, it is important to mention this aspect of the experimental design for two reasons. First, it explains why our sample collections were chosen. Second, we unexpectedly discovered that the infestations with *I. scapularis* larvae reduced the presence and abundance of *B. burgdorferi* in the mouse tissues (see Results and Discussion), which is relevant to the main objective of the present study.

Ear tissue biopsies were taken from each mouse prior to their experimental infection (-2 to -1 weeks PI), and before each larval infestation (days 29, 59, and 89 PI). Mice were anaesthetized by isoflurane prior to collection of a 2 mm ear tissue biopsy by punch. The pre-infection tissue biopsy was taken from the left ear, and the 3 post-infection tissue biopsies were taken from the right ear. Blood samples were taken from each mouse at pre-infection (-2 to -1

weeks PI), day 28 PI, and at euthanasia (day 97 PI). Pre-euthanasia blood samples were taken by submandibular bleeding with Goldenrod lancets (Golde et al., 2005) and 10-50 µL of blood were collected. At day 97 PI, all mice were euthanized by isoflurane overdose followed by cervical dislocation, cardiac puncture, and exsanguination.

2.4.4 Necropsy and tissue sample collection

Mice were necropsied immediately following euthanasia, and seven organs/tissues were collected including the kidney, left ear, right ear, ventral skin (from belly of mouse), right rear tibiotarsal joint, heart, and bladder. Each mouse was processed with sterile equipment disinfected with Virkon between uses. Tissues were kept at 4 ºC before being trimmed and weighed to the nearest 0.1 mg within 24 hours of their collection. Final samples were held at -80 ºC prior to DNA extraction.

2.4.5 Homogenization and DNA extraction of tissue samples

Necropsy and ear biopsy samples were homogenized by micropestle or by 3.6 mm stainless steel beads with the Qiagen TissueLyser II. For all organs, extractions were done on partial samples, hereafter also referred to as tissue. DNA was extracted from homogenized tissue samples using the Qiagen DNEasy Blood and Tissue kit individual spin columns following the manufacturer's instructions (see Appendix A Section 2).

2.4.6 qPCR to measure the abundance of *B. burgdorferi* in mouse organs

To test for the presence and quantity of *B. burgdorferi*, a probe and primer assay targeting the *23S rRNA* intergenic spacer gene was used as described previously (Courtney et al.,

2004; see Appendix A Section 2). Quantification cycle (Cq) values were transformed using a synthetic gene standard (IDTDNA, gBlock; see Appendix A Section 3). The repeatability of the sample Cq for the *23S rRNA* intergenic spacer gene was 85.3% and was based on 70 necropsy samples.

A second qPCR was performed on each sample to quantify the *M. musculus* housekeeping gene *Beta-actin* using a previously described protocol (Dai et al., 2009; see Appendix A Section 2). Quantification cycle (Cq) values were transformed using a synthetic gene standard (IDTDNA, gBlock; see Appendix A Section 3). The repeatability of the sample (Cq) for the mouse *Beta-actin* gene was 85.8% and was based on 70 necropsy samples.

2.4.7 Statistical Methods

We analyzed 4 infection phenotypes: (1) prevalence of *B. burgdorferi* in the ear biopsies over the course of the infection, (2) abundance of *B. burgdorferi* in the subset of infected ear biopsies over the course of the infection, (3) prevalence of *B. burgdorferi* in the tissues at euthanasia, and (4) abundance of *B. burgdorferi* in the subset of infected tissues at euthanasia.

2.4.8 Analysis of presence of *B. burgdorferi* in ear tissues and necropsy tissues

For all tissues, the presence of *B. burgdorferi* infection was a binomial variable (0 = absent = uninfected, 1 = present = infected). These response variables were analysed by generalized linear mixed effect models (GLMMs) with binomial errors. For the analysis of *B. burgdorferi* infection presence in the ear tissues over time, the fixed factors included ear punch (4 levels: days 29, 59, 89, and 97 PI), strain (11 levels; see Table 2.1), sex (2 levels: female, male), and their interactions. Temporal block (2 levels: A, B) was included but not in the

interaction terms. The right ear necropsy sample from day 97 PI was included in this analysis because all post-infection biopsies were from the right ear. For the analysis of *B. burgdorferi* infection presence in the tissues at euthanasia, the fixed factors included tissue (7 levels: kidney, left ear, right ear, ventral skin, tibiotarsal joint, heart, and bladder), strain, sex, their interactions, and temporal block. Mouse identity was included as a random factor in both analyses. Both analyses were restricted to samples from the subset of 84 mice that became infected following the infectious nymphal challenge (see below). Non-significant interaction terms were sequentially removed to generate the final models. Factor significance was estimated using type II Wald tests, post-hoc analyses were performed and estimated marginal means were calculated.

2.4.9 Analysis of abundance of *B. burgdorferi* in ear tissues and necropsy tissues

For the subset of infected tissue samples, we standardized the abundance of *B. burgdorferi* (measured as the number of *B. burgdorferi 23S rRNA* copies) relative to three estimates of the amount of mouse tissue: (1) mass of tissue used in the DNA extraction, (2) DNA concentration of the resultant DNA extraction, and (3) number of mouse *Beta-actin* gene copies. We found that all three of these methods of standardizing the tissue spirochete load were highly correlated with each other and that method 3 yielded the best quality results (see Appendix A Section 4). For this reason, we present the abundance of *B. burgdorferi* (also referred to as spirochete load) as the log10-transformed ratio of the number of *B. burgdorferi 23S rRNA* copies per one million mouse *Beta-actin* copies.

Analyses of the spirochete loads were run on the subset of infected tissues using linear mixed effect models (LMMs). For the analysis of spirochete loads in the ear biopsies over time, the fixed factors included ear punch, strain, sex, their interactions, and temporal block. For the

analysis of spirochete loads in the necropsy tissues, the fixed factors included tissue, strain, sex, their interactions, and temporal block. Mouse identity was included as a random factor in both analyses. Like the analyses on *B. burgdorferi* infection presence, non-significant interactions were sequentially removed to generate the final simplified models. Post-hoc analyses were done in the same manner as for the analysis of the tissue infection presence.

2.4.10 Effect of region on the 4 infection phenotypes

For each of the 4 infection phenotypes, a separate model was run to analyse the effect of region (Midwestern Canada versus Eastern Canada). As the strains are nested within region, region and strain could not both be included as fixed factors and the strain was therefore included in the random effects for these analyses.

2.4.11 Correlation analyses

We performed a correlation analysis across the set of 11 strains of *B. burgdorferi* to determine whether there were correlations among the 4 measures of infection: (1) infection presence in third ear biopsy, (2) spirochete abundance in third ear biopsy, (3) infection presence in the 7 necropsy tissues, (4) spirochete abundance in the 7 necropsy tissues. The estimated marginal means of these 4 infection phenotypes were calculated for each of the 11 *B. burgdorferi* strains and the pairwise correlations were tested using Pearson's correlation test. As mouse sex had a significant effect on the 4 infection phenotypes, we repeated the previous analysis for the 22 combinations of mouse sex and strain. For the sample of infected mice (n = 84), a separate correlation analyses were done to determine whether the presence of infection or spirochete loads were correlated among the 7 necropsy tissues.

2.4.12 Estimates of the frequencies of *B. burgdorferi* strains in nature

To determine whether our laboratory estimates of the strain-specific spirochete infection prevalence and/or abundance in the mouse tissues predict the frequencies of these *B. burgdorferi* strains in nature, we used the PubMLST database and the published literature to estimate the latter. The PubMLST database for *B. burgdorferi* sensu lato contains almost 2,500 MLST profiles that include samples from wildlife, ticks, and patients (Jolley et al., 2018). We used two published studies that investigated the frequencies of *B. burgdorferi* MLSTs in questing *I. scapularis* ticks in the USA (n = 741) and Canada (n = 153) (Ogden et al., 2011; Travinsky et al., 2010). For each of our strains, we determined the number of times its MLST occurred in the database. These counts were converted to frequencies by dividing them by the total count for the MLSTs in our set of strains (see Appendix A Section 5). We used generalized linear models (GLMs) with binomial errors to test the relationship between these 2 estimates of the strain-specific frequency in nature (response variable) and 3 different estimates of strain-specific abundance in the mouse tissues (explanatory variables): (1) proportion of infected mouse tissues, (2) mean spirochete load in subset of infected mouse tissues, and (3) mean spirochete load in all mouse tissues (see Appendix A Section 5).

2.4.13 Statistical software:

We used R version 4.0.4 for all statistical analyses (Team, 2021). The list of R packages and R functions we used are given in Appendix A (See Appendix A Section 2).

2.5 Results

2.5.1 *Borrelia burgdorferi* infection status of the mice

One of the 12 strains (strain 111) failed to establish infection in the 4 mice in block A, and therefore this strain was not included in block B, resulting in a total of 92 mice in the infected group. Of the 24 mice in the uninfected control group, 20 completed the study (9 in block A, 11 in block B). For a mouse to be considered infected, it had to meet one of three criteria: (1) an IgG antibody response significantly greater than the negative control mice (See Appendix A Section 6), (2) detection of *B. burgdorferi* in an ear tissue biopsy, or (3) detection of *B. burgdorferi* in a necropsy tissue sample. As expected, all 20 mice in the uninfected control group met 0 of our 3 infection criteria. Of the 92 mice in the infected group, 84 mice met 3 of our 3 infection criteria and were considered infected with *B. burgdorferi*, whereas 8 mice met 0 of our 3 infection criteria and were considered uninfected. Of the 8 mice that remained uninfected after the nymphal challenge, 2 mice (challenged with strain 174) had no engorged infected nymphs recovered, and 6 mice (1, 1, and 4 challenged with strain 174, strain 66, and strain 111, respectively) were uninfected despite recovery of engorged infected nymphs. These 8 mice were excluded from subsequent analyses because this study is focused on the differences between infected mice.

Each of the 84 infected mice were challenged with at least one infected nymph (range = 1 to 3, mean = 2.3). There was no significant difference in the number of engorged infected nymphs recovered between strains ($p = 0.712$; see Appendix A Section 7). The number of infected nymphs was not a significant covariate for the presence or abundance of *B. burgdorferi* in the necropsy tissues (see Appendix A Section 7). These results suggest that the infectious challenge via nymphal tick bite was similar among the 11 strains of *B. burgdorferi*.

Table 2.1 The genetic identity and location of origin are shown for the 12 strains of *B. burgdorferi* used in the study. Strain identity numbers are from the reference publication (Tyler et al., 2018). All successfully infected mice (n = 84) had direct detection of *B. burgdorferi* in their ear biopsies and necropsy tissues by qPCR and a strong serum IgG antibody response. The mice that failed to become infected (n = 8) had no detection of *B. burgdorferi* in any of their ear biopsies and necropsy tissues and no detectable serum IgG antibody response.

Strain ID	MLST	*ospC* type	Region	Town (Province)	Infected mice
111	29	A	West	Buffalo Point (MB)	0/4
57	29	Y	West	Buffalo Point (MB)	8/8
174	37	D	East	Lunenburg (NS)	5/8
167	12	C	East	Shelburne (NS)	8/8
178*	3	K	East	Lunenburg (NS)	8/8
198	3	K	East	Bedford (NS)	8/8
22.2	55	A	West	Buffalo Point (MB)	8/8
150	19	E, E1	East	Lunenburg (NS)	8/8
10.2	32	H	West	Roseau River (MB)	8/8
66	237	J	West	Buffalo Point (MB)	7/8
54	741	I	West	Buffalo Point (MB)	8/8
126	43	N, N*	West	Big Grassy (ON)	8/8
Total					84/92
Uninfected**	NA	NA	NA	NA	0/20

*This strain was originally intended to be 178-2 but is 178-1 (Tyler et al., 2018), thus we have two isolates of the same strain in this study (MLST 3, *ospC* K). We refer to this strain as 178 in this study.
** Uninfected control mice were fed upon by uninfected *I. scapularis* nymphs. As expected, these 20 mice all tested negative for the 3 *B. burgdorferi* infection criteria.

2.5.2 Presence of *B. burgdorferi* in the ear tissue biopsies

Ear tissue biopsies were taken prior to the nymphal infestation (pre-infection), prior to each larval infestation (days 29, 59, 89 PI), and a final necropsy sample was taken at euthanasia (day 97 PI). For the subset of the 84 infected mice, the mean prevalence of *B. burgdorferi* infection at pre-infection, days 29, 59, 89, and 97 PI were 0.0% (0/84), 98.9% (83/84), 100.0% (84/84), 91.7% (77/84), and 14.3% (12/84). Only 6 of 11 strains were detected in the terminal ear tissue samples from day 97 PI. For the subset of the 28 uninfected mice (20 uninfected control

mice plus 8 mice with failed infections), all 112 ear tissue biopsies tested negative for *B. burgdorferi*.

The infection presence of *B. burgdorferi* in the post-infection right ear tissue samples was analyzed with a GLMM with the fixed factors of strain, sex, punch (days 29, 59, 89, and 97 PI), and temporal block. There were no significant interactions among the fixed factors, and temporal block was not significant (See Appendix A Section 8). Strain ($p = 0.004$), sex ($p = 0.019$) and punch ($p = 3.004*10^{-10}$) were significant. In general, the presence of *B. burgdorferi* in the right ear at euthanasia (day 97 PI) was significantly lower compared to the three right ear biopsies (days 29, 59, and 89 PI), and males had a higher infection presence in the right ear compared to females.

2.5.3 Abundance of *B. burgdorferi* in the ear tissue biopsies

The abundance of *B. burgdorferi* in the right ear biopsies was expressed as the log10-transformed ratio of the number of *B. burgdorferi 23S rRNA* copies per million mouse *Beta-actin* copies. For the subset of infected ear biopsies ($n = 256$), an LMM was used to test the tissue spirochete load. Strain ($p = 0.004$), sex ($p = 0.027$), punch ($p = 2.2*10^{-16}$), and the interactions between strain and punch ($p = 3.467*10^{-8}$), and between sex and punch ($p = 0.017$) were significant. The other interactions, and temporal block were not significant (See Appendix A Section 8). For the 6 strains that had positive terminal right ear samples at day 97 PI, the spirochete load was significantly lower compared to the ear biopsies on days 29, 59, and 89 PI (Figure 2.1). After excluding the terminal ear sample on day 97 PI, we found that the spirochete loads did not differ between the three ear biopsies (days 29, 59, and 89 PI) for most strains (Figure 2.1). The exceptions were strains 66, 57, and 54, which had significantly higher

spirochete loads on day 29 PI compared to days 59 and 89 PI (Figure 2.1). Strain 66 had the greatest decrease in spirochete load with the ear biopsy at day 59 PI having 0.03x the number of spirochetes as the ear biopsy at day 29 PI (day 29 PI ear biopsy: mean = 13,182.6 *23S rRNA*/10^6 *Beta-actin*; day 59 PI ear biopsy: mean = 389.0 *23S rRNA*/10^6 *Beta-actin*; $p < 0.001$).

Separate linear models were run for each of the 3 ear biopsies to remove the interaction terms (see vSection 8). The terminal ear tissue sample on day 97 PI was excluded because there were so few infected samples (12/84). Strain had a significant effect on ear tissue spirochete load for each of the 3 ear biopsies (day 29 PI: $p = 2.547*10^{-5}$; day 59 PI: $p = 0.002$; day 89 PI: $p = 0.029$). Sex had a significant effect on ear tissue spirochete load on day 59 PI ($p = 2.280*10^{-4}$) and day 89 PI ($p = 0.030$), but not on day 29 PI ($p = 0.408$; see Appendix A Section 8). At 59 days PI and 89 days PI, male mice had 1.95x and 1.48x more *23S rRNA*/10^6 *Beta-actin* compared to female mice, respectively.

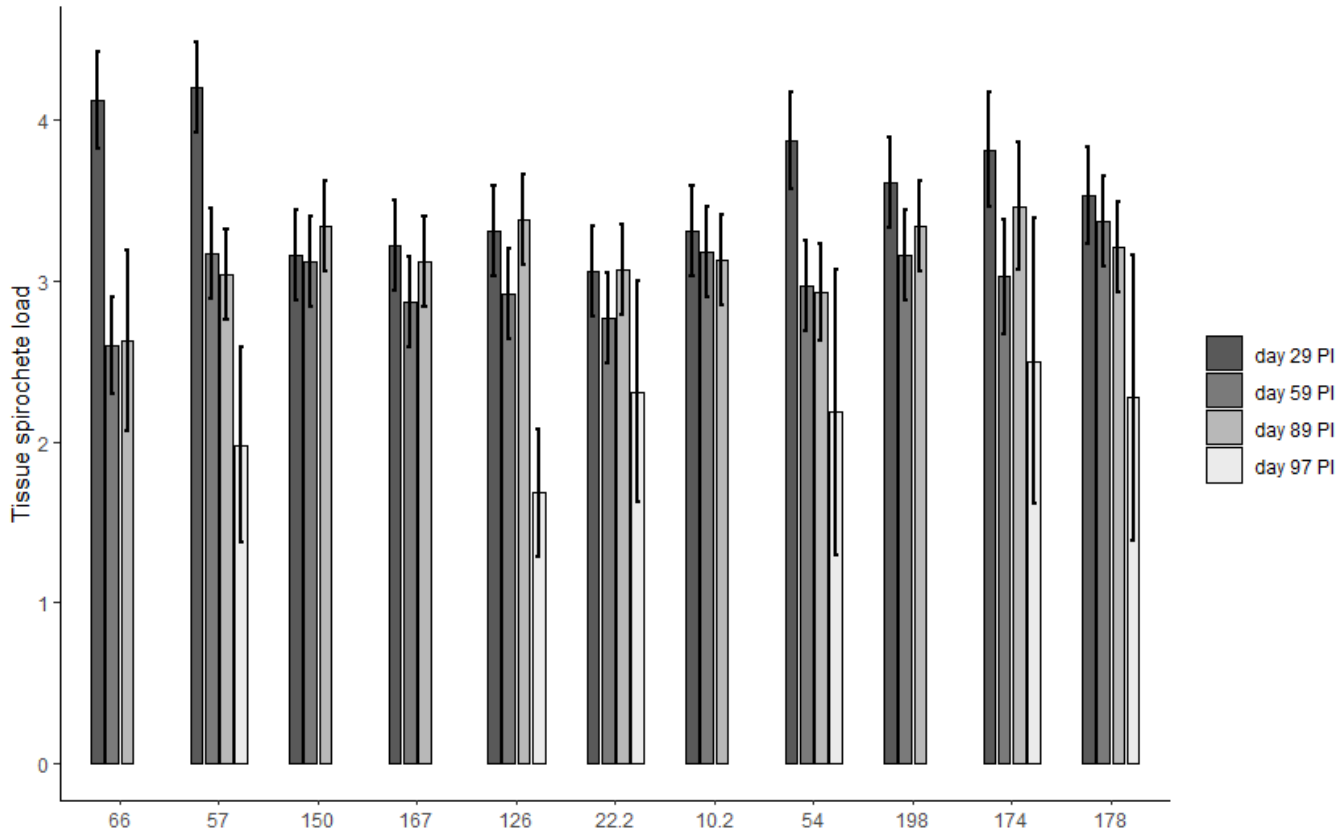

Figure 2.1 The spirochete load in the right ear tissue samples over the course of the infection separated by strain. The spirochete loads were calculated as the log10-transformed ratio of the number of *B. burgdorferi 23S rRNA* copies/10^6 mouse *Beta-actin* copies. The right ear was sampled on days 29, 59, 89, and 97 post-infection (PI). The spirochete loads are estimated marginal means (EMMs) based on a total of 256 infected ear samples from the 84 infected mice. Only 6 of 11 strains had positive ear samples at day 97 PI (euthanasia). The spirochete loads in right ear tissue biopsies (days 29, 59, and 89 PI) were generally consistent for most strains except for strains 66, 57, and 54, which showed significant decreases.

2.5.4 Presence of *B. burgdorferi* in the mouse necropsy tissues

For the subset of infected mice (n = 84), the mean number of infected necropsy tissues was 3.96 (range = 2–7 infected necropsy tissues). Infection presence of necropsy tissues was analysed in the same manner as the infection presence of the ear biopsies. The main effects of strain ($p = 0.004$), sex ($p = 0.008$), tissue ($p = 2.2*10^{-16}$), and temporal block ($p = 0.013$) were

significant, and the interactions between strain and sex ($p = 0.033$), and between sex and tissue ($p = 7.442*10^{-9}$) were significant. The effect sizes are given below.

The prevalence of *B. burgdorferi* infection differed among the 7 necropsy tissues (Figure 2.2A): kidney (29.8% = 25/84), left ear (38.1% = 32/84), right ear (14.3% = 12/84), ventral skin (52.4% = 44/84), tibiotarsal joint (71.4% = 60/84), heart (92.9% = 78/84), and bladder (97.6% = 82/84). Mice infected with strain 66 had the lowest number of infected tissues (2.88/7) and mice infected with strain 126 had the highest number of infected tissues (5.50/7; Figure 2.3A). In general, *B. burgdorferi* was detected in more tissues in male mice (65.4% = 197/301) compared to female mice (50.5% = 145/287; Figures 2.2A and 2.3A). Males had a significantly higher infection prevalence than females in their joints (90.7% versus 51.2%), ventral skin (93.0% versus 9.8%), and right ears (23.3% versus 4.9%), whereas females had a significantly higher infection prevalence than males in their kidneys (61.0% versus 20.9%; Figure 2.2A). For 10 of the 11 strains, males had a significantly higher infection prevalence than females (Figure 2.3A; strain 126 was the exception). Block B had a higher infection prevalence in the mouse tissues compared to block A (61.0% versus 52.5%).

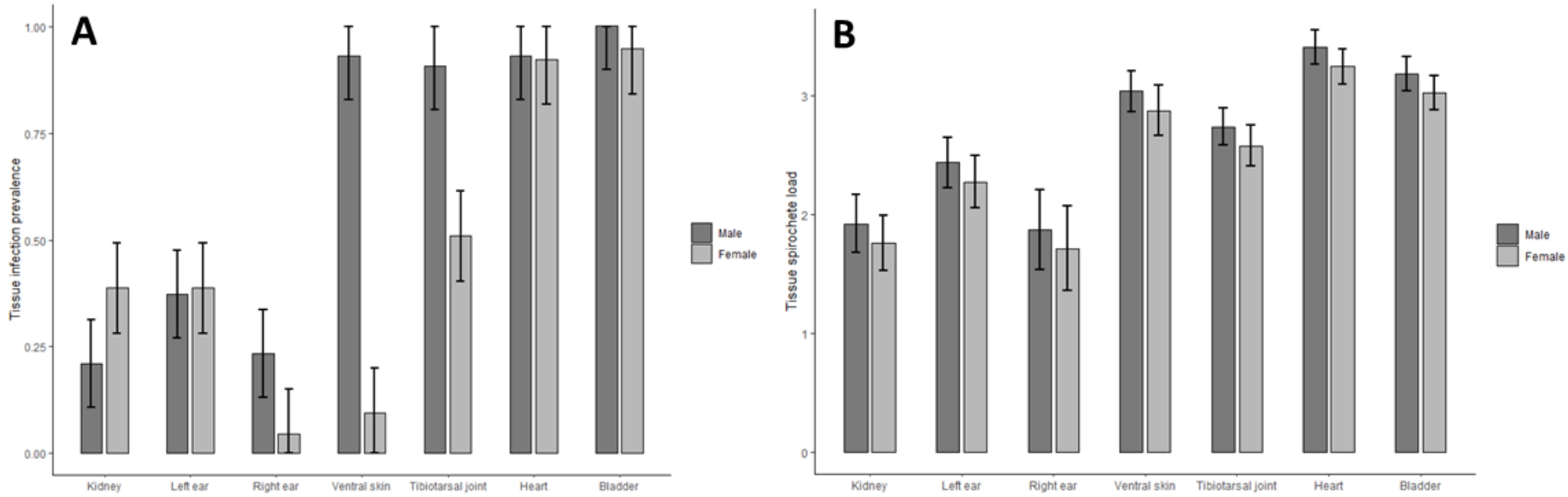

Figure 2.2 The prevalence (A) and abundance (B) of *B. burgdorferi* in the mouse necropsy tissues on day 97 PI is shown for the 7 necropsy tissues and the two sexes. The 7 mouse necropsy tissues include the kidney, left ear, right ear, ventral skin, right rear tibiotarsal joint, heart, and bladder. (A) Infection prevalence is the proportion of necropsy tissues infected with *B. burgdorferi*. The infection prevalence was higher in the internal tissues (bladder, heart, tibiotarsal joints) compared to external tissues (ventral skin, left ear, right ear). The infection prevalence of the right ear, ventral skin, and tibiotarsal joint was significantly higher in males compared to females. Each bar is based on 43 male and 41 female mice, respectively. (B) Abundance is the log10-transformed ratio of the number of *B. burgdorferi 23S rRNA* copies/10^6 mouse *Beta-actin* copies. The abundance of *B. burgdorferi* was highest in the bladder and heart and lowest in the kidney and ears. Male mice had significantly more (1.45x) spirochetes in their tissues compared to female mice. The estimated marginal means were generated from the final models from which non-significant interactions had been removed. Error bars represent the 95% confidence intervals.

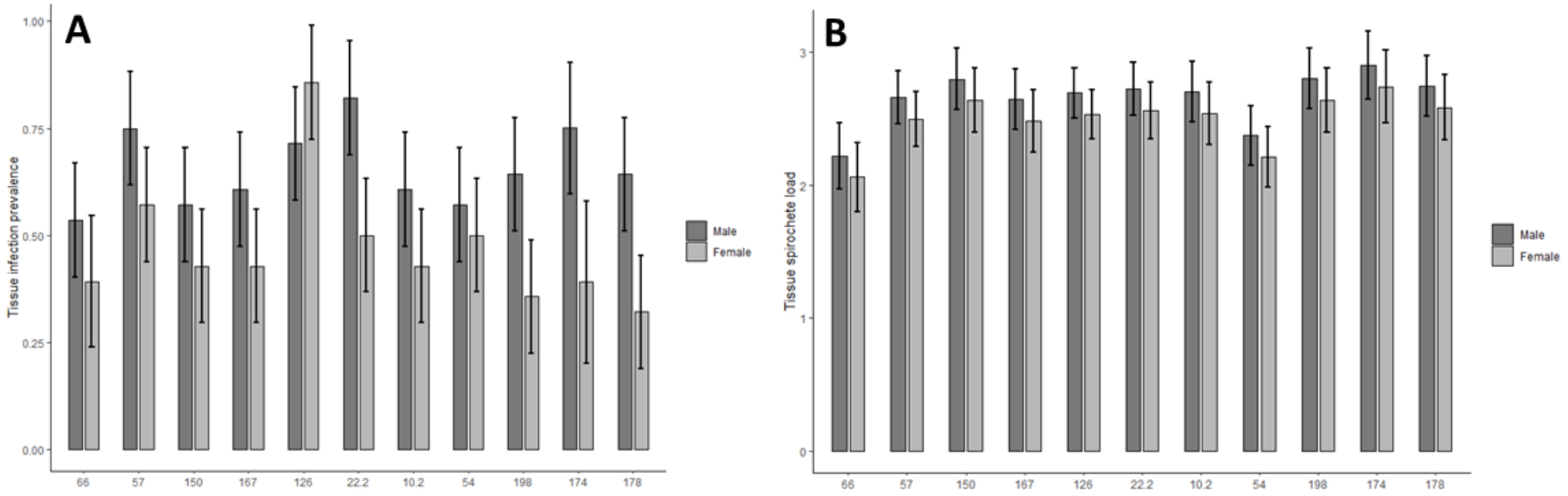

Figure 2.3 The prevalence (A) and abundance (B) of *B. burgdorferi* in the mouse necropsy tissues on day 97 PI is shown for 11 *B. burgdorferi* strains and the two sexes. The 7 mouse necropsy tissues include the kidney, left ear, right ear, ventral skin, right rear tibiotarsal joint, heart, and bladder. (A) Infection prevalence is the proportion of necropsy tissues infected with *B. burgdorferi*. The tissue infection prevalence was significantly higher in male mice compared to female mice for all strains except strain 126. (B) Abundance is the log10-transformed ratio of *B. burgdorferi 23S rRNA* copies/10^6 mouse *Beta-actin* copies. Strain 66 had the lowest tissue abundance, and strain 174 had the highest tissue abundance. Male mice had consistently higher tissue abundance than female mice for all 11 strains. The estimated marginal means were generated from the final models from which non-significant interactions had been removed. Error bars represent the 95% confidence intervals.

2.5.5 Abundance of *B. burgdorferi* in the mouse necropsy tissues

For the subset of tissues that were infected with *B. burgdorferi* (n = 333 infected necropsy tissues from 84 infected mice), the abundance of *B. burgdorferi* was analyzed. There were significant effects of strain ($p = 0.001$), sex ($p = 0.005$), and tissue ($p = 2.2*10^{-16}$) on the abundance of *B. burgdorferi* in the necropsy tissues. There were also significant interactions between strain and tissue ($p = 0.010$), and between sex and tissue ($p = 0.006$). Temporal block was not significant ($p = 0.122$). The effect sizes are given below.

Using kidney as the reference tissue, the mean spirochete load in the other 6 tissues is as follows: left ear (3.27x), right ear (0.90x), ventral skin (12.98x), tibiotarsal joint (6.55x), heart (30.36x), and bladder (18.19x) (Figure 2.2B). A main effects model was used to generate estimates of the mean spirochete load across tissues for each strain (Figure 2.3B). Strain 66 had a significantly lower spirochete load than the three isolates with the highest spirochete loads (strain 174: $p = 0.013$; strain 198: $p = 0.031$; strain 150: $p = 0.034$). All other strains had similar spirochete loads (Figure 2.3B). The mean spirochete load in the necropsy tissues for strain 174 (659.2 *23S rRNA*/10^6 *Beta-actin*) was 4.79x higher compared to strain 66 (137.5 *23S rRNA*/10^6 *Beta-actin*). In general, the mean spirochete load in the necropsy tissues was 1.45x higher in males compared to females across tissues and strains (male: 457.1 *23S rRNA*/10^6 *Beta-actin*; female: 316.2 *23S rRNA*/10^6 *Beta-actin*; $p = 0.005$; Figures 2.2B and 2.3B).

Separate linear models were run for each necropsy tissue to remove the two interactions (see Appendix A Section 9). Male mice had a spirochete load in their ventral skin that was 15.3x higher compared to female mice (male: 1266 *23S rRNA*/10^6 *Beta-actin*; female: 83 *23S rRNA*/10^6 *Beta-actin*; $p = 0.012$) and a spirochete load in their tibiotarsal joints that was 3.8x higher

compared to females (male: 604; female: 160; $p = 4.504*10^{-4}$). There were significant differences in spirochete load among strains in the heart ($p = 0.012$) and bladder ($p = 0.031$).

2.5.6 Infection phenotypes did not differ by region

There were no significant effects of region (Midwestern Canada versus eastern Canada) on the 4 infection phenotypes and the presentation of these results is restricted to the supplementary material (see Appendix A Section 10).

2.5.7 Correlations among the *B. burgdorferi* infection phenotypes in the mouse tissues

For the 142 combinations of strain, sex, and tissue, there was a strong positive correlation between the presence of *B. burgdorferi* in the necropsy tissues and the abundance of *B. burgdorferi* in the necropsy tissues ($r = 0.676$, $p = 2.2*10^{-16}$; see Appendix A Section 11). This result shows that *B. burgdorferi* strains with high abundance in the mouse tissues are more likely to be detected than strains with low abundance. For the 22 combinations of mouse sex and *B. burgdorferi* strain, there was also a strong positive correlation between the spirochete load in the necropsy tissues on day 97 PI versus the spirochete load in the third biopsy of the right ear on day 89 PI (Figure 2.4; $r = 0.923$, $p = 9.551*10^{-10}$). This result shows that the third larval infestation did not change the ranking of the strains with respect to the spirochete load in the mouse tissues.

Correlation tests were done to determine whether the infection presence or spirochete load was correlated among pairs of the seven necropsy tissues. Infection presence and spirochete load were strongly and positively correlated for many pairs of necropsy tissues and there were no negative correlations (see Appendix A Section 11). These pairwise correlations were especially

strong for the internal tissues of heart, bladder, and kidney (see Appendix A Section 11). Heart and bladder were the most strongly correlated (infection presence: $r = 0.828$, $p < 0.001$; spirochete load: $r = 0.918$, $p < 0.001$).

We used GLMs with quasibinomial errors to examine the relationship between 3 different estimates of strain-specific abundance in the mouse tissues and 2 estimates of the strain-specific frequency in nature (see Appendix A Section 5 for details). For the proportion of infected mouse tissues and for the mean spirochete load in all mouse tissues, there was no relationship with the strain-specific frequencies in nature. There was a positive relationship between the mean spirochete load in the subset of infected mouse tissues and the strain-specific frequencies in nature for the pubMLST database (see Appendix A Section 5; $p = 0.055$) and for the *I. scapularis* ticks (Figure 2.5; $p = 0.045$).

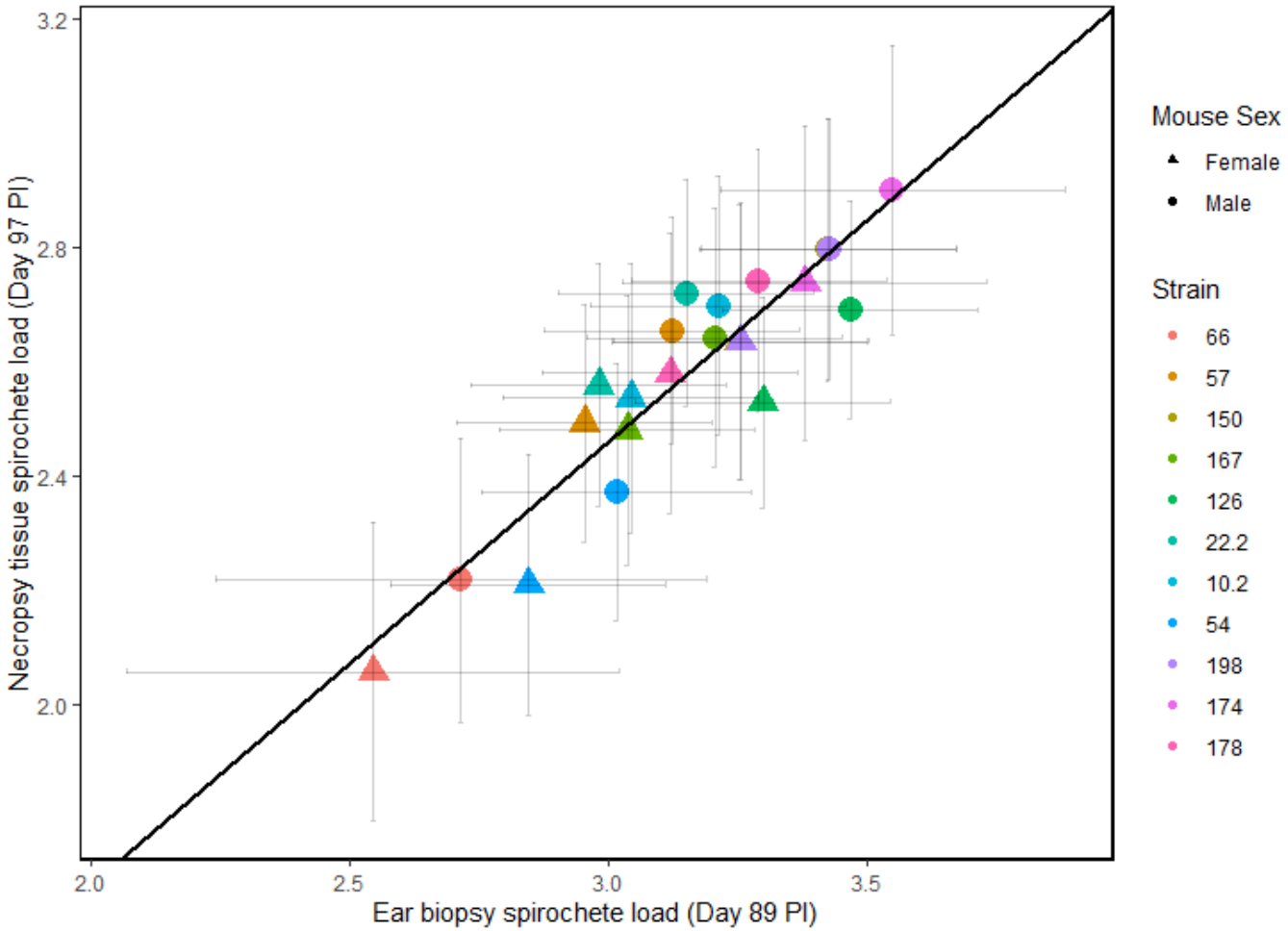

Figure 2.4 Correlation between the spirochete load in the necropsy tissues versus the spirochete load in the last right ear biopsy across the 22 combinations of *B. burgdorferi* strain and mouse sex. The necropsy tissue spirochete load is based on the 7 mouse tissues tested at necropsy (day 97 PI) using qPCR. The ear biopsy spirochete load is based on the last biopsy of the right ear (day 89 PI) using qPCR. Both values are expressed as the log10-transformed ratio of the *B. burgdorferi 23S rRNA* copies/10^6 mouse *Beta-actin* copies. The correlation between the two variables is positive and highly significant ($r = 0.923$, $p = 9.551*10^{-10}$).

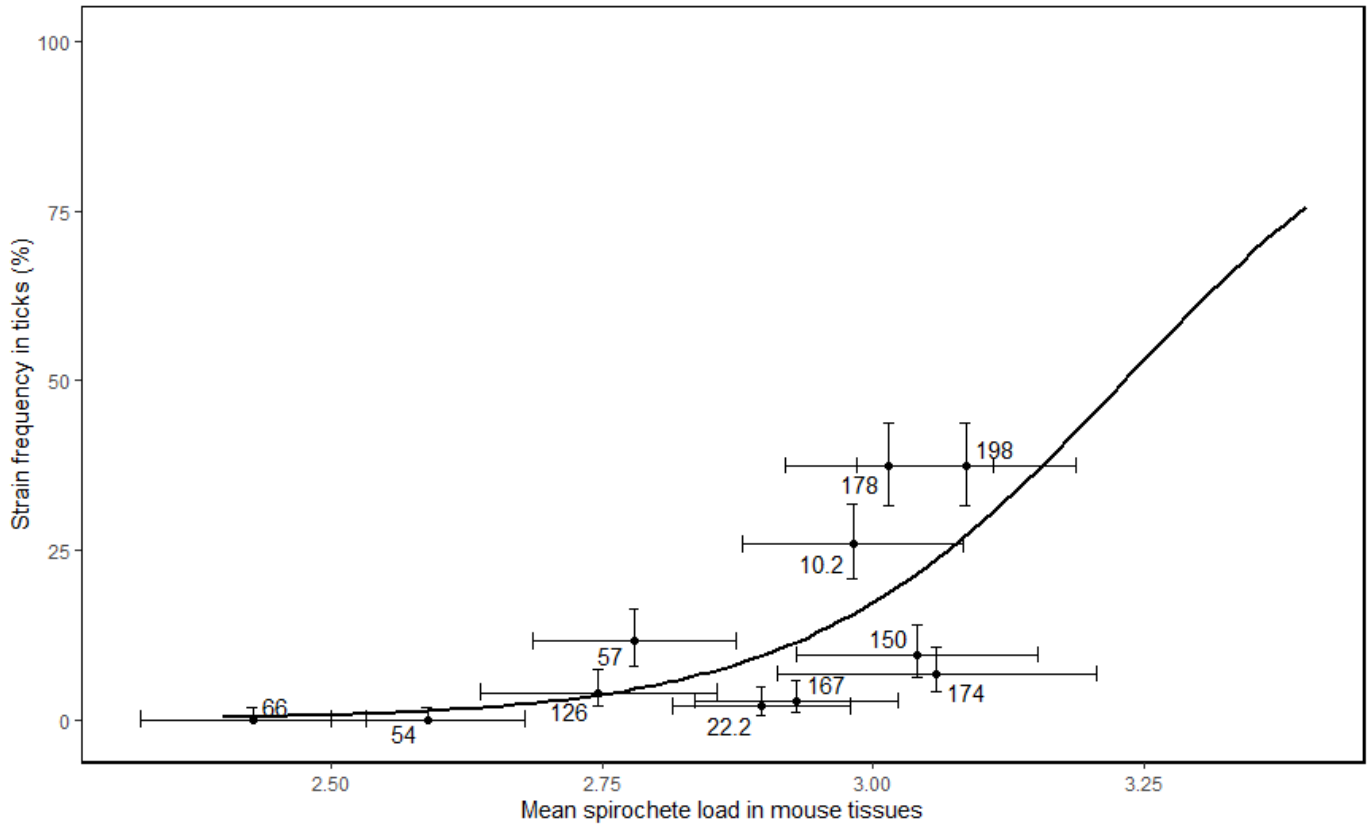

Figure 2.5 Relationship between the strain-specific estimates of the mean spirochete load in the mouse tissues and the strain-specific frequency in *I. scapularis* ticks in North America. The MLST was used to determine how many times each strain appeared in *I. scapularis* ticks based on two published studies (Ogden et al., 2011; Travinsky et al., 2010). The strain-specific frequencies were calculated by dividing the counts for each strain by the sum of the counts for all our strains (n = 251). The mean spirochete load in the mouse tissues is based on the subset of infected mouse tissues tested at necropsy (day 97 PI) and is averaged over the 2 sexes and the 7 necropsy tissue types. Spirochete loads are expressed as the log10-transformed ratio of the *B. burgdorferi 23S rRNA* copies/10^6 mouse *Beta-actin* copies. A GLM with quasibinomial errors found a significant relationship between the two variables (p = 0.045). Horizontal and vertical error bars represent the 95% confidence intervals for each variable.

2.6 Discussion

2.6.1 Strain-specific estimates of spirochete abundance in lab mice are related to strain-specific frequencies in nature

We found significant differences among the 11 *B. burgdorferi* strains in the percentage of infected tissues at necropsy and in the mean abundance of spirochetes in the necropsy tissues. These results indicate that some strains are present in more mouse tissues and establish higher abundance in those mouse tissues compared to other strains. Strains with higher infection prevalence and higher abundance in mouse tissue are expected to have higher transmission to feeding *I. scapularis* ticks and to have higher frequencies in nature. Interestingly, we found a significant positive relationship between our strain-specific estimates of the mean spirochete load in mouse tissues and our estimates of the strain frequencies in nature (Figure 2.5; see Appendix A Section 5). Thus, strains of *B. burgdorferi* that established a higher spirochete load in the tissues of the C3H/HeJ mice were more commonly found in the PubMLST database and in field-collected *I. scapularis* ticks. This result agrees with another study, which found that *B. burgdorferi* strains with high versus low prevalence in *I. scapularis* nymphs established high versus low abundance in the tissues of the white-footed mouse (*Peromyscus leucopus*), an important reservoir host of *B. burgdorferi* in nature (Baum et al., 2012). Studies on the European Lyme disease spirochete *Borrelia afzelii* found a positive relationship between spirochete abundance in the host tissues and spirochete transmission to feeding *I. ricinus* ticks (Genné et al., 2021; Råberg, 2012). We have previously shown that *B. afzelii* strains with higher transmission from infected hosts to *I. ricinus* ticks are more common in nature (Durand et al., 2017; Tonetti et al., 2015). We therefore hypothesize that *B. burgdorferi* strains with higher abundance in mouse tissues have higher host-to-tick transmission, which causes these strains to have higher frequencies in nature.

The multi-locus sequence type (MLST) was used to match our strains to the PubMLST database and the published literature and to estimate their frequencies in nature. The *Borrelia* MLST is based on 8 house-keeping genes that are located on the bacterial chromosome (Hoen et al., 2009; Margos et al., 2008; Margos et al., 2012), but this strain typing system does not provide any information on the many linear and circular plasmids that carry the genes necessary for infection in the vertebrate host and the tick vector (Casjens et al., 2017; Casjens et al., 2012; Grimm et al., 2005; Stewart et al., 2005). However, numerous studies have found strong linkage disequilibrium between the chromosomal MLST and plasmid-encoded genes such as *ospC* (Bunikis, Garpmo, et al., 2004; Hellgren et al., 2011; Qiu et al., 2004; Travinsky et al., 2010), suggesting that MLST might be a reasonable guide to link variation in strain-specific life history traits measured in the lab (e.g., abundance in host tissues and host-to-tick transmission) to variation in strain-specific frequencies in nature.

2.6.2 Most *B. burgdorferi* strains establish persistent infections in C3H/HeJ mice

Of the 12 strains of *B. burgdorferi* used in this study, 11 strains established persistent infections in C3H/HeJ mice. The strain that failed to infect mice (strain 111) was missing a plasmid shared by the other 11 strains (see Appendix A Section 1). Each infected mouse had consistent detection of *B. burgdorferi* in ear biopsies and in the necropsy tissues at 97 days PI. This result was similar to another study demonstrating that 6 strains of *B. burgdorferi* were able to establish persistent infection in the white-footed mouse (*P. leucopus*) up to 35 days PI following needle inoculation (Baum et al., 2012). For most strains, the spirochete loads in the right ear tissue biopsies of infected mice remained stable over time but for strains 66, 57, and 54 there was a significant decrease in abundance in the right ear tissue over time. Interestingly,

these 3 strains also had the highest abundance in the right ear on day 29 PI. This observation suggests that there is a trade-off between high abundance early in the infection versus the ability to maintain high abundance over the duration of the infection. Others have suggested that *B. burgdorferi* strains can evolve different life history strategies, such as persistent strains versus rapidly cleared strains (Haven et al., 2012).

2.6.3 Sex-specific differences of *B. burgdorferi* prevalence and abundance in C3H/HeJ mice

Our study found that male mice had a higher infection prevalence and abundance of *B. burgdorferi* in their tissues than female mice. This was true for 10 of the 11 successful strains, whereas strain 126 had equal tissue infection prevalence between the sexes. We screened 27 experimental studies of rodent hosts infected with different *B. burgdorferi* sl genospecies but found no reports of such differences between the sexes (Table 2.2, see Appendix A Section 12). A study of a relapsing fever spirochete, *Borrelia hermsii,* found a non-significant trend of male mice having a higher bacteremia than female mice (Benoit et al., 2010). We found four field studies where the infection prevalence of *B. burgdorferi* sl was higher in male rodents compared to female rodents (Hamer et al., 2012; Tschirren et al., 2013; Voordouw et al., 2015; Zawada et al., 2020). One limitation with field studies is that they do not control for sex-specific differences in exposure rate, and previous studies have shown that male rodents are more likely to be parasitized by ticks than female rodents (Devevey & Brisson, 2012; Ostfeld et al., 2018; Perkins et al., 2003). In our study, both sexes were equally susceptible to infection with *B. burgdorferi*, but the abundance of *B. burgdorferi* in the host tissues was 1.45x higher in male mice compared to female mice. One potential explanation for this sex-specific difference is the immunosuppressive effect of testosterone in male vertebrate hosts (Klein, 2004; Klein &

Flanagan, 2016; Trigunaite et al., 2015). In mice, testosterone has been directly linked to a greater host impact of infection with males having higher pathogen burden or prolonged infection compared to females (Arroyo-Mendoza et al., 2020; Benten et al., 1997; Hughes & Randolph, 2001; Sasaki et al., 2013). In summary, our study shows that with equal exposure, male and female mice are both susceptible to *B. burgdorferi*, but male mice have a higher tissue infection prevalence and higher spirochete abundance compared to female mice.

Table 2.2 A literature search for sex-specific differences in *B. burgdorferi* sensu lato infection in rodent hosts. The included studies all experimentally infected rodent hosts with *B. burgdorferi* sensu lato. The sex of mouse used is shown if this information was indicated in the study. The mouse species and *Borrelia* genospecies used in the study are listed. One study (2) used sex in their statistical analyses and found no difference in tissue spirochete loads.

Number	Study	Sex of mice	Mouse species [1]	*Borrelia* species [2]
1	(Barthold et al., 1990)	N/A	MM	*burg*
2	(Yang et al., 1994)	M+F	MM	*burg*
3	(Ma et al., 1998)	F	MM	*burg*
4	(Zeidner et al., 2001)	N/A	MM	*burg*
5	(Wang et al., 2001)	M + F	MM	*burg*
6	(Wang et al., 2002)	M + F	MM	*burg*
7	(Dolan et al., 2004)	F	MM	*burg*
8	(Derdáková et al., 2004)	N/A	PL	*burg*
9	(Liang, Yan, et al., 2004)	N/A	MM	*burg*
10	(Lima et al., 2005)	N/A	MM	*burg*
11	(Hanincova et al., 2008)	M+F	PL, MM	*burg*
12	(Craig-Mylius et al., 2009)	N/A	MM	*burg*
13	(Schwanz et al., 2011)	M	PL	*burg*
14	(Baum et al., 2012)	F	PL, MM	*burg*
15	(Golovchenko et al., 2014)	F	MM	*burg*
16	(Kern et al., 2015)	N/A	MM	*burg*
17	(Tonetti et al., 2015)	M	MM	*afz*
18	(Elsner et al., 2015)	M + F	MM	*burg*
18	(Devevey et al., 2015)	F	MM	*burg*
20	(Jacquet et al., 2015)	F	MM	*afz*
21	(Belli et al., 2017)	F	MM	*afz*
22	(Grillon et al., 2017)	M + F	MM	*burg, afz, gar*
23	(Rynkiewicz et al., 2017)	M + F	PL	*burg*
24	(Sertour et al., 2018)	F	MM	*burg, afz, bav*
25	(Genné et al., 2018)	F	MM	*afz*

26	(Gomez-Chamorro, Battilotti, et al., 2019)*	M+F	MG	*afz*
27	(Gomez-Chamorro, Heinrich, et al., 2019)	M+F	MG	*afz*

[1] Mouse species: MG = *Myodes glareolus*, MM = *Mus musculus*, PL = *Peromyscus leucopus*

[2] *Borrelia burgdorferi* sensu lato genospecies abbreviations: *Borrelia afzelii* (*afz*), *Borrelia bavariensis* (*bav*), *Borrelia burgdorferi* sensu stricto (*burg*), *Borrelia garinii* (*gar*)

*This study investigated whether host sex impacted susceptibility to infection with *B. afzelii* and found it did not, which agrees with our results. This is not included as this search was restricted to differences in infection, not susceptibility to infection.

2.6.4 Tissue tropism of *B. burgdorferi* in the vertebrate host

B. burgdorferi sl is an extracellular pathogen that targets the extracellular matrix of the host tissues (Cabello et al., 2007), and it is found in a variety of host tissues including skin, joints, bladder, and heart. While many vector-borne pathogens are found in the blood of their vertebrate hosts, for *B. burgdorferi* sl it is the host skin that is the most important organ for transmission to feeding ticks (Genné et al., 2021; Grillon et al., 2017; Råberg, 2012; Tsao, 2009). In contrast, the internal organs (joints, bladder, heart), which are distant from the sites of tick attachment, are believed to be a dead-end for spirochete transmission (Tsao, 2009). Thus, natural selection should favour those strains that can persist in the skin of their reservoir hosts and in this study, all strains established persistent infections in the skin as shown by the ear biopsies. The presence and abundance of *B. burgdorferi* in the host tissues is also influenced by the host immune response, which consists of both humoral and cellular components (Bockenstedt et al., 2021). This surveillance by the cells and molecules of the host immune system is reduced in immune privileged tissues, such as articular cartilage and heart valves, which might explain why the joints and the heart have a high abundance of *B. burgdorferi* despite being dead end tissues for transmission to feeding ticks (Embers et al., 2004; Hill et al., 2021).

In our study, the infection status and spirochete load of *B. burgdorferi* differed significantly among the 7 necropsy tissues on day 97 PI. The internal tissues (heart and bladder, but not the kidney) had higher infection prevalence and higher spirochete abundance compared to the external tissues (ventral skin, left ear, right ear). In studies on *B. burgdorferi* in C3H/HeJ mice taking place over a shorter infection time (7-21 days), the heart and ears were the tissues with the higher spirochete abundance compared to the bladder (Wang et al., 2002; Wang et al., 2001). In a study on *B. burgdorferi* in *P. leucopus* over a shorter infection time (5 weeks), the spirochete abundance in the ear and tail was much higher compared to the heart (Baum et al., 2012). One explanation is that the spirochete load in the host tissues changes with the age of the infection in the host. We therefore observed a different pattern of spirochete loads in the host tissues because we sacrificed our mice substantially later (97 days PI) compared to these other experimental infection studies. A second explanation is that our mice were infected via tick bite whereas the other studies infected mice via needle inoculation. A third explanation is that we sacrificed our mice immediately after the third larval infestation and we suspect that larval feeding might reduce the spirochete load in the external tissues but not the internal tissues (see below). In summary, tissue infection prevalence and tissue spirochete load are influenced by many factors including the *B. burgdorferi* sl genospecies or strain, the species of vertebrate host, the time of euthanasia, and the mode of inoculation (i.e., needle versus tick).

2.6.5 Limited evidence for differences in tissue tropism among *B. burgdorferi* strains

Pathogen species and pathogen strains can differ in their tissue tropism, which influences their transmission and virulence (McCall et al., 2016). For example, the three most common causative agents of Lyme borreliosis in humans, *B. burgdorferi* ss, *B. afzelii*, and *B. garinii*, are

often clinically differentiated by their symptoms in the joints, skin, and nervous system, respectively (Stanek et al., 2012). In experimental infection studies where the presence and abundance of pathogen strains are measured across a set of tissues, strain-specific tissue tropisms manifest themselves as a significant strain x tissue interaction. For infection presence, the strain x tissue interaction was not significant, which suggests that the *B. burgdorferi* strains did not differ in their preference for the 7 different tissues tested at necropsy (day 97 PI). With respect to the abundance of *B. burgdorferi*, our study found a significant strain x tissue interaction ($p = 0.010$), but this interaction was largely driven by the difference between the strain with the highest abundance in the skin, strain 126 (MLST 43, *ospC* N), and two strains with the lowest abundance in the skin, strain 66 (MLST 237 *ospC* type J) and strain 54 (MLST 741 *ospC* type I). Furthermore, the fact that both the presence and abundance of *B. burgdorferi* were strongly and positively correlated among pairs of the 7 necropsy tissues further indicates that highly infectious strains (e.g., strain 126) established high presence and abundance in all tissues, whereas moderately infectious strains (e.g., strains 66 and 54) established intermediate presence and abundance in all tissues.

2.6.6 Larval infestation may transiently decrease abundance of *B. burgdorferi* in mouse skin

Our study found that the prevalence of infection in the right ear was 91.7% in the last biopsy (day 89 PI) but dropped to 14.3% at necropsy (day 97 PI). This observation suggests that the spirochete abundance in the right ear decreased by 94.0% over a period of 8 days (see Appendix A Section 13). In this 8-day period, each mouse was infested with ~100 larvae that fed to repletion from day 90 PI to day 95 PI. Thus, the third larval infestation reduced the abundance of *B. burgdorferi* in the mouse tissues below our qPCR detection limit thereby causing the

dramatic drop in infection prevalence in the right ear on day 97 PI. The underlying mechanism involves spirochete loss from the mouse skin during tick feeding followed by a slow recovery of the spirochete population. Spirochetes have periplasmic flagella and are constantly moving within the skin of the mice (Motaleb et al., 2015). During tick feeding, spirochetes migrate to the tick bite site where upon ingestion by the tick they are lost from the spirochete population in the mouse skin (Bockenstedt et al., 2014). *B. burgdorferi* has a slow intrinsic growth rate with a doubling time of 12 hours at 34 ºC (Jutras et al., 2013), and it might take days or even weeks for the spirochete population in the mouse skin to recover following a larval infestation. This transient loss of spirochetes from the mouse skin following the larval infestation might explain why the infection prevalence and tissue spirochete abundance were lower in the external organs (skin and ears) compared to the internal organs (bladder, heart, kidney) at necropsy. Importantly, despite the potential impact of the third larval infestation, the abundance of spirochetes in the necropsy tissues was strongly positively correlated with the abundance in the last ear biopsy (Figure 2.4; Appendix A Sections 11 and 13). This result suggests that the impact of the third larval infestation on the abundance of spirochetes in the necropsy tissues was consistent across strains.

2.6.7 Limitations of using *M. musculus* as a model host for *B. burgdorferi*

One limitation of this study is that we used a laboratory strain of the house mouse (*Mus musculus*; strain C3H/HeJ) to compare variation in tissue infection prevalence and abundance among strains of *B. burgdorferi* rather than a common natural reservoir host, such as the white-footed mouse (*P. leucopus*) (Barbour, 2017). Strain C3H/HeJ possesses a mutation in Toll-like receptor 4 which makes them highly susceptible to Gram-negative bacteria compared to the

wild-type C3H/HeN. While this may further impact the performance of *B. burgdorferi* in this host, previous studies have found that C3H/HeJ mice are no different than wild-type in their response to infection with *B. burgdorferi* (Barthold et al., 1991; Ma et al., 1998). Both *M. musculus* and *P. leucopus* have a high probability of becoming infected following exposure to *B. burgdorferi* via needle inoculation or via tick bite (Barbour, 2017; Baum et al., 2012; Derdáková et al., 2004; Devevey et al., 2015; Hanincova et al., 2008; Rynkiewicz et al., 2017; Wang et al., 2002; Wang et al., 2001). Experimental infections of *M. musculus* and the European bank vole (*Myodes glareolus*) with the same strains of *B. afzelii* have likewise found no differences in susceptibility (Belli et al., 2017; Genné et al., 2021; Gomez-Chamorro, Battilotti, et al., 2019; Gomez-Chamorro, Heinrich, et al., 2019). Host species can influence the abundance of *B. burgdorferi* sl in the tissues of the rodent reservoir host; for example, bank voles (*Myodes glareolus*) have higher abundance of *B. afzelii* in their tissues compared to yellow-necked mice (*Apodemus flavicollis*) (Råberg, 2012; Zhong et al., 2019). However, we are not aware of any studies that have compared the tissue abundance of different strains of *B. burgdorferi* among different host species. A study that experimentally infected *P. leucopus* mice with 6 different *B. burgdorferi* strains found similar levels of variation in tissue spirochete load among strains compared to the present study (Baum et al., 2012). For our study to be relevant to the situation in nature, the variation due to differences among strains averaged across host species should be much larger compared to the variation due to interactions between host species and strains (Råberg et al., 2017). In other words, strains that have high versus low fitness in lab mice should have a similar ranking in natural rodent reservoir hosts. One study that compared host-to-tick transmission of two *B. burgdorferi* strains in C3H/HeJ mice and *P. leucopus* mice found that the same strain had higher transmission in both host species (Hanincova et al., 2008). Future studies

should investigate whether the strain-specific mean tissue spirochete loads and strain-specific host-to-tick transmission are correlated between different host species.

In the present study, the mice were sexually mature but relatively young (7 to 9 weeks of age) at the time of the nymphal infestation, and the spirochete loads in the necropsy tissues were determined on day 97 PI when the mice were much older (21 to 23 weeks of age). Although we are not aware of any studies that have shown that the age at which mice are infected with *B. burgdorferi* influences the spirochete load in necropsy tissues, we acknowledge that the inferences of this study are restricted to C3H/HeJ mice that are infected and dissected according to the time schedule used in the present study. Field studies have repeatedly shown that the prevalence of *B. burgdorferi* infection is much higher in adult mice compared to juvenile and sub-adult mice (Bunikis, Tsao, et al., 2004; Hofmeister et al., 1999; Tschirren et al., 2013; Voordouw et al., 2015), which suggests that many mice become infected during the transition from the sub-adult stage to the adult stage. In Lyme disease-endemic areas, the monthly probability that a mouse acquires *B. burgdorferi* can be as high as 60%, which suggests that most mice (>80%) will have become infected at 8 weeks of age (Bunikis, Tsao, et al., 2004; Voordouw et al., 2015). Thus, our decision to infect 7- to 9-week-old mice via tick bite is representative of when naïve rodent reservoir hosts encounter *B. burgdorferi* in nature.

2.6.8 Conclusions

Using experimental infections of a laboratory model host with the Lyme borreliosis agent *B. burgdorferi*, we found that estimates of the strain-specific abundance in the host tissues were positively correlated with the frequencies of these strains in wild populations of *I. scapularis* ticks. Thus, strains that established a higher abundance in the tissues of lab mice were more

common in nature. While male and female mice were equally susceptible to infection, male mice had consistently higher infection prevalence and abundance of *B. burgdorferi* in their tissues compared to female mice. In this study, there was no evidence for strain-specific tissue tropism. There were big differences for all strains in the presence and abundance of *B. burgdorferi* among the 7 different necropsy tissues. There was also a 4.8-fold range in the mean spirochete load in the mouse necropsy tissues among strains. In contrast, there was limited evidence for significant strain x tissue interactions indicating that the highly infectious strains were better at establishing themselves in all tissues compared to the moderately infectious strains. An unexpected result was that infestation with *I. scapularis* larvae dramatically reduced the presence of *B. burgdorferi* in the mouse ear tissues. Future studies will investigate whether strain-specific variation in tissue presence and abundance influences strain-specific variation in host-to-tick transmission.

3 Variation among strains of *Borrelia burgdorferi* in host tissue abundance and lifetime transmission determine the population strain structure in nature

Zinck, C.B., Thanpy, P. R., Uhlemann, E.E., Wachter, J., Suchan, D., Cameron, A. D. S., Rego, R. O. M., Brisson, D., Bouchard, C., Ogden, N. H., & Voordouw, M. (2023). Variation among strains of *Borrelia burgdorferi* in host tissue abundance and lifetime transmission determine the population strain structure in nature. (Submitted, April 7, 2023; Reviews received May 17, 2023)

Authors' contributions
MJV, CBZ, DB and NHO designed the study. CB and NHO helped with obtaining funding. CBZ and PRT executed the experimental infection study. CBZ and EU performed the molecular work. JW cultured strains of *B. burgdorferi.* ROMR performed the plasmid content analysis on the strains of B. burgdorferi. DS and AC confirmed genetic identity of strains. CBZ conducted statistical analyses of the data. CBZ and MJV wrote the manuscript. All authors read and approved the final version of the manuscript.

Acknowledgements
The authors would like to thank Dr. Susan Detmer and Dr. Pini Zvionow for their assistance in necropsy and tissue collection. The authors would like to thank Georgia Hurry, Alexandra Foley-Eby and the staff of the WCVM animal care unit for their assistance with the experimental infection study. We would like to thank Dr Robbin Lindsay and Antonia DiBernardo for kindly providing the strains of *B. burgdorferi* that were used in this study, and for their advice on how to culture these strains.

3.1 Transition Statement

In chapter 2, we established pathogen abundance in the host tissues for the 11 strains of *B. burgdorferi* in this study. We found that the abundance of a strain in the host tissues was predictive of its strain frequency in nature, and that males had significantly higher pathogen abundance in their tissues compared to females. In this chapter we now focus on transmission, the ability of *B. burgdorferi* to transit from an infected host to a feeding tick. These data are from the same experiment and the same mice as the previous chapter. We measured lifetime host-to-tick transmission by infesting the mice with larval *I. scapularis* ticks on days 30, 60, and 90 post-infection (PI). After feeding, tick larvae were allowed to moult and these nymphs were tested to estimate transmission to compare against our estimates of abundance from Chapter 2, and the frequency of these strains in nature. We also investigated variation among strains in the larval infection prevalence and the larval spirochete load, measures that are often overlooked in *B. burgdorferi* research.

3.2 Abstract

Theoretical models of pathogen life history evolution assume a positive genetic correlation between pathogen abundance in the host tissues and pathogen transmission. Empirical evidence requires measuring both traits across a set of naturally occurring pathogen strains in a common host and a controlled environment. This study used 11 field-collected strains of the spirochete *Borrelia burgdorferi*, a rodent host (*Mus musculus*, C3H/HeJ) and the tick vector (*Ixodes scapularis*) to investigate the genetic correlation between pathogen abundance and lifetime host-to-tick transmission (HTT) of the Lyme disease spirochete. Male and female mice were experimentally infected with 1 of 11 strains of *B. burgdorferi*. Lifetime HTT was measured by infesting mice with *I. scapularis* ticks over the duration of the infection. Abundance of each strain was estimated using host tissues collected at necropsy. The prevalence and abundance of the strains in the host tissues and ticks were determined by qPCR. Spirochete abundance in host tissues and lifetime HTT varied significantly among the 11 strains of *B. burgdorferi*. Strains with higher spirochete loads in the host tissues were more likely to infect feeding larvae, which molted into nymphs with a higher probability of *B. burgdorferi* infection (*i.e.*, higher HTT). Finally, we found that our laboratory-based estimates of lifetime HTT were predictive of the frequencies of these strains in wild *I. scapularis* populations (obtained from the literature). For *B. burgdorferi*, the strains that establish high abundance in host tissues and that have high lifetime transmission are the strains that are most common in nature.

Keywords

Borrelia burgdorferi, Lyme borreliosis, transmission, pathogen life-history, tick-borne disease

3.3 Introduction

Pathogen evolution is classically determined by the trade-offs between three key life history traits: replication, transmission, and virulence (Alizon et al., 2009; Anderson & May, 1982; Cressler et al., 2016; Frank, 1996; Mackinnon et al., 2008; Visher et al., 2021). Pathogen strains that have higher within-host replication (*i.e.*, establish higher abundance in host tissues) are expected to have higher transmission success, but they will reduce the survival of the host (*i.e.*, have higher virulence), which shortens the duration of the infection. Pathogens are therefore expected to evolve intermediate virulence, which balance the costs of a shorter lifespan of infection with the benefits of higher transmission (De Roode et al., 2008; Fraser et al., 2007; Jensen et al., 2006; Mackinnon & Read, 2004; Visher et al., 2021). Life history theory assumes that variation in these three key pathogen traits and their trade-offs are determined at least in part by pathogen genetics (Alizon et al., 2009; Anderson & May, 1982; Cressler et al., 2016; Frank, 1996; Mackinnon et al., 2008; Visher et al., 2021). A powerful approach for demonstrating the genetic basis of trade-offs is the comparative method, which requires measurement of pathogen traits across a set of genetically distinct pathogen clones or strains in a common host and a common environment (Cressler et al., 2016; Mackinnon & Read, 1999, 2004; Stearns, 1992).

Numerous empirical studies have reported the expected positive relationship between pathogen abundance (or pathogen load) in the host tissues and pathogen transmission (Acevedo et al., 2019; De Roode et al., 2008; Fraser et al., 2007; Jensen et al., 2006; Mackinnon & Read, 2004; Råberg, 2012; Schneider et al., 2012). However, upon closer inspection only one study demonstrates the presence of a genetic correlation between these two pathogen traits by measuring them across a set of parasite clones in experimentally infected hosts (Mackinnon & Read, 1999). Studies on human pathogens have demonstrated the expected positive relationship

but cannot control for host or environmental factors (Fraser et al., 2007; Mackinnon & Read, 2004). Some studies using arthropod hosts as model systems have measured genetic variation among pathogen strains in load or virulence but not in transmission (De Roode et al., 2008; Jensen et al., 2006). Thus, there are surprisingly few examples of a genetic correlation between pathogen load and pathogen transmission and recent reviews have highlighted the need for more such studies (Acevedo et al., 2019; Cressler et al., 2016; Visher et al., 2021).

Studies that measure pathogen life history traits are typically conducted in the lab under carefully controlled conditions. An open question is whether these lab-based estimates of strain fitness are relevant to the real world. The revolution in next generation sequencing methods has allowed scientists to document pathogen strain diversity in host populations with great accuracy and precision (Bambini et al., 2013; Buckee et al., 2010; Durand et al., 2017; Råberg et al., 2017; Weinberger et al., 2009). All else being equal, the frequency of a strain in the pathogen population is a measure of its fitness; common strains are expected to have higher fitness compared to rare strains. Thus, one way to validate our lab-based estimates of pathogen strain fitness would be to test whether they can explain variation in frequencies among strains in the real world (Durand et al., 2017; Weinberger et al., 2009). Such validation would increase our confidence that our lab-based estimates of the genetic variation underlying pathogen life history traits is relevant to their evolution in nature.

Lyme borreliosis is the most common vector-borne disease in Europe and North America (Steere et al., 2016) and is caused by tick-borne spirochetes belonging to the *Borrelia burgdorferi* sensu lato (sl) genospecies complex. The three most important *Borrelia* genospecies are *B. afzelii* and *B. garinii* in Europe, and *B. burgdorferi* sensu stricto (hereafter *B. burgdorferi*) in North America (Stanek & Reiter, 2011). These genospecies are transmitted among vertebrate

hosts through the bite of *Ixodes* ticks, which include *I. scapularis* in North America and *I. ricinus* in Europe. *Ixodes* ticks consist of three developmental stages: larva, nymph, and adult. Larval ticks acquire spirochetes after feeding on infected hosts and moult into infected nymphs, which infect the next generation of vertebrate hosts. Adult female ticks feed on larger vertebrate hosts that are incompetent for *B. burgdorferi* sl pathogens (Kurtenbach et al., 2006; Piesman & Gern, 2004). In summary, the two transmission steps that maintain *B. burgdorferi* in nature are from infected vertebrate hosts to naïve larvae and from infected nymphs to naïve vertebrate hosts.

Each *Borrelia* genospecies consists of multiple strains that coexist in natural populations. These strains can vary in their life history traits, such as replication or abundance in host tissues (Baum et al., 2012; Genné et al., 2021; Jacquet et al., 2015; Wang et al., 2002; Wang et al., 2001) or host-to-tick transmission (Brisson & Dykhuizen, 2004; Derdáková et al., 2004; Genné et al., 2018; Genné et al., 2019; Hanincova et al., 2008; Jacquet et al., 2016; Rynkiewicz et al., 2017; Tonetti et al., 2015). A study of two strains of *B. afzelii* found that the strain abundance in host tissues was predictive of host-to-tick transmission success (Genné et al., 2021). Other studies have found that estimates of these life history traits in a controlled experiment are predictive of strain frequencies in nature (Baum et al., 2012; Durand et al., 2017; Zinck et al., 2022). Studying the relationships between these life history traits is important to understand the ecological and evolutionary forces that shape the current strain structure, and to predict which strains are likely to become dominant in new and emerging areas.

In this study, we investigated the variation in host-to-tick transmission (HTT) among 11 different strains of *B. burgdorferi*. We have previously shown that there is significant variation in host tissue abundance among these strains (Zinck et al., 2022). The present study had four objectives. First, characterize the variation in lifetime HTT among 11 strains of *B. burgdorferi*.

Second, quantify the relationship between tissue burden and the number of spirochetes acquired by *I. scapularis* larvae during feeding for 11 strains of *B. burgdorferi*. Third, quantify the relationship between host tissue burden (replication) and lifetime HTT for 11 strains of *B. burgdorferi*. Fourth, determine whether our laboratory estimates of strain-specific lifetime HTT are predictive of strain frequencies in nature. We hypothesize that strains with higher tissue abundance will transmit more spirochetes to feeding larval ticks and will have a greater lifetime HTT. Finally, we predict that the strains with a greater lifetime HTT will be more common in nature.

3.4 Materials and Methods

3.4.1 Strains, ticks, and mice

For this study, 11 low passage strains of *B. burgdorferi* were obtained from the isolate collection of the Public Health Agency of Canada (PHAC). Initially 12 strains were used however one failed to infect mice and is not included here (Zinck et al., 2022). These strains were originally isolated from wild *I. scapularis* ticks collected from field sites in Canada (Tyler et al., 2018). The strains were selected by maximizing the multi-locus sequence type (MLST) diversity while also considering the *ospC* type and geographic region of origin. We selected 5 strains from Eastern Canada, and 6 from Midwestern Canada (Table 3.1) because previous work found substantial differences in strain diversity between these two regions (Margos et al., 2012; Mechai et al., 2015; Ogden et al., 2011). All strains were validated for the presence of plasmids necessary for the natural transmission cycle of *B. burgdorferi* (Zinck et al., 2022).

Laboratory-reared, specific-pathogen-free *I. scapularis* larvae were obtained from the National Tick Research and Education Resource at Oklahoma State University. This colony is regularly outbred with wild *I. scapularis* to prevent inbreeding and screened for multiple tick-

borne pathogens including *B. burgdorferi*. Six batches of larvae were purchased over the course of the study (2 temporal blocks x 3 larval infestations per block). The larvae for each infestation came from egg clutches of multiple different adult female ticks.

Specific-pathogen-free, 6 to 8-week-old, female and male *Mus musculus* C3H/HeJ mice were purchased from The Jackson Laboratory and used as the reservoir host in this study. This strain of mouse has been used in numerous experimental infection studies with *B. burgdorferi* (Dolan et al., 2004; Wang et al., 2002; Wang et al., 2001).

3.4.2 Creation of *I. scapularis* nymphs infected with one of the 12 strains of *B. burgdorferi*

The *I. scapularis* nymphs infected with one of the 11 strains were created as described previously (Zinck et al., 2022). Briefly, each strain was cultured from frozen stock in BSK-H media for 9-14 days. C3H-HeJ mice were then needle-inoculated with single strains (n = 2-4 mice per strain). At 2-4 weeks post-infection (PI), mice were infested with naïve *I. scapularis* larvae that were left to feed to repletion following our infestation procedure (see below). These larvae were maintained in humidity chambers to moult into nymphs. To minimize plasmid loss during culture, the *B. burgdorferi* strains had undergone only 4 passages from the time of isolation from field-collected *I. scapularis* ticks to needle inoculation into our mice.

3.4.3 Infecting mice via nymphal tick bite with one of the 11 strains of *B. burgdorferi*

A total of 112 mice (56 male, 56 female) were used in this study. Each of the 11 strains had 8 mice (4 male, 4 female) with an additional 24 (12 male, 12 female) uninfected control mice. To mimic a natural infection cycle, experimental mice were infected by allowing three putatively infected *I. scapularis* nymphs feed to repletion as previously described (Zinck et al.,

2022). Control mice were infested with 3 uninfected *I. scapularis* nymphs. To manage the workload, the study was run in two orthogonal temporal blocks (A, B) processed ~6 months apart; each block contained half the experimental mice and half the control mice. To confirm the infectious challenge, replete nymphs were recovered and tested for the presence of *B. burgdorferi* by qPCR targeting the *23S rRNA* gene of *B. burgdorferi* (see below).

3.4.4 Infestations of mice with *I. scapularis* larvae

At days 30, 60, and 90 post-infection (PI), mice were infested with 50-100 naïve *I. scapularis* larval ticks that were allowed to feed to repletion. All mice were anaesthetized for ~20 min with xylazine and ketamine for each infestation, and larvae were brushed onto their fur. Mice were housed in a cage setup that facilitated the collection of engorged larvae as described previously (Jacquet et al., 2015). For each mouse and infestation, 5 engorged larvae were frozen immediately at -80 ºC following recovery (no engorged larvae were collected for the first infestation of the mice in the first block). The remaining engorged larvae were kept at high humidity (~99%) and room temperature and were allowed to moult into nymphs. Four weeks after the engorged larvae moulted into nymphs, a sample of 10 nymphs per mouse per infestation were frozen at -80 ºC for DNA extraction.

3.4.5 Collection of tissues from C3H/HeJ mice

At 97 days post-infection, the C3H/HeJ mice were euthanized, and we dissected and collected 7 tissues: (1) bladder, (2) heart, (3) kidney, (4) left ear, (5) right ear, (6) right rear tibiotarsal joint, and (7) dorsal skin. Mouse tissue samples were frozen at -80 ºC for DNA extraction.

3.4.6 DNA extraction of whole *I. scapularis* ticks

For each mouse, there were 45 ticks (3 infestations * (5 larvae + 10 nymphs) per infestation) for a total of 5,040 ticks (112 mice x 45 ticks). Tick extractions were done as previously described (Jacquet et al., 2015). Ticks were homogenized using bead beating with the Qiagen TissueLyser II. DNA was extracted from the homogenized ticks using the Qiagen DNEasy 96-well plate extraction kit following the manufacturer's instructions. All extractions were eluted with a final volume of 65 µL and stored at -80 ºC prior to use in qPCR.

3.4.7 Detection of *Borrelia burgdorferi* in *I. scapularis* ticks by qPCR

To test for the presence of *B. burgdorferi* in experimental samples, a qPCR targeting the *23S rRNA* intergenic spacer of *B. burgdorferi* was used (Courtney et al., 2004). Every plate was run with a synthetic gene fragment to use as a standard (Zinck et al., 2022). A strict lower detection limit of 1 gene copy/µL was used as a cut-off based on the lower detection limit of the standards. To generate copy numbers, a single regression was done on multiple runs of standards (range: $1 – 10^5$ copies/µL, n = 81) so that the same equation was used for every transformation (Zinck et al., 2022). As whole ticks were used in every extraction, values are reported as the $\log_{10}$ *23S rRNA* copies per tick.

In comparison to nymphs, replete larvae have a lower abundance of *B. burgdorferi* in addition to the presence of mammalian blood which can inhibit amplification of DNA (Schrader et al., 2012; Sidstedt et al., 2018). For this reason, a qPCR targeting the *I. scapularis calreticulin* gene was developed (See Appendix B Section 1) to determine DNA extraction success by using

a tick housekeeping gene present in all samples. Like with the *23S rRNA* qPCR, a synthetic gene fragment was designed to use as a standard (See Appendix B Section 2).

3.4.8 Detection of *Borrelia burgdorferi* in mouse tissues by qPCR

The abundance of *B. burgdorferi* in the 7 mouse tissues was also estimated using *23S rRNA* qPCR and were standardized relative to the number of mouse *Beta-actin* gene copies, as previously described (Zinck et al., 2022).

3.4.9 Statistical Methods

We analyzed 4 measures of transmission of *B. burgdorferi*: (1) proportion of engorged larvae infected with *B. burgdorferi*, hereafter larval infection prevalence (LIP), (2) abundance of *B. burgdorferi* in the subset of infected larvae, hereafter larval spirochete load (LSL) (3) proportion of unfed nymphs infected with *B. burgdorferi*, hereafter nymphal infection prevalence (NIP), and (4) abundance of *B. burgdorferi* in the subset of infected unfed nymphs, hereafter nymphal spirochete load (NSL).

3.4.10 Analysis of *B. burgdorferi* infection prevalence in larvae and nymphs

For larvae and nymphs, the presence of *B. burgdorferi* infection was a binomial variable (0 = uninfected, 1 = infected). Means of infection presence (prevalence) were done by infestation, by mouse, and by strain. The LIP and the NIP were analyzed by generalized linear mixed effect models (GLMMs) with binomial errors. For both analyses, the fixed factors included strain (11 levels; see Table 3.1), mouse sex (2 levels: female, male), infestation (days 30, 60, 90 PI), and their interactions. Temporal block (2 levels: A, B) was included in the

GLMM but not in the interaction terms. Mouse identity was included as a random factor. Analyses were restricted to ticks from the subset of 84 mice that became infected following nymphal challenge (see below). To generate the final models, interactions were sequentially removed if they were not significant and/or if their inclusion prevented the GLMM from converging on precise parameter estimates (i.e., standard error is orders of magnitude larger than parameter estimate). Factor significance was estimated using type II Wald tests, post-hoc analyses were performed and estimated marginal means were calculated.

3.4.11 Analysis of *B. burgdorferi* abundance in infected larvae and infected nymphs

For the subset of infected larvae and nymphs, analyses were run using linear mixed effect models (LMMs). For both analyses, the fixed factors included strain, mouse sex, infestation, and their interactions. Temporal block was included but not in the interaction terms. Mouse identity was included as a random factor. For the larvae only, *calreticulin* copies per tick were also included as a covariate to control for random variation in the efficiency of DNA extraction. Non-significant interactions were sequentially removed to generate the final models. Estimated marginal means and post-hoc analyses were done as mentioned above.

3.4.12 Correlations of strain phenotypes

In this study, we generated 4 measures of transmission for each strain: (1) larval infection prevalence (LIP), (2) larval spirochete load (LSL), (3) nymphal infection prevalence (NIP), and (4) nymphal spirochete load (NSL). For each of the 11 strains of *B. burgdorferi*, we have previously estimated (5) presence in 7 mouse tissues and (6) abundance in 7 mouse tissues (Zinck et al., 2022). Finally, we have estimated (7) frequencies of our 11 *B. burgdorferi* strains

in nature based on different datasets (Ogden et al., 2011; Travinsky et al., 2010). For each of the 11 strains of *B. burgdorferi*, a mean value was calculated for each of the 7 life history traits. These mean values were averaged across mouse sex and infestation such that a single value was used to represent each strain. To determine the pairwise relationships between these 7 variables across the 11 strains, simple linear regressions, and/or quasibinomial generalized linear models (GLMs) were used.

3.4.13 Statistical software

We used R version 4.0.4 for all statistical analyses (Team, 2021). The list of R packages and R functions we used are given in Appendix B (See Appendix B Section 1).

3.5 Results

3.5.1 Infestations of mice and recovery and testing of immature *I. scapularis* ticks

Each strain had 5-8 infected mice (total n = 84 infected mice) that survived to the end of the study (Table 3.1). In addition, 20 uninfected control mice survived to the end of the study. For each mouse and each infestation, we froze a maximum of 5 engorged larvae and 10 unfed nymphs. The infection status of these mice was previously determined by performing qPCR on 3 ear tissue biopsies and 7 necropsies and by performing ELISA on 2 blood samples per mouse (Zinck et al., 2022). In the present study, a maximum of 45 immature ticks were tested for their infection status for each mouse. Every infected mouse was found positive for *B. burgdorferi* in mouse tissues, xenodiagnostic ticks, and with respect to the IgG antibody response on a commercial ELISA. No uninfected control mouse, or mouse that failed to become infected had any detection of *B. burgdorferi.* In summary, there is no ambiguity about the infection status of

the 84 infected mice, the 4 experimental mice that failed to become infected following nymphal challenge, and the 20 uninfected control mice.

Table 3.1 The genetic identity and location of origin are shown for the 11 strains of *B. burgdorferi* used in the study. Strain identity numbers are from the reference publication (Tyler et al., 2018). Counts of larvae and nymphs are only for the subset of infected mice as mice that failed to become infected were excluded from analysis.

PubMLST Strain ID	NML Strain ID	MLST	*ospC* type	Region	Infected mice	Infected larvae	Infected nymphs
2439	57-1	29	Y, A3	West	8/8	70/90	212/230
2418	174	37	T	East	5/8	47/58	148/150
2416	167	12	M	East	8/8	74/106	201/241
2420	178-1*	3	K	East	8/8	85/89	233/236
2429	198	3	K	East	8/8	83/96	229/240
2392	22-2	55	A	West	8/8	53/83	176/226
2413	150	19	E	East	8/8	61/94	205/239
2388	10-2	32	H, C3	West	8/8	54/74	201/233
2443	66	237	J	West	7/8	27/77	114/210
2038	54	741	I	West	8/8	33/93	155/230
2399	126	43	N	West	8/8	58/90	210/236
	Total				84/92	645/950	2,084/2,471
	Uninfected**	NA	NA	NA	0/20	0/200	0/558

*This strain was originally intended to be 178-2 but turned out to be 178-1 (Tyler et al., 2018), thus we have two isolates of the same strain in this study (MLST 3, *ospC* K). We refer to this strain as 178 in this study.
** Uninfected control mice were fed upon by uninfected *I. scapularis* nymphs. As expected, all the ticks that fed on the uninfected control mice tested negative for *B. burgdorferi*.

3.5.2 Larval infection prevalence

Each mouse had up to 5 engorged larvae frozen from three separate infestations at days 30, 60, and 90 PI. In total, 950 and 200 engorged larvae were recovered and tested from the 84 infected mice and 20 uninfected control mice, respectively. The infection prevalence in the engorged larvae was 67.9% (645/950) and 0.0% (0/200) from the 84 infected mice and 20

uninfected control mice, respectively (Table 3.1). For the 84 infected mice (i.e., across the 11 strains), the mean number of infected larvae per infestation on days 30, 60, and 90 PI were 4.12 (range = 0 – 5), 2.73 (range = 0 – 5), and 3.20 (range = 0 – 5), respectively. Every infected mouse had *B. burgdorferi*-infected in larvae in at least one infestation.

The analysis of the larval infection prevalence (LIP) found that there were no significant interactions among the model, and mouse sex was not significant (See Appendix B Section 3). Strain ($p = 1.346*10^{-15}$), infestation ($p = 3.359*10^{-5}$), and temporal block ($p = 8.088*10^{-10}$) were all significant. The overall LIP varied 2.7-fold among strains (strain 54: 35.5%; strain 178: 95.5%). The LIP decreased from the first infestation at day 30 to the subsequent infestations (30 days PI: 89.7%; 60 days PI: 60.5%; 90 days PI: 64.6%). Temporal block B had a higher LIP than temporal block A (block A: 51.3%; block B: 79.6%). One explanation for this difference between blocks is that no larvae were collected from the first infestation (30 days PI) of mice in block A (See Appendix B Section 3).

3.5.3 Larval spirochete load

The analysis of the larval spirochete load (LSL) in the subset of infected engorged larvae ($n = 645$) found that strain ($p = 5.968*10^{-12}$), temporal block ($p = 6.236*10^{-5}$), infestation ($p = 4.773*10^{-11}$), and *calreticulin* copy number ($p = 2.2*10^{-16}$) were all significant (See Appendix B Section 4). The LSL varied 12-fold between the lowest and highest abundance strains (strain 54: 1,317.4 *23S rRNA* copies/larva; strain 178: 15,635.5 *23S rRNA* copies/larva). As with the LIP, the LSL was highest in the first infestation (30 days PI: 10,501.0 *23S rRNA* copies/larva; 60 days PI: 2,115.3 *23S rRNA* copies/larva; 90 days PI: 5,538.3 *23S rRNA* copies/larva). Like the LIP, the LSL was higher in block B than block A (block A: 1,867.1 *23S rRNA* copies/larva; block B:

7,071.7 *23S rRNA* copies/larva). As expected, there was a positive relationship between the number of *calreticulin* copies per engorged larva and the spirochete abundance (See Appendix B Section 4). These results suggest that the absolute abundance of *B. burgdorferi* measured in an engorged larval tick (*i.e.*, total copies of *23S rRNA*) is dependent on the size of the tick, larval engorgement time, and/or the DNA extraction efficacy.

3.5.4 Nymphal infection prevalence (host-to-tick transmission)

Each mouse had up to 10 unfed, 4-week-old nymphs frozen from the three separate infestations at days 30, 60, and 90 PI. In total, 2,471 and 558 unfed nymphs were tested from the 84 infected mice and 20 uninfected control mice, respectively. The infection prevalence in the unfed nymphs was 84.3% (2,084/2,471) and 0.0% (0/558) from the 84 infected mice and 20 uninfected control mice, respectively. For the 84 infected mice (i.e., across the 11 strains), the mean number of infected nymphs per infestation on days 30, 60, and 90 PI were 9.44 (range = 1 – 10), 8.02 (range = 0 – 10), and 7.41 (range = 0 – 10), respectively. All 84 mice had detection of *B. burgdorferi* in unfed nymphs in at least two of the three infestations; 79/84 mice had detection in all three infestations.

The analysis of the nymphal infection prevalence (NIP) found that strain ($p = 1.758*10^{-14}$), mouse sex ($p = 0.001$), infestation ($p = 2.2*10^{-16}$), and the 2-way interactions between sex and infestation ($p = 1.625*10^{-4}$) were significant. The interactions of strain and infestation ($p = 0.017$), and strain and sex ($p = 0.022$) were significant but were removed so the model could converge on parameter estimates (See Appendix B Section 5). For 8 of the 11 strains, the NIP decreased with successive larval infestations, whereas it remained consistently high (above 90%) for 3 strains (strains: 198, 174, 178; Figure 3.1). At day 30 PI, the NIP for male and female mice

were similar (males: 94.8%, females: 97.8%), but declined more for females by day 90 PI (males: 82.6%, females: 67.1%; Figure 3.2). Thus, the NIP decreased over time in both sexes, but the decrease in NIP was significantly greater for female mice compared to male mice (Figure 3.2). Overall, the lifetime NIP was greater in males compared to females for 9 of 11 strains (males: 87.8% [1,113/1,268], females: 80.7% [971/1,203]).

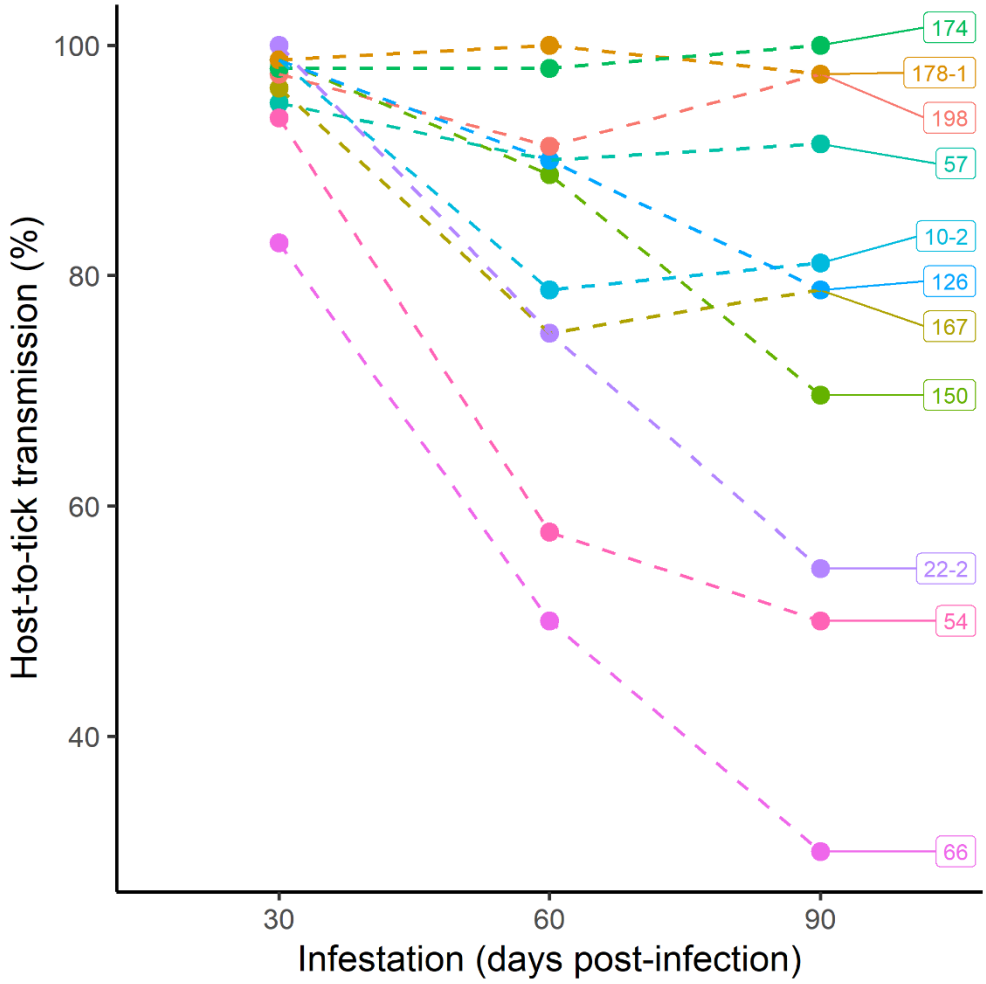

Figure 3.1 The transmission of *B. burgdorferi* from infected mice to immature *I. scapularis* ticks decreased over the 3 successive larval infestations for some strains but remained constant over time for other strains. Lifetime host-to-tick transmission (HTT) was measured by infesting mice with *I. scapularis* larvae on 3 occasions (days 30, 60, and 90 post-infection), allowing the engorged larvae to moult into nymphs, and testing the nymphs for infection with *B. burgdorferi*. Each of the 33 estimates of HTT (11 strains x 3 infestations) was based on a maximum of 80

unfed nymphs (8 mice per strain x 10 unfed nymphs per infestation). Labels on datapoints are strain ID numbers.

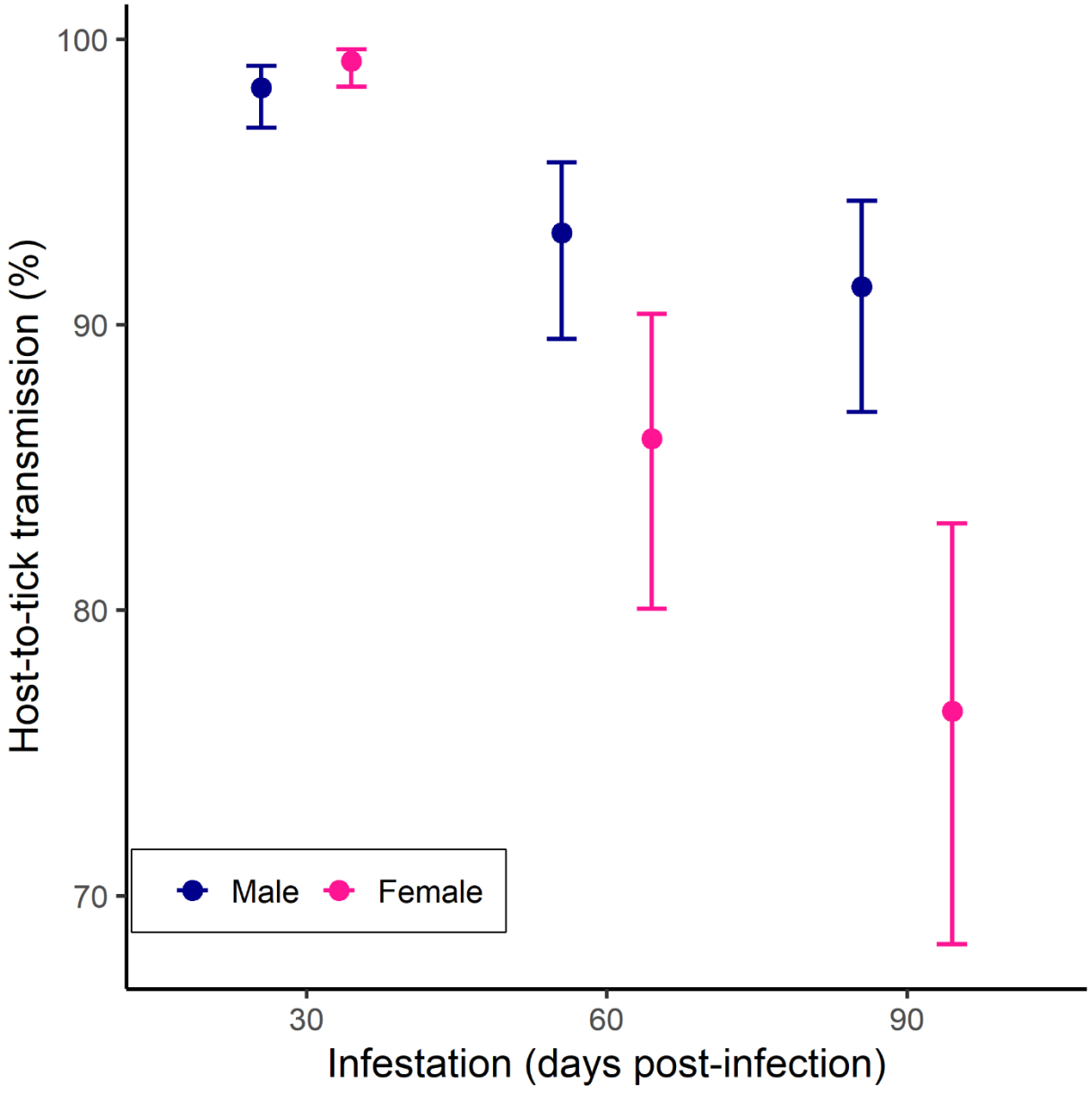

Figure 3.2 Host-to-tick transmission of *B. burgdorferi* from infected male and female C3H/HeJ mice to immature *I. scapularis* ticks decreased over the course of the infection. Male mice had higher lifetime HTT compared to female mice for all 11 strains of *B. burgdorferi*. Lifetime HTT was measured by infesting mice with *I. scapularis* larvae on 3 occasions (days 30, 60, and 90 post-infection), allowing the engorged larvae to moult into nymphs, and testing the nymphs for infection

with *B. burgdorferi*. The highly significant 2-way interaction between mouse sex and infestation ($p = 0.0002$) indicates that the decrease in the HTT over time was larger in the female mice compared to the male mice.

3.5.5 Nymphal spirochete load

The analysis of the nymphal spirochete load (NSL) in the subset of infected unfed nymphs (n = 2,084) found that strain ($p = 2.2*10^{-16}$), infestation ($p = 8.914*10^{-12}$), and the 2-way interactions between strain and infestation ($p = 7.561*10^{-5}$), and between mouse sex and infestation ($p = 0.026$) were all significant. The other interactions, and the main effects of mouse sex and temporal block were not significant (See Appendix B Section 6). The mean NSL in unfed nymphs averaged across all infestations varied by 8.57x between the lowest and highest abundance strains (strain 66: 7,707.3 *23S rRNA* copies/tick; strain 174: 66,069.3 *23S rRNA* copies/tick). Unlike the larval spirochete loads, the NSL in the unfed nymphs increased for some strains with successive infestations, whereas it decreased for others. Like the NIP, the NSL in ticks fed on female mice decreased more with successive infestations than the NSL in ticks fed on male mice (Males: 30 days PI: 26,525.2 *23S rRNA* copies/tick; 90 days PI: 19,075.1 *23S rRNA* copies /tick; Females: 30 days PI: 32,587.7 *23S rRNA* copies/tick; 90 days PI: 17,937.3 *23S rRNA* copies/tick).

3.5.6 Pairwise relationships of the transmission variables across 11 strains of *B. burgdorferi*

Pairwise relationships across the 11 strains of *B. burgdorferi* were estimated among the 4 measures of transmission (LIP, LSL, NIP, NSL), the 2 measures of mouse tissue prevalence/abundance, and the strain frequencies in nature (Figure 3.3). Binomial response variables (i.e., LIP, NIP, strain frequencies) were analyzed with a GLM using quasibinomial

errors, whereas normal response variables (i.e., larval spirochete load and nymphal spirochete load) were analyzed with simple linear regression. All 4 transmission measures were positively related (Figure 3.3; See Appendix B Section 7). For both larvae and nymphs, there was a positive relationship between the spirochete load within infected ticks and the prevalence of infected ticks (GLM for larvae: slope = 1.925, SE = 0.691, p = 0.021; GLM for nymphs: slope = 2.129, SE = 0.976, p = 0.057). The LIP and LSL were positively correlated with the NIP and NSL (Figure 3.3; See Appendix B Section 7).

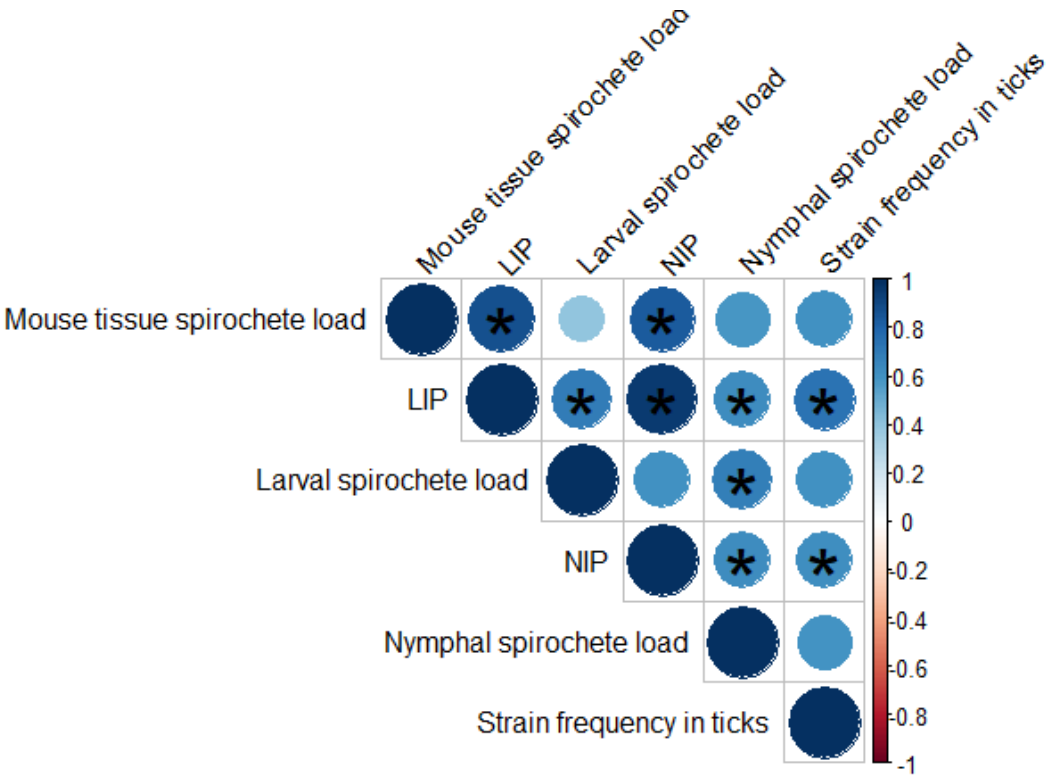

Figure 3.3 Pairwise correlations between 6 different variables across the 11 strains of *B. burgdorferi*. The six variables include (1) mouse tissue spirochete load, (2) larval infection prevalence (LIP), (3) Larval spirochete load, (4) nymphal infection prevalence (NIP), (5) nymphal spirochete load, and (6) frequency of strain in I. scapularis tick populations in nature. All 15 correlations were positive as indicated by the blue colours and the size of the circles. Of the 15 correlations, 9 correlations were statistically significant at an $\alpha = 0.05$ as indicated by the asterisks.

The pairwise relationship between pathogen abundance in the mouse tissues and the 4 measures of transmission was tested. Across the 11 strains, the abundance of spirochetes in the host tissues at necropsy was not related to the abundance of spirochetes in engorged larvae (r^2 = 0.062, p = 0.228) or in the post-moult unfed nymphs (r^2 = 0.266, p = 0.060). The spirochete abundance in mouse tissues did determine the LIP (GLM: slope = 3.445, SE = 0.751, p = 0.001, Figure 3.4) and most importantly the NIP (GLM: slope = 3.551, SE = 0.902, p = 0.003, Figure 3.5).

GLMs with quasibinomial errors were used to analyze the relationship between our laboratory-based estimates of host-to-tick transmission (i.e., the NIP) and literature-based estimates of the strain frequency in nature (Figure 3.6; See Appendix B Section 7). Our laboratory-based estimates of NIP were significantly positively related with the literature-based frequencies of these strains in natural populations of *I. scapularis* ticks (Figure 3.6; GLM slope = 10.750, SE = 4.287, p = 0.033).

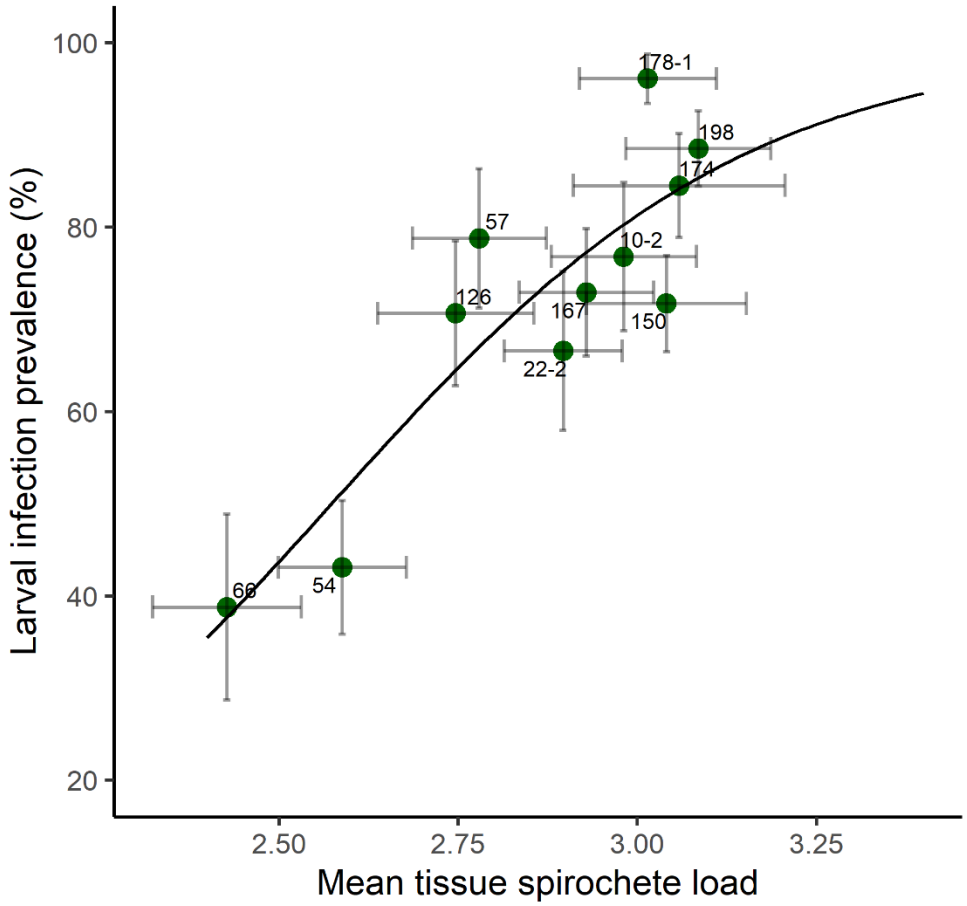

Figure 3.4 The mean spirochete load in the mouse tissues determines the larval infection prevalence (LIP) across the 11 strains of *B. burgdorferi*. The mean spirochete load in the mouse tissues was based on the infected necropsy tissues and was calculated as log10(*23S rRNA*/10^6 *Beta-actin*). The LIP was based on the percentage of fed larvae that tested positive for *B. burgdorferi*; these larvae had fed on the mice at either day 30, 60, or 90 post-infection. The slope of the logistic regression is positive and significant (slope = 3.44, SE = 0.75, p = 0.001). Labels on datapoints are strain ID numbers. Error bars represent the 95% confidence intervals.

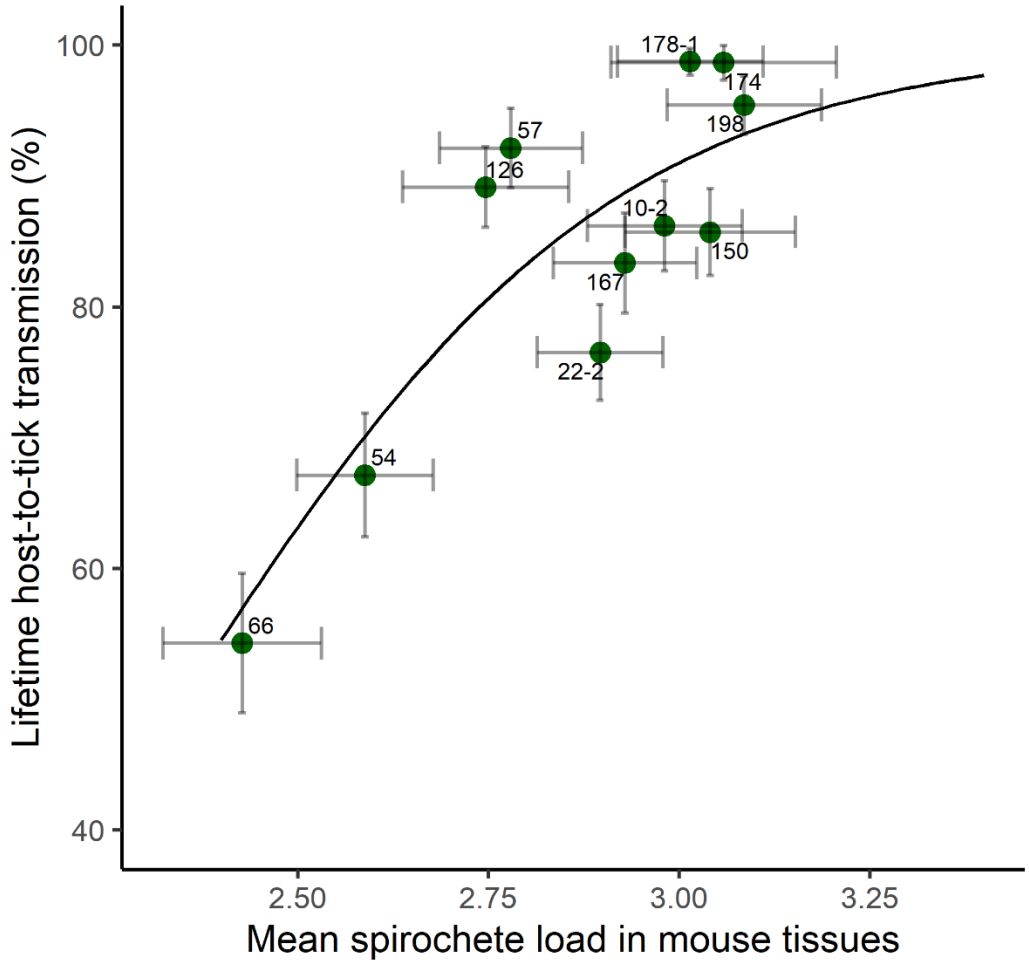

Figure 3.5 The mean spirochete load in the mouse tissues determines the lifetime host-to-tick transmission across the 11 strains of *B. burgdorferi*. The mean spirochete load in the mouse tissues was based on the infected necropsy tissues and was calculated as log10(*23S rRNA*/10^6 *Beta-actin*). The lifetime host-to-tick transmission (HTT) was based on the percentage of nymphs that tested positive for *B. burgdorferi*; these nymphs had taken their larval blood meal on the mice at either day 30, 60, or 90 post-infection. The slope of the logistic regression is positive and significant (slope = 3.55, SE = 0.90, p = 0.003). Labels on datapoints are strain ID numbers. Error bars represent the 95% confidence intervals.

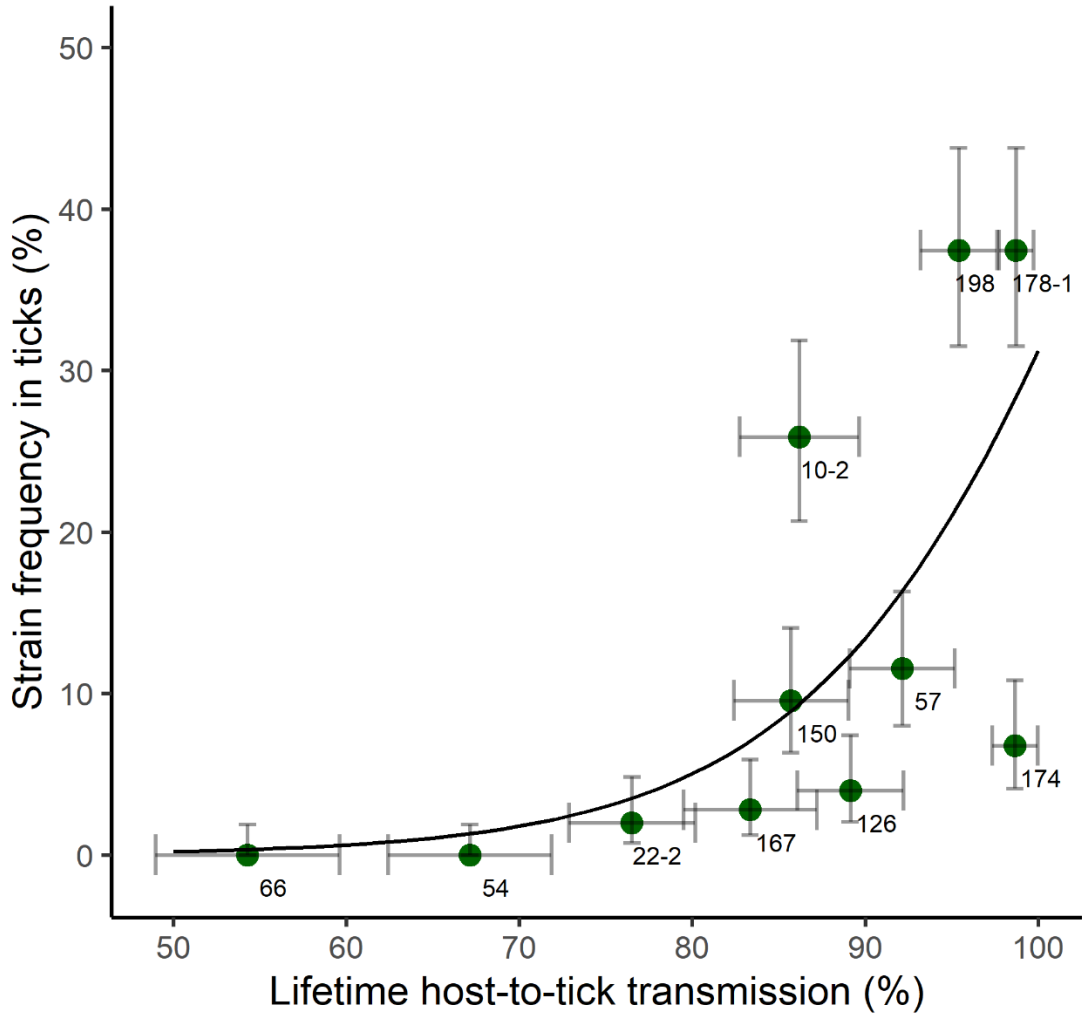

Figure 3.6 Our laboratory-based estimates of the lifetime host-to-tick transmission for the 11 strains of *B. burgdorferi* are positively related to the frequencies of these strains in natural populations of *I. scapularis* ticks in Canada and the USA. The slope of the logistic regression is positive and significant (slope = 10.75, SE = 4.29, p = 0.033). The error bars represent the 95% confidence intervals.

3.6 Discussion

3.6.1 Strain-specific estimates of host tissue abundance predict lifetime HTT

Our primary measure of host-to-tick transmission success for the 11 strains of *B. burgdorferi* was the nymphal infection prevalence (NIP), a common metric of HTT of *Borrelia*

burgdorferi genospecies (LoGiudice et al., 2003; Rynkiewicz et al., 2017; Tonetti et al., 2015). We found that our estimates of lifetime HTT for the 11 strains of *B. burgdorferi* were significantly positively correlated with both host tissue spirochete load (Figure 3.5) and larval infection prevalence (Figure 3.3). Our results agree with previous studies that found a positive phenotypic correlation between host tissue spirochete load and HTT (Genné et al., 2021; Jacquet et al., 2015; Råberg, 2012). The demonstration of a positive correlation between host tissue spirochete load and HTT across 11 genetically distinct strains of *B. burgdorferi* suggests an underlying genetic correlation between these two life history traits, which shapes their evolution. The present study suggests that strains of *B. burgdorferi* are under strong selection to maintain high abundance in the tissues of their reservoir hosts to achieve high HTT to feeding *I. scapularis* ticks. Although the present study did not examine the costs of maintaining high abundance in the host tissues, possible mechanisms include reduced survival of reservoir hosts (i.e., virulence) and/or increased surveillance and attack by the host immune system (Alizon et al., 2009; Anderson & May, 1982). In summary, this study demonstrates the following causal chain linking spirochete replication inside the host to lifetime HTT, high spirochete load in the host tissues results in more feeding larvae acquiring spirochetes, and these engorged infected larvae have a high probability of moulting into infected nymphs.

Many vector-borne pathogens maintain high abundance in the blood to achieve transmission to feeding arthropod vectors (De Roode et al., 2005; Komar et al., 2003; Mackinnon & Read, 1999). *B. burgdorferi* has low abundance in the blood of vertebrate hosts (Lee et al., 2010) and bacteremia is not important for host-to-tick transmission (Tsao, 2009). The host skin has previously been identified as the crucial site of transmission for the closely related spirochete *B. afzelii* (Genné et al., 2021; Jacquet et al., 2015; Råberg, 2012). To obtain the best estimate of

strain-specific tissue abundance in the host tissues, this trait was averaged over 7 necropsy tissues, including skin, ears, and internal organs. This approach is valid because we had previously shown that strain abundances were positively related among all 7 necropsy tissues (Zinck et al., 2022). Our study found that strains of *B. burgdorferi* that established a higher spirochete load in the host tissues had a greater LIP but not necessarily a higher LSL. The engorged larvae were frozen shortly after drop-off, and their spirochete loads are a combination of acquisition and replication. The accurate detection of spirochetes in engorged larvae is complicated by the low spirochete loads leading to false negatives (Eisen, 2020; Genné et al., 2019; Jacquet et al., 2017).

The NIP was consistently higher than the LIP. The LIP estimates the proportion of larvae that acquired the strain after feeding on an infected mouse. The NIP is the product of the LIP and the probability of larva-to-nymph transstadial transmission of the strain. In theory, the LIP should be higher than the NIP. This lower LIP is caused by the reduced sensitivity to detect *B. burgdorferi* in the fed larvae (Eisen, 2020; Genné et al., 2019; Jacquet et al., 2017). Despite this, the strong correlation between our larval and nymphal measures of transmission suggest that the impact of reduced detection is consistent across strains.

3.6.2 Strain-specific estimates of lifetime HTT are related to strain-specific frequencies in nature

Our estimates of lifetime HTT were significantly positively related to the frequency of these strains in nature (Figure 3.6). The strains that have higher HTT in an experimental setting were also the ones that are more commonly found in ticks in nature. We recently showed that our mouse tissue spirochete load estimates are also significantly positively related to strain frequency

(Zinck et al., 2022). This result agrees with a previous study that found that laboratory-based estimates of the R_0 values of six strains of *B. afzelii* were related to their frequencies at a local field site in Switzerland (Durand et al., 2017). The present study is more general because the strain-specific frequencies were obtained from *I. scapularis* tick populations that were distributed across North America (Ogden et al., 2011; Travinsky et al., 2010).

Previous studies have shown that strains of *B. burgdorferi* can be transmitted by many different vertebrate hosts including chipmunks, squirrels, shrews, and other species, but across North America the closely related white-footed and deer mice (*P. leucopus, P. maniculatus*) are the common reservoir hosts (Brisson & Dykhuizen, 2004; Hanincová et al., 2006; Mechai et al., 2016; Vuong et al., 2014). Some of these studies have found associations between vertebrate host species and *B. burgdorferi* strains in transmission to immature *I. scapularis* ticks (Brisson & Dykhuizen, 2004; Mechai et al., 2016). For this reason, we were surprised that our laboratory estimates of strain-specific lifetime HTT in C3H/HeJ mice (*Mus musculus*) were predictive of the frequencies of these *B. burgdorferi* strains in *I. scapularis* tick populations. The estimates of strain frequency we used represent a broad geographic range, and they are likely to be predominantly influenced by *P. leucopus* and *P. maniculatus*. Importantly, these 11 strains are not known to all colocalize in a single area. Our study suggests that the strains that have high HTT in lab mice also have high HTT in the widespread reservoir hosts that are important for the epidemiology of *B. burgdorferi* in nature.

3.6.3 Host sex affects transmission of *B. burgdorferi*

An interesting result was that the lifetime HTT was higher for male mice compared to female mice and this was true for 9 of 11 strains (Figure 3.2). We had recently shown that male

mice have a significantly higher spirochete load in their tissues compared to female mice (Bourgeois et al., 2022; Zinck et al., 2022). The present study suggests that male mice have higher HTT because they have higher spirochete loads in their tissues compared to female mice. In nature, male mice are more likely to be infected with *B. burgdorferi* sl than female mice (Hamer et al., 2012; Tschirren et al., 2013; Voordouw et al., 2015; Zawada et al., 2020), and importantly they are more likely to be parasitized by ticks (Bouchard et al., 2011; Devevey & Brisson, 2012; Ostfeld et al., 2018; Perkins et al., 2003). Independent of susceptibility and given equal exposure to feeding larval *I. scapularis*, ticks feeding on male mice had a higher likelihood of becoming infected with *B. burgdorferi*. This result suggests that male mice contribute more to the prevalence of infected ticks in nature and hence to the risk of Lyme borreliosis compared to their female counterparts.

3.6.4 HTT decreases over time for most *B. burgdorferi* strains

Host-to-tick transmission was above 85% for the first infestation (30 days PI) for all 11 strains and above 90% for all three infestations in 3 strains (Figure 3.1). For the other 8 strains, HTT decreased over the 3 successive infestations and the magnitude of the decrease determined variation in lifetime HTT (Figure 3.1), which agrees with other studies (Donahue et al., 1987; Hanincova et al., 2008; Jacquet et al., 2016; Richter et al., 2004). Three strains (22-2, 54, and 66) had the most dramatic decrease in HTT over time (Figure 3.1). Interestingly, two of these three strains (54 and 66) had been previously shown to have the most dramatic decrease in ear tissue spirochete load over the course of the infection (Zinck et al., 2022). *B. burgdorferi* can create antigenic variation at the immunodominant VlsE protein, which allows it to evade the host antibody response and establish a persistent infection in the tissues of the vertebrate host (Graves

et al., 2013). Thus, one mechanistic explanation for the dramatic decrease in HTT over time in strains 22-2, 54, and 66 is that these strains are less able to evade the host antibody response.

3.6.5 Conclusions

We tested the variation in host-to-tick transmission among strains of *B. burgdorferi* using a laboratory model host. We found that these estimates of HTT were positively correlated with measures of host tissue spirochete load, and with the strain frequencies in nature. From this we suggest a simple mechanistic explanation, where strains that establish a higher spirochete load in the tissues of the vertebrate host are more likely to be acquired by feeding larvae, which in turn results in more infected questing nymphs. The strains with higher spirochete loads in the host tissues and higher lifetime host-to-tick transmission are thus more common in nature.

4 Strains of *Borrelia burgdorferi* exhibit different virulence in a laboratory model host

Acknowledgements
I would like to thank Dr. Susan Detmer and Dr. Pini Zvionow for their assistance in necropsy and tissue collection. I would like to thank Georgia Hurry, Alexandra Foley-Eby, Prasobh Thampy, and the staff of the WCVM animal care unit for their assistance with the experimental infection study. I would like to thank Dr. Pini Zvionow for his work preparing and scoring the pathology tissues.

4.1 Transition Statement

Virulence is the last of the three pathogen life history traits to be analyzed for our 11 strains of *B. burgdorferi*. Chapters 2 and 3 estimated pathogen abundance in the host tissues and pathogen transmission. These two pathogen life history traits were significantly positively correlated as expected by evolutionary virulence theory. Both measures were also predictive of the frequencies of these *B. burgdorferi* strains in nature. Virulence is defined as the pathogen-induced reduction in host fitness. Evolutionary theory predicts a positive correlation between virulence, pathogen abundance in the host tissues and pathogen transmission. *Borrelia burgdorferi* can cause debilitating disease in human Lyme disease patients. In some strains of laboratory mice (*Mus musculus*), *B. burgdorferi* causes arthritis and carditis. However, there is not much evidence that *B. burgdorferi* causes pathology or virulence in its common reservoir host, the white-footed mouse *Peromyscus leucopus*. In this chapter, we investigate the virulence caused by *B. burgdorferi* in C3H/HeJ mice and whether it conforms to the relationship predicted by evolutionary virulence theory.

4.2 Abstract

The defining feature of a pathogen is virulence, the damage it causes to its host. Evolutionary virulence theory predicts that virulence should be positively correlated with pathogen abundance in the host tissues and pathogen transmission. These relationships can be altered by host factors like immunopathology, where virulence may depend more on the strength of the host immune response rather than pathogen abundance in the host tissues. This study investigated the relationship between measures of virulence and pathogen abundance in the host tissues among 11 field-collected strains of the tick-borne spirochete *Borrelia burgdorferi* in a model rodent host (*Mus musculus*, C3H/HeJ). Male and female mice were experimentally infected with 1 of 11 strains of *B. burgdorferi* and virulence measures of change in body weight, ankle swelling, and histopathology were taken. These were then compared against the abundance of *B. burgdorferi* in host tissues and the host IgG antibody response. Virulence measures differed among the 11 *B. burgdorferi* strains, but there was no relationship between measures of virulence and spirochete abundance in host tissues. Across the 11 strains, there was a significant positive relationship between ankle swelling at day 28 PI and the strength of the mouse IgG antibody response. Female mice had more carditis and higher IgG antibody responses despite lower abundances of *B. burgdorferi* compared to male mice. Variation in virulence phenotypes of *B. burgdorferi* in *Mus musculus* appears to be linked to the host immune response rather than spirochete load in the host tissues.

Keywords

Borrelia burgdorferi, Lyme borreliosis, virulence, pathogen life-history, immunopathology

4.3 Introduction

Parasites (including pathogens) exploit the resources of their hosts, which causes disease and reduces host fitness (Anderson & May, 1982; Musser, 1996). Evolutionary biologists use the term 'virulence' to refer to the negative effect of the parasite on host fitness (e.g., reduced host survival and/or host reproduction). As host fitness is often difficult to measure, virulence is often used to refer to any parasite-induced reduction in host health that correlates with host fitness. In evolutionary theory, virulence is seen as a trait of the parasite, but it is always measured in the host. Virulence is influenced by both parasite and host factors (Klein & Flanagan, 2016; Mackinnon & Read, 1999; Wooten & Weis, 2001).

Pathogen populations often consist of multiple strains that differ in their virulence (Bell et al., 2006; De Roode et al., 2005; Forbes et al., 2008; Lysenko et al., 2010). Evolutionary virulence theory predicts that there are trade-offs between pathogen abundance in the host tissues, transmission, and virulence (Acevedo et al., 2019; Anderson & May, 1982). Strains with high abundance in the host tissues are expected to have the benefit of higher transmission but incur the cost of higher host exploitation, higher virulence, and thus a shorter lifespan of infection. In human HIV-1 infections, patients with a higher viral titre have a higher likelihood of transmitting HIV-1 per sex act but they have earlier onset of AIDS and hence a shorter infectious period (Fraser et al., 2007). In the rodent malaria parasite *Plasmodium chabaudi,* strains with high parasitemia have higher transmission to blood-feeding *Anopheles* mosquitoes, but they cause more severe anemia and are more likely to kill the rodent host (Bell et al., 2006; Mackinnon & Read, 1999). For *Streptococcus pneumoniae*, high abundance strains are more likely to transmit but cause more inflammation in the nasopharynges (Richard et al., 2014).

These examples demonstrate the positive relationship between pathogen abundance in host tissues and host damage, as expected by evolutionary virulence theory.

In response to infection, the host mounts an immune response that feeds back on the pathogen population, which in turn influences the severity of disease and virulence (Klein, 2004; Klein & Flanagan, 2016; Li et al., 2012). A competent host immune response clears the pathogen from the host tissues thereby resolving disease and virulence. In contrast, the host sometimes mounts an inappropriate immune response to infection that causes further damage to the host, and this phenomenon is referred to as immunopathology (Graham et al., 2005). In the previous example of *S. aureus*, the inflammation is produced by the host immune system in response to the infection rather than a function of the pathogen directly (Richard et al., 2014). When immunopathology contributes to virulence, virulence may be correlated with the strength of the host immune response rather than the abundance of the pathogen in the host tissues. The host immune response is also affected by additional host factors such as age, nutritional condition, and host sex (Barthold et al., 2006; Fleming-Davies et al., 2018; Klein & Flanagan, 2016). Host sex is important because testosterone-based immunosuppression makes males more susceptible to infections and have higher pathogen loads compared to females. In contrast, females tend to have stronger immune responses, leading to greater immunopathology than males (Klein, 2004; Klein & Flanagan, 2016; Roved et al., 2017).

Globally, zoonoses, which includes vector-borne diseases, pose the fastest growing risk of emerging infectious diseases to humans (Jones et al., 2008; Taylor et al., 2001). In North America and Europe, Lyme borreliosis (LB) is the most common vector-borne disease and the annual incidence of LB is increasing in many places (Mead, 2015; Steere et al., 2016; Steinbrink et al., 2022). LB is caused by spirochete bacteria belonging to the *Borrelia burgdorferi* sensu lato

genospecies complex, principally *B. burgdorferi* sensu stricto (herein *B. burgdorferi*), *B. afzelii*, and *B. garinii* (Baranton, Assous, et al., 1992). In North America, *B. burgdorferi* is the main cause of LB and east of the Rocky Mountains it is transmitted by the blacklegged tick, *Ixodes scapularis* (Ogden et al., 2011; Sperling & Sperling, 2009). The zoonotic cycle of *B. burgdorferi* involves the immature stages of *I. scapularis* (larvae and nymphs), which feed on the same vertebrate reservoir hosts (Anderson et al., 1987; Barbour, 2017). Larvae acquire the infection after feeding on an infected host and subsequently moult into an infected nymph that transmits the spirochetes to the next generation of reservoir hosts the following year (Radolf et al., 2012).

Virulence theory applies to pathogens that have a negative impact on the fitness of their host organism. *Borrelia burgdorferi* causes debilitating disease in human LB patients and symptoms include arthritis, carditis, and neurological problems (Steere et al., 2016; Wooten & Weis, 2001; Wormser et al., 2006). However, humans are accidental dead-end hosts (i.e., they do not transmit the infection back to feeding ticks) that are not expected to influence the evolution of *B. burgdorferi*. The white-footed mouse, *Peromyscus leucopus*, is a key reservoir host for the epidemiology of LB because *B. burgdorferi* can establish chronic infections in this host (Bunikis, Tsao, et al., 2004; Donahue et al., 1987; Rynkiewicz et al., 2017) and because it feeds large numbers of immature *I. scapularis* ticks (Brunner & Ostfeld, 2008; Keesing et al., 2009). However, there is not much evidence to suggest that *B. burgdorferi* causes significant reductions in fitness in white-footed mice (Hofmeister et al., 1999; Moody et al., 1994; Schwanz et al., 2011; Voordouw et al., 2015). *Borrelia burgdorferi* does cause pathology in the laboratory model species house mouse (*Mus musculus*), although we emphasize that the house mouse is not a natural reservoir host. *Mus musculus* infected with *B. burgdorferi* develop arthritis and carditis (Barthold et al., 1990; Weis et al., 1997). Spirochete abundance in mouse tissues and disease

severity differ among mouse strains (Armstrong et al., 1992; Barthold et al., 1990; Ma et al., 1998; McKisic et al., 2000; Wooten & Weis, 2001). Experimental infections with lab mice have also shown that strains of *B. burgdorferi* can differ in their abundance in host tissues, induction of the host immune response, and pathology (Dolan et al., 2004; Lin et al., 2014; Lin et al., 2020; Strle et al., 2011; Wang et al., 2002; Wang et al., 2001; Zeidner et al., 2001; Zinck et al., 2022). In summary, host factors (mouse strain) and pathogen factors (*B. burgdorferi* strain) both influence virulence.

We recently performed experimental infections where C3H/HeJ mice (male and female) were experimentally infected with 11 strains of *B. burgdorferi*. We measured various pathogen life history traits including spirochete abundance in the host tissues, lifetime host-to-tick transmission, host serum antibody response, and six measures of pathology (or virulence), which included mouse body weight, mouse ankle swelling, and lesions in 4 mouse tissues including the kidney, ventral skin, heart, and rear tibiotarsal joint. In previous studies, we showed that the spirochete abundance in the host tissues is positively correlated with lifetime host-to-tick transmission across 11 strains of *B. burgdorferi*. Importantly, we validated these laboratory estimates of pathogen fitness by showing that they were correlated with strain frequency in nature (Zinck et al., 2022). We also found that male mice have significantly higher tissue spirochete loads and host-to-tick transmission compared to female mice for 9 of the 11 *B. burgdorferi* strains. The present study has three aims. First, test whether there is significant variation in the host antibody response and the virulence traits among strains. Second, investigate the pattern of correlations across the 11 *B. burgdorferi* strains between spirochete load in the host tissues, host serum antibody response, and the six measures of virulence. Third, test whether host sex influences *B. burgdorferi*-induced pathology.

We hypothesize that there will be significant variation in pathology (or virulence) among the 11 strains of *B. burgdorferi*. The classic virulence model predicts that virulence will be positively correlated with spirochete abundance in the mouse tissues across the 11 *B. burgdorferi* strains. As male mice have higher tissue spirochete loads compared to female mice (Zinck et al., 2022), we predict that male mice will have more pathology than female mice. The immunopathology model predicts that pathology will be correlated with the mouse antibody response across the 11 *B. burgdorferi* strains. As females have stronger antibody responses to *B. burgdorferi* infection compared to male mice, the immunopathology model predicts that female mice will have more pathology than male mice.

4.4 Materials & Methods

4.4.1 *Borrelia burgdorferi* strains, C3H/HeJ mice, and ticks

In this study, 11 low passage strains of *B. burgdorferi* were used from the isolate collection of the Public Health Agency of Canada. Initially, 12 strains were selected however one failed to infect the mice and is not included here (Zinck et al., 2022). These strains originated from *I. scapularis* ticks collected in Canada (Tyler et al., 2018). All strains were whole genome sequenced and their multi-locus sequence type and *ospC* type were determined prior to use (Tyler et al., 2018). During culture, strains of *B. burgdorferi* sometimes lose plasmids that are critical for establishing infection in the mouse host or the tick vector. For this reason, the plasmid content of the strains was checked using PCR to confirm the presence of the critical plasmids (Zinck et al., 2022).

Female and male specific-pathogen-free 6- to 8-week-old *Mus musculus* C3H/HeJ mice were purchased from The Jackson Laboratory for use as the host in this study. C3H/HeJ mice

develop noticeable tissue lesions and ankle swelling in response to infection with *B. burgdorferi* and this mouse strain has previously been used to compare pathology between different strains of *B. burgdorferi* (Barthold et al., 1990; Dolan et al., 2004; Wang et al., 2002; Wang et al., 2001). The use of mice and all procedures in this study were reviewed and approved by the Animal Research Ethics Board at the University of Saskatchewan (permit number 20190012).

Laboratory-reared specific-pathogen-free *I. scapularis* larvae were obtained from the National Tick Research and Education Resource at Oklahoma State University. This colony is regularly outbred with wild *I. scapularis* to prevent inbreeding and screened for multiple tick-borne pathogens including *B. burgdorferi*.

4.4.2 Experimental infection of mice with *B. burgdorferi*

For each of the 11 *B. burgdorferi* strains, 8 mice (4 female, 4 male) were experimentally infected via nymphal tick bite for a total of 88 mice in the infected group (44 female, 44 male). Each mouse was infested with 3 *I. scapularis* nymphs putatively infected with the strain of interest, and the nymphs were allowed to feed to repletion. Subsequent testing of these blood-engorged nymphs found that each mouse was exposed to 1-3 infected nymphs (Zinck et al., 2022). There were 20 mice in the uninfected control group (10 female, 10 male); each mouse was infested with 3 uninfected control nymphs. To manage the workload, the study was split in two orthogonal temporal blocks (A, B) that were started ~6 months apart. Each block contained half the control mice and half the mice for each of the 11 strains.

Mice had ear tissue biopsies taken at days 29, 59, and 89 PI, and blood samples taken at pre-infection (-2 to -1 weeks PI) and at day 28 PI as previously described (Zinck et al., 2022). To

measure the lifetime host-to-tick transmission of the 11 strains of *B. burgdorferi*, mice were infested with larval *I. scapularis* at days 30, 60, and 90 PI.

4.4.3 Mouse body mass measurements

Mouse body mass measurements were recorded weekly from day -10 PI to day 96 PI, except during periods of larval infestation. Mouse body mass was measured by placing mice in a sterile plastic container on a balance and recording to the nearest 0.1 g.

4.4.4 Mouse ankle width measurements

Previous studies have shown that infection with *B. burgdorferi* causes joint swelling in C3H/HeJ mice (Wang et al., 2002; Wang et al., 2001). To measure *B. burgdorferi*-induced joint swelling, the width of both the left and right rear tibiotarsal joints (i.e., ankles) were recorded weekly from day -10 PI to day 96 PI, except during periods of larval infestation. Ankle measurements were done following a modified version of the protocol used by Wang et al. (2002). Each mouse was scruffed and held supine so the hind legs would be accessible. Digital calipers (0.01 mm) were used to measure the width of the thickest part of the joint, along the anteroposterior line. The calipers and plane of measurement were kept parallel with the plane of movement of the joint. This process was repeated for the left and right rear tibiotarsal joints.

4.4.5 Necropsy and tissue sample preparation

At 97 days PI, mice were euthanized with an isoflurane overdose followed by cervical dislocation, and exsanguination via cardiac puncture. Immediately following euthanasia, mice were necropsied, and 4 mouse tissues were dissected including kidney, ventral skin (from the

belly of each mouse), right rear tibiotarsal joint, and heart. All necropsies were done using pre-sterilized instruments, and Virkon was used to sterilize surfaces between mice to prevent cross contamination. Mouse tissues were prepared for histopathological analysis or DNA extraction and subsequent qPCR.

Fresh tissue samples of the 4 mouse necropsy tissues were frozen at – 80 ºC for DNA extraction. Histopathological samples were taken from the kidney, ventral skin, left rear tibiotarsal joint, and heart. These samples were fixed in 10% neutral buffered formalin for 24 hours following dissection. After fixation, osseous tissues were placed in a 20% formic acid decalcifying solution for an additional 48 hours. Tissues were trimmed down and embedded in paraffin blocks for 5 µm sectioning on glass slides for standard hematoxylin and eosin staining.

4.4.6 DNA extraction and qPCR of mouse tissue samples

Mouse tissue samples for DNA extraction and qPCR were processed as described previously (Zinck et al., 2022). Briefly, tissue samples were homogenized by 3.6 mm stainless steel beads using a Qiagen TissueLyser II followed by overnight digestion with proteinase K. The DNA of these homogenized mouse tissue samples was extracted using the Qiagen DNEasy Blood and Tissue kit individual spin columns following the manufacturer's instructions. The extracted DNA was then tested for the presence of *B. burgdorferi* using a qPCR assay that targets the *23S rRNA* intergenic spacer gene (Courtney et al., 2004). A qPCR assay that targets the mouse *Beta-actin* gene was used to quantify the amount of mouse tissue in each DNA extraction (Dai et al., 2009). Quantification cycle (Cq) values for both qPCR assays were transformed using a synthetic gene standard (IDTDNA, gBlock). The abundance of *B.*

burgdorferi in the mouse tissues was reported as the number of *23S rRNA* gene copies per 10^6 mouse *Beta-actin* gene copies.

4.4.7 ELISA to measure mouse IgG antibodies against *B. burgdorferi*

The strength of the mouse serum IgG antibody response to *B. burgdorferi* was measured using a commercial ELISA. Blood samples were allowed to clot for 10–15 min at room temperature followed by centrifugation at 1,500 rcf for 15 min. The serum was transferred to sterile microcentrifuge tubes and stored at -80 ºC until use. All ELISA assays were done using the Zeus Scientific *B. burgdorferi* IgG test system (3Z9651G). This ELISA is prepared with *B. burgdorferi* whole cell adsorption and detects all strains of *B. burgdorferi*. Modifications were made to the manufacturer's protocol to adapt this test to mice. The kit-supplied secondary antibody was substituted with goat anti-mouse IgG conjugated to horseradish peroxidase (Thermo Scientific, #31430) at a 1:5,000 dilution in sterile PBS (0.1 M, pH 7.2). In addition, 1 µL of mouse serum was used with 104 µL of sample diluent. All TMB reactions were stopped at 12.5 min and the absorbance values were read within 30 min at 450 nm (Varioskan Lux multimode microplate reader). The repeatability of the absorbance measurements was 97.7% based on 135 samples retested using separate plates.

4.4.8 Histopathology of *B. burgdorferi*-infected mouse tissues

The prepared slides of the mouse tissues were randomly renumbered to blind the pathologists with respect to the infection status, sex, and infecting *B. burgdorferi* strain of the animal. Mouse tissues were examined by a single pathologist (PZ) to determine deviations from the normal background lesions present in uninfected mouse tissues and a scoring matrix was

developed. Each sample was given a score of no lesions (0), mild lesions (1), or moderate to severe lesions (2). This matrix was validated by two additional pathologists and after consensus was reached, final scores were given for each tissue by PZ. Tissue lesions were scored for 4 tissues: kidney, ventral skin, left rear tibiotarsal joint (ankle), and heart.

4.4.9 Statistical analyses

The strength of the mouse serum IgG antibody response to infection with *B. burgdorferi* was analyzed. Six virulence phenotypes were analyzed: (1) mouse body mass, (2) mouse ankle swelling, and lesions in (3) kidney, (4) ventral skin, (5) left rear tibiotarsal joint, and (6) heart.

4.4.10 Analysis of mouse serum IgG antibody response to *B. burgdorferi*

The IgG antibody response was measured for 3 serum samples: pre-infection, 28 days PI, and 97 days PI (terminal). Linear mixed effect models (LMMs) were run on the post-infection IgG antibody responses of infected mice using the fixed factors of strain (11 levels; see Table 4.1), mouse sex (2 levels: female, male), blood draw (2 levels: 28 days PI, 97 days PI), and their interactions. Block (2 levels: A, B) was included as a fixed factor. Mouse identity was included as a random factor. Non-significant interactions were iteratively removed to generate the final simplified model. Factor significance was estimated using type II Wald tests, and post-hoc analyses were performed and estimated marginal means (EMMs) were calculated.

4.4.11 Analysis of mouse body mass

The mouse body mass on day 84 PI was calculated for each mouse using linear interpolation. A two-way ANOVA was used to test whether mouse sex and *B. burgdorferi* infection status influenced mouse body mass on day 84 PI.

4.4.12 Analysis of mouse ankle swelling

A Pearson correlation was done to test whether the widths of the left rear ankle and the right rear ankle were correlated. To minimize measurement error, the widths of the left rear ankle and the right rear ankle were averaged for each sampling occasion. This mean rear ankle width was used as the response variable in a generalized additive model (GAM) with 3 fixed factors including mouse infection status (2 levels: uninfected, infected), mouse sex (2 levels: female, male), and block (2 levels: A, B). The GAM also included a smoother function of days post-infection conditioned on infection status, and mouse as a random effect. To determine the effect of *B. burgdorferi* strain on mean rear ankle width, the same GAM was used but mouse infection status was replaced with strain (11 levels) in both the fixed effects structure and the smoother function. This GAM was used to generate estimated marginal means (EMMs) of peak ankle width at day 28 PI for each *B. burgdorferi* strain.

4.4.13 Analysis of histopathology scoring

Tissue lesions were scored for 4 tissues: kidney, ventral skin, left rear tibiotarsal joint, and heart. These scores were given on an ordinal scale with three categories, no lesions (0), mild lesions (1), and moderate lesions (2). Mouse tissue lesion score was analyzed separately for each of the 4 tissues using ordinal logistic regression (OLR). The first set of OLRs analyzed tissue

lesion scores as a function of mouse infection status (2 levels), mouse sex (2 levels), and block (2 levels). Once these OLRs had demonstrated that *B. burgdorferi* infection influenced lesion scores in the four mouse tissues, a second set of OLRs was used to determine the importance of *B. burgdorferi* strain. This second set of OLRs analyzed tissue lesion scores as a function of strain (11 levels), mouse sex (2 levels), their interaction, and block (2 levels). The mean spirochete load in each of the 4 mouse tissues, $\log_{10}$(*23S rRNA* copies per 10^6 *Beta-actin*), was included as a covariate. For the analysis of lesions in the left rear tibiotarsal joint, the mean rear ankle width at day 28 PI was also included as a covariate. Factor significance was estimated using type II Wald tests, post-hoc analyses were performed and EMMs were calculated.

4.5 Results

4.5.1 Infection success of the mice

Of the 88 mice in the infected group, 84 were successfully infected (Table 4.1, Zinck et al., 2022). The 4 mice that failed to become infected were excluded from all analyses. Infection status of the mice was confirmed by detection of *B. burgdorferi* in ear tissue biopsies and necropsy tissues (via qPCR), and detection of IgG antibodies in mouse serum samples (via ELISA) (Zinck et al., 2022). All 20 uninfected control mice tested negative for *B. burgdorferi* in all tissues. All tissues for all mice were successfully processed and tested for both histopathology and qPCR, except the ventral skin sample for one uninfected control mouse.

Table 4.1 The genetic identity and location of origin are shown for the 11 strains of *B. burgdorferi* used in the study. Strain identity numbers are from the reference publication (Tyler et al., 2018). All successfully infected mice (n = 84) had direct detection of *B. burgdorferi* in ear biopsies and necropsy tissues by qPCR and a strong serum IgG antibody response.

Strain ID	MLST	*ospC* type	Origin: Town (Province)	Infected mice
57	29	Y, A3	Buffalo Point (MB)	8/8
174	37	T	Lunenburg (NS)	5/8
167	12	M	Shelburne (NS)	8/8
178-1*	3	K	Lunenburg (NS)	8/8
198	3	K	Bedford (NS)	8/8
22-2	55	A	Buffalo Point (MB)	8/8
150	19	E	Lunenburg (NS)	8/8
10-2	32	H, C3	Roseau River (MB)	8/8
66	237	J	Buffalo Point (MB)	7/8
54	741	I	Buffalo Point (MB)	8/8
126	43	N	Big Grassy (ON)	8/8
Total				84/92
Uninfected**	NA	NA	NA	0/20

*This strain was originally intended to be 178-2 but is 178-1 (Tyler et al., 2018), thus we have two isolates of the same strain in this study (MLST 3, *ospC* K).
** Uninfected control mice were fed upon by uninfected *I. scapularis* nymphs. As expected, these 20 mice all tested negative for the 3 *B. burgdorferi* infection criteria.

4.5.2 Mouse serum IgG antibody response against *B. burgdorferi*

The mouse serum IgG antibody response to *B. burgdorferi* was measured in blood samples taken at pre-infection (Pre), day 28 PI (Post), and day 97 PI (Terminal). Of the 84 infected mice, all showed a significant increase in their serum IgG antibody levels to *B. burgdorferi* from pre-infection to post-infection (paired t-test, $p = 2.2*10^{-16}$). The serum IgG antibody response to *B. burgdorferi* was analyzed using an LMM with mouse infection status (infected, uninfected) and blood sample (pre-infection, day 28 PI, day 97 PI) as fixed factors. Uninfected mice had non-existent IgG antibody response (0.05–0.06). Infected mice showed an increased IgG antibody response in their post-infection samples (day 28 PI: 1.73, day 97 PI: 2.77) compared to their pre-infection sample (0.05).

For the subset of the 84 infected mice, the IgG antibody response was analyzed using an LMM with the fixed factors of strain, blood sample (day 28 PI, day 97 PI), sex, their interactions,

and the main effect of temporal block. All interactions were not significant and therefore removed from the model. The main effects of strain ($p = 2.276*10^{-16}$), blood sample ($p = 2.2*10^{-16}$), mouse sex ($p = 0.012$), and temporal block ($p = 9.465*10^{-4}$) were significant. Across all strains, the IgG antibody response of females was 1.06x higher compared to males ($p = 0.015$). The IgG antibody response on day 97 PI was 1.60x higher compared to day 28 PI (see Appendix C). The IgG antibody response of block B was 1.09x higher compared to block A. There were strain-specific differences in the IgG antibody response to *B. burgdorferi* (Figure 4.1). Most strains had similar IgG antibody response values (range: 2.1–2.5), two strains had a low IgG antibody response (strain 174: mean = 1.7; strain 167: mean = 1.8) and one strain had a high IgG antibody response (strain 22-2: mean = 2.8).

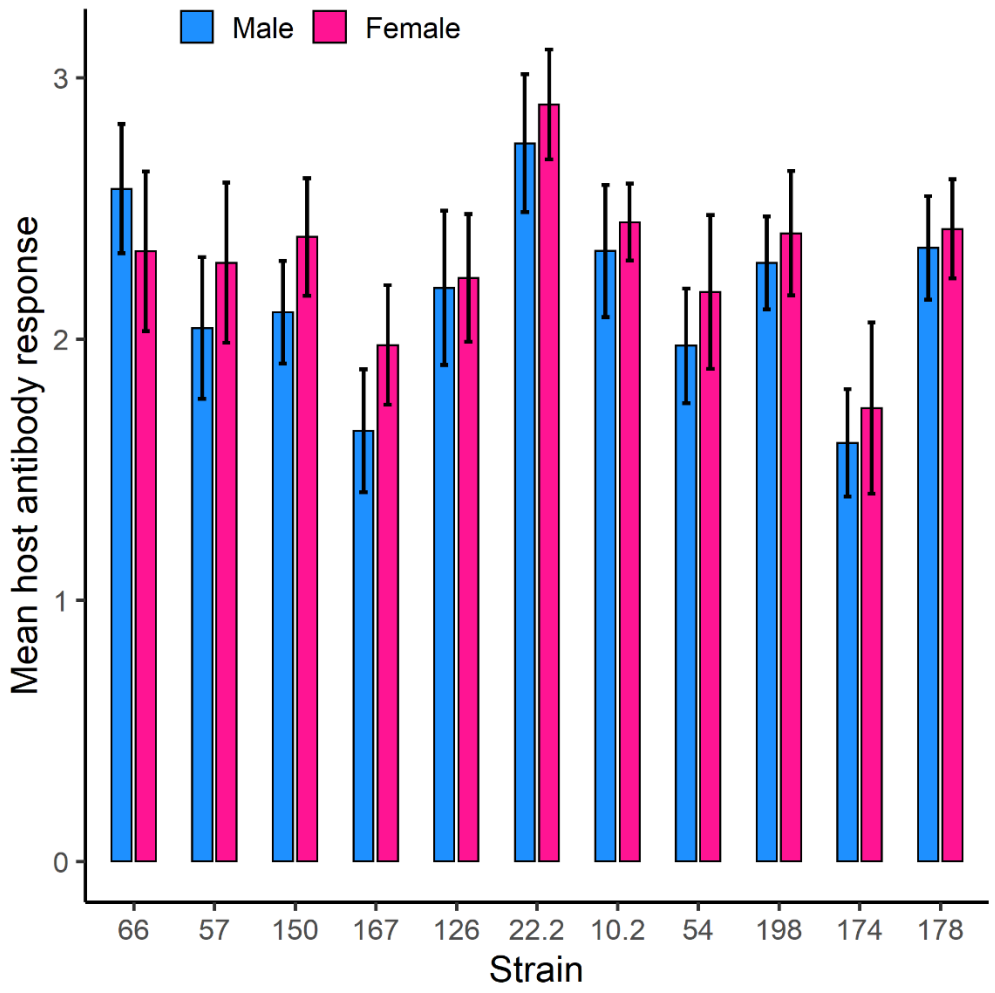

Figure 4.1 The strength of the mouse serum Ig antibody response differed among *B. burgdorferi* strains and between the mouse sexes. The mouse serum IgG antibody response was measured using the Zeus ELISA kit, which uses whole spirochetes. Female C3H/HeJ mice generally had a stronger serum IgG antibody response compared to male mice. Shown are the estimated marginal means and the 95% confidence intervals.

4.5.3 Mouse body mass

The analysis of mouse body mass included 104 C3H/HeJ mice, of which 20 were uninfected (12 females and 8 males) and 84 were infected (41 females and 43 males). The body mass measurements were taken on a weekly basis over a period for which the start and end corresponded to a median mouse age of 61 days (range 55 to 63 days) and 168 days (range 141

to 213 days), respectively. At the time of infection via tick bite, the median age of the mice was 64 days (range = 56 to 86 days). With respect to the age of the infection, the body mass measurements were taken on a weekly basis over a period for which the start and end corresponded to a median age of infection of 1.5 days pre-infection (range 25 to 1 days pre-infection) and 105 days post-infection (PI; range 84 to 127 days PI). For the 104 mice we obtained a total of 1149 body mass measurements; the mean was 11 measurements per mouse (range: 10 to 13 body mass measurements).

A two-way ANOVA was used to test whether mouse sex and *B. burgdorferi* infection status influenced the mouse body mass on day 84 PI (see Appendix C). The interaction between sex and *B. burgdorferi* infection status was not significant ($F_{1, 100} = 0.115$, $p = 0.736$). The effect of sex was highly significant ($F_{1, 100} = 187.299$, $p < 2.2*10^{-16}$), but the effect of *B. burgdorferi* infection status was not ($F_{1, 100} = 2.221$, $p = 0.139$). The mean body size on day 84 for males (n = 53 male mice; mean ± SE = 31.03 g ± 0.381 g) was 25.4% heavier compared to the females (n = 51 female mice; mean ± SE = 24.74 ± 0.356 g). In summary, there was no evidence that infection with *B. burgdorferi* influenced the body mass of C3H/HeJ mice.

4.5.4 Mouse ankle joint swelling

There was a strong positive correlation in the ankle width between the left and right rear tibiotarsal joints ($r = 0.692$, $t = 33.832$, $df = 1247$, $p < 2.2*10^{-16}$). Mouse infection status ($p = 4.81*10^{-15}$), mouse sex ($p = 8.62*10^{-11}$), and block ($p = 0.004$) had significant effects on the mouse mean ankle width (see Appendix C. The effects of days post-infection, infection status, and mouse sex on the ankle width are shown in Figure 4.2. Peak ankle swelling for infected mice occurred on day 28 PI. Averaged across sexes and blocks and on day 28 PI, the mean ankle

width for infected mice (4.33 ± 0.016) was 9.5% bigger compared to uninfected mice (3.96 ± 0.014). Averaged across infection status and blocks and on day 28 PI, the mean ankle width for male mice (4.21 ± 0.012) was 2.9% bigger compared to female mice (4.09 ± 0.012). Averaged across infection status and sex and on day 28 PI, the mean ankle width for mice in block B (4.12 ± 0.013) was 1.0% lower compared to mice in block A (4.17 ± 0.012).

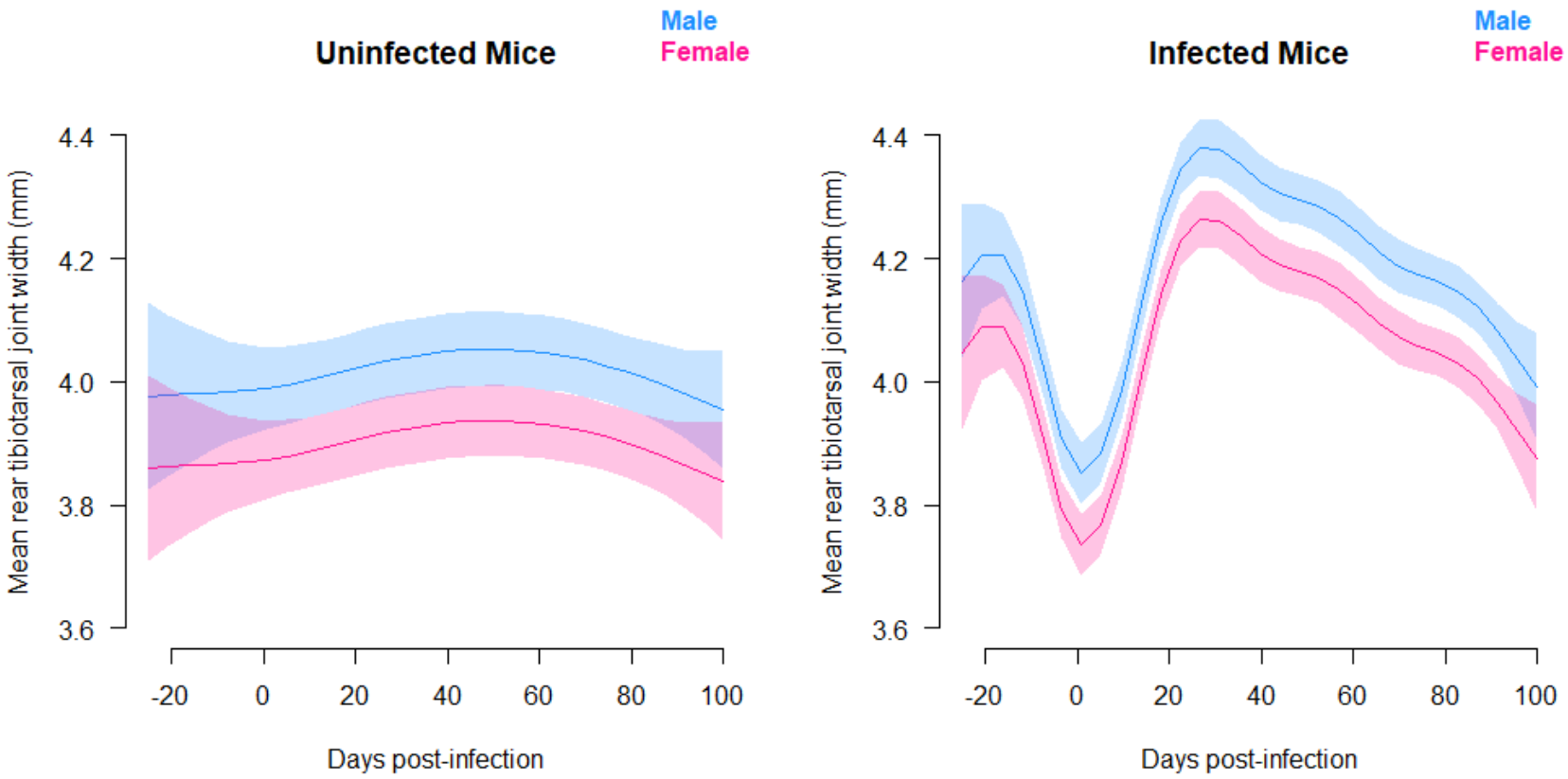

Figure 4.2 Parameter estimates of the GAM of rear tibiotarsal joint as a function of days post-infection, mouse infection status, and mouse sex. The diameter of the rear tibiotarsal joint (ankle width) was averaged for the left and right leg and was measured in mm. Day 0 corresponds to the day of infection with *B. burgdorferi* via nymphal tick bite. For uninfected mice, there is a concave relationship between ankle width and days post-infection. For infected mice, the ankle width increases dramatically after infection via nymphal tick bite and then decreases slowly over time.

A separate GAM was used to determine the effect of *B. burgdorferi* strain on mouse ankle swelling (see Appendix C). Strain ($p = 1.186*10^{-27}$), sex ($p = 9.052*10^{-15}$), and block ($p = 0.0008$) all had significant effects on the mouse mean ankle width. To evaluate differences among strains, mouse ankle swelling was expressed as a percent increase in ankle width relative to the uninfected control mice on day 28 PI. Strain 22-2 increased mouse ankle width by 13.6%, whereas strain 167 only increased mouse ankle width by 1.6% (Figure 4.3). All strains except 167 produced significant ankle swelling on day 28 PI compared to the uninfected control mice. The mean ankle width on day 28 PI was 2.7% bigger in male mice compared to female mice. The mean ankle width on day 28 PI was 1.5% bigger in block A compared to block B. In summary, ankle swelling at day 28 PI differed among strains of *B. burgdorferi* and was more severe in male mice.

There was no correlation between the abundance of *B. burgdorferi* in joint tissues at necropsy (day 97 PI) and the mean ankle width on day 28 PI ($r = 0.054$, $t = 0.715$, $df = 9$, $p = 0.493$, see Appendix C). There was a significant positive correlation between mouse serum IgG antibody response on day 28 PI and mean ankle width on day 28 PI ($r = 0.428$, $t = 2.594$, $df = 9$, $p = 0.029$, Figure 4.4). Strains of *B. burgdorferi* that induced a higher serum IgG antibody response on day 28 PI (as measured by IgG antibody binding to whole spirochetes) also caused more ankle swelling on day 28 PI.

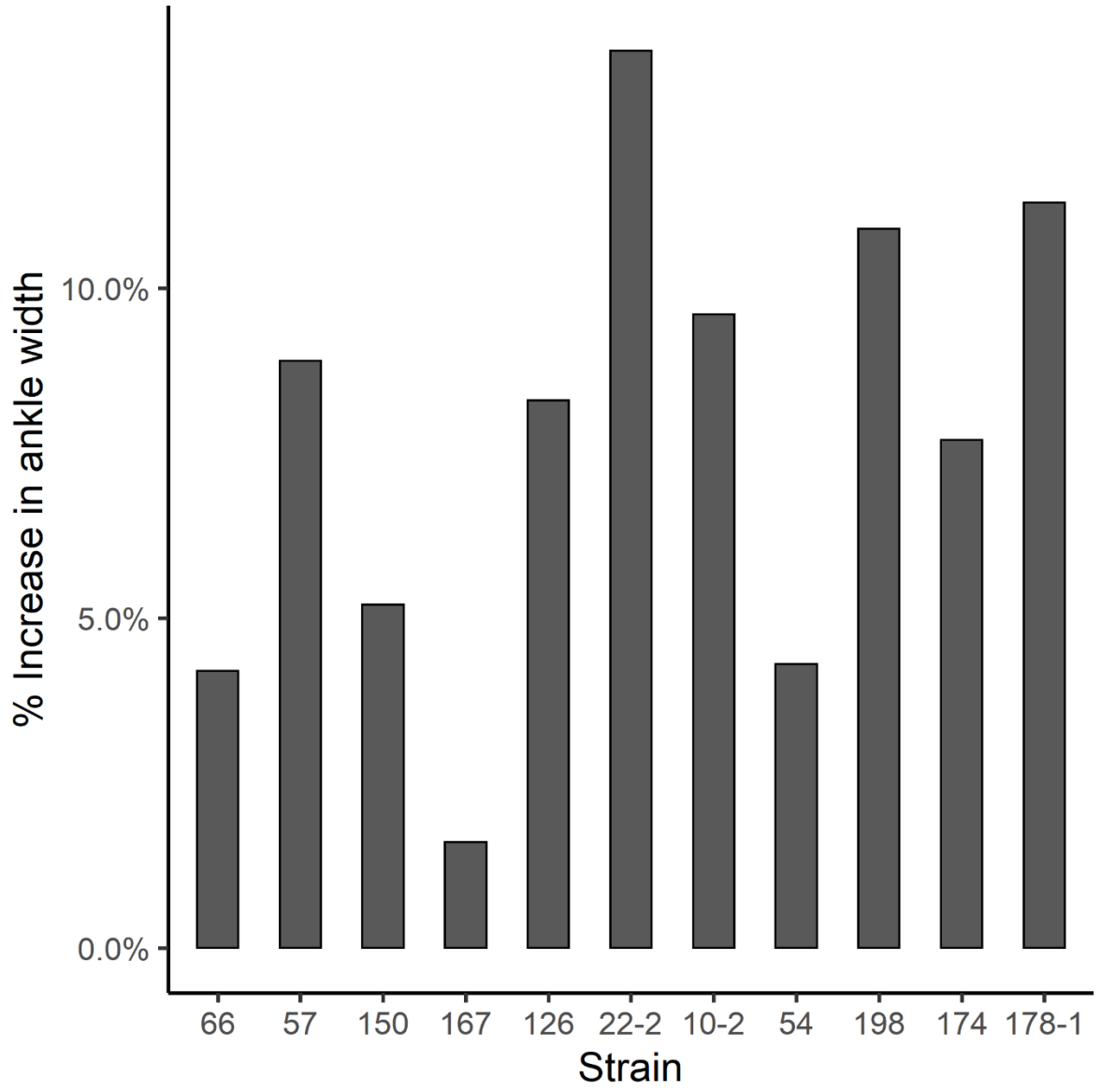

Figure 4.3 Estimated marginal means (EMMs) of strain-specific ankle swelling at day 28 PI expressed as their percent increase over uninfected control mice. For the 11 strains of *B. burgdorferi*, the EMMs were averaged over the two sexes and the two blocks.

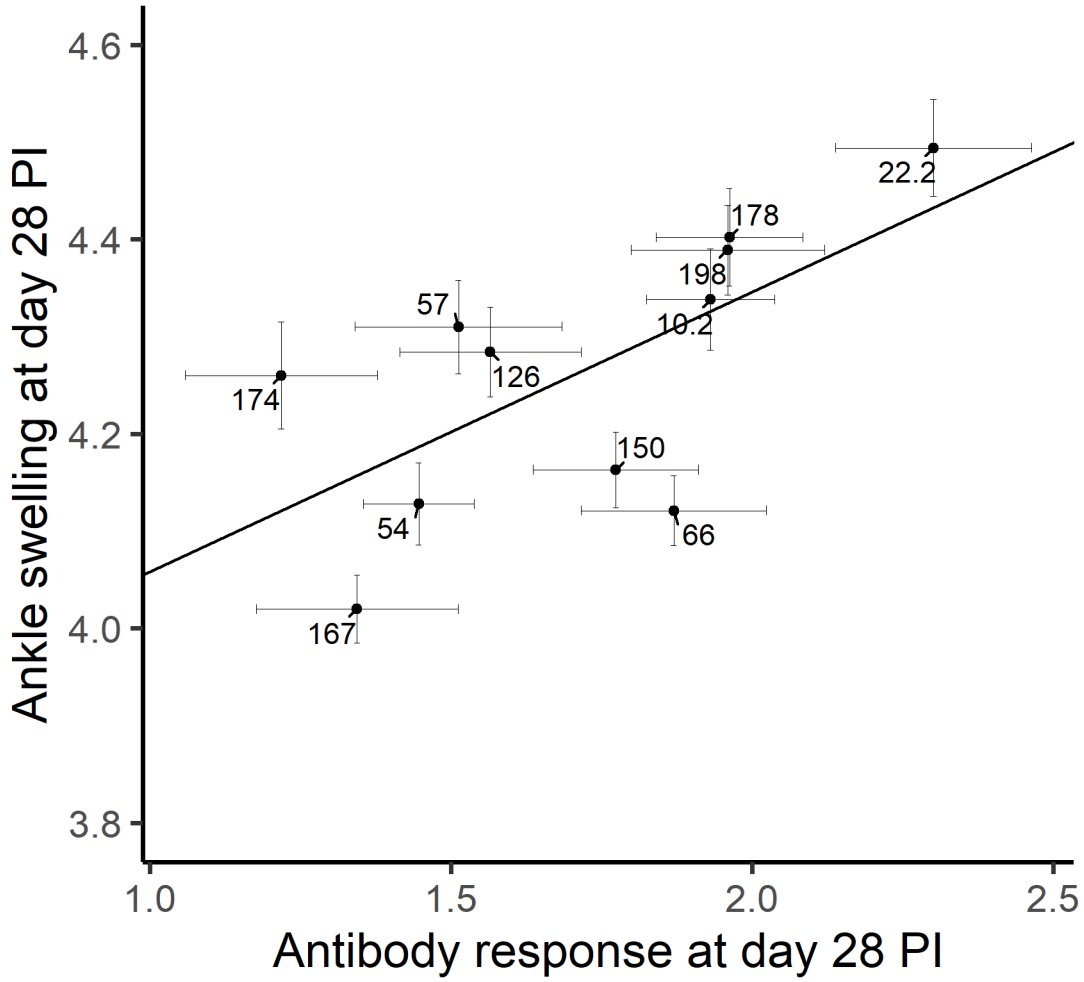

Figure 4.4 Relationship between mouse ankle swelling at day 28 PI versus the mouse serum IgG antibody response at day 28 PI across the 11 strains of *B. burgdorferi* (r = 0.428, t = 2.594, df = 9, p = 0.029). For each strain the 95% confidence interval is shown for the mean mouse ankle swelling and the mean mouse serum IgG antibody response.

4.5.5 *B. burgdorferi*-induced lesions in mouse tissues

For all 4 tissue types (kidney, ventral skin, rear left tibiotarsal joint, and heart), mouse tissues infected with *B. burgdorferi* had significantly more lesions compared to tissues of uninfected control mice ($p < 0.05$, see Appendix C). The increase in lesion scores over uninfected mice varied among tissue types based on the parameter estimates with kidney having the least difference (kidney: 1.490; ventral skin: 19.575; tibiotarsal joint: 19.701; heart: 19.574).

The strain-specific EMMs generated from the OLRs were highly correlated with the strain-specific averages of the histopathology scores for all 4 tissue types ($p <<< 0.05$, $r > 0.97$, see Appendix C). All results will be reported using the strain-specific averages of the tissue lesion scores.

In the kidney, there was a significant effect of *B. burgdorferi* strain ($p = 0.011$), block ($p = 0.007$), and the strain and sex interaction ($p = 0.020$), but not sex ($p = 0.064$) on the lesion score. Strain-specific kidney lesion scores ranged from 0.600 in strain 174 to 1.625 in strain 198. Female mice had higher mean kidney lesion scores compared to male mice for 9 of 11 strains, but not strains 174 and 178, which drove the strain x sex interaction. Mice in block A had a higher mean kidney lesion score compared to mice in block B. Across the 11 strains, there was no correlation between the mean spirochete load in the kidney and the mean lesion score in the kidney ($r = 0.053$, $t = 0.711$, $df = 9$, $p = 0.495$).

In the ventral skin, there was no significant effect of *B. burgdorferi* strain, mouse sex, or temporal block on the lesion score. Across the 11 strains, there was no correlation between the mean spirochete load in the ventral skin and the mean lesion score in the ventral skin ($r = 0.189$, $t = 1.446$ $df = 9$ $p = 0.182$).

In the tibiotarsal joint, strain was highly significant ($p = 2.896*10^{-4}$) but no other factors, including peak joint width on day 28 PI ($p = 0.755$), had significant effects on the lesion score. Strain-specific tibiotarsal joint lesion scores ranged from 0.25 in strain 57 to 1.625 in strain 178. Across the 11 strains, there was no correlation between the spirochete load in the right rear tibiotarsal joint and the mean lesion score in the left rear tibiotarsal joint ($r = 0.171$, $t = 1.363$, $df = 9$, $p = 0.206$). Across the 11 strains, there was no correlation between the ankle width at day 28 PI and the mean lesion score in the tibiotarsal joint at day 97 PI ($r = 0.381$, $p = 0.248$).

In the heart, strain ($p = 7.280*10^{-4}$), mouse sex ($p = 1.944*10^{-4}$), and the interaction between strain and sex ($p = 0.002$) had significant effects on the lesion score. Strain-specific heart lesion scores ranged from 0.25 in strain 150 to 1.625 in strains 57 and 178. Averaged across the 11 strains, the mean heart lesion score in female mice was 1.81x higher compared to male mice. Across the 11 strains, there was no correlation between the mean spirochete load in the heart and the mean lesion score in the heart ($r = 0.032$, $t = 0.547$, $df = 9$, $p = 0.598$).

4.6 Discussion

4.6.1 Mouse ankle swelling is determined by the mouse antibody response

Infection with *B. burgdorferi* causes joint swelling and joint lesions in human Lyme disease patients (Steere et al., 2004; Steere & Glickstein, 2004; Steere et al., 2016) and in mice (Barthold et al., 2006; McKisic et al., 2000; Wooten & Weis, 2001). Our study found that infection with *B. burgdorferi* caused significant ankle joint swelling and ankle joint lesions in C3H/HeJ mice compared to uninfected control mice. Mouse ankle swelling peaked at day 28 PI and then decreased over time, which agrees with other studies (Craig-Mylius et al., 2009; Keane-Myers & Nickell, 1995). Our study found signification variation in ankle joint swelling and ankle joint lesions among *B. burgdorferi* strains. This result agrees with other studies that classified *B. burgdorferi* strains according to RST type where RST1 type strains are more invasive and cause more pathology including ankle swelling and ankle lesions compared to RST3 type strains (Wang et al., 2002; Wang et al., 2001).

The two explanations for strain-specific differences in ankle swelling are the virulence hypothesis and the immunopathology hypothesis. The virulence hypothesis suggests that strain-specific differences in spirochete abundance in the ankle joint drive strain-specific differences in

ankle swelling, whereas the immunopathology hypothesis suggests that strain-specific differences in the host immune response are responsible. Our study found no relationship between spirochete abundance in the ankle joint at day 97 PI versus peak ankle swelling at day 28 PI. One limitation of our study was that the spirochete load in the ankle joint was determined ~70 days after peak ankle swelling. In contrast, studies that measure these two variables at the same time have found significant correlations between spirochete abundance in the ankle joint and ankle joint swelling (Wang et al., 2002; Wang et al., 2001).

Our study supports the immunopathology hypothesis of strain-specific ankle swelling in the C3H/HeJ mice. Across the 11 strains of *B. burgdorferi*, we found a significant positive relationship between the mouse serum IgG antibody response on day 28 PI and mouse ankle swelling on day 28 PI. This result suggests that *B. burgdorferi*-induced joint swelling is an immune-mediated response to infection (Barthold et al., 2006; McKisic et al., 2000; Wooten & Weis, 2001) where a stronger antibody response leads to higher inflammation, and more ankle swelling. Our results agree with the two studies that classified *B. burgdorferi* strains according to RST type (Wang et al., 2002; Wang et al., 2001). Both studies found that RST1 strains caused more ankle swelling and induced a stronger IgG antibody response (as measured on Western blot) compared to RST3 strains (Wang et al., 2002; Wang et al., 2001).

Our study found no correlations between joint lesions at day 97 PI, spirochete abundance in the joint at day 97 PI, and the serum IgG antibody response at day 97 PI. In contrast, Wang et al. (2002) found a correlation across *B. burgdorferi* strains between the spirochete abundance in the joints and the joint lesion scores at day 21 PI. One explanation for this difference between studies is that Wang et al. (2002) scored mouse joint pathology on day 21 PI versus day 97 PI in the present study. Another explanation is that Wang et al. (2002) infected the mice via needle

inoculation, whereas our study infected the mice via tick bite. The mode of infection (needle versus tick) can alter the resultant infection phenotype (Gern et al., 1993; Ramamoorthi et al., 2005; Roehrig et al., 1992; Sertour et al., 2018). Studies that used tick-based infection of C3H mice did not find the correlation between tissue spirochete load and tissue lesion score (Dolan et al., 2004).

Evolutionary virulence theory assumes that higher pathogen abundance in host tissues is positively correlated with higher levels of damage to host tissues, a greater reduction in host fitness, and hence higher virulence (Acevedo et al., 2019; Anderson & May, 1982). In the rodent malaria parasite *Plasmodium chabaudi* for example, strains with high parasitemia cause higher levels of erythrocyte destruction, anemia, and body weight loss in the mouse host (Alizon et al., 2009; Mackinnon & Read, 1999). In this system, high parasitemia is positively correlated with parasite transmission to feeding *Anopheles* mosquitoes. In summary, the malaria parasite has a tropism for blood and high parasitemia enhances parasite transmission but also increases parasite virulence.

In contrast, *B. burgdorferi* does not cause severe disease in either laboratory mice or natural reservoir hosts, such as the white-footed mouse *P. leucopus* (Balderrama-Gutierrez et al., 2021; Moody et al., 1994; Schwanz et al., 2011; Voordouw et al., 2015; Wright & Nielsen, 1990) and the search for a virulence phenotype for this pathogen has been elusive. If *B. burgdorferi* has negligible virulence in its natural reservoir hosts, this trait is not expected to contribute to the evolution of its life history in nature. However, our demonstration that *B. burgdorferi* strains differ in the severity of disease agrees with numerous other studies (Dolan et al., 2004; Wang et al., 2002; Wang et al., 2001; Wormser et al., 2008; Wormser et al., 1999; Zeidner et al., 2001).

4.6.2 Mouse IgG antibody response to *B. burgdorferi* increased over time

The infected C3H/HeJ mice developed a strong serum IgG antibody response against *B. burgdorferi*, which agrees with previous studies on this mouse strain (Barthold, 1991). The serum IgG antibody response against *B. burgdorferi* increased over the course of the infection for all 11 strains of *B. burgdorferi*. The spirochete abundance in the ear tissue biopsies remained consistent over time for most strains (Zinck et al., 2022), which suggests that the IgG antibody response did not reduce the spirochete burden. Over the course of infection, *B. burgdorferi* modifies expression of its surface antigens to evade the host antibody response. For example, spirochetes reduce expression of the immunodominant OspC antigen after establishing infection in the host tissues (Liang, Yan, et al., 2004). *B. burgdorferi* also uses recombination of its *vmp*-like sequence (*vls*) cassettes to generate novel variants of the variable lipoprotein surface-exposed protein (VlsE) thereby evading the host antibody response. Genetic variation in these immune evasion strategies will result in differences in the ability of the host immune system to detect and respond to these *B. burgdorferi* strains (Norris, 2014).

In North America, conventional two-tiered serologic testing for Lyme disease includes a sensitive ELISA followed by a more specific Western blot. A recent study on human Lyme disease patients in Canada suggested that the sensitivity of this conventional two-tiered serologic testing was lower in western Canada compared to eastern Canada (Ogden et al., 2017). Genetic studies have shown that eastern and western Canada contain different strains of *B. burgdorferi* (Mechai et al., 2015). Thus, one explanation is that regional differences in *B. burgdorferi* strains are causing these regional differences in diagnostic sensitivity (Ogden et al., 2017). The Zeus ELISA found significant variation in the strength of the IgG antibody response among the 11 *B. burgdorferi* strains, but this assay was always able to differentiate between uninfected and

infected mice. In summary, C3H/HeJ mice experimentally infected with *B. burgdorferi* via tick bite developed a robust IgG antibody response that was always detectable with the Zeus ELISA, regardless of the identity of the *B. burgdorferi* strain.

4.6.3 Female mice have more severe carditis compared to male mice

Our study found that the mean heart tissue lesion score in female mice was 1.81x higher compared to male mice across the 11 strains of *B. burgdorferi*. While the difference in tissue lesion severity between male and female mice differed among strains, female mice had more carditis compared to male mice for all strains. The severity of disease often differs between the sexes; males are more susceptible to infectious diseases, whereas females are more susceptible to autoimmune disorders (Klein, 2004; Klein & Flanagan, 2016). In mice, testosterone has been directly linked to increasing the pathogen abundance in host tissues or the duration of infection (Arroyo-Mendoza et al., 2020; Benten et al., 1997; Sasaki et al., 2013). Importantly, carditis is caused by the host immune response (McKisic et al., 2000) and these immune-mediated effects are typically stronger in females (Klein & Flanagan, 2016). Infected female mice had a significantly stronger IgG antibody response to *B. burgdorferi* compared to infected male mice, suggesting that females are more immune-reactive to *B. burgdorferi* infection than males. We have previously shown a significant sex-specific difference in the tissue spirochete load, where male mice harbored 1.41x more spirochetes in their heart tissue than female mice (Zinck et al., 2022). We suggest that female mice had a stronger immune response, which reduced their heart spirochete load but also led to increased carditis compared to male mice.

The sex-specific difference in lesion scores was also seen in the kidneys where females had more lesions in 9 of 11 strains, but there was little difference in lesion scores between the sexes

in the ventral skin and rear tibiotarsal joint. In the C3H model of Lyme borreliosis, the severity of lesions generally peaks around weeks 2–4 PI, followed by resolution of symptoms by day 45 PI (Barthold et al., 1990; Barthold et al., 1991; Barthold et al., 1992; Ma et al., 1998). In studies where mice were infected via nymphal tick bite (such as the present study), lesions in the joints and heart have persisted to 18 weeks PI (Dolan et al., 2004; Zeidner et al., 2001). Surprisingly, few experimental studies have investigated sex-specific differences in *B. burgdorferi* infection (Zinck et al., 2022). Given that *B. burgdorferi* induces strong arthritis in C3H mice, we were surprised that we did not find a sex-specific difference in the joint lesion score. One explanation is that the joint is a site of immune evasion for *B. burgdorferi*, which may mitigate the effect of the greater immune response in females (Liang, Brown, et al., 2004). In summary, our study demonstrates that host sex is a critical factor in the study of Lyme borreliosis, where male mice have greater spirochete loads in their tissues, but females have a stronger immune response and more pathology.

4.6.4 Conclusions

Among the 11 strains of *B. burgdorferi* there was significant variation in their virulence in a laboratory model host. We tested whether this variation could be explained by strain-specific differences in tissue abundance as expected by virulence theory but did not find any relationship. We found that ankle swelling was positively correlated with host immune response suggesting it is caused by immunopathology rather than by spirochete load in the host tissues. We also found that female mice had a stronger IgG antibody response and more severe carditis compared to male mice, which had higher heart spirochete loads. Our study demonstrates that future studies should include host sex when studying the pathology of *B. burgdorferi* in the vertebrate host.

5 General Discussion

5.1 Differences among strains in host infection

My PhD thesis used an experimental infection of a laboratory host, *Mus musculus* strain C3H/HeJ to allow for comparative analyses of 11 strains of *B. burgdorferi* in their performance across multiple life history traits. In Chapter 2, we demonstrated that the abundance of *B. burgdorferi* in necropsy tissues significantly varied among strains, and that this variation was meaningful because it was significantly positively correlated to the frequencies of these strains in nature. We measured the presence and abundance of the strains in 7 different tissues including kidney, left ear, right ear, ventral skin, tibiotarsal joint, heart, and bladder. The presence and abundance of *B. burgdorferi* was much higher in some tissues (e.g., heart and bladder) compared to others (e.g., kidney and ears). Across the 11 *B. burgdorferi* strains, the infection presence and spirochete abundance were positively correlated among the 7 tissues. This result shows that strains that have high abundance in one tissue will have a high abundance in all tissues and vice versa for low abundance strains. Currently there is not much evidence of differences in tissue tropism among strains of *B. burgdorferi*, with research instead focusing on genes that contribute to species level tropisms (Lin et al., 2014; Lin et al., 2020; Wager et al., 2015). In our study the strain x tissue interaction was not significant indicating that there was no evidence that some strains had a preference for certain tissues.

The virulence-transmission trade-off hypothesis predicts that pathogen replication in host tissues is positively related to pathogen transmission (Anderson & May, 1982). In this study, we used the abundance of *B. burgdorferi* in the host tissues as an estimate of pathogen replication. In a disseminated infection, not every localized pathogen population will contribute to transmission, and these would then be considered evolutionary dead ends (Lysenko et al., 2010; Tsao, 2009; Zafar et al., 2017). With *B. burgdorferi*, it is unclear what host tissues transmit spirochetes to

feeding ticks. In *B. afzelii*, the skin of the rodent host has been identified as the critical tissue for transmission (Genné et al., 2021; Grillon et al., 2017; Råberg, 2012; Tsao, 2009). *Borrelia burgdorferi* persists in 'immune privileged' sites like cartilaginous tissue and the heart (Cadavid et al., 2000; Embers et al., 2004; Hill et al., 2021). If abundance in these tissues benefits transmission in some way, this could be adaptive. Given the lack of identifiable virulence in the typical reservoir host *P. leucopus* (Hofmeister et al., 1999; Moody et al., 1994; Schwanz et al., 2011; Voordouw et al., 2015), it may not be adaptive through indirect benefits (i.e., slowing the host to increase tick encounter rate). It remains an open question as to whether these populations may directly contribute to the spirochetes transmitted to ticks.

Borrelia burgdorferi also persists in the skin (Barthold et al., 1993), though in our study it was detectable in fewer mice and less abundant relative to the internal tissues. Skin is the largest organ and is approximately 17% of a mouse by weight (Blackburn et al., 1997). Our abundance estimates are based on testing a fraction of the total organ, always taken from the same location on each mouse. The first consideration is how reflective our measurements are of the true abundance of *B. burgdorferi* in the skin. A potential solution would be to drastically increase the sampling for each mouse (i.e., 10 samples from skin sites) to get a better estimated value. To determine whether it is the skin specifically that is responsible for transmission is more difficult, especially given the correlation with other tissues. A recent study by our group showed that the abundance of *B. burgdorferi* could be transiently increased in the skin, but not the internal organs, by topical application of clobetasol (Bourgeois et al., 2022). If the skin population is contributing the most to transmission, a new experiment incorporating clobetasol treatment as a factor would expect to find increased transmission for all strains in the clobetasol treatment group.

5.2 Tissue abundance and lifetime host-to-tick transmission

Closely related pathogen species or strains with differences in their in-host abundance should have correlated differences in their transmission success. The main purpose of this PhD thesis was to test the relationship between pathogen tissue abundance and pathogen transmission. In Chapter 3, we showed a strong relationship across 11 strains of *B. burgdorferi* between the spirochete load in the host tissues and their lifetime host-to-tick transmission (HTT). The strain-specific estimates of lifetime HTT were significantly positively correlated with the frequencies of these strains in wild *I. scapularis* tick populations in the USA and Canada.

The biggest difference between this project and similar studies done in the past was the scope, both in terms of the number of strains used (11 strains), and our attempt to measure lifetime HTT by infesting mice with larval *I. scapularis* ticks at 30, 60, and 90 days PI. Most studies that investigate lifetime HTT use one or two strains of *B. burgdorferi* sl (Donahue et al., 1987; Gern et al., 1994; Hanincova et al., 2008; Jacquet et al., 2016; Rynkiewicz et al., 2017), which makes it difficult to make any generalizations. Studies that investigate a larger strain diversity typically measure other variables like abundance in tissues, pathology, and host antibody response, but not HTT (Baum et al., 2012; Dolan et al., 2004; Wang et al., 2002). Tonetti et al. (2015) measured HTT for 8 strains of *B. afzelii*, but only at 30 days PI. Thus, our study is unique in having measured lifetime HTT for many *B. burgdorferi* strains.

Most experimental studies that have measured lifetime HTT for different strains of *B. burgdorferi* and *B. afzelii* have shown that HTT peaks at 30 days PI and then declines over time (Donahue et al., 1987; Gern et al., 1994; Hanincova et al., 2008; Jacquet et al., 2016; Rynkiewicz et al., 2017). Studies have also shown that this decline in HTT over time is much more dramatic

for some strains than others (Derdáková et al., 2004; Hanincova et al., 2008). In our study, HTT declined dramatically over the course of infection for 3 strains: 66, 54, and 22-2; there were no significant differences in HTT among the strains at 30 days PI. These studies clearly show that a single measurement of HTT at 30 days PI may not be representative of the lifetime HTT for these strains.

In nature, naïve *P. leucopus* mice are born in the spring at which time they can be infected by *I. scapularis* nymphs carrying *B. burgdorfer*i (Bunikis, Tsao, et al., 2004; Hofmeister et al., 1999). The larvae feed on these infected mice later in the summer, and each infected mouse can be repeatedly infested with larval ticks over the course of infection (Devevey & Brisson, 2012). There were three strains, 66, 54, 22-2, where HTT decreased rapidly over time and these strains had the lowest lifetime HTT. Interestingly, strains 54 and 66 had the highest spirochete loads in their ear tissue biopsies at 28 days PI. Previous studies have suggested that there are some strains that have boom-and-bust dynamics where they have high HTT in early infection followed by a dramatic drop in HTT in late infection, whereas other strains after a slow start have persistently high transmission (Derdáková et al., 2004; Hanincova et al., 2008; Haven et al., 2012; Jacquet et al., 2016; Kurtenbach et al., 2006). A theoretical model showed that boom-and-bust strains can co-exist with persister strains (Haven et al., 2012), however differences in synchrony can select for boom-and-bust or persister strains (Gatewood et al., 2009; Ogden et al., 2007). When nymphal and larval feeding peaks are highly synchronous (i.e., the larval peak closely follows the nymphal peak), boom-and-bust strains are favored. In contrast, asynchronous feeding peaks (i.e., there is a delay between the nymphal and larval peaks) will favor persistent strains. Gatewood et al. (2009) found that seasonal temperature variation influenced synchrony, and that tick feeding times were more synchronous in the

midwestern USA. The three strains (66, 54, 22-2) that may have this life strategy all came from sampling locations in midwestern Canada (Table 2.1, Tyler et al., 2018). While in our study these strains had the lowest tissue abundance at day 97 PI, and the lowest lifetime HTT, the persistence of these strains in nature could be explained by a different life history strategy that maximizes their transmission based on the feeding synchrony in their environment.

Finally, it is important to remember that mixed strain infections or co-infections are common in nature. Experimental infection studies have shown that co-infection influences the strain-specific spirochete load in host tissues and strain-specific HTT (Derdáková et al., 2004; Genné et al., 2021; Rogovskyy & Bankhead, 2014; Rynkiewicz et al., 2017). These studies have also shown that performance in single strain infections is not necessarily predictive of performance in mixed infections (Genné et al., 2021; Rynkiewicz et al., 2017). For example, a study with *B. afzelii* strains Fin-Jyv-A3 and NE4049, found that in single strain infections strain Fin-Jyv-A3 had higher HTT than NE4049, but that in simultaneous co-infections, NE4049 had higher HTT than Fin-Jyv-A3. As these were single strain infections, it is possible that their relative fitness to the other strains is not reflective of their success in coinfections. The maintenance of *B. burgdorferi* strain diversity is a complex question influenced by multiple factors, with lifetime transmission and its relationship to host tissue abundance being a part of the larger puzzle.

5.3 Predicting natural frequencies with experimental infection data

The demonstration that our lab-based estimates of strain-specific life history traits are correlated with the frequencies of these strains in wild *I. scapularis* tick populations is a validation of the experimental results and their relevance to the epidemiology of *B. burgdorferi*

strains in nature. When testing assumptions of pathogen evolutionary theory experimentally, decisions about what measures will represent the key life history traits have to be made. For example, in studies of malaria, the density of parasites in the blood is the common measure for replication because malaria parasites have a synchronous 24-hour reproduction cycle (Mackinnon & Read, 1999). The choice of measure to represent a phenotype is critical to the validity of the phenotype for comparisons.

Our host tissue abundance phenotype was based on an average of the 7 necropsy tissue spirochete loads. One limitation of these necropsy spirochete loads is that they represent a single point in time when the infection was 97 days old. The spirochete load was also measured in the ear tissue biopsies at days 29, 59, and 89 post-infection (i.e., the day before each larval infestation) which gives measures of abundance over time. While it would be interesting to test whether temporal changes in HTT are correlated with temporal changes in ear biopsy spirochete load, these represent spirochete abundances in one tissue. Given that we do not know which tissue-specific measures of abundance are the most relevant, we chose to use an average of all the tissues at one time rather than a single tissue over time. Like HTT, a better measure would be lifetime abundance based on cohorts of mice sacrificed after each infestation. As the in-host abundance declines over time (Barthold et al., 1993), and is affected by the host immune response (Barthold et al., 2006; Bockenstedt et al., 2021), this would give abundance averaged over time, or the relationship can be tested at three separate times over the course of infection.

To estimate lifetime HTT, each mouse was infested with naïve *I. scapularis* larvae on days 30, 60, and 90 PI. A subset of engorged larvae were frozen for testing and the remainder were allowed to moult into nymphs. For each of the 312 combinations of mouse and infestation (104 x 3 = 312), a maximum of 5 engorged larvae and 10 unfed nymphs were tested for their *B.*

burgdorferi infection status. A total of 1150 engorged larvae and 3029 unfed nymphs were tested for their *B. burgdorferi* infection status. Allowing engorged larvae to moult and testing the resultant unfed nymphs is the definitive standard for measuring HTT for 3 reasons. First, the nymph is the infectious stage that determines the risk of LB. Second, this measure includes the probability of transstadial transmission of spirochetes between stages, and third, there is reduced ability to detect *B. burgdorferi* in engorged larvae due to low spirochete load and presence of mouse blood (Eisen, 2020; Genné et al., 2019; Jacquet et al., 2017). In summary, our study gave good estimates of the lifetime HTT for the 11 strains of *B. burgdorferi*.

Our experimental infection study used strains from locations that are geographically separated: Manitoba (Buffalo Point, Roseau River) and Ontario (Big Grassy) in midwestern Canada, and Nova Scotia (Lunenburg, Shelburne, Bedford) in eastern Canada (Tyler et al., 2018). To estimate the frequencies of our strains in nature, we combined the results of two studies that surveyed *B. burgdorferi* MLST strains in *I. scapularis* populations across the USA and Canada (Ogden et al., 2011; Travinsky et al., 2010). There is one other study (Tonetti et al., 2015) that estimated strain-specific fitness for large number of *B. afzelii* strains (n = 8). Most of these *B. afzelii* strains were sampled from Neuchatel, Switzerland and were identified by their *ospC* type. This study measured host-to-tick, tick-to-host, and co-feeding transmission and combined these 3 transmission components into a single estimate of the reproduction number (R_0) for each strain (Durand et al., 2017; Tonetti et al., 2015). The frequencies of these *B. afzelii* strains in nature were estimated using an 11-year collection of *B. afzelii* isolates cultured from wild *I. ricinus* ticks sampled at a single forest location in Neuchatel, Switzerland (Durand et al., 2015; Durand et al., 2017). Similar to the present PhD thesis, the authors found a positive correlation between the strain-specific R_0 values and the frequencies of the *ospC* types in wild *I.*

ricinus ticks. An advantage of this study is that the strain-specific fitness estimates and the strain-specific frequencies were all sampled from the same local *B. afzelii* population.

In contrast, our strain-specific estimates of lifetime HTT and strain-specific frequencies were collected over a much larger geographic scale (continent of North America) compared to the study by Durand et al. (2017), which was conducted at a highly local scale (one forest in the Canton of Neuchatel). Given the large spatial scale of our study, it was entirely possible that regional differences in strain frequency and strain fitness could cancel each other out and eliminate any correlation between these two variables. Despite the continental scale of our study, we still found a significant positive relationship between our laboratory estimates of fitness and the strain frequencies in nature, and we take this as evidence of the strength of the relationship. If our strain fitness estimates had been compared with strain frequencies at the locations where the strains had been collected (Buffalo Point Manitoba, Lunenburg Nova Scotia), we believe the relationship between lab fitness and strain frequency would be even stronger.

5.4 Virulence in a model host does not explain tissue abundance

Virulence is the third canonical pathogen life history trait and was broadly defined as infection-induced damage to the host (Mackinnon & Read, 2004). In Chapter 4, we found significant differences in virulence among the 11 strains of *B. burgdorferi*. We found that peak ankle swelling on day 28 PI was significantly positively correlated to the host antibody response at day 28 PI, but not to tissue spirochete load on day 97 PI. Tissue lesion scores at day 97 PI for the kidney, ventral skin, rear tibiotarsal joint, and heart were also not correlated with their spirochete loads at day 97 PI. Thus, our study did not support a basic prediction of virulence theory, which is that strains with high abundance in the host tissues have more virulence.

Virulence theory requires that the pathogen has a negative effect on the survival and/or reproduction of its natural reservoir host. There is not much evidence that *B. burgdorferi* sl pathogens reduce the fitness of their reservoir hosts (Balderrama-Gutierrez et al., 2021; Schwanz et al., 2011; Voordouw et al., 2015). Experimental infection with *B. burgdorferi* in *P. leucopus* caused carditis and arthritis in infant mice but not in adult mice (Moody et al., 1994). Nevertheless, even though *B. burgdorferi* sl does not appear to cause virulence in its rodent reservoir hosts, we felt that it was still worthwhile to test whether strains that established high abundance in the mouse tissues caused more virulence.

In Chapter 4, we showed that the host antibody response and ankle swelling were positively related to each other. Like many pathogens, *B. burgdorferi* has developed strategies for immune evasion. Recombination at the *vls* locus allows *B. burgdorferi* to change the immunodominant VlsE antigen over the course of the infection (Norris, 2014). Reduced expression of OspC following dissemination allows spirochetes to avoid antibodies developed against this immunodominant antigen (Liang, Brown, et al., 2004; Lin et al., 2014; Lin et al., 2020). In simplest terms, determining the spirochete load-virulence relationship across strains of *B. burgdorferi* is confounded by the host immune system. Even when a single host background is used (i.e., C3H/HeJ mice), strains differ in their immune evasion potential. For example, strains 22-2 and 167 had similar estimates of tissue spirochete load yet strain 22-2 had a stronger host antibody response and more ankle swelling. One possibility is that strain 167 is more effective at evading the host immune response. Strain 22-2 might have a higher *in vivo* replication rate, but the stronger antibody response coupled with higher spirochete clearance results in the same net spirochete load.

Studies on the effect of the host immune response show that SCID mice that lack B and T lymphocytes have higher tissue spirochete loads and more severe arthritis and carditis compared to their WT counterparts (Barthold et al., 1996; Barthold et al., 1997; Barthold et al., 2006; Hodzic et al., 2003). Interestingly, the increased virulence in SCID can be negated by passive transfer of antibodies from infected WT mice without reducing the tissue spirochete load. This means that virulence is shaped by the host immune response rather than tissue spirochete load.

5.5 Host sex is a critical factor in *B. burgdorferi* experimental infection

One of the greatest moments in research is the unexpected discovery, revealing some novel insight that you had not considered previously that can refocus future research efforts and your own perspective. In this study, the dramatic effect of host sex on each of the phenotypes measured was certainly unexpected. We found that male mice had more *B. burgdorferi* in their tissues and had greater transmission to ticks than female mice. We also found that male mice had less virulence (carditis) than female mice and lower antibody responses. To the best of our knowledge, this is the first experimental study to report sex-specific impacts of infections with *B. burgdorferi*. In our research group, two studies have since also found sex effects on tissue spirochete loads. A study using *B. burgdorferi* strain 198 and C3H/HeJ mice found the tissue spirochete load was higher in males than females at ~40 days PI (Bourgeois et al., 2022). A study using strains 22-2 and 54 in C57/BL6 mice found a greater spirochete load in male tissues at days 88 and 112 PI respectively (C. Koloski, unpubl.). In summary, there are now three independent studies from our research group that have shown that males have higher tissue spirochete loads compared to females. Importantly, one strain (126) did not have this sex-

specific difference which makes it an ideal strain to include in future studies to interrogate why it is not similarly affected.

Field studies on rodent reservoir hosts have found that the infection prevalence of *B. burgdorferi* sl pathogens is higher in males than females (Tschirren et al., 2013; Voordouw et al., 2015; Zawada et al., 2020). However, these field studies do not control for possible sex-specific differences in the probability of exposure to ticks. Other field studies have shown that male rodents tend to have higher tick burdens compared to female rodents (Devevey & Brisson, 2012; Ostfeld et al., 2018; Perkins et al., 2003). Our study found no difference in susceptibility to infection between the sexes (84/88 mice exposed to infected ticks became infected with *B. burgdorferi*), nor was it designed to answer that question. For 9 of the 11 strains, host-to-tick transmission was greater in males than in females. In summary, field studies suggest that males are more likely to encounter ticks and thus more likely to be infected. Our study suggests that infected males are more likely to transmit *B. burgdorferi* to feeding ticks than females.

Why do males have higher tissue spirochete loads and higher HTT compared to females? Our study found sex-specific differences in tissue spirochete load differed among tissue types. For the ventral skin, the tissue spirochete load was 15x higher in male mice compared to female mice. Bourgeois et al. (2022) found the spirochete load in the skin was 70x higher in males than females, and there was no difference in internal tissues (i.e., heart, bladder). Finally, C. Koloski (unpubl.) found that the spirochete load in male skin was 8x higher than females, and this difference increased to 200x in SCID mice. The skin is structurally different between male and female mice. Males have relatively more dermis which is the preferred skin layer for *B. burgdorferi* (Azzi et al., 2005; Imai et al., 2013). However, the fact that males have higher spirochete loads in all tissues compared to females in our study suggests a systemic cause. We

suggest that sex-specific differences found in this study are attributable to immune differences between male and female mice.

Immune differences among sexes are common and contribute to differences in numerous infections (Ingersoll, 2017; Klein, 2004; Klein & Flanagan, 2016; Roved et al., 2017). The male sex hormone testosterone, which is more abundant in males than females, is known to suppress the immune system (Furman et al., 2014; Trigunaite et al., 2015). In *Mus musculus*, testosterone has been shown to reduce the efficacy of the mouse immune response (Benten et al., 1997; Fujii et al., 1975; Sasaki et al., 2013). In our study, females had a stronger serum IgG antibody response against *B. burgdorferi* than males, which is consistent with testosterone-based immunosuppression. In pathogens that cause direct damage to the host (e.g., hemolysis by *Babesia microti* and *Plasmodium chabaudi*), the reduced immune response in males results in higher pathogen loads, which causes higher virulence in males (Benten et al., 1997; Sasaki et al., 2013). In pathogens that induce immunopathology, the stronger immune response of females can result in more damage to the host tissues compared to males. *B. burgdorferi*-induced carditis in mice is immune-mediated, which suggests that carditis severity should be higher in females compared to males (McKisic et al., 2000). In our study, the heart lesion score was higher in female mice compared to male mice. In summary, we believe that testosterone-mediated immunosuppression causes higher spirochete loads in the tissues of male mice and higher levels of pathology in the tissues of female mice.

5.6 Challenges in teasing apart evolutionary relationships

Evolutionary virulence theory assumes that there is genetic variation in pathogen life history traits (Mackinnon & Read, 2004). The genetic relationships between pathogen tissue

abundance, transmission, and virulence can be shown using the comparative approach with closely related pathogen strains. Importantly, genetic variation in the pathogen population for these life history traits must be separated from host factors, which may also cause the expected relationships between pathogen tissue abundance, transmission, and virulence.

In studies of *B. burgdorferi*, host immune function is often used to demonstrate that the relationship between pathogen abundance in the host tissues and virulence can change (Moody & Barthold, 1998; Wooten & Weis, 2001). In our study, we compared 11 strains of *B. burgdorferi* in the same inbred host under the same environmental conditions. The only additional factors considered were the temporal block, as the experiment was performed in separate groups, and host sex. The experimental groups were split orthogonally to avoid any confounds with these factors. In summary, we are confident that the relationships observed in this study are the result of genetic variation among strains, and thus show a genetic basis for differences in spirochete tissue abundance leading to transmission differences.

This study compared the three main pathogen life history traits among 11 strains of *B. burgdorferi* with comparable effort on pathogen tissue abundance and pathology to past work, and a much greater effort on *B. burgdorferi* transmission than typically found. As with any study bound by practical limitations, this does involve compromises in the data collected that may have limited our ability to detect differences among traits.

First and foremost, the decision to use 11 strains meant fewer mice per strain. This decision was made to give the best chance of sampling outliers with extreme phenotypes (i.e., low transmission). Fewer mice per strain meant there was more error of the estimates for each strain. For each measured trait there were some high and low strains, but most clustered toward intermediate values and were not significantly different from each other. It is possible that with

fewer strains and thus more mice per strain, we would have been able to resolve differences among these strains, but without any *a priori* knowledge, the risk would have been missing the overall relationship.

Most studies that investigate the virulence of *B. burgdorferi* in a rodent host sacrifice their mice for histopathology between 4-6 weeks PI because this is when the greatest virulence is observed, allowing for better ability to differentiate between groups (Wang et al., 2002; Wang et al., 2001; Zeidner et al., 2001). We sacrificed our mice at day 97 PI which is well beyond peak virulence. This was a necessary compromise to allow for measuring lifetime HTT but resulted in much less strain-specific variation in virulence in our mice compared to past studies (Wang et al., 2002; Wang et al., 2001). We failed to detect consistent strain-specific variation in tissue lesions and did not observe any correlation between tissue lesions and tissue pathogen abundance. While this relationship has yet to be demonstrated using mice infected via tick bite (Dolan et al., 2004; Zeidner et al., 2001), confidence in this negative result would be greater if the lesion scores were taken at peak virulence. Ultimately, experimental design involves trade-offs and in this study our emphasis on measuring lifetime HTT limited our ability to investigate virulence.

5.7 Future Directions

The 11 *B. burgdorferi* strains used in the present study were obtained from the Public Health Agency of Canada (PHAC). All these *B. burgdorferi* strains were whole genome sequenced by PHAC (Tyler et al., 2018). Thus, the data from this PhD thesis could be used to examine the relationship between *B. burgdorferi* genetics and the various infection phenotypes measured in this study. Closely related strains should have similar infection phenotypes. There

were two strains in this study (178-1, 198) that had the same MLST and *ospC* type (MLST 3, *ospC* type K). These two closely related strains had very similar estimates for each life history trait. Future studies should investigate the linkages between the genomes of these 11 strains of *B. burgdorferi* (Tyler et al., 2018) and their infection phenotypes in C3H/HeJ mice.

As we have repeatedly stressed, all work in this study was done in a laboratory model host (*M. musculus*) and not a natural reservoir. Repeating this experiment in a natural reservoir like *P. leucopus* would be a way to validate strain performance directly in a natural host. The relative performance of these strains in a second host would be useful to study how much host adaptation may differ among strains of *B. burgdorferi.*

The life cycle of *B. burgdorferi* involves two transmission steps, host-to-tick and tick-to-host transmission. In this study we only investigated HTT. Each mouse was challenged with 1-3 putatively infected nymphs to ensure we successfully infected them. In effect this study has looked at variation in life history traits throughout most of the life cycle of *B. burgdorferi* and investigating tick-to-host transmission is a logical next step to complete the cycle. We have demonstrated that HTT and abundance are positively linked, so the question yet remains what is the trade-off? One possibility is that maximizing transmission from the host to the tick (i.e., maximizing fitness in the host) reduces transmission from the tick to the host. A previous study found that both transmission measures were positively related in *B. afzelii* (Tonetti et al., 2015), but this remains an understudied area. We found a nine-fold difference in the nymphal spirochete loads among strains. Presumably, higher abundance should again lead to greater transmission but this needs to be tested.

We found a significant effect of host sex on the abundance of *B. burgdorferi*. Now the question is what is causing it? We hypothesized that the host immune response is responsible

based on measures of host serum IgG antibody response. These can give a general overview of the strength of the response, but specifics of the immune response should be investigated more rigorously. More informative tests (i.e., western blot) on the specific antibodies and their abundance by each strain would be a first step. If immunosuppression by testosterone is indeed contributing to this difference, then another experimental infection would be needed to compare abundance and virulence in mice across a range of testosterone levels.

5.8 Conclusions

Using a single overarching experiment, we measured three canonical life history traits of *B. burgdorferi* and found a significant positive relationship between tissue spirochete load and transmission among the 11 strains. We also found that these two life history traits were related to the frequencies of these strains in wild tick populations, which supports the applicability of these results to the natural system. We did not see the expected positive relationships between pathogen tissue abundance and virulence. The most obvious explanation is that the absence of a strong virulence phenotype for *B. burgdorferi* suggests that the virulence transmission trade-off may not be applicable for this pathogen. Strain-specific virulence (ankle swelling) was positively related to the strength of the host antibody response, which decouples virulence from pathogen abundance in the host tissues. We found that regardless of strain, male mice had greater tissue spirochete load and transmission, but less severe pathology than female mice. This is the first experimental study to report sex-specific differences in *B. burgdorferi* infection in the rodent host. In an ecological context, our study demonstrates how strain-specific abundance differences in the host influence their frequency in nature, providing an easy phenotype to predict emerging strains of *B. burgdorferi*. From a public health perspective, our study demonstrates that strains

with higher pathogen load in host tissues have higher transmission and are the strains that are more commonly found in nature and thus more likely to be encountered by humans.

6 References

Acevedo, M. A., Dillemuth, F. P., Flick, A. J., Faldyn, M. J., & Elderd, B. D. (2019). Virulence-driven trade-offs in disease transmission: A meta-analysis. *Evolution*, *73*(4), 636-647. https://doi.org/10.1111/evo.13692

Achtman, M., Wain, J., Weill, F. X., Nair, S., Zhou, Z., Sangal, V., Krauland, M. G., Hale, J. L., Harbottle, H., Uesbeck, A., Dougan, G., Harrison, L. H., & Brisse, S. (2012). Multilocus sequence typing as a replacement for serotyping in *Salmonella enterica*. *PLOS Pathogens*, *8*(6), 1002776. https://doi.org/10.1371/journal.ppat.1002776

Adams, B., Walter, K. S., & Diuk-Wasser, M. A. (2021). Host Specialisation, Immune Cross-Reaction and the Composition of Communities of Co-circulating Borrelia Strains. *Bulletin of Mathematical Biology*, *83*(6), 66. https://doi.org/10.1007/s11538-021-00896-2

Adeolu, M., & Gupta, R. S. (2014). A phylogenomic and molecular marker based proposal for the division of the genus Borrelia into two genera: The emended genus Borrelia containing only the members of the relapsing fever Borrelia, and the genus Borreliella gen. nov. containing the members o. *Antonie van Leeuwenhoek, International Journal of General and Molecular Microbiology*, *105*(6), 1049-1072. https://doi.org/10.1007/s10482-014-0164-x

Agre, F., & Schwartz, R. (1993). The value of early treatment of deer tick bites for the prevention of Lyme disease. *American journal of diseases of children*, *147*(9), 945-947.

Alizon, S., de Roode, J. C., & Michalakis, Y. (2013). Multiple infections and the evolution of virulence. *Ecology Letters*, *16*(4), 556-567. https://doi.org/10.1111/ele.12076

Alizon, S., Hurford, A., Mideo, N., & Van Baalen, M. (2009). Virulence evolution and the trade-off hypothesis: history, current state of affairs and the future. *J Evol Biol*, *22*(2), 245-259. https://doi.org/10.1111/j.1420-9101.2008.01658.x

Alizon, S., & Lion, S. (2011). Within-host parasite cooperation and the evolution of virulence. *Proceedings of the Royal Society B: Biological Sciences*, *278*(1725), 3738-3747. https://doi.org/10.1098/rspb.2011.0471

Anderson, J. F., Johnson, R. C., & Magnarelli, L. A. (1987). Seasonal prevalence of Borrelia burgdorferi in natural populations of white-footed mice, Peromyscus leucopus. *JOURNAL OF CLINICAL MICROBIOLOGY*, *25*(8), 1564-1566.

Anderson, J. F., Magnarelli, L. A., Burgdorfer, W., & Barbour, A. G. (1983). Spirochetes in Ixodes dammini and mammals from Connecticut. *Am J Trop Med Hyg*, *32*(4), 818-824. https://doi.org/10.4269/ajtmh.1983.32.818

Anderson, R. M., & May, R. M. (1982). Coevolution of hosts and parasites. *Parasitology*, 16.

Anguita, J., Hedrick, M. N., & Fikrig, E. (2003). Adaptation of Borrelia burgdorferi in the tick and the mammalian host. *FEMS Microbiology Reviews*, *27*(4), 493-504. https://doi.org/10.1016/S0168-6445(03)00036-6

Anguita, J., Ramamoorthi, N., Hovius, J. W. R., Das, S., Thomas, V., Persinski, R., Conze, D., Askenase, P. W., Rincón, M., Kantor, F. S., & Fikrig, E. (2002). Salp15, an Ixodes scapularis salivary protein, inhibits CD4+ T cell activation. *Immunity*, *16*(6), 849-859. https://doi.org/10.1016/S1074-7613(02)00325-4

Armstrong, A. L., Barthold, S. W., Persing, D. H., & Beck, D. S. (1992). Carditis in Lyme disease susceptible and resistant strains of laboratory mice infected with Borrelia burgdorferi. *Am J Trop Med Hyg*, *47*(2), 249-258. https://doi.org/10.4269/ajtmh.1992.47.249

Arroyo-Mendoza, M., Peraza, K., Olson, J., Adler-Moore, J. P., & Buckley, N. E. (2020). Effect of testosterone and estrogen supplementation on the resistance to systemic Candida albicans infection in mice. *Heliyon*, *6*(7), e04437. https://doi.org/10.1016/j.heliyon.2020.e04437

Attie, O., Bruno, J. F., Xu, Y., Qiu, D., Luft, B. J., & Qiu, W.-G. (2007). Co-evolution of the outer surface protein C gene (ospC) and intraspecific lineages of Borrelia burgdorferi sensu stricto in the northeastern United States. *Infection, Genetics and Evolution, 7*, 1-12. https://doi.org/10.1016/j.meegid.2006.02.008

Aucott, J. N., Crowder, L. A., & Kortte, K. B. (2013). Development of a foundation for a case definition of post-treatment Lyme disease syndrome. *International Journal of Infectious Diseases*, *17*(6), e443-e449. https://doi.org/https://doi.org/10.1016/j.ijid.2013.01.008

Aucott, J. N., Seifter, A., & Rebman, A. W. (2012). Probable late lyme disease: a variant manifestation of untreated Borrelia burgdorferi infection. *BMC Infectious Diseases*, *12*(1), 173. https://doi.org/10.1186/1471-2334-12-173

Azzi, L., El-Alfy, M., Martel, C., & Labrie, F. (2005). Gender Differences in Mouse Skin Morphology and Specific Effects of Sex Steroids and Dehydroepiandrosterone. *Journal of Investigative Dermatology*, *124*(1), 22-27. https://doi.org/10.1111/j.0022-202X.2004.23545.x

Baalen, M. v., & Sabelis, M. W. (1995). The dynamics of multiple infection and the evolution of virulence. *The American Naturalist*, *146*(6), 881-910.

Balderrama-Gutierrez, G., Milovic, A., Cook, V. J., Islam, M. N., Zhang, Y., Kiaris, H., Belisle, J. T., Mortazavi, A., & Barbour, A. G. (2021). An Infection-Tolerant Mammalian Reservoir for Several Zoonotic Agents Broadly Counters the Inflammatory Effects of Endotoxin. *mBio*, *12*(2). https://doi.org/10.1128/mBio.00588-21

Balmelli, T., & Piffaretti, J. C. (1995). Association between different clinical manifestations of Lyme disease and different species of Borrelia burgdorferi sensu lato. *Research in Microbiology*, *146*(4), 329-340. https://doi.org/https://doi.org/10.1016/0923-2508(96)81056-4

Balmer, O., & Tanner, M. (2011). Prevalence and implications of multiple-strain infections. *The Lancet Infectious Diseases*, *11*(11), 868-878. https://doi.org/10.1016/S1473-3099(11)70241-9

Bambini, S., Piet, J., Muzzi, A., Keijzers, W., Comandi, S., De Tora, L., Pizza, M., Rappuoli, R., van de Beek, D., van der Ende, A., & Comanducci, M. (2013). An Analysis of the Sequence Variability of Meningococcal fHbp, NadA and NHBA over a 50-Year Period in the Netherlands [Article]. *PLOS ONE*, *8*(5), 10, Article e65043. https://doi.org/10.1371/journal.pone.0065043

Baranton, G., Assous, M., & Postic, D. (1992). [Three bacterial species associated with Lyme borreliosis. CLinical and diagnostic implications]. *Bull Acad Natl Med*, *176*(7), 1075-1085; discussion 1085-1076. (Trois espèces bactériennes associées à la borréliose de Lyme. Conséquences cliniques et diagnostiques.)

Baranton, G., Postic, D., Saint Girons, I., Boerlin, P., Piffaretti, J. C., Assous, M., & Grimont, P. A. (1992). Delineation of Borrelia burgdorferi sensu stricto, Borrelia garinii sp. nov., and group VS461 associated with Lyme borreliosis. *Int J Syst Bacteriol*, *42*(3), 378-383. https://doi.org/10.1099/00207713-42-3-378

Barbour, A. G. (2017). Infection resistance and tolerance in Peromyscus spp., natural reservoirs of microbes that are virulent for humans. *Seminars in Cell and Developmental Biology*, *61*, 115-122. https://doi.org/10.1016/j.semcdb.2016.07.002

Barbour, A. G., Bunikis, J., Travinsky, B., Hoen, A. G., Diuk-Wasser, M. A., Fish, D., & Tsao, J. I. (2009). Niche partitioning of Borrelia burgdorferi and Borrelia miyamotoi in the same tick vector and mammalian reservoir species. *The American Journal of Tropical Medicine and Hygiene*, *81*(6), 1120-1131. https://doi.org/10.4269/ajtmh.2009.09-0208

Barbour, A. G., & Travinsky, B. (2010). Evolution and distribution of the *ospC* gene, a transferable serotype determinant of *Borrelia burgdorferi*. *mBio, 1*(4). https://doi.org/10.1128/mBio.00153-10

Barclay, V. C., Sim, D., Chan, B. H. K., Nell, L. A., Rabaa, M. A., Bell, A. S., Anders, R. F., & Read, A. F. (2012). The evolutionary consequences of blood-stage vaccination on the rodent malaria *Plasmodium chabaudi*. *PLOS Biology*, *10*(7), e1001368. https://doi.org/10.1371/journal.pbio.1001368

Barthold, S. W. (1991). Infectivity of *Borrelia burgdorferi* relative to route of inoculation and genotype in laboratory mice. *The Journal of Infectious Diseases*, *163*(2), 419-420. https://doi.org/10.1093/infdis/163.2.419

Barthold, S. W., Beck, D. S., Hansen, G. M., Terwilliger, G. A., & Moody, K. D. (1990). Lyme borreliosis in selected strains and ages of laboratory mice. *The Journal of Infectious Diseases*, *162*(1), 133-138. https://doi.org/10.1093/infdis/162.1.133

Barthold, S. W., de Souza, M. S., Janotka, J. L., Smith, A. L., & Persing, D. H. (1993). Chronic Lyme borreliosis in the laboratory mouse. *The American Journal of Pathology*, *143*(3), 959-971.

Barthold, S. W., deSouza, M., & Feng, S. (1996). Serum-mediated resolution of Lyme arthritis in mice. *Lab Invest*, *74*(1), 57-67.

Barthold, S. W., Feng, S., Bockenstedt, L. K., Fikrig, E., & Feen, K. (1997). Protective and Arthritis-Resolving Activity in Sera of Mice Infected with Borrelia burgdorferi. *Clinical Infectious Diseases*, *25*(s1), S9--S17. https://doi.org/10.1086/516166

Barthold, S. W., Hodzic, E., Tunev, S., & Feng, S. (2006). Antibody-Mediated Disease Remission in the Mouse Model of Lyme Borreliosis. *INFECTION AND IMMUNITY*, *74*(8), 4817-4825. https://doi.org/10.1128/iai.00469-06

Barthold, S. W., Persing, D. H., Armstrong, A. L., & Peeples, R. A. (1991). Kinetics of *Borrelia burgdorferi* dissemination and evolution of disease after intradermal inoculation of mice. *The American Journal of Pathology*, *139*(2), 263-273.

Barthold, S. W., Sidman, C. L., & Smith, A. L. (1992). Lyme borreliosis in genetically resistant and susceptible mice with severe combined immunodeficiency. *The American Journal of Tropical Medicine and Hygiene*, *47*(5), 605-613. https://doi.org/10.4269/ajtmh.1992.47.605

Bashey, F., Reynolds, C., Sarin, T., & Young, S. K. (2011). Virulence and competitive ability in an obligately killing parasite. *Oikos*, *120*(10), 1539-1545. https://doi.org/10.1111/j.1600-0706.2011.19304.x

Baum, E., Hue, F., & Barbour, A. G. (2012). Experimental infections of the reservoir species Peromyscus leucopus with diverse strains of Borrelia burgdorferi, a Lyme disease agent. *mBio*, *3*(6), e00434-00412. https://doi.org/10.1128/mBio.00434-12

Beery, A. K., & Zucker, I. (2011). Sex bias in neuroscience and biomedical research. *Neuroscience and Biobehavioral Reviews*, *35*(3), 565-572. https://doi.org/10.1016/j.neubiorev.2010.07.002

Bekker, L. G., Moreira, A. L., Bergtold, A., Freeman, S., Ryffel, B., & Kaplan, G. (2000). Immunopathologic effects of tumor necrosis factor alpha in murine mycobacterial infection are dose dependent. *Infect Immun*, *68*(12), 6954-6961. https://doi.org/10.1128/iai.68.12.6954-6961.2000

Bell, A. S., Roode, J. C. d., Sim, D., & Read, A. F. (2006). Within-host competition in genetically diverse malaria infections: Parasite virulence and competitive success. *Evolution*, *60*(7), 1358-1371. https://doi.org/10.1554/05-611.1

Belli, A., Sarr, A., Rais, O., Rego, R. O. M., & Voordouw, M. J. (2017). Ticks infected via co-feeding transmission can transmit Lyme borreliosis to vertebrate hosts. *Scientific Reports*, *7*(1), 5006. https://doi.org/10.1038/s41598-017-05231-1

Ben-Ami, F., Mouton, L., & Ebert, D. (2008). The effects of multiple infections on the expression and evolution of virulence in a *Daphnia*-endoparasite system. *Evolution*, *62*(7), 1700-1711. https://doi.org/10.1111/j.1558-5646.2008.00391.x

Benoit, V. M., Petrich, A., Alugupalli, K. R., Marty-Roix, R., Moter, A., Leong, J. M., & Boyartchuk, V. L. (2010). Genetic control of the innate immune response to *Borrelia hermsii* influences the course of relapsing fever in inbred strains of mice. *INFECTION AND IMMUNITY*, *78*(2), 586-594. https://doi.org/10.1128/IAI.01216-09

Benten, W. P. M., Ulrich, P., Kühn-Velten, W. N., Vohr, H.-W., & Wunderlich, F. (1997). Testosterone-induced susceptibility to Plasmodium chabaudi malaria: persistence after withdrawal of testosterone. *Journal of Endocrinology*, *153*(2), 275-281. https://doi.org/10.1677/joe.0.1530275

Bernard, Q., Grillon, A., Lenormand, C., Ehret-Sabatier, L., & Boulanger, N. (2020). Skin Interface, a Key Player for Borrelia Multiplication and Persistence in Lyme Borreliosis. *Trends in Parasitology*, *36*(3), 304-314. https://doi.org/https://doi.org/10.1016/j.pt.2019.12.017

Billingham, R. (1986). Immunologic advantages and disadvantages of being a female. *Reproductive immunology*, 1-9.

Blackburn, A., Schmitt, A., Schmidt, P., Wanke, R., Hermanns, W., Brem, G., & Wolf, E. (1997). Actions and interactions of growth hormone and insulin-like growth factor-II: body and organ growth of transgenic mice. *Transgenic Research*, *6*(3), 213-222. https://doi.org/10.1023/A:1018494108654

Bockenstedt, L. K., Gonzalez, D., Mao, J., Li, M., Belperron, A. A., & Haberman, A. (2014). What ticks do under your skin: two-photon intravital imaging of Ixodes scapularis feeding in the presence of the lyme disease spirochete. *Yale J Biol Med*, *87*(1), 3-13.

Bockenstedt, L. K., Hodzic, E., Feng, S., Bourrel, K. W., De Silva, A., Montgomery, R. R., Fikrig, E., Radolf, J. D., & Barthold, S. W. (1997). *Borrelia burgdorferi* strain-specific Osp C-mediated immunity in mice. *INFECTION AND IMMUNITY*, *65*(11), 4661-4667. https://doi.org/10.1128/iai.65.11.4661-4667.1997

Bockenstedt, L. K., Wooten, R. M., & Baumgarth, N. (2021). Immune Response to Borrelia: Lessons from Lyme Disease Spirochetes. *Curr Issues Mol Biol*, *42*, 145-190. https://doi.org/10.21775/cimb.042.145

Bonneaud, C., Tardy, L., Hill, G. E., McGraw, K. J., Wilson, A. J., & Giraudeau, M. (2020). Experimental evidence for stabilizing selection on virulence in a bacterial pathogen. *Evolution Letters*, *4*(6), 491-501. https://doi.org/10.1002/evl3.203

Bouchard, C., Beauchamp, G., Nguon, S., Trudel, L., Milord, F., Lindsay, L. R., Bélanger, D., & Ogden, N. H. (2011). Associations between Ixodes scapularis ticks and small mammal hosts in a newly endemic zone in southeastern Canada: Implications for Borrelia burgdorferi transmission. *Ticks and Tick-borne Diseases*, *2*(4), 183-190. https://doi.org/https://doi.org/10.1016/j.ttbdis.2011.03.005

Bouchard, C., Leighton, P. A., Beauchamp, G., Nguon, S., Trudel, L., Milord, F., Lindsay, L. R., Bélanger, D., & Ogden, N. H. (2013). Harvested White-Tailed Deer as Sentinel Hosts for Early Establishing *Ixodes scapularis* Populations and Risk From Vector-Borne Zoonoses in Southeastern Canada. *Journal of Medical Entomology*, *50*(2), 384-393. https://doi.org/10.1603/me12093

Bourgeois, B., Koloski, C., Foley-Eby, A., Zinck, C. B., Hurry, G., Boulanger, N., & Voordouw, M. J. (2022). Clobetasol increases the abundance of Borrelia burgdorferi in the skin 70 times more in male mice compared to female mice. *Ticks Tick Borne Dis*, *13*(6), 102058. https://doi.org/10.1016/j.ttbdis.2022.102058

Brisson, D., Baxamusa, N., Schwartz, I., & Wormser, G. P. (2011). Biodiversity of *Borrelia burgdorferi* strains in tissues of Lyme disease patients. *PLOS ONE*, *6*(8), e22926. https://doi.org/10.1371/journal.pone.0022926

Brisson, D., Drecktrah, D., Eggers, C. H., & Samuels, D. S. (2012). Genetics of *Borrelia burgdorferi*. *Annual Review of Genetics*, *46*, 515-536. https://doi.org/10.1146/annurev-genet-011112-112140

Brisson, D., & Dykhuizen, D. E. (2004). *ospC* diversity in *Borrelia burgdorferi*: Different hosts are different niches. *Genetics*, *168*(2), 713-722. https://doi.org/10.1534/genetics.104.028738

Brown, S. P., Le Chat, L., & Taddei, F. (2008). Evolution of virulence: triggering host inflammation allows invading pathogens to exclude competitors. *Ecology Letters*, *11*(1), 44-51. https://doi.org/10.1111/j.1461-0248.2007.01125.x

Brunner, J. L., & Ostfeld, R. S. (2008). Multiple causes of variable tick burdens on small-mammal hosts. *Ecology*, *89*(8), 2259-2272. https://doi.org/10.1890/07-0665.1

Buckee, C. O., Gupta, S., Kriz, P., Maiden, M. C. J., & Jolley, K. A. (2010). Long-term evolution of antigen repertoires among carried meningococci [Article]. *Proceedings of the Royal Society B-Biological Sciences*, *277*(1688), 1635-1641. https://doi.org/10.1098/rspb.2009.2033

Bull, J. J. (1994). VIRULENCE. *Evolution*, *48*(5), 1423-1437. https://doi.org/https://doi.org/10.1111/j.1558-5646.1994.tb02185.x

Bunikis, J., Garpmo, U., Tsao, J., Berglund, J., Fish, D., & Barbour, A. G. (2004). Sequence typing reveals extensive strain diversity of the Lyme borreliosis agents Borrelia burgdorferi in North America and Borrelia afzelii in Europe. *Microbiology*, *150*, 1741-1755. https://doi.org/10.1099/mic.0.26944-0

Bunikis, J., Tsao, J., Luke, C. J., Luna, M. G., Fish, D., & Barbour, A. G. (2004). *Borrelia burgdorferi* infection in a natural population of *Peromyscus leucopus* mice: A longitudinal study in an area where Lyme borreliosis is highly endemic. *The Journal of Infectious Diseases*, *189*(8), 1515-1523. https://doi.org/10.1086/382594

Burgdorfer, W. (1984). THE NEW-ZEALAND WHITE-RABBIT - AN EXPERIMENTAL HOST FOR INFECTING TICKS WITH LYME-DISEASE SPIROCHETES [Article]. *Yale Journal of Biology and Medicine*, *57*(4), 609-612. <Go to ISI>://WOS:A1984TV77500031

https://www.ncbi.nlm.nih.gov/pmc/articles/PMC2590024/pdf/yjbm00100-0157.pdf

Butterworth, M., McClellan, B., & Aklansmith, M. (1967). Influence of sex on immunoglobulin levels. *Nature*, *214*, 1224-1225.

Cabello, F. C., Godfrey, H. P., & Newman, S. A. (2007). Hidden in plain sight: Borrelia burgdorferi and the extracellular matrix. *Trends Microbiol*, *15*(8), 350-354. https://doi.org/10.1016/j.tim.2007.06.003

Cadavid, D., O'Neill, T., Schaefer, H., & Pachner, A. R. (2000). Localization of Borrelia burgdorferi in the nervous system and other organs in a nonhuman primate model of lyme disease. *Laboratory Investigation*, *80*(7), 1043-1054. https://doi.org/10.1038/labinvest.3780109

Caine, J. A., & Coburn, J. (2015). A Short-Term Borrelia burgdorferi Infection Model Identifies Tissue Tropisms and Bloodstream Survival Conferred by Adhesion Proteins. https://doi.org/10.1128/IAI.00349-15

Cameron, D. J. (2007). Consequences of treatment delay in Lyme disease. *Journal of Evaluation in Clinical Practice*, *13*(3), 470-472. https://doi.org/https://doi.org/10.1111/j.1365-2753.2006.00734.x

Canica, M. M., Nato, F., du Merle, L., Mazie, J. C., Baranton, G., & Postic, D. (1993). Monoclonal antibodies for identification of Borrelia afzelii sp. nov. associated with late cutaneous manifestations of Lyme borreliosis. *Scand J Infect Dis*, *25*(4), 441-448. https://doi.org/10.3109/00365549309008525

Casjens, S. R., Gilcrease, E. B., Vujadinovic, M., Mongodin, E. F., Luft, B. J., Schutzer, S. E., Fraser, C. M., & Qiu, W.-G. (2017). Plasmid diversity and phylogenetic consistency in the Lyme disease agent Borrelia burgdorferi. *BMC Genomics*, *18*(1), 165. https://doi.org/10.1186/s12864-017-3553-5

Casjens, S. R., Mongodin, E. F., Qiu, W. G., Luft, B. J., Schutzer, S. E., Gilcrease, E. B., Huang, W. M., Vujadinovic, M., Aron, J. K., Vargas, L. C., Freeman, S., Radune, D., Weidman, J. F., Dimitrov, G. I., Khouri, H. M., Sosa, J. E., Halpin, R. A., Dunn, J. J., & Fraser, C. M. (2012). Genome stability of Lyme disease spirochetes: comparative genomics of Borrelia burgdorferi plasmids. *PLOS ONE*, *7*(3), e33280. https://doi.org/10.1371/journal.pone.0033280

Castillo-Ramírez, S., Fingerle, V., Jungnick, S., Straubinger, R. K., Krebs, S., Blum, H., Meinel, D. M., Hofmann, H., Guertler, P., Sing, A., & Margos, G. (2016). Trans-Atlantic exchanges have shaped the population structure of the Lyme disease agent Borrelia burgdorferi sensu stricto. *Scientific Reports*, *6*(1), 22794. https://doi.org/10.1038/srep22794

Chauhan, R. P., & Gordon, M. L. (2021). Deciphering transmission dynamics and spillover of avian influenza viruses from avian species to swine populations globally. *Virus Genes*, *57*(6), 541-555. https://doi.org/10.1007/s11262-021-01873-6

Cheung, G. Y. C., Bae, J. S., & Otto, M. (2021). Pathogenicity and virulence of Staphylococcus aureus. *Virulence*, *12*(1), 547-569. https://doi.org/10.1080/21505594.2021.1878688

Choo-Kang, C., Tang, E., & Mattappallil, A. (2010). The Treatment of Early Lyme Disease. *US Pharm*, *35*(9), 41-48.

Cobey, S. (2014). Pathogen evolution and the immunological niche. *Annals of the New York Academy of Sciences*, *1320*(1), 1-15. https://doi.org/10.1111/nyas.12493
Conway, D. J., & Polley, S. D. (2002). Measuring immune selection. *Parasitology*, *125 Suppl*, S3-16. https://doi.org/10.1017/s0031182002002214
Costello, C. M., Steere, A. C., Pinkerton, R. E., & Feder, H. M., Jr. (1989). A Prospective Study of Tick Bites in an Endemic Area for Lyme Disease. *The Journal of Infectious Diseases*, *159*(1), 136-139. https://doi.org/10.1093/infdis/159.1.136
Courtney, J. W., Kostelnik, L. M., Zeidner, N. S., & Massung, R. F. (2004). Multiplex real-time PCR for detection of *Anaplasma phagocytophilum* and *Borrelia burgdorferi*. *JOURNAL OF CLINICAL MICROBIOLOGY*, *42*(7), 3164-3168. https://doi.org/10.1128/JCM.42.7.3164-3168.2004
Craig-Mylius, K. A., Lee, M., Jones, K. L., & Glickstein, L. J. (2009). Arthritogenicity of Borrelia burgdorferi and Borrelia garinii: comparison of infection in mice. *Am J Trop Med Hyg*, *80*(2), 252-258. https://www.ncbi.nlm.nih.gov/pubmed/19190223
Cressler, C. E., McLeod, D. V., Rozins, C., van den Hoogen, J., & Day, T. (2016). The adaptive evolution of virulence: a review of theoretical predictions and empirical tests. *Parasitology*, *143*(7), 915-930. https://doi.org/10.1017/s003118201500092x
Dai, J., Wang, P., Adusumilli, S., Booth, C. J., Narasimhan, S., Anguita, J., & Fikrig, E. (2009). Antibodies against a tick protein, Salp15, protect mice from the Lyme disease agent. *Cell Host and Microbe*, *6*(5), 482-492. https://doi.org/10.1016/j.chom.2009.10.006
Darwin, C. (1859). *On the Origin of Species, 1859*. https://doi.org/10.4324/9780203509104
Dattwyler, R. J., Luft, B. J., Kunkel, M. J., Finkel, M. F., Wormser, G. P., Rush, T. J., Grunwaldt, E., Agger, W. A., Franklin, M., Oswald, D., Cockey, L., & Maladorno, D. (1997). Ceftriaxone Compared with Doxycycline for the Treatment of Acute Disseminated Lyme Disease. *New England Journal of Medicine*, *337*(5), 289-295. https://doi.org/10.1056/nejm199707313370501
De Roode, J. C., Pansini, R., Cheesman, S. J., Helinski, M. E. H., Huijben, S., Wargo, A. R., Bell, A. S., Chan, B. H. K., Walliker, D., & Read, A. F. (2005). Virulence and competitive ability in genetically diverse malaria infections. *Proceedings of the National Academy of Sciences of the United States of America*, *102*(21), 7624-7628. https://doi.org/10.1073/pnas.0500078102
De Roode, J. C., Yates, A. J., & Altizer, S. (2008). Virulence-transmission trade-offs and population divergence in virulence in a naturally occurring butterfly parasite. *Proceedings of the National Academy of Sciences of the United States of America*, *105*(21), 7489-7494. https://doi.org/10.1073/pnas.0710909105
de Silva, A. M., & Fikrig, E. (1995). Growth and Migration of Borrelia burgdorferi in Ixodes Ticks during Blood Feeding. *The American Journal of Tropical Medicine and Hygiene*, *53*(4), 397-404. https://doi.org/10.4269/ajtmh.1995.53.397
Derdáková, M., Dudiò, V., Brei, B., Brownstein, J. S., Schwartz, I., & Fish, D. (2004). Interaction and transmission of two *Borrelia burgdorferi* sensu stricto strains in a tick-rodent maintenance system. *Applied and Environmental Microbiology*, *70*(11), 6783-6788. https://doi.org/10.1128/AEM.70.11.6783-6788.2004
des Vignes, F., Piesman, J., Heffernan, R., Schulze, T. L., Stafford, K. C., 3rd, & Fish, D. (2001). Effect of tick removal on transmission of Borrelia burgdorferi and Ehrlichia phagocytophila by Ixodes scapularis nymphs. *J Infect Dis*, *183*(5), 773-778. https://doi.org/10.1086/318818

Devevey, G., & Brisson, D. (2012). The effect of spatial heterogenity on the aggregation of ticks on white-footed mice. *Parasitology*, *139*(7), 915-925. https://doi.org/10.1017/S003118201200008X

Devevey, G., Dang, T., Graves, C. J., Murray, S., & Brisson, D. (2015). First arrived takes all: inhibitory priority effects dominate competition between co-infecting *Borrelia burgdorferi* strains. *BMC Microbiology*, *15*(1), 61. https://doi.org/10.1186/s12866-015-0381-0

Diuk-Wasser, M. A., Gatewood, A. G., Cortinas, M. R., Yaremych-Hamer, S., Tsao, J., Kitron, U., Hickling, G., Brownstein, J. S., Walker, E., Piesman, J., & Fish, D. (2006). Spatiotemporal patterns of host-seeking Ixodes scapularis nymphs (Acari: Ixodidae) in the United States. *J Med Entomol*, *43*(2), 166-176. https://doi.org/10.1603/0022-2585(2006)043[0166:spohis]2.0.co;2

Dolan, M. C., Hojgaard, A., Hoxmeier, J. C., Replogle, A. J., Respicio-Kingry, L. B., Sexton, C., Williams, M. A., Pritt, B. S., Schriefer, M. E., & Eisen, L. (2016). Vector competence of the blacklegged tick, Ixodes scapularis, for the recently recognized Lyme borreliosis spirochete Candidatus Borrelia mayonii. *Ticks Tick Borne Dis*, *7*(5), 665-669. https://doi.org/10.1016/j.ttbdis.2016.02.012

Dolan, M. C., Piesman, J., Mbow, M. L., Maupin, G. O., Peter, O., Brossard, M., & Golde, W. T. (1998). Vector competence of Ixodes scapularis and Ixodes ricinus (Acari: Ixodidae) for three genospecies of Borrelia burgdorferi. *J Med Entomol*, *35*(4), 465-470. https://doi.org/10.1093/jmedent/35.4.465

Dolan, M. C., Piesman, J., Schneider, B. S., Schriefer, M., Brandt, K., & Zeidner, N. S. (2004). Comparison of disseminated and nondisseminated strains of *Borrelia burgdorferi* sensu stricto in mice naturally infected by tick bite. *INFECTION AND IMMUNITY*, *72*(9), 5262-5266. https://doi.org/10.1128/IAI.72.9.5262-5266.2004

Donahue, J. G., Piesman, J., & Spielman, A. (1987). Reservoir competence of white-footed mice for Lyme disease spirochetes. *American Journal of Tropical Medicine and Hygiene*, *36*(1), 92-96. https://doi.org/10.4269/ajtmh.1987.36.92

Dressler, F., Whalen, J. A., Reinhardt, B. N., & Steere, A. C. (1993). Western Blotting in the Serodiagnosis of Lyme Disease. *The Journal of Infectious Diseases*, *167*(2), 392-400. https://doi.org/10.1093/infdis/167.2.392

Dunham-Ems, S. M., Caimano, M. J., Pal, U., Wolgemuth, C. W., Eggers, C. H., Balic, A., & Radolf, J. D. (2009). Live imaging reveals a biphasic mode of dissemination of Borrelia burgdorferi within ticks. *J Clin Invest*, *119*(12), 3652-3665. https://doi.org/10.1172/JCI39401

Durand, J., Jacquet, M., Paillard, L., Rais, O., Gern, L., & Voordouw, M. J. (2015). Cross-Immunity and Community Structure of a Multiple-Strain Pathogen in the Tick Vector. *Applied and Environmental Microbiology*, *81*(22), 7740-7752. https://doi.org/10.1128/aem.02296-15

Durand, J., Jacquet, M., Rais, O., Gern, L., & Voordouw, M. J. (2017). Fitness estimates from experimental infections predict the long-term strain structure of a vector-borne pathogen in the field. *Scientific Reports*, *7*(1). https://doi.org/10.1038/s41598-017-01821-1

Earnhart, C. G., Buckles, E. L., Dumler, J. S., & Marconi, R. T. (2005). Demonstration of *OspC* type diversity in invasive human Lyme disease isolates and identification of previously uncharacterized epitopes that define the specificity of the *OspC* murine antibody

response. *INFECTION AND IMMUNITY*, *73*(12), 7869-7877. https://doi.org/10.1128/iai.73.12.7869-7877.2005
Ebert, D., & Bull, J. J. (2003). Challenging the trade-off model for the evolution of virulence: is virulence management feasible? *TRENDS in Microbiology*, *11*(1), 15-20. https://doi.org/10.1016/S0966-842X(02)00003-3
Eisen, L. (2018). Pathogen transmission in relation to duration of attachment by Ixodes scapularis ticks. *Ticks and Tick-borne Diseases*, *9*(3), 535-542. https://doi.org/10.1016/J.TTBDIS.2018.01.002
Eisen, L. (2020). Vector competence studies with hard ticks and Borrelia burgdorferi sensu lato spirochetes: A review. *Ticks Tick Borne Dis*, *11*(3), 101359. https://doi.org/10.1016/j.ttbdis.2019.101359
Eisen, L., Dolan, M. C., Piesman, J., & Lane, R. S. (2003). Vector competence of Ixodes pacificus and I. spinipalpis (Acari: Ixodidae), and reservoir competence of the dusky-footed woodrat (Neotoma fuscipes) and the deer mouse (Peromyscus maniculatus), for Borrelia bissettii. *J Med Entomol*, *40*(3), 311-320. https://doi.org/10.1603/0022-2585-40.3.311
Elsner, R. A., Hastey, C. J., Olsen, K. J., & Baumgarth, N. (2015). Suppression of long-lived humoral immunity following *Borrelia burgdorferi* infection. *PLOS Pathogens*, *11*(7), e1004976. https://doi.org/10.1371/journal.ppat.1004976
Embers, M. E., Ramamoorthy, R., & Philipp, M. T. (2004). Survival strategies of *Borrelia burgdorferi*, the etiologic agent of Lyme disease. *Microbes and Infection*, *6*(3), 312-318. https://doi.org/10.1016/j.micinf.2003.11.014
Enright, M. C., & Spratt, B. G. (1999). Multilocus sequence typing. *TRENDS in Microbiology*, *7*(12), 482-487. https://doi.org/10.1016/S0966-842X(99)01609-1
Fairlie-Clarke, K. J., Allen, J. E., Read, A. F., & Graham, A. L. (2013). Quantifying variation in the potential for antibody-mediated apparent competition among nine genotypes of the rodent malaria parasite Plasmodium chabaudi. *Infect Genet Evol*, *20*, 270-275. https://doi.org/10.1016/j.meegid.2013.09.013
Falco, R., & Fish, D. (1988). A survey of tick bites acquired in a Lyme disease endemic area in southern New York State. *Annals of the New York Academy of Sciences (USA)*.
Feder, H. M., Jr, Gerber, M. A., Krause, P. J., Shapiro, E. D., & Ryan, R. (1993). Early Lyme Disease: A Flu-Like Illness Without Erythema Migrans. *Pediatrics*, *91*(2), 456-459. https://doi.org/10.1542/peds.91.2.456
Fiset, J., Tessier, N., Millien, V., & Lapointe, F. J. (2015). Phylogeographic structure of the white-footed mouse and the deer mouse, two lyme disease reservoir hosts in Québec. *PLOS ONE*, *10*(12), 1-18. https://doi.org/10.1371/journal.pone.0144112
Flajnik, M. F., & Kasahara, M. (2010). Origin and evolution of the adaptive immune system: genetic events and selective pressures. *Nat Rev Genet*, *11*(1), 47-59. https://doi.org/10.1038/nrg2703
Fleming-Davies, A. E., Williams, P. D., Dhondt, A. A., Dobson, A. P., Hochachka, W. M., Leon, A. E., Ley, D. H., Osnas, E. E., & Hawley, D. M. (2018). Incomplete host immunity favors the evolution of virulence in an emergent pathogen. *Science*, *359*(6379), 1030-1033. https://doi.org/10.1126/science.aao2140
Forbes, M. L., Horsey, E., Hiller, N. L., Buchinsky, F. J., Hayes, J. D., Compliment, J. M., Hillman, T., Ezzo, S., Shen, K., Keefe, R., Barbadora, K., Post, J. C., Hu, F. Z., & Ehrlich, G. D. (2008). Strain-specific virulence phenotypes of *Streptococcus pneumoniae*

assessed using the *Chinchilla laniger* model of otitis media. *PLOS ONE, 3*(4), e1969. https://doi.org/10.1371/journal.pone.0001969

Frank, S. A. (1996). Models of parasite virulence. *Quarterly Review of Biology, 71*(1), 37-78. <Go to ISI>://A1996UE27500002

Fraser, C., Hollingsworth, T. D., Chapman, R., de Wolf, F., & Hanage, W. P. (2007). Variation in HIV-1 set-point viral load: epidemiological analysis and an evolutionary hypothesis. *Proc Natl Acad Sci U S A, 104*(44), 17441-17446. https://doi.org/10.1073/pnas.0708559104

Fujii, H., Nawa, Y., Tsuchiya, H., Matsuno, K., Fukumoto, T., Fukuda, S., & Kotani, M. (1975). Effect of a single administration of testosterone on the immune response and lymphoid tissues in mice. *Cellular Immunology*, *20*(2), 315-326. https://doi.org/10.1016/0008-8749(75)90108-2

Furman, D., Hejblum, B. P., Simon, N., Jojic, V., Dekker, C. L., Thiébaut, R., Tibshirani, R. J., & Davis, M. M. (2014). Systems analysis of sex differences reveals an immunosuppressive role for testosterone in the response to influenza vaccination. *Proceedings of the National Academy of Sciences*, *111*(2), 869-874. https://doi.org/10.1073/pnas.1321060111

Futse, J. E., Brayton, K. A., Dark, M. J., Knowles, D. P., & Palmer, G. H. (2008). Superinfection as a driver of genomic diversification in antigenically variant pathogens. *Proceedings of the National Academy of Sciences*, *105*(6), 2123-2127. https://doi.org/doi:10.1073/pnas.0710333105

Gandon, S., Mackinnon, M. J., Nee, S., & Read, A. F. (2001). Imperfect vaccines and the evolution of pathogen virulence. *Nature*, *414*(6865), 751-756. https://doi.org/10.1038/414751a

Gasmi, S., Ogden, N. H., Lindsay, L. R., Burns, S., Fleming, S., Badcock, J., Hanan, S., Gaulin, C., Leblanc, M. A., Russell, C., Nelder, M., Hobbs, L., Graham-Derham, S., Lachance, L., Scott, A. N., Galanis, E., & Koffi, J. K. (2017). Surveillance for Lyme disease in Canada: 2009-2015. *Canada communicable disease report = Releve des maladies transmissibles au Canada*, *43*(10), 194-199.

Gatewood, A. G., Liebman, K. A., Vourc'h, G., Bunikis, J., Hamer, S. A., Cortinas, R., Melton, F., Cislo, P., Kitron, U., Tsao, J., Barbour, A. G., Fish, D., & Diuk-Wasser, M. A. (2009). Climate and tick seasonality are predictors of Borrelia burgdorferi genotype distribution. *Appl Environ Microbiol*, *75*(8), 2476-2483. https://doi.org/10.1128/AEM.02633-08

Genné, D., Rossel, M., Sarr, A., Battilotti, F., Rais, O., Rego, R. O. M., & Voordouw, M. J. (2021). Competition between strains of *Borrelia afzelii* in the host tissues and consequences for transmission to ticks. *The ISME Journal*, *15*(8), 2390-2400. https://doi.org/10.1038/s41396-021-00939-5

Genné, D., Sarr, A., Gomez-Chamorro, A., Durand, J., Cayol, C., Rais, O., & Voordouw, M. J. (2018). Competition between strains of *Borrelia afzelii* inside the rodent host and the tick vector. *Proceedings of the Royal Society B: Biological Sciences*, *285*(1890), 17-20. https://doi.org/10.1098/rspb.2018.1804

Genné, D., Sarr, A., Rais, O., & Voordouw, M. J. (2019). Competition between strains of *Borrelia afzelii* in immature *Ixodes ricinus* ticks is not affected by season. *Frontiers in Cellular and Infection Microbiology | www.frontiersin.org, 9*, 431. https://doi.org/10.3389/fcimb.2019.00431

Gern, L. (2008, 2008). Borrelia burgdorferi sensu lato, the agent of Lyme borreliosis: Life in the wilds.

Gern, L., Schaible, U. E., & Simon, M. M. (1993). Mode of inoculation of the Lyme disease agent *Borrelia burgdorferi* influences infection and immune responses in inbred strains of mice. *Journal of Infectious Diseases, 167*(4), 971-975. https://doi.org/10.1093/infdis/167.4.971

Gern, L., Siegenthaler, M., Hu, C. M., Leuba-Garcia, S., Humair, P. F., & Moret, J. (1994). *Borrelia burgdorferi* in rodents (*Apodemus flavicollis* and *A. sylvaticus*): Duration and enhancement of infectivity for *Ixodes ricinus* ticks. *European Journal of Epidemiology, 10*(1), 75-80. https://doi.org/10.1007/BF01717456

Ginsberg, H. S., Buckley, P. A., Balmforth, M. G., Zhioua, E., Mitra, S., & Buckley, F. G. (2005). Reservoir Competence of Native North American Birds for the Lyme Disease Spirochete, Borrelia burgdorferi. *Journal of Medical Entomology, 42*(3), 445-449. https://doi.org/10.1093/jmedent/42.3.445

Goddard, J., Embers, M., Hojgaard, A., & Piesman, J. (2015). Comparison of Tick Feeding Success and Vector Competence for Borrelia burgdorferi Among Immature Ixodes scapularis (Ixodida: Ixodidae) of Both Southern and Northern Clades. *Journal of Medical Entomology, 52*(1), 81-85. https://doi.org/10.1093/jme/tju005

Golde, W. T., Gollobin, P., & Rodriguez, L. L. (2005). A rapid, simple, and humane method for submandibular bleeding of mice using a lancet. *Lab Animal, 34*(9), 39-43. https://doi.org/10.1038/laban1005-39

Golovchenko, M., Sima, R., Hajdusek, O., Grubhoffer, L., Oliver, J. H., & Rudenko, N. (2014). Invasive potential of *Borrelia burgdorferi* sensu stricto *ospC* type L strains increases the possible disease risk to humans in the regions of their distribution. *Parasites & Vectors, 7*(1), 538. https://doi.org/10.1186/s13071-014-0538-y

Gomez-Chamorro, A., Battilotti, F., Cayol, C., Mappes, T., Koskela, E., Boulanger, N., Genné, D., Sarr, A., & Voordouw, M. J. (2019). Susceptibility to infection with *Borrelia afzelii* and TLR2 polymorphism in a wild reservoir host. *Scientific Reports, 9*(1), 6711. https://doi.org/10.1038/s41598-019-43160-3

Gomez-Chamorro, A., Heinrich, V., Sarr, A., Roethlisberger, O., Genné, D., Bregnard, C., Jacquet, M., & Voordouw, M. J. (2019). Maternal antibodies provide bank voles with strain-specific protection against infection by the Lyme disease pathogen. *Applied and Environmental Microbiology, 85*(23), e01887-01819. https://doi.org/10.1128/AEM.01887-19

Graham, A. L., Allen, J. E., & Read, A. F. (2005). Evolutionary Causes and Consequences of Immunopathology. *Annual Review of Ecology, Evolution, and Systematics, 36*(1), 373-397. https://doi.org/10.1146/annurev.ecolsys.36.102003.152622

Graves, C. J., Ros, V. I., Stevenson, B., Sniegowski, P. D., & Brisson, D. (2013). Natural selection promotes antigenic evolvability. *PLoS Pathog, 9*(11), e1003766. https://doi.org/10.1371/journal.ppat.1003766

Grillon, A., Westermann, B., Cantero, P., Jaulhac, B., Voordouw, M. J., Kapps, D., Collin, E., Barthel, C., Ehret-Sabatier, L., & Boulanger, N. (2017). Identification of *Borrelia* protein candidates in mouse skin for potential diagnosis of disseminated Lyme borreliosis. *Scientific Reports, 7*(1), 1-13. https://doi.org/10.1038/s41598-017-16749-9

Grimm, D., Tilly, K., Bueschel, D. M., Fisher, M. A., Policastro, P. F., Gherardini, F. C., Schwan, T. G., & Rosa, P. A. (2005). Defining Plasmids Required by Borrelia

burgdorferi for Colonization of Tick Vector Ixodes scapularis (Acari: Ixodidae). *Journal of Medical Entomology*, *42*(4), 676-684. https://doi.org/10.1093/jmedent/42.4.676
Grimm, D., Tilly, K., Byram, R., Stewart, P. E., Krum, J. G., Bueschel, D. M., Schwan, T. G., Policastro, P. F., Elias, A. F., & Rosa, P. A. (2004). Outer-surface protein C of the Lyme disease spirochete: a protein induced in ticks for infection of mammals. *Proc Natl Acad Sci U S A*, *101*(9), 3142-3147. https://doi.org/10.1073/pnas.0306845101
Gupta, S., & Anderson, R. M. (1999). Population structure of pathogens: The role of immune selection. *Parasitology Today*, *15*(12), 497-501. https://doi.org/10.1016/S0169-4758(99)01559-8
Gupta, S., Ferguson, N., & Anderson, R. (1998). Chaos, persistence, and evolution of strain structure in antigenically diverse infectious agents. *Science*, *280*(5365), 912-915. https://doi.org/10.1126/science.280.5365.912
Gupta, S., Maiden, M. C. J., Feavers, I. M., Nee, S., May, R. M., & Anderson, R. M. (1996). The maintenance of strain structure in populations of recombining infectious agents. *Nature Medicine*, *2*(4), 437-442. https://doi.org/10.1038/nm0496-437
Hamer, S. A., Hickling, G. J., Keith, R., Sidge, J. L., Walker, E. D., & Tsao, J. I. (2012). Associations of passerine birds, rabbits, and ticks with Borrelia miyamotoi and Borrelia andersonii in Michigan, U.S.A. *Parasites and Vectors*, *5*(1), 1-11. https://doi.org/10.1186/1756-3305-5-231
Hanincová, K., Kurtenbach, K., Diuk-Wasser, M., Brei, B., & Fish, D. (2006). Epidemic spread of Lyme borreliosis, northeastern United States. *Emerging Infectious Diseases*, *12*(4), 604-611. https://doi.org/10.3201/eid1204.051016
Hanincova, K., Ogden, N. H., Diuk-Wasser, M., Pappas, C. J., Iyer, R., Fish, D., Schwartz, I., & Kurtenbach, K. (2008). Fitness variation of Borrelia burgdorferi sensu stricto strains in mice. *Appl Environ Microbiol*, *74*(1), 153-157. https://doi.org/10.1128/AEM.01567-07
Hanincová, K., Schafer, S. M., Etti, S., Sewell, H. S., Taragelova, V., Ziak, D., Labuda, M., & Kurtenbach, K. (2003). Association of Borrelia afzelii with rodents in Europe. *Parasitology*, *126*(Pt 1), 11-20. https://doi.org/10.1017/s0031182002002548
Hanincová, K., TARAGELOVÁ, V., Koci, J., Schäfer, S. M., Hails, R., Ullmann, A. J., Piesman, J., Labuda, M., & Kurtenbach, K. (2003). Association of Borrelia garinii and B. valaisiana with Songbirds in Slovakia. *Applied and Environmental Microbiology*, *69*(5), 2825-2830. https://doi.org/10.1128/aem.69.5.2825-2830.2003
Haven, J., Magori, K., & Park, A. W. (2012). Ecological and inhost factors promoting distinct parasite life-history strategies in Lyme borreliosis. *Epidemics*, *4*(3), 152-157. https://doi.org/10.1016/j.epidem.2012.07.001
Haven, J., Vargas, L. C., Mongodin, E. F., Xue, V., Hernandez, Y., Pagan, P., Fraser-Liggett, C. M., Schutzer, S. E., Luft, B. J., Casjens, S. R., & Qiu, W. G. (2011). Pervasive recombination and sympatric genome diversification driven by frequency-dependent selection in *Borrelia burgdorferi*, the Lyme disease bacterium. *Genetics*, *189*(3), 951-966. https://doi.org/10.1534/genetics.111.130773
Hellgren, O., Andersson, M., & Råberg, L. (2011). The genetic structure of Borrelia afzelii varies with geographic but not ecological sampling scale. *Journal of Evolutionary Biology*, *24*, 159-167. https://doi.org/10.1111/j.1420-9101.2010.02148.x
Hershberg, R. (2015). Mutation--The Engine of Evolution: Studying Mutation and Its Role in the Evolution of Bacteria. *Cold Spring Harb Perspect Biol*, *7*(9), a018077. https://doi.org/10.1101/cshperspect.a018077

Hill, M. A., Kwon, J. H., Gerry, B., Hardy, W. A., Walkowiak, O. A., Kavarana, M. N., Nadig, S. N., & Rajab, T. K. (2021). Immune Privilege of Heart Valves. *Front Immunol*, *12*, 731361. https://doi.org/10.3389/fimmu.2021.731361

Hodzic, E., Feng, S., Freet, K. J., & Barthold, S. W. (2003). Borrelia burgdorferi population dynamics and prototype gene expression during infection of immunocompetent and immunodeficient mice. *INFECTION AND IMMUNITY*, *71*(9), 5042-5055. https://doi.org/10.1128/IAI.71.9.5042-5055.2003

Hoen, A. G., Margos, G., Bent, S. J., Diuk-Wasser, M. A., Barbour, A., Kurtenbach, K., & Fish, D. (2009). Phylogeography of Borrelia burgdorferi in the eastern United States reflects multiple independent Lyme disease emergence events. *Proceedings of the National Academy of Sciences of the United States of America*, *106*(35), 15013-15018. https://doi.org/10.1073/pnas.0903810106

Hofmeister, E. K., Ellis, B. A., Childs, J. E., & Glass, G. E. (1999). Longitudinal study of infection with *Borrelia burgdorferi* in a population of *Peromyscus leucopus* at a Lyme disease-enzootic site in Maryland. *The American Journal of Tropical Medicine and Hygiene*, *60*(4), 598-609. https://doi.org/10.4269/ajtmh.1999.60.598

Hojgaard, A., Eisen, R. J., & Piesman, J. (2008). Transmission dynamics of Borrelia burgdorferi s.s. during the key third day of feeding by nymphal Ixodes scapularis (Acari: Ixodidae). *J Med Entomol*, *45*(4), 732-736. https://doi.org/10.1603/0022-2585(2008)45[732:TDOBBS]2.0.CO;2

Hughes, V. L., & Randolph, S. E. (2001). Testosterone increases the transmission potential of tick-borne parasites. *Parasitology*, *123*(4), 365-371. https://doi.org/10.1017/S0031182001008599

Humphrey, P. T., Caporale, D. A., & Brisson, D. (2010). Uncoordinated phylogeography of *Borrelia burgdorferi* and its tick vector, *Ixodes scapularis*. *Evolution*, *64*(9), 2653-2663. https://doi.org/10.1111/j.1558-5646.2010.01001.x

Hunfeld, K. P., Ruzic-Sabljic, E., Norris, D. E., Kraiczy, P., & Strle, F. (2005). In vitro susceptibility testing of Borrelia burgdorferi sensu lato isolates cultured from patients with erythema migrans before and after antimicrobial chemotherapy. *Antimicrob Agents Chemother*, *49*(4), 1294-1301. https://doi.org/10.1128/aac.49.4.1294-1301.2005

Hussell, T., Pennycook, A., & Openshaw, P. J. (2001). Inhibition of tumor necrosis factor reduces the severity of virus-specific lung immunopathology. *Eur J Immunol*, *31*(9), 2566-2573. https://doi.org/10.1002/1521-4141(200109)31:9<2566::aid-immu2566>3.0.co;2-l

Hyde, J. A. (2017). *Borrelia burgdorferi* keeps moving and carries on: A review of borrelial dissemination and invasion. *Frontiers in Immunology*, *8*, 114. https://doi.org/10.3389/fimmu.2017.00114

Imai, D. M., Feng, S., Hodzic, E., & Barthold, S. W. (2013). Dynamics of connective-tissue localization during chronic Borrelia burgdorferi infection. *Laboratory Investigation*, *93*(8), 900-910. https://doi.org/https://doi.org/10.1038/labinvest.2013.81

Ingersoll, M. A. (2017). Sex differences shape the response to infectious diseases. *PLoS Pathog*, *13*(12), e1006688. https://doi.org/10.1371/journal.ppat.1006688

Jacobs, M. B., Purcell, J. E., & Philipp, M. T. (2003). Ixodes scapularis ticks (Acari: Ixodidae) from Louisiana are competent to transmit Borrelia burgdorferi, the agent of Lyme borreliosis. *J Med Entomol*, *40*(6), 964-967. https://doi.org/10.1603/0022-2585-40.6.964

Jacquet, M., Durand, J., Rais, O., & Voordouw, M. J. (2015). Cross-reactive acquired immunity influences transmission success of the Lyme disease pathogen, *Borrelia afzelii*. *Infection, Genetics and Evolution*, *36*, 131-140. https://doi.org/10.1016/j.meegid.2015.09.012

Jacquet, M., Genné, D., Belli, A., Maluenda, E., Sarr, A., & Voordouw, M. J. (2017). The abundance of the Lyme disease pathogen Borrelia afzelii declines over time in the tick vector Ixodes ricinus. *Parasites & Vectors*, *10*(257). https://doi.org/10.1186/s13071-017-2187-4

Jacquet, M., Margos, G., Fingerle, V., & Voordouw, M. J. (2016). Comparison of the lifetime host-to-tick transmission between two strains of the Lyme disease pathogen *Borrelia afzelii*. *Parasites & Vectors*, *9*(1), 645. https://doi.org/10.1186/s13071-016-1929-z

Janeway, C. A. J., Travers, P., Walport, M., & Schlomchik, M. J. (2001). *Immunobiology: the immune system in health and disease* (5 ed.). Garland.

Jauris-Heipke, S., Liegl, G., Preac-Mursic, V., Rössler, D., Schwab, E., Soutschek, E., Will, G., & Wilske, B. (1995). Molecular analysis of genes encoding outer surface protein C ({OspC}) of Borrelia burgdorferi sensu lato: relationship to {ospA} genotype and evidence of lateral gene exchange of {ospC}. *JOURNAL OF CLINICAL MICROBIOLOGY*, *33*(7), 1860-1866. https://doi.org/10.1128/jcm.33.7.1860-1866.1995

Jenkins, A., Diep, B. A., Mai, T. T., Vo, N. H., Warrener, P., Suzich, J., Stover, C. K., & Sellman, B. R. (2015). Differential expression and roles of Staphylococcus aureus virulence determinants during colonization and disease. *mBio*, *6*(1), e02272-02214. https://doi.org/10.1128/mBio.02272-14

Jensen, K. H., Little, T., Skorping, A., & Ebert, D. (2006). Empirical support for optimal virulence in a castrating parasite. *PLOS Biology*, *4*(7), 1265-1269, Article e197. https://doi.org/10.1371/journal.pbio.0040197

Jolley, K. A., Bray, J. E., & Maiden, M. C. J. (2018). Open-access bacterial population genomics: BIGSdb software, the PubMLST.org website and their applications. *Wellcome Open Research*, *3*, 124. https://doi.org/10.12688/wellcomeopenres.14826.1

Jones, K. E., Patel, N. G., Levy, M. A., Storeygard, A., Balk, D., Gittleman, J. L., & Daszak, P. (2008). Global trends in emerging infectious diseases. *Nature*, *451*(7181), 990-993. https://doi.org/10.1038/nature06536

Jutras, B. L., Chenail, A. M., & Stevenson, B. (2013). Changes in bacterial growth rate govern expression of the Borrelia burgdorferi OspC and Erp infection-associated surface proteins. *J Bacteriol*, *195*(4), 757-764. https://doi.org/10.1128/jb.01956-12

Keane-Myers, A., & Nickell, S. P. (1995). T cell subset-dependent modulation of immunity to Borrelia burgdorferi in mice. *J Immunol*, *154*(4), 1770-1776.

Keesing, F., Brunner, J., Duerr, S., Killilea, M., LoGiudice, K., Schmidt, K., Vuong, H., & Ostfeld, R. S. (2009). Hosts as ecological traps for the vector of Lyme disease. *Proceedings of the Royal Society B: Biological Sciences*, *276*(1675), 3911-3919. https://doi.org/10.1098/rspb.2009.1159

Kenedy, M. R., Lenhart, T. R., & Akins, D. R. (2012). The role of Borrelia burgdorferi outer surface proteins. *FEMS Immunology and Medical Microbiology*, *66*(1), 1-19. https://doi.org/10.1111/j.1574-695X.2012.00980.x

Kern, A., Collin, E., Barthel, C., Michel, C., Jaulhac, B., & Boulanger, N. (2011). Tick Saliva Represses Innate Immunity and Cutaneous Inflammation in a Murine Model of Lyme Disease. *Vector-Borne and Zoonotic Diseases*, *11*(10), 1343-1350. https://doi.org/10.1089/vbz.2010.0197

Kern, A., Schnell, G., Bernard, Q., Bœuf, A., Jaulhac, B., Collin, E., Barthel, C., Ehret-Sabatier, L., & Boulanger, N. (2015). Heterogeneity of *Borrelia burgdorferi* sensu stricto population and its involvement in *Borrelia* pathogenicity: study on murine model with specific emphasis on the skin interface. *PLOS ONE*, *10*(7), e0133195. https://doi.org/10.1371/journal.pone.0133195

Klein, S. L. (2000). Hormones and mating system affect sex and species differences in immune function among vertebrates. *Behavioural Processes*, *51*(1), 149-166. https://doi.org/https://doi.org/10.1016/S0376-6357(00)00125-X

Klein, S. L. (2004). Hormonal and immunological mechanisms mediating sex differences in parasite infection. *Parasite Immunology*, *26*(6-7), 247-264. https://doi.org/10.1111/j.0141-9838.2004.00710.x

Klein, S. L., & Flanagan, K. L. (2016). Sex differences in immune responses. *Nature Reviews Immunology*, *16*(10), 626-638. https://doi.org/10.1038/nri.2016.90

Komar, N., Langevin, S., Hinten, S., Nemeth, N., Edwards, E., Hettler, D., Davis, B., Bowen, R., & Bunning, M. (2003). Experimental infection of north American birds with the New York 1999 strain of West Nile virus. *Emerging Infectious Diseases*, *9*(3), 311-322. https://doi.org/10.3201/eid0903.020628

Kurtenbach, K., De Michelis, S., Etti, S., Schäfer, S. M., Sewell, H. S., Brade, V., & Kraiczy, P. (2002). Host association of Borrelia burgdorferi sensu lato - The key role of host complement. *TRENDS in Microbiology*, *10*(2), 74-79. https://doi.org/10.1016/S0966-842X(01)02298-3

Kurtenbach, K., De Michelis, S., Sewell, H. S., Etti, S., Schäfer, S. M., Hails, R., Collares-Pereira, M., Santos-Reis, M., Haninçová, K., Labuda, M., Bormane, A., & Donaghy, M. (2001). Distinct combinations of Borrelia burgdorferi sensu lato genospecies found in individual questing ticks from Europe. *Appl Environ Microbiol*, *67*(10), 4926-4929. https://doi.org/10.1128/aem.67.10.4926-4929.2001

Kurtenbach, K., Hanincová, K., Tsao, J. I., Margos, G., Fish, D., & Ogden, N. H. (2006). Fundamental processes in the evolutionary ecology of Lyme borreliosis. *Nature Reviews Microbiology*, *4*(9), 660-669. https://doi.org/10.1038/nrmicro1475

Lee, W. Y., Moriarty, T. J., Wong, C. H. Y., Zhou, H., Strieter, R. M., Van Rooijen, N., Chaconas, G., & Kubes, P. (2010). An intravascular immune response to Borrelia burgdorferi involves Kupffer cells and iNKT cells. *Nature Immunology*, *11*(4), 295-302. https://doi.org/10.1038/ni.1855

Leo, S. S. T., Gonzalez, A., & Millien, V. (2017). The genetic signature of range expansion in a disease vector—the black-legged tick. *Journal of Heredity*, *108*(2), 176-183. https://doi.org/10.1093/jhered/esw073

Li, Y., Gierahn, T., Thompson, C. M., Trzciński, K., Ford, C. B., Croucher, N., Gouveia, P., Flechtner, J. B., Malley, R., & Lipsitch, M. (2012). Distinct Effects on Diversifying Selection by Two Mechanisms of Immunity against Streptococcus pneumoniae. *PLOS Pathogens*, *8*(11), e1002989. https://doi.org/10.1371/journal.ppat.1002989

Liang, F. T., Brown, E. L., Wang, T., Iozzo, R. V., & Fikrig, E. (2004). Protective niche for *Borrelia burgdorferi* to evade humoral immunity. *The American Journal of Pathology*, *165*(3), 977-985. https://doi.org/10.1016/S0002-9440(10)63359-7

Liang, F. T., Yan, J., Mbow, M. L., Sviat, S. L., Gilmore, R. D., Mamula, M., & Fikrig, E. (2004). *Borrelia burgdorferi* changes its surface antigenic expression in response to host

immune responses. *INFECTION AND IMMUNITY*, *72*(10), 5759-5767. https://doi.org/10.1128/iai.72.10.5759-5767.2004

Liang, L., Wang, J., Schorter, L., Nguyen Trong, T. P., Fell, S., Ulrich, S., & Straubinger, R. K. (2020). Rapid clearance of Borrelia burgdorferi from the blood circulation. *Parasit Vectors*, *13*(1), 191. https://doi.org/10.1186/s13071-020-04060-y

Lieske, D. J., & Lloyd, V. K. (2018). Combining public participatory surveillance and occupancy modelling to predict the distributional response of Ixodes scapularis to climate change. *Ticks and Tick-borne Diseases*, *9*(3), 695-706. https://doi.org/10.1016/j.ttbdis.2018.01.018

Lima, C. M. R., Zeidner, N. S., Beard, C. B., Soares, C. A. G., Dolan, M. C., Dietrich, G., & Piesman, J. (2005). Differential infectivity of the Lyme disease spirochete *Borrelia burgdorferi* derived from *Ixodes scapularis* salivary glands and midgut. *Journal of Medical Entomology*, *42*(3), 506-510. https://doi.org/10.1603/0022-2585(2005)042[0506:diotld]2.0.co;2

Lin, Y.-P., Benoit, V., Yang, X., Martínez-Herranz, R., Pal, U., & Leong, J. M. (2014). Strain-Specific Variation of the Decorin-Binding Adhesin DbpA Influences the Tissue Tropism of the Lyme Disease Spirochete. *PLOS Pathogens*, *10*(7). https://doi.org/10.1371/journal.ppat.1004238

Lin, Y. P., Tan, X., Caine, J. A., Castellanos, M., Chaconas, G., Coburn, J., & Leong, J. M. (2020). Strain-specific joint invasion and colonization by Lyme disease spirochetes is promoted by outer surface protein C. *PLOS Pathogens*, *16*(5), 1-29. https://doi.org/10.1371/journal.ppat.1008516

Lindsay, L. R., Barker, I. K., Surgeoner, G. A., McEwen, S. A., & Campbell, G. D. (1997). Duration of Borrelia burgdorferi infectivity in white-footed mice for the tick vector Ixodes scapularis under laboratory and field conditions in Ontario. *Journal of Wildlife Diseases*, *33*(4), 766-775. https://doi.org/10.7589/0090-3558-33.4.766

Lipsitch, M., & O'Hagan, J. J. (2007). Patterns of antigenic diversity and the mechanisms that maintain them. *Journal of the Royal Society Interface*, *4*(16), 787-802. https://doi.org/10.1098/rsif.2007.0229

Lloyd, V. K., & Hawkins, R. G. (2018). Under-Detection of Lyme Disease in Canada. *Healthcare (Basel, Switzerland)*, *6*(4), E125. https://doi.org/10.3390/healthcare6040125

Loewe, L., & Hill, W. G. (2010). The population genetics of mutations: good, bad and indifferent. *Philos Trans R Soc Lond B Biol Sci*, *365*(1544), 1153-1167. https://doi.org/10.1098/rstb.2009.0317

LoGiudice, K., Ostfeld, R. S., Schmidt, K. A., & Keesing, F. (2003). The ecology of infectious disease: Effects of host diversity and community composition on Lyme disease risk. *Proceedings of the National Academy of Sciences*, *100*(2), 567-571. https://doi.org/10.1073/pnas.0233733100

Lysenko, E. S., Lijek, R. S., Brown, S. P., & Weiser, J. N. (2010). Within-Host Competition Drives Selection for the Capsule Virulence Determinant of Streptococcus pneumoniae. *Current Biology*, *20*(13), 1222-1226. https://doi.org/10.1016/j.cub.2010.05.051

Ma, Y., Seiler, K. P., Eichwald, E. J., Weis, J. H., Teuscher, C., & Weis, J. J. (1998). Distinct characteristics of resistance to *Borrelia burgdorferi*- induced arthritis in C57BL / 6N mice. *INFECTION AND IMMUNITY*, *66*(1), 161-168.

Mackinnon, M. J., Gandon, S., & Read, A. F. (2008). Virulence evolution in response to vaccination: The case of malaria. *Vaccine*, *26*, C42-C52. https://doi.org/10.1016/j.vaccine.2008.04.012

Mackinnon, M. J., & Read, A. F. (1999). Genetic Relationships between Parasite Virulence and Transmission in the Rodent Malaria Plasmodium Chabaudi. *Evolution*, *53*(3), 689-703. https://doi.org/10.1111/j.1558-5646.1999.tb05364.x

Mackinnon, M. J., & Read, A. F. (2004). Virulence in malaria: an evolutionary viewpoint. *Philos Trans R Soc Lond B Biol Sci*, *359*(1446), 965-986. https://doi.org/10.1098/rstb.2003.1414

Madhav, N. K., Brownstein, J. S., Tsao, J. I., & Fish, D. (2009). A Dispersal Model for the Range Expansion of Blacklegged Tick (Acari: Ixodidae). *Journal of Medical Entomology*, *41*(5), 842-852. https://doi.org/10.1603/0022-2585-41.5.842

Magid, D., Schwartz, B., Craft, J., & Schwartz, J. S. (1992). Prevention of Lyme disease after tick bites. A cost-effectiveness analysis. *N Engl J Med*, *327*(8), 534-541. https://doi.org/10.1056/nejm199208203270806

Magnarelli, L. A., Anderson, J. F., & Chappell, W. A. (1984). Antibodies to spirochetes in white-tailed deer and prevalence of infected ticks from foci of Lyme disease in Connecticut. *J Wildl Dis*, *20*(1), 21-26. https://doi.org/10.7589/0090-3558-20.1.21

Marcus, L. C., Steere, A. C., Duray, P. H., Anderson, A. E., & Mahoney, E. B. (1985). Fatal pancarditis in a patient with coexistent Lyme disease and babesiosis. Demonstration of spirochetes in the myocardium. *Ann Intern Med*, *103*(3), 374-376. https://doi.org/10.7326/0003-4819-103-3-374

Margos, G., Binder, K., Dzaferovic, E., Hizo-Teufel, C., Sing, A., Wildner, M., Fingerle, V., & Jolley, K. A. (2015). {PubMLST}.org {\textendash} The new home for the Borrelia {MLSA} database. *Ticks and Tick-borne Diseases*, *6*(6), 869-871. https://doi.org/10.1016/j.ttbdis.2015.06.007

Margos, G., Gatewood, A. G., Aanensen, D. M., Hanincová, K., Terekhova, D., Vollmer, S. A., Cornet, M., Piesman, J., Donaghy, M., Bormane, A., Hurn, M. A., Feil, E. J., Fish, D., Casjens, S., Wormser, G. P., Schwartz, I., & Kurtenbach, K. (2008). MLST of housekeeping genes captures geographic population structure and suggests a European origin of Borrelia burgdorferi. *Proceedings of the National Academy of Sciences of the United States of America*, *105*(25), 8730-8735. https://doi.org/10.1073/pnas.0800323105

Margos, G., Tsao, J. I., Castillo-Ramírez, S., Girard, Y. A., Hamer, S. A., Hoen, A. G., Lane, R. S., Raper, S. L., & Ogden, N. H. (2012). Two boundaries separate *Borrelia burgdorferi* populations in North America. *Applied and Environmental Microbiology*, *78*(17), 6059-6067. https://doi.org/10.1128/AEM.00231-12

Margos, G., Vollmer, S. A., Ogden, N. H., & Fish, D. (2011). Population genetics, taxonomy, phylogeny and evolution of *Borrelia burgdorferi* sensu lato. *Infection, Genetics and Evolution*, *11*(7), 1545-1563. https://doi.org/10.1016/j.meegid.2011.07.022

Margos, G., Wilske, B., Sing, A., Hizo-Teufel, C., Cao, W.-C., Chu, C., Scholz, H., Straubinger, R. K., & Fingerle, V. (2013). Borrelia bavariensis sp. nov. is widely distributed in Europe and Asia. *International Journal of Systematic and Evolutionary Microbiology*, *63*(Pt_11), 4284-4288. https://doi.org/10.1099/ijs.0.052001-0

Margos, G., Wilske, B., Sing, A., Hizo-Teufel, C., Cao, W. C., Chu, C., Scholz, H., Straubinger, R. K., & Fingerle, V. (2013). Borrelia bavariensis sp. nov. is widely distributed in Europe and Asia. *Int J Syst Evol Microbiol*, *63*(Pt 11), 4284-4288. https://doi.org/10.1099/ijs.0.052001-0

Markowski, D., Ginsberg, H. S., Hyland, K. E., & Hu, R. (1998). Reservoir Competence of the Meadow Vole (Rodentia: Cricetidae) for the Lyme Disease Spirochete Borrelia burgdorferi. *Journal of Medical Entomology*, *35*(5), 804-808. https://doi.org/10.1093/jmedent/35.5.804

Marques, A., Telford, S. R., 3rd, Turk, S. P., Chung, E., Williams, C., Dardick, K., Krause, P. J., Brandeburg, C., Crowder, C. D., Carolan, H. E., Eshoo, M. W., Shaw, P. A., & Hu, L. T. (2014). Xenodiagnosis to detect Borrelia burgdorferi infection: a first-in-human study. *Clin Infect Dis*, *58*(7), 937-945. https://doi.org/10.1093/cid/cit939

Marsh, K., & Snow, R. W. (1997). Host-parasite interaction and morbidity in malaria endemic areas. *Philos Trans R Soc Lond B Biol Sci*, *352*(1359), 1385-1394. https://doi.org/10.1098/rstb.1997.0124

Massad, E. (1987). Transmission rates and the evolution of pathogenicity. *Evolution*, *41*(5), 1127-1130. https://doi.org/10.2307/2409198

Mather, T. N., & Mather, M. E. (1990). INTRINSIC COMPETENCE OF 3 IXODID TICKS (ACARI) AS VECTORS OF THE LYME-DISEASE SPIROCHETE [Article]. *Journal of Medical Entomology*, *27*(4), 646-650. https://doi.org/10.1093/jmedent/27.4.646

May, R. M., & Nowak, M. A. (1995). Coinfection and the evolution of parasite virulence. *Proceedings: Biological Sciences*, *261*(1361), 209-215.

Mbow, M. L., Gilmore, R. D., Jr., & Titus, R. G. (1999). An OspC-specific monoclonal antibody passively protects mice from tick-transmitted infection by Borrelia burgdorferi B31. *Infect Immun*, *67*(10), 5470-5472. https://doi.org/10.1128/iai.67.10.5470-5472.1999

McCall, L. I., Siqueira-Neto, J. L., & McKerrow, J. H. (2016). Location, Location, Location: Five Facts about Tissue Tropism and Pathogenesis. *PLoS Pathog*, *12*(5), e1005519. https://doi.org/10.1371/journal.ppat.1005519

McKisic, M. D., Redmond, W. L., & Barthold, S. W. (2000). Cutting edge: T cell-mediated pathology in murine Lyme borreliosis. *J Immunol*, *164*(12), 6096-6099. https://doi.org/10.4049/jimmunol.164.12.6096

Mead, P. S. (2015). Epidemiology of Lyme Disease. *Infectious Disease Clinics of North America*, *29*(2), 187-210. https://doi.org/10.1016/j.idc.2015.02.010

Mechai, S., Margos, G., Feil, E. J., Barairo, N., Lindsay, L. R., Michel, P., & Ogden, N. H. (2016). Evidence for host-genotype associations of *Borrelia burgdorferi* sensu stricto. *PLOS ONE*, *11*(2), 1-25. https://doi.org/10.1371/journal.pone.0149345

Mechai, S., Margos, G., Feil, E. J., Lindsay, L. R., & Ogden, N. H. (2015). Complex Population Structure of Borrelia burgdorferi in Southeastern and South Central Canada as Revealed by Phylogeographic Analysis. *Applied and Environmental Microbiology*, *81*(4), 1309-1318. https://doi.org/10.1128/aem.03730-14

Middelveen, M. J., Sapi, E., Burke, J., Filush, K. R., Franco, A., Fesler, M. C., & Stricker, R. B. (2018). Persistent Borrelia Infection in Patients with Ongoing Symptoms of Lyme Disease. *Healthcare (Basel)*, *6*(2). https://doi.org/10.3390/healthcare6020033

Moody, K. D., & Barthold, S. W. (1998). Lyme Borreliosis in Laboratory Mice. *Laboratory Animal Science*, 4.

Moody, K. D., Terwilliger, G. A., Hansen, G. M., & Barthold, S. W. (1994). EXPERIMENTAL BORRELIA BURGDORFERI INFECTION IN PEROMYSCUS LEUCOPUS. *Journal of Wildlife Diseases*, *30*(2), 155-161. https://doi.org/10.7589/0090-3558-30.2.155

Moriarty, T. J., Norman, M. U., Colarusso, P., Bankhead, T., Kubes, P., & Chaconas, G. (2008). Real-time high resolution 3D imaging of the lyme disease spirochete adhering to and

escaping from the vasculature of a living host. *PLOS Pathogens*, *4*(6), e1000090. https://doi.org/10.1371/journal.ppat.1000090

Motaleb, M. A., Liu, J., & Wooten, R. M. (2015). Spirochetal motility and chemotaxis in the natural enzootic cycle and development of Lyme disease. *Curr Opin Microbiol*, *28*, 106-113. https://doi.org/10.1016/j.mib.2015.09.006

Muehlenbachs, A., Bollweg, B. C., Schulz, T. J., Forrester, J. D., DeLeon Carnes, M., Molins, C., Ray, G. S., Cummings, P. M., Ritter, J. M., Blau, D. M., Andrew, T. A., Prial, M., Ng, D. L., Prahlow, J. A., Sanders, J. H., Shieh, W. J., Paddock, C. D., Schriefer, M. E., Mead, P., & Zaki, S. R. (2016). Cardiac Tropism of Borrelia burgdorferi: An Autopsy Study of Sudden Cardiac Death Associated with Lyme Carditis. *American Journal of Pathology*, *186*(5), 1195-1205. https://doi.org/10.1016/j.ajpath.2015.12.027

Murfin, K. E., Kleinbard, R., Aydin, M., Salazar, S. A., & Fikrig, E. (2019). Borrelia burgdorferi chemotaxis toward tick protein Salp12 contributes to acquisition. *Ticks and Tick-borne Diseases*, *10*(5), 1124-1134. https://doi.org/10.1016/j.ttbdis.2019.06.002

Musser, J. M. (1996). Molecular Population Genetic Analysis of Emerged Bacterial Pathogens: Selected Insights. *Emerging Infectious Diseases*, *2*(1), 1-17. https://doi.org/10.3201/eid0201.960101

Nelson, C. A., Saha, S., Kugeler, K. J., Delorey, M. J., Shankar, M. B., Hinckley, A. F., & Mead, P. S. (2015). Incidence of Clinician-Diagnosed Lyme Disease, United States, 2005-2010. *Emerg Infect Dis*, *21*(9), 1625-1631. https://doi.org/10.3201/eid2109.150417

Niewiesk, S., & Gans, H. (2014). Maternal antibodies: clinical significance, mechanism of interference with immune responses, and possible vaccination strategies. https://doi.org/10.3389/fimmu.2014.00446

Norris, S. J. (2014). vls Antigenic Variation Systems of Lyme Disease Borrelia: Eluding Host Immunity through both Random, Segmental Gene Conversion and Framework Heterogeneity. *Microbiol Spectr*, *2*(6), 2.6.27. https://doi.org/10.1128/microbiolspec.MDNA3-0038-2014

Ogden, N. H., Arsenault, J., Hatchette, T. F., Mechai, S., & Lindsay, L. R. (2017). Antibody responses to *Borrelia burgdorferi* detected by western blot vary geographically in Canada. *PLOS ONE*, *12*(2), e0171731. https://doi.org/10.1371/journal.pone.0171731

Ogden, N. H., Bigras-Poulin, M., O'Callaghan, C. J., Barker, I. K., Kurtenbach, K., Lindsay, L. R., & Charron, D. F. (2007). Vector seasonality, host infection dynamics and fitness of pathogens transmitted by the tick Ixodes scapularis. *Parasitology*, *134*(2), 209-227. https://doi.org/10.1017/S0031182006001417

Ogden, N. H., Bouchard, C., Badcock, J., Drebot, M. A., Elias, S. P., Hatchette, T. F., Koffi, J. K., Leighton, P. A., Lindsay, L. R., Lubelczyk, C. B., Peregrine, A. S., Smith, R. P., & Webster, D. (2019). What is the real number of Lyme disease cases in Canada? *BMC Public Health*, *19*(1), 849. https://doi.org/10.1186/s12889-019-7219-x

Ogden, N. H., Feil, E. J., Leighton, P. A., Lindsay, L. R., Margos, G., Mechai, S., Michel, P., & Moriarty, T. J. (2015). Evolutionary aspects of emerging Lyme disease in Canada. *Applied and Environmental Microbiology*, *81*(21), 7350-7359. https://doi.org/10.1128/AEM.01671-15

Ogden, N. H., Lindsay, L. R., Hanincová, K., Barker, I. K., Bigras-Poulin, M., Charron, D. F., Heagy, A., Francis, C. M., O'Callaghan, C. J., Schwartz, I., & Thompson, R. A. (2008). Role of migratory birds in introduction and range expansion of Ixodes scapularis ticks

and of Borrelia burgdorferi and Anaplasma phagocytophilum in Canada. *Applied and Environmental Microbiology*, *74*(6), 1780-1790. https://doi.org/10.1128/AEM.01982-07

Ogden, N. H., Lindsay, L. R., Morshed, M., Sockett, P. N., & Artsob, H. (2009). The emergence of Lyme disease in Canada. *Cmaj*, *180*(12), 1221-1224. https://doi.org/10.1503/cmaj.080148

Ogden, N. H., Margos, G., Aanensen, D. M., Drebot, M. A., Feil, E. J., Hanincova, K., Schwartz, I., Tyler, S., & Lindsay, L. R. (2011). Investigation of genotypes of Borrelia burgdorferi in Ixodes scapularis ticks collected during surveillance in Canada. *Appl Environ Microbiol*, *77*(10), 3244-3254. https://doi.org/10.1128/AEM.02636-10

Ogden, N. H., St.-Onge, L., Barker, I. K., Brazeau, S., Bigras-Poulin, M., Charron, D. F., Francis, C. M., Heagy, A., Lindsay, L. R., Maarouf, A., Michel, P., Milord, F., O'Callaghan, C. J., Trudel, L., & Thompson, R. A. (2008). Risk maps for range expansion of the Lyme disease vector, *Ixodes scapularis*, in Canada now and with climate change. *International Journal of Health Geographics*, *7*, 1-15. https://doi.org/10.1186/1476-072X-7-24

Ostfeld, R. S., Brisson, D., Oggenfuss, Kelly, Devine, J., Levy, M. Z., & Keesing, F. (2018). Effects of a zoonotic pathogen, *Borrelia burgdorferi*, on the behavior of a key reservoir host. *4074 | Ecology and Evolution*, *8*, 4074-4083. https://doi.org/10.1002/ece3.3961

Pal, U., Yang, X., Chen, M., Bockenstedt, L. K., Anderson, J. F., Flavell, R. A., Norgard, M. V., & Fikrig, E. (2004). OspC facilitates Borrelia burgdorferi invasion of Ixodes scapularis salivary glands. *Journal of Clinical Investigation*, *113*(2), 220-230. https://doi.org/10.1172/JCI200419894

Perkins, S. E., Cattadori, I. M., Tagliapietra, V., Rizzoli, A. P., & Hudson, P. J. (2003). Empirical evidence for key hosts in persistence of a tick-borne disease. *International Journal for Parasitology*, *33*(9), 909-917. https://doi.org/10.1016/s0020-7519(03)00128-0

Piesman, J. (1993). Dynamics of Borrelia burgdorferi Transmission by Nymphal Ixodes dammini Ticks. *Journal of Infectious Diseases*, *167*(5), 1082-1085. https://doi.org/10.1093/infdis/167.5.1082

Piesman, J., Dolan, M. C., Happ, C. M., Luft, B. J., Rooney, S. E., Mather, T. N., & Golde, W. T. (1997). Duration of immunity to reinfection with tick-transmitted Borrelia burgdorferi in naturally infected mice. *INFECTION AND IMMUNITY*, *65*(10), 4043-4047. https://doi.org/10.1128/iai.65.10.4043-4047.1997

Piesman, J., & Gern, L. (2004). Lyme borreliosis in Europe and North America. *Parasitology*, *129*(S1), S191--S220. https://doi.org/10.1017/s0031182003004694

Piesman, J., Oliver, J. R., & Sinsky, R. J. (1990). Growth Kinetics of the Lyme Disease Spirochete (Borrelia Burgdorferi) in Vector Ticks (Ixodes Dammini). *The American Journal of Tropical Medicine and Hygiene*, *42*(4), 352-357. https://doi.org/10.4269/ajtmh.1990.42.352

Piesman, J., & Sinsky, R. J. (1988). Ability to Ixodes scapularis, Dermacentor variabilis, and Amblyomma americanum (Acari: Ixodidae) to acquire, maintain, and transmit Lyme disease spirochetes (Borrelia burgdorferi) [Article]. *J Med Entomol*, *25*(5), 336-339. https://doi.org/10.1093/jmedent/25.5.336

Pospisilova, T., Urbanova, V., Hes, O., Kopacek, P., Hajdusek, O., & Sima, R. (2019). Tracking of Borrelia afzelii Transmission from Infected Ixodes ricinus Nymphs to Mice. *INFECTION AND IMMUNITY*. https://doi.org/10.1128/IAI.00896-18

Preac-Mursic, V., Wilske, B., Jauris, S., Will, G., Reinhardt, S., Lehnert, G., Patsouris, E., Mehraein, P., Soutschek, E., & Klockmann, U. (1992). Active immunization with pC protein ofBorrelia burgdorferi protects gerbils againstB. burgdorferi infection. *Infection*, *20*(6), 342-349. https://doi.org/10.1007/BF01710681

Priem, S., Burmester, G. R., Kamradt, T., Wolbart, K., Rittig, M. G., & Krause, A. (1998). Detection of Borrelia burgdorferi by polymerase chain reaction in synovial membrane, but not in synovial fluid from patients with persisting Lyme arthritis after antibiotic therapy. *Ann Rheum Dis*, *57*(2), 118-121. https://doi.org/10.1136/ard.57.2.118

Probert, W. S., Crawford, M., Cadiz, R. B., & LeFebvre, R. B. (1997). Immunization with Outer Surface Protein (Osp) A, but Not {OspC}, Provides Cross-Protection of Mice Challenged with North American Isolates of Borrelia burgdorferi. *Journal of Infectious Diseases*, *175*(2), 400-405. https://doi.org/10.1093/infdis/175.2.400

Probert, W. S., & LeFebvre, R. B. (1994). Protection of C3H/HeN mice from challenge with Borrelia burgdorferi through active immunization with OspA, OspB, or OspC, but not with OspD or the 83-kilodalton antigen. *Infect Immun*, *62*(5), 1920-1926. https://doi.org/10.1128/iai.62.5.1920-1926.1994

Public Health Agency of Canada. (2023). *Lyme disease: Surveillance*. Public Health Agency of Canada. Retrieved May 21 from https://www.canada.ca/en/public-health/services/diseases/lyme-disease/surveillance-lyme-disease.html

Qiu, W.-G., Dykhuizen, D. E., Acosta, M. S., & Luft, B. J. (2002). Geographic uniformity of the Lyme disease spirochete (*Borrelia burgdorferi*) and its shared history with tick vector (*Ixodes scapularis*) in the Northeastern United States. *Genetics*, *160*(3), 833-849.

Qiu, W.-G., Schutzer, S. E., Bruno, J. F., Attie, O., Xu, Y., Dunn, J. J., Fraser, C. M., Casjens, S. R., & Luft, B. J. (2004). Genetic exchange and plasmid transfers in Borrelia burgdorferi sensu stricto revealed by three-way genome comparisons and multilocus sequence typing. *PNAS*, *101*(39), 14150-14155. https://doi.org/10.1073

Qiu, W. G., Bosler, E. M., Campbell, J. R., Ugine, G. D., Wang, I. N., Luft, B. J., & Dykhuizen, D. E. (1997). A population genetic study of Borrelia burgdorferi sensu stricto from eastern Long Island, New York, suggested frequency-dependent selection, gene flow and host adaptation. *Hereditas*, *127*(3), 203-216. https://doi.org/10.1111/j.1601-5223.1997.00203.x

Råberg, L. (2012). Infection intensity and infectivity of the tick-borne pathogen *Borrelia afzelii*. *Journal of Evolutionary Biology*, *25*(7), 1448-1453. https://doi.org/10.1111/j.1420-9101.2012.02515.x

Råberg, L., de Roode, Jacobus C., Bell, Andrew S., Stamou, P., Gray, D., & Read, Andrew F. (2006). The role of immune-mediated apparent competition in genetically diverse malaria infections. *The American Naturalist*, *168*(1), 41-53. https://doi.org/10.1086/505160

Råberg, L., Hagström, Andersson, M., Bartkova, S., Scherman, K., Strandh, M., & Tschirren, B. (2017). Evolution of antigenic diversity in the tick-transmitted bacterium *Borrelia afzelii*: a role for host specialization? *Journal of Evolutionary Biology*, *30*(5), 1034-1041. https://doi.org/10.1111/jeb.13075

Radolf, J. D., Caimano, M. J., Stevenson, B., & Hu, L. T. (2012). Of ticks, mice and men: understanding the dual-host lifestyle of Lyme disease spirochaetes. *Nat Rev Microbiol*, *10*(2), 87-99. https://doi.org/10.1038/nrmicro2714

Rahman, S., Shering, M., Ogden, N. H., Lindsay, R., & Badawi, A. (2016). Toll-like receptor cascade and gene polymorphism in host-pathogen interaction in Lyme disease. *J Inflamm Res*, *9*, 91-102. https://doi.org/10.2147/jir.S104790

Ramamoorthi, N., Narasimhan, S., Pal, U., Bao, F., Yang, X. F., Fish, D., Anguita, J., Norgard, M. V., Kantor, F. S., Anderson, J. F., Koski, R. A., & Fikrig, E. (2005). The Lyme disease agent exploits a tick protein to infect the mammalian host. *Nature*, *436*(7050), 573-577. https://doi.org/10.1038/nature03812

Rand, P. W., Lacombe, E. H., Smith, R. P., Jr., Rich, S. M., Kilpatrick, W. C., Dragoni, C. A., & Caporale, D. (1993). Competence of Peromyscus maniculatus (Rodentia: Cricetidae) as a Reservoir Host for Borrelia burgdorferi (Spirochaetares: Spirochaetaceae) in the Wild. *Journal of Medical Entomology*, *30*(3), 614-618. https://doi.org/10.1093/jmedent/30.3.614

Read, A. F., Baigent, S. J., Powers, C., Kgosana, L. B., Blackwell, L., Smith, L. P., Kennedy, D. A., Walkden-Brown, S. W., & Nair, V. K. (2015). Imperfect vaccination can enhance the transmission of highly virulent pathogens. *PLOS Biology*, *13*(7), e1002198. https://doi.org/10.1371/journal.pbio.1002198

Richard, A. L., Siegel, S. J., Erikson, J., & Weiser, J. N. (2014). TLR2 signaling decreases transmission of Streptococcus pneumoniae by limiting bacterial shedding in an infant mouse Influenza A co-infection model. *PLoS Pathog*, *10*(8), e1004339. https://doi.org/10.1371/journal.ppat.1004339

Richter, D., Klug, B., Spielman, A., & Matuschka, F. R. (2004). Adaptation of diverse Lyme disease spirochetes in a natural rodent reservoir host. *INFECTION AND IMMUNITY*, *72*(4), 2442-2444. https://doi.org/10.1128/iai.72.4.2442-2444.2004

Richter, D., Matuschka, F. R., Spielman, A., & Mahadevan, L. (2013). How ticks get under your skin: insertion mechanics of the feeding apparatus of Ixodes ricinus ticks. *Proc Biol Sci*, *280*(1773), 20131758. https://doi.org/10.1098/rspb.2013.1758

Richter, D., Spielman, A., Komar, N., & Matuschka, F. R. (2000a). Competence of American robins as reservoir hosts for Lyme disease spirochetes. *Emerg Infect Dis*, *6*(2), 133-138. https://doi.org/10.3201/eid0602.000205

Richter, D., Spielman, A., Komar, N., & Matuschka, F. R. (2000b). Response to dr. Randolph and drs. Gern and humair. *Emerg Infect Dis*, *6*(6), 659-662.

Roehrig, J. T., Piesman, J., Hunt, A. R., Keen, M. G., Happ, C. M., & Johnson, B. J. B. (1992). The hamster immune response to tick-transmitted *Borrelia burgdorferi* differs from the response to needle-inoculated, cultured organisms. *Journal of Immunology*, *149*(11), 3648-36453.

Rogovskyy, A. S., & Bankhead, T. (2014). Bacterial Heterogeneity Is a Requirement for Host Superinfection by the Lyme Disease Spirochete. *INFECTION AND IMMUNITY*, *82*(11), 4542-4552. https://doi.org/10.1128/iai.01817-14

Rollend, L., Fish, D., & Childs, J. E. (2013). Transovarial transmission of *Borrelia* spirochetes by *Ixodes scapularis*: A summary of the literature and recent observations. *Ticks and Tick-borne Diseases*, *4*(1-2), 46-51. https://doi.org/10.1016/j.ttbdis.2012.06.008

Roved, J., Westerdahl, H., & Hasselquist, D. (2017). Sex differences in immune responses: Hormonal effects, antagonistic selection, and evolutionary consequences. *Horm Behav*, *88*, 95-105. https://doi.org/10.1016/j.yhbeh.2016.11.017

Rynkiewicz, E. C., Brown, J., Tufts, D. M., Huang, C.-I., Kampen, H., Bent, S. J., Fish, D., & Diuk-Wasser, M. A. (2017). Closely-related *Borrelia burgdorferi* (sensu stricto) strains

exhibit similar fitness in single infections and asymmetric competition in multiple infections. *Parasites & Vectors*, *10*(1), 64. https://doi.org/10.1186/s13071-016-1964-9
Sadziene, A., Wilske, B., Ferdows, M. S., & Barbour, A. G. (1993). The cryptic {ospC} gene of Borrelia burgdorferi B31 is located on a circular plasmid. *INFECTION AND IMMUNITY*, *61*(5), 2192-2195. https://doi.org/10.1128/iai.61.5.2192-2195.1993
Salkeld, D. J., Leonhard, S., Girard, Y. A., Hahn, N., Mun, J., Padgett, K. A., & Lane, R. S. (2008). Identifying the Reservoir Hosts of the Lyme Disease Spirochete Borrelia burgdorferi in California: The Role of the Western Gray Squirrel (Sciurus griseus). *The American Journal of Tropical Medicine and Hygiene*, *79*(4), 535-540. https://doi.org/10.4269/ajtmh.2008.79.535
Sanders, F. H., Jr., & Oliver, J. H., Jr. (1995). Evaluation of Ixodes scapularis, Amblyomma americanum, and Dermacentor variabilis (Acari: Ixodidae) from Georgia as vectors of a Florida strain of the Lyme disease spirochete, Borrelia burgdorferi. *J Med Entomol*, *32*(4), 402-406. https://doi.org/10.1093/jmedent/32.4.402
Sasaki, M., Fujii, Y., Iwamoto, M., & Ikadai, H. (2013). Effect of Sex Steroids on Babesia microti Infection in Mice. *The American Journal of Tropical Medicine and Hygiene*, *88*(2), 367-375. https://doi.org/10.4269/ajtmh.2012.12-0338
Schmid-Hempel, P. (2009). Immune defence, parasite evasion strategies and their relevance for 'macroscopic phenomena' such as virulence. *Philosophical Transactions of the Royal Society B: Biological Sciences*, *364*(1513), 85-98. https://doi.org/10.1098/rstb.2008.0157
Schmid-Hempel, P. (2021). *Evolutionary parasitology: the integrated study of infections, immunology, ecology, and genetics* (2 ed.). Oxford University Press.
Schneider, P., Bell, A. S., Sim, D. G., O'Donnell, A. J., Blanford, S., Paaijmans, K. P., Read, A. F., & Reece, S. E. (2012). Virulence, drug sensitivity and transmission success in the rodent malaria, Plasmodium chabaudi. *Proceedings of the Royal Society B: Biological Sciences*, *279*(1747), 4677-4685. https://doi.org/10.1098/rspb.2012.1792
Schotthoefer, A. M., & Frost, H. M. (2015). Ecology and Epidemiology of Lyme Borreliosis. *Clinics in Laboratory Medicine*, *35*(4), 723-743. https://doi.org/10.1016/j.cll.2015.08.003
Schrader, C., Schielke, A., Ellerbroek, L., & Johne, R. (2012). PCR inhibitors - occurrence, properties and removal. *J Appl Microbiol*, *113*(5), 1014-1026. https://doi.org/10.1111/j.1365-2672.2012.05384.x
Schuurs, A., & Verheul, H. (1990). Effects of gender and sex steroids on the immune response. *Journal of steroid biochemistry*, *35*(2), 157-172.
Schwanz, L. E., Voordouw, M. J., Brisson, D., & Ostfeld, R. S. (2011). Borrelia burgdorferi Has Minimal Impact on the Lyme Disease Reservoir Host Peromyscus leucopus. *Vector-Borne and Zoonotic Diseases*, *11*(2), 117-124. https://doi.org/10.1089/vbz.2009.0215
Schwartz, A. M., Hinckley, A. F., Mead, P. S., Hook, S. A., & Kugeler, K. J. (2017). Surveillance for Lyme Disease — United States, 2008–2015. *MMWR Surveill Summ*. https://doi.org/ http://dx.doi.org/10.15585/mmwr.ss6622a1
Segerman, B. (2012). The genetic integrity of bacterial species: the core genome and the accessory genome, two different stories. *Frontiers in Cellular and Infection Microbiology*, *2*, 116. https://doi.org/10.3389/fcimb.2012.00116
Sertour, N., Cotté, V., Garnier, M., Malandrin, L., Ferquel, E., & Choumet, V. (2018). Infection kinetics and tropism of *Borrelia burgdorferi* sensu lato in mouse after natural (via ticks) or artificial (needle) infection depends on the bacterial strain. *Frontiers in Microbiology*, *9*, 1722. https://doi.org/10.3389/fmicb.2018.01722

Shadick, N. A., Phillips, C. B., Logigian, E. L., Steere, A. C., Kaplan, R. F., Berardi, V. P., Duray, P. H., Larson, M. G., Wright, E. A., Ginsburg, K. S., Katz, J. N., & Liang, M. H. (1994). The long-term clinical outcomes of Lyme disease. A population-based retrospective cohort study. *Ann Intern Med*, *121*(8), 560-567. https://doi.org/10.7326/0003-4819-121-8-199410150-00002

Shapiro, E., Gerber, M., Persing, D., Berg, A., & Feder, H. (1992). Prevention of Lyme disease: a randomized clinical trial of antimicrobial prophylaxis for people bitten by a deer tick. Proceedings and abstracts of the Fifth International Conference on Lyme Borreliosis, Washington, DC,

Shih, C.-M., Pollack, R. J., Telford, S. R., & Spielman, A. (1992). Delayed dissemination of Lyme disease spirochetes from the site of deposition in the skin of mice. *Journal of Infectious Diseases*, *166*(4), 827-831. https://doi.org/10.1093/infdis/166.4.827

Sidstedt, M., Hedman, J., Romsos, E. L., Waitara, L., Wadso, L., Steffen, C. R., Vallone, P. M., & Radstrom, P. (2018). Inhibition mechanisms of hemoglobin, immunoglobulin G, and whole blood in digital and real-time PCR. *Anal Bioanal Chem*, *410*(10), 2569-2583. https://doi.org/10.1007/s00216-018-0931-z

Skare, J. T., Shaw, D. K., Trzeciakowski, J. P., & Hyde, J. A. (2016). In vivo imaging demonstrates that borrelia burgdorferi ospC is uniquely expressed temporally and spatially throughout experimental infection. *PLOS ONE*, *11*(9), 1-28. https://doi.org/10.1371/journal.pone.0162501

Soares, C. A. G., Zeidner, N. S., Beard, C. B., Dolan, M. C., Dietrich, G., & Piesman, J. (2006). Kinetics of *Borrelia burgdorferi* infection in larvae of refractory and competent tick vectors. *Journal of Medical Entomology*, *43*(1), 61-67. https://doi.org/10.1093/jmedent/43.1.61

Sonenshine, D. (2018). Range Expansion of Tick Disease Vectors in North America: Implications for Spread of Tick-Borne Disease. *International Journal of Environmental Research and Public Health*, *15*(3), 478. https://doi.org/10.3390/ijerph15030478

Sperling, J. L. H., & Sperling, F. A. H. (2009). Lyme borreliosis in canada: Biological diversity and diagnostic complexity from an entomological perspective. *Canadian Entomologist*, *141*(6), 521-549. https://doi.org/10.4039/n08-CPA04

Srivastava, S. Y., & De Silva, A. M. (2008). Reciprocal expression of ospA and ospC in single cells of borrelia burgdorferi. *Journal of Bacteriology*, *190*(10), 3429-3433. https://doi.org/10.1128/JB.00085-08

Stanek, G., & Reiter, M. (2011). The expanding Lyme *Borrelia* complex-clinical significance of genomic species? *Clinical Microbiology and Infection*, *17*(4), 487-493. https://doi.org/10.1111/j.1469-0691.2011.03492.x

Stanek, G., Wormser, G. P., Gray, J., & Strle, F. (2012). Lyme borreliosis. *Lancet*, *379*(9814), 461-473. https://doi.org/10.1016/s0140-6736(11)60103-7

Stearns, S. C. (1992). *The evolution of life histories*. Oxford University Press.

Steere, A. C., Bartenhagen, N. H., Craft, J. E., Hutchinson, G. J., Newman, J. H., Rahn, D. W., Sigal, L. H., Spieler, P. N., Stenn, K. S., & Malawista, S. E. (1983). The Early Clinical Manifestations of Lyme Disease. *Annals of Internal Medicine*, *99*(1), 76-82. https://doi.org/10.7326/0003-4819-99-1-76

Steere, A. C., Coburn, J., & Glickstein, L. (2004). The emergence of Lyme disease. *Journal of Clinical Investigation*, *113*(8), 1093-1101. https://doi.org/10.1172/jci21681

Steere, A. C., Dhar, A., Hernandez, J., Fischer, P. A., Sikand, V. K., Schoen, R. T., Nowakowski, J., McHugh, G., & Persing, D. H. (2003). Systemic symptoms without erythema migrans as the presenting picture of early Lyme disease. *Am J Med*, *114*(1), 58-62. https://doi.org/10.1016/s0002-9343(02)01440-7

Steere, A. C., & Glickstein, L. (2004). Elucidation of Lyme arthritis. *Nat Rev Immunol*, *4*(2), 143-152. https://doi.org/10.1038/nri1267

Steere, A. C., Malawista, S. E., Snydman, D. R., Shope, R. E., Andiman, W. A., Ross, M. R., & Steele, F. M. (1977). Lyme arthritis: an epidemic of oligoarticular arthritis in children and adults in three connecticut communities. *Arthritis Rheum*, *20*(1), 7-17. https://doi.org/10.1002/art.1780200102

Steere, A. C., Strle, F., Wormser, G. P., Hu, L. T., Branda, J. A., Hovius, J. W. R., Li, X., & Mead, P. S. (2016). Lyme borreliosis. *Nature Reviews Disease Primers*, *2*(1), 1-19. https://doi.org/10.1038/nrdp.2016.90

Steinbrink, A., Brugger, K., Margos, G., Kraiczy, P., & Klimpel, S. (2022). The evolving story of Borrelia burgdorferi sensu lato transmission in Europe. *Parasitology Research*, *121*(3), 781-803. https://doi.org/10.1007/s00436-022-07445-3

Stewart, P. E., Byram, R., Grimm, D., Tilly, K., & Rosa, P. A. (2005). The plasmids of Borrelia burgdorferi: essential genetic elements of a pathogen. *Plasmid*, *53*, 1-13. https://doi.org/10.1016/j.plasmid.2004.10.006

Strandh, M., & Råberg, L. (2015). Within-host competition between *Borrelia afzelii ospC* strains in wild hosts as revealed by massively parallel amplicon sequencing. *Philosophical Transactions of the Royal Society B: Biological Sciences*, *370*(1675). https://doi.org/10.1098/rstb.2014.0293

Strle, F., & Stanek, G. (2009). Clinical manifestations and diagnosis of lyme borreliosis. *Curr Probl Dermatol*, *37*, 51-110. https://doi.org/10.1159/000213070

Strle, K., Jones, K. L., Drouin, E. E., Li, X., & Steere, A. C. (2011). Borrelia burgdorferi RST1 (OspC type A) genotype is associated with greater inflammation and more severe Lyme disease. *Am J Pathol*, *178*(6), 2726-2739. https://doi.org/10.1016/j.ajpath.2011.02.018

Swanson, K. I., & Norris, D. E. (2008). Presence of multiple variants of Borrelia burgdorferi in the natural reservoir Peromyscus leucopus throughout a transmission season. *Vector Borne Zoonotic Dis*, *8*(3), 397-405. https://doi.org/10.1089/vbz.2007.0222

Talbot, B., Leighton, P. A., & Kulkarni, M. A. (2020). Genetic melting pot in blacklegged ticks at the northern edge of their expansion front. *Journal of Heredity*, *111*(4), 371-378. https://doi.org/10.1093/jhered/esaa017

Taylor, L. H., Latham, S. M., & Woolhouse, M. E. (2001). Risk factors for human disease emergence. *Philos Trans R Soc Lond B Biol Sci*, *356*(1411), 983-989. https://doi.org/10.1098/rstb.2001.0888

Team, R. C. (2021). *R: A language and environment for statistical computing*. In R Foundation for Statistical Computing.

Telford, S. R., Mather, T. N., Moore, S. I., Wilson, M. L., & Spielman, A. (1988). Incompetence of deer as reservoirs of the Lyme disease spirochete. *American Journal of Tropical Medicine and Hygiene*, *39*(1), 105-109. https://doi.org/10.4269/ajtmh.1988.39.105

Theisen, M., Frederiksen, B., Lebech, A. M., Vuust, J., & Hansen, K. (1993). Polymorphism in ospC gene of Borrelia burgdorferi and immunoreactivity of OspC protein: implications for taxonomy and for use of OspC protein as a diagnostic antigen. *JOURNAL OF*

CLINICAL MICROBIOLOGY, *31*(10), 2570-2576. https://doi.org/10.1128/jcm.31.10.2570-2576.1993

Tonetti, N., Voordouw, M. J., Durand, J., Monnier, S., & Gern, L. (2015). Genetic variation in transmission success of the Lyme borreliosis pathogen Borrelia afzelii. *Ticks and Tick-borne Diseases*, *6*(3), 334-343. https://doi.org/https://doi.org/10.1016/j.ttbdis.2015.02.007

Travinsky, B., Bunikis, J., & Barbour, A. G. (2010). Geographic differences in genetic locus linkages for Borrelia burgdorferi. *Emerg Infect Dis*, *16*(7), 1147-1150. https://doi.org/10.3201/eid1607.091452

Trigunaite, A., Dimo, J., & Jørgensen, T. N. (2015). Suppressive effects of androgens on the immune system. *Cellular Immunology*, *294*(2), 87-94. https://doi.org/10.1016/j.cellimm.2015.02.004

Tsao, J. I. (2009). Reviewing molecular adaptations of Lyme borreliosis spirochetes in the context of reproductive fitness in natural transmission cycles. *Vet Res*, *40*(2), 36. https://doi.org/10.1051/vetres/2009019

Tschirren, B., Andersson, M., Scherman, K., Westerdahl, H., Mittl, P. R., & Råberg, L. (2013). Polymorphisms at the innate immune receptor TLR2 are associated with Borrelia infection in a wild rodent population. *Proc Biol Sci*, *280*(1759), 20130364. https://doi.org/10.1098/rspb.2013.0364

Tyler, S., Tyson, S., Dibernardo, A., Drebot, M., Feil, E. J., Graham, M., Knox, N. C., Lindsay, L. R., Margos, G., Mechai, S., Van Domselaar, G., Thorpe, H. A., & Ogden, N. H. (2018). Whole genome sequencing and phylogenetic analysis of strains of the agent of Lyme disease *Borrelia burgdorferi* from Canadian emergence zones. *Scientific Reports*, *8*(1), 1-12. https://doi.org/10.1038/s41598-018-28908-7

Urwin, R., & Maiden, M. C. J. (2003). Multi-locus sequence typing: a tool for global epidemiology. *TRENDS in Microbiology*, *11*(10), 479-487. https://doi.org/10.1016/j.tim.2003.08.006

Van Gundy, T. J., Ullmann, A. J., Brandt, K. S., & Gilmore, R. D. (2021). A transwell assay method to evaluate Borrelia burgdorferi sensu stricto migratory chemoattraction toward tick saliva proteins. https://doi.org/10.1016/j.ttbdis.2021.101782

Visher, E., Evensen, C., Guth, S., Lai, E., Norfolk, M., Rozins, C., Sokolov, N. A., Sui, M., & Boots, M. (2021). The three Ts of virulence evolution during zoonotic emergence. *Proceedings of the Royal Society B-Biological Sciences*, *288*(1956), Article 20210900. https://doi.org/10.1098/rspb.2021.0900

Voordouw, M. J., Lachish, S., & Dolan, M. C. (2015). The Lyme disease pathogen has no effect on the survival of its rodent reservoir host. *PLOS ONE*, *10*(2), e0118265. https://doi.org/10.1371/journal.pone.0118265

Vuong, H. B., Canham, C. D., Fonseca, D. M., Brisson, D., Morin, P. J., Smouse, P. E., & Ostfeld, R. S. (2014). Occurrence and transmission efficiencies of Borrelia burgdorferi ospC types in avian and mammalian wildlife. *Infection, Genetics and Evolution*, *27*, 594-600. https://doi.org/https://doi.org/10.1016/j.meegid.2013.12.011

Wager, B., Shaw, D. K., Groshong, A. M., Blevins, J. S., & Skare, J. T. (2015). BB0744 Affects Tissue Tropism and Spatial Distribution of Borrelia burgdorferi. *INFECTION AND IMMUNITY*, *83*(9), 3693-3703. https://doi.org/10.1128/IAI.00828-15

Wang, G., Liveris, D., Mukherjee, P., Jungnick, S., Margos, G., & Schwartz, I. (2014). Molecular typing of Borrelia burgdorferi. *Current Protocols in Microbiology*, *2014*, 12C.15.11-12C.15.31. https://doi.org/10.1002/9780471729259.mc12c05s34

Wang, G., Ojaimi, C., Wu, H., Saksenberg, V., Iyer, R., Liveris, D., McClain, Steve A., Wormser, Gary P., & Schwartz, I. (2002). Disease severity in a murine model of Lyme borreliosis is associated with the genotype of the infecting *Borrelia burgdorferi* sensu stricto strain. *The Journal of Infectious Diseases*, *186*(6), 782-791. https://doi.org/10.1086/343043

Wang, G., Ojaimi, C., Wu, H., Saksenberg, V., Iyer, R., McClain, S. A., Wormser, G. P., & Schwartz, I. (2001). Impact of genotypic variation of *Borrelia burgdorferi* sensu stricto on kinetics of dissemination and severity of disease in C3H/HeJ mice. *Abstracts of the General Meeting of the American Society for Microbiology*, *101*(7), 294-295. https://doi.org/10.1128/IAI.69.7.4303

Wang, I. N., Dykhuizen, D. E., Qiu, W., Dunn, J. J., Bosler, E. M., & Luft, B. J. (1999). Genetic diversity of *ospC* in a local population of *Borrelia burgdorferi* sensu stricto. *Genetics*, *151*(1), 15-30. https://doi.org/10.1093/genetics/151.1.15

Weedall, G. D., & Conway, D. J. (2010). Detecting signatures of balancing selection to identify targets of anti-parasite immunity. *Trends Parasitol*, *26*(7), 363-369. https://doi.org/10.1016/j.pt.2010.04.002

Weinberger, D. M., Trzciński, K., Lu, Y.-J., Bogaert, D., Brandes, A., Galagan, J., Anderson, P. W., Malley, R., & Lipsitch, M. (2009). Pneumococcal Capsular Polysaccharide Structure Predicts Serotype Prevalence. *PLOS Pathogens*, *5*(6), e1000476. https://doi.org/10.1371/journal.ppat.1000476

Weis, J. J., Yang, L., Seiler, K. P., & Silver, R. M. (1997). Pathological Manifestations in Murine Lyme Disease: Association with Tissue Invasion and Spirochete Persistence. *Clinical Infectious Diseases*, *25*(Supplement_1), S18-S24. https://doi.org/10.1086/516172

Wooten, R. M., & Weis, J. J. (2001). Host-pathogen interactions promoting inflammatory Lyme arthritis: Use of mouse models for dissection of disease processes. *Current Opinion in Microbiology*, *4*(3), 274-279. https://doi.org/10.1016/S1369-5274(00)00202-2

Wormser, G. P. (2006). Early Lyme Disease. *New England Journal of Medicine*, *354*(26), 2794-2801. https://doi.org/10.1056/NEJMcp061181

Wormser, G. P., Brisson, D., Liveris, D., Hanincová, K., Sandigursky, S., Nowakowski, J., Nadelman, R. B., Ludin, S., & Schwartz, I. (2008). *Borrelia burgdorferi* genotype predicts the capacity for hematogenous dissemination during early Lyme disease. *Journal of Infectious Diseases*, *198*(9), 1358-1364. https://doi.org/10.1086/592279

Wormser, G. P., Dattwyler, R. J., Shapiro, E. D., Halperin, J. J., Steere, A. C., Klempner, M. S., Krause, P. J., Bakken, J. S., Strle, F., Stanek, G., Bockenstedt, L., Fish, D., Dumler, J. S., & Nadelman, R. B. (2006). The clinical assessment, treatment, and prevention of lyme disease, human granulocytic anaplasmosis, and babesiosis: clinical practice guidelines by the Infectious Diseases Society of America. *Clin Infect Dis*, *43*(9), 1089-1134. https://doi.org/10.1086/508667

Wormser, G. P., Liveris, D., Nowakowski, J., Nadelman, R. B., Cavaliere, L. F., McKenna, D., Holmgren, D., & Schwartz, I. (1999). Association of Specific Subtypes of Borrelia burgdorferi with Hematogenous Dissemination in Early Lyme Disease. *The Journal of Infectious Diseases*, *180*(3), 720-725. https://doi.org/10.1086/314922

Wright, S. D., & Nielsen, S. W. (1990). Experimental infection of the white-footed mouse with Borrelia burgdorferi. *Am J Vet Res*, *51*(12), 1980-1987.

Xu, L., Yoon, H., Zhao, M. Q., Liu, J., Ramana, C. V., & Enelow, R. I. (2004). Cutting edge: pulmonary immunopathology mediated by antigen-specific expression of TNF-alpha by antiviral CD8+ T cells. *J Immunol*, *173*(2), 721-725. https://doi.org/10.4049/jimmunol.173.2.721

Yang, L., Weis, J. H., Eichwald, E., Kolbert, C. P., Persing, D. H., & Weis, J. J. (1994). Heritable susceptibility to severe *Borrelia burgdorferi*-induced arthritis is dominant and is associated with persistence of large numbers of spirochetes in tissues. *INFECTION AND IMMUNITY*, *62*(2), 492-500. https://doi.org/10.1128/iai.62.2.492-500.1994

Yang, X. F., Pal, U., Alani, S. M., Fikrig, E., & Norgard, M. V. (2004). Essential role for OspA/B in the life cycle of the Lyme disease spirochete. *J Exp Med*, *199*(5), 641-648. https://doi.org/10.1084/jem.20031960

Zafar, M. A., Wang, Y., Hamaguchi, S., & Weiser, J. N. (2017). Host-to-Host Transmission of Streptococcus pneumoniae Is Driven by Its Inflammatory Toxin, Pneumolysin. *Cell Host & Microbe*, *21*(1), 73-83. https://doi.org/10.1016/j.chom.2016.12.005

Zawada, S. G., Fricken, M. E. v., Weppelmann, T. A., Sikaroodi, M., & Gillevet, P. M. (2020). Optimization of tissue sampling for *Borrelia burgdorferi* in white-footed mice (*Peromyscus leucopus*). *PLOS ONE*, *15*(1), e0226798. https://doi.org/10.1371/journal.pone.0226798

Zeidner, N. S., Schneider, B. S., Dolan, M. C., & Piesman, J. (2001). An analysis of spirochete load, strain, and pathology in a model of tick-transmitted Lyme borreliosis. *Vector-Borne and Zoonotic Diseases*, *1*(1), 35-44. https://doi.org/10.1089/153036601750137642

Zhi, H., Xie, J., & Skare, J. T. (2018). The Classical Complement Pathway Is Required to Control Borrelia burgdorferi Levels During Experimental Infection. *Front Immunol*, *9*, 959. https://doi.org/10.3389/fimmu.2018.00959

Zhong, X., Nouri, M., & Råberg, L. (2019). Colonization and pathology of Borrelia afzelii in its natural hosts. *Ticks and Tick-borne Diseases*, *10*(4), 822-827. https://doi.org/10.1016/j.ttbdis.2019.03.017

Zinck, C. B., Thampy, P. R., Rego, R. O. M., Brisson, D., Ogden, N. H., & Voordouw, M. (2022). Borrelia burgdorferi strain and host sex influence pathogen prevalence and abundance in the tissues of a laboratory rodent host. *Mol Ecol*. https://doi.org/10.1111/mec.16694

Zuk, M., & McKean, K. A. (1996). Sex differences in parasite infections: patterns and processes. *International Journal for Parasitology*, *26*(10), 1009-1024.

Appendix A – Supplementary material for Ch. 2

This appendix is the supplementary materials for a manuscript published in Molecular Ecology,

Zinck, C. B., Thampy, P. R., Rego, R. O. M., Brisson, D., Ogden, N. H., & Voordouw, M. (2022). *Borrelia burgdorferi* strain and host sex influence pathogen prevalence and abundance in the tissues of a laboratory rodent host. Molecular Ecology. https://doi.org/10.1111/mec.16694

Section 1 – Plasmid profiles for the 12 strains of *B. burgdorferi*

We used PCR to determine whether the *Borrelia burgdorferi* strains used in this study contained the plasmids necessary to complete the tick-borne life cycle. We tested the strains for the following 20 plasmids: lp5, lp17, lp21, lp25, lp28-1, lp28-2, lp28-3, lp28-4, lp36, lp38, lp54, lp56, cp9, cp26, cp32-1, cp32-2, cp32-3, cp32-6, cp32-8, and cp32-9. Total genomic DNA was prepared from approximately 7 ml of *B. burgdorferi* culture using the Wizard genomic DNA kit (Promega, Madison, WI) as per the manufacturer's instructions. The total plasmid content of the strains of *B. burgdorferi* were compared using primers specific for plasmids based on the complete genome sequence of *B. burgdorferi* strain B31 (Elias et al., 2002; Purser & Norris, 2000). DNA from strains B31 and N40 were used as positive controls.

The plasmid profile of the *B. burgdorferi* strains are shown in Table S1. The plasmid number ranged from 10 plasmids for strain 150 to 15 plasmids for strains 57, 22.2, 10.2, and 178 (Table S1). Most of the *B. burgdorferi* strains contained the same 10 plasmids, which were as follows: lp17, lp25, lp28-2, lp28-3, lp28-4, lp36, lp54, cp26, cp32-2, and cp32-9. The exceptions were strain 111, which did not contain lp28-2 and cp32-2, and strain 66, which did not include cp32-2.

Plasmid lp28-1 was not detected using the designated primers in 10 of the 12 strains (the exceptions were strains 22.2 and 10.2). The plasmid profile for those 10 strains where lp28-1 was missing is similar to strain N40. It has been shown that the important *vlsE* gene present on lp28-1 is present on plasmid lp36 in strain N40. Given the fact that all 10 strains were able to establish a chronic infection in the mouse, we conclude that the *vlsE* gene is present on the lp36 plasmid in strains where lp28-1 was determined to be absent. The plasmids that are relevant for infection in ticks and mammalian hosts are present (personal communication with Ryan Rego). The plasmids that are missing for the *B. burgdorferi* strains have not been shown to be important for infection in the tick or the mammalian host. For example, several of the cp32 plasmids are copies with redundancy. The loss of these redundant plasmids does not lead to loss of infection in a lab setting. Another example, the loss of plasmid lp38 from *B. burgdorferi* strain B31 did not lead to any change in infection in a lab setting (Dulebohn et al., 2011). Of the 10 strains that we tested, 2 have a plasmid profile similar to strain B31 and 8 have a plasmid profile similar to strain N40.

Table S1. The plasmid profile is shown for 10 strains of *B. burgdorferi*: 57, 150, 167, 126, 22.2, 10.2, 54, 198, 178, and 178. The 20 plasmids tested were as follows: lp5, lp17, lp21, lp25, lp28-1, lp28-2, lp28-3, lp28-4, lp36, lp38, lp54, lp56, cp9, cp26, cp32-1, cp32-2, cp32-3, cp32-6, cp32-8, cp32-9. The '+' and '-' symbols indicate whether a plasmid was present or absent for a given strain.

Plasmid	111	66	57	150	167	126	22.2	10.2	54	198	174	178
lp5	+	-	+	-	-	-	+	+	-	-	-	+
lp17	+	+	+	+	+	+	+	+	+	+	+	+
lp21	-	-	-	-	-	-	-	-	-	+	-	+
lp25	+	+	+	+	+	+	+	+	+	+	+	+
lp28-1	-	-	-	-	-	-	+	+	-	-	-	-
lp28-2	-	+	+	+	+	+	+	+	+	+	+	+
lp28-3	+	+	+	+	+	+	+	+	+	+	+	+

lp28-4	+	+	+	+	+	+	+	+	+	+	+	+
lp36	+	+	+	+	+	+	+	+	+	+	+	+
lp38	-	+	-	-	-	-	-	-	-	-	-	-
lp54	+	+	+	+	+	+	+	+	+	+	+	+
lp56	-	-	-	-	-	-	-	-	-	-	-	-
cp9	+	+	+	-	+	+	+	+	+	+	+	+
cp26	+	+	+	+	+	+	+	+	+	+	+	+
cp32-1	-	+	+	-	+	+	+	+	+	-	+	-
cp32-2	-	-	+	+	+	+	+	+	+	+	+	+
cp32-3	-	-	+	-	-	+	+	-	-	+	-	+
cp32-6	+	+	+	-	-	-	+	+	+	+	+	+
cp32-8	-	-	-	-	-	-	-	-	-	-	-	-
cp32-9	+	+	+	+	+	+	+	+	+	+	+	+
Plasmid count	11	13	15	10	12	13	15	15	13	14	13	15

Section 2 – Additional Methods

Nymphal infestation of mice: The *Mus musculus* mice (strain C3H/HeJ) were infected with the *B. burgdorferi* strains via nymphal tick bite. Each mouse was infested with 3 nymphs that were putatively infected with the strain of interest. To protect nymphs against the mouse grooming response and to enhance recovery of engorged nymphs, the nymphs were placed in a capsule attached to the lower back of the mouse using the following procedure. Each mouse was anaesthetized for ~40 min with a mixture of xylazine and ketamine and had its lower back shaved (~1 cm above the base of the tail to their midback). A capsule made from a cut 1.5 mL microcentrifuge tube attached to a neoprene base was glued to the mouse with latex costume glue. The nymphs were placed in the capsule which was sealed with a nylon mesh to allow air transfer. Each mouse was fixed with an Elizabethan collar for the duration of the infestation to prevent the mouse from removing the capsule. Nymphs were allowed to feed to repletion and were recovered after detaching. After all nymphs had detached (5-7 days), the Elizabethan collars were removed, and the capsule was removed using mineral oil to dissolve the glue.

Larval infestation of mice: At days 30, 60, and 90 PI, each mouse was infested with 50-100 naïve *I. scapularis* larval ticks. All mice were anaesthetized for ~40 min with a mixture of xylazine and ketamine for each of the 3 larval infestations. The larvae fed on the mice for 3 to 5 days before dropping off in the engorged state.

DNA extraction of tissues: All samples were processed using the Qiagen blood and tissue kit. All samples were processed following the manufacturer's tissue DNA extraction protocol. Samples were incubated in a shaking incubator overnight at 56 ºC at 600 rpm. The DNA of the necropsy tissues and the ear biopsies was resuspended in 100 µL and 55 µL of elution buffer, respectively. Tissues from uninfected control mice (i.e., uninfected DNA controls) and reagent controls (no tissue added) were processed with experimental samples to check for contamination. All samples had their DNA concentration measured via Nanodrop™ (Thermo Fisher Scientific). All DNA extractions were stored at -80 ºC prior to use in qPCR.

***23s rRNA* intergenic spacer qPCR:** To determine the presence and abundance of *B. burgdorferi* in the mouse tissues, a qPCR was used that targeted the *23s rRNA* intergenic spacer

gene of *B. burgdorferi*. The primers and reaction protocol for this qPCR are previously described (Courtney et al., 2004). Each reaction used 3 µL of template in a total volume of 20 µL. A synthetic gene fragment was created to use as a standard (IDTDNA, gBlock). All transformed values used the same linear equation created by combining all standards into one regression (range: $1 – 10^5$ copies/µL, n = 81). A strict lower detection limit of 1 gene copy/µL was applied based on the lower detection limit of the standards.

Mouse *Beta-actin* qPCR: To determine the number of mouse genomes in the mouse tissues, a qPCR was used that targeted the *Beta-actin* gene of *M. musculus*. The primers and reaction protocol for this qPCR are previously described (Dai et al., 2009). Each reaction was done with 1 µL of template in a total volume of 20 µL. A separate synthetic standard (IDTDNA, gBlock) was designed for this reaction, and again the linear equation used to determine the gene copy number was made by performing a single regression on all standards run (range: $20 – 2x10^8$ copies/µL, n = 118).

Statistical software: We used R version 4.0.4 for all statistical analyses (R Core Team, 2021). We used the *lmer()* function in the lme4 package to run the LMMs (Bates et al., 2015) and the *Anova()* function in the car package to run the Wald tests of statistical significance (Fox & Weisberg, 2019). Post-hoc analysis and calculation of estimated marginal means were done using *emmeans(), pairs(), pwpm()* functions in the emmeans package (Lenth, 2021) and *ggemmeans()* function in the ggeffects package (Lüdecke, 2018). Correlations were calculated using the *cor.test()* function in the base package. Correlation matrices and correlation plots were calculated using the *rcorr()* function in the Hmisc package (Harrell Jr., 2021).

Section 3 – Synthetic standards used in qPCR

Synthetic *23S rRNA* gene standard: The presence and abundance of *B. burgdorferi* in the mouse tissues was estimated using a *23S rRNA* quantitative-PCR that was previously described (Courtney et al., 2004). To translate the quantification cycle (Cq) values produced by the *23S rRNA* qPCR to estimates of the abundance of *B. burgdorferi* requires a standard curve. We created this standard curve by repeatedly performing the *23S rRNA* qPCR on a dilution series of a synthetic *23S rRNA* gene of known concentrations. The synthetic standard was purchased as a gblock from IDTDNA. The standard was based on the *B. burgdorferi* B31 reference sequence (Genbank Accession number: AE000783.1) to encompass the region targeted by the *23S rRNA* primers (Table S2). A total sequence length of 181 nt was used to ensure that the forward and reverse primer sites were not at the ends of the gblock where degradation could impact binding. The *23S rRNA* gene sequence was modified from the reference genome to allow for two methods of differentiation between the synthetic standard and a real gene copy for contamination checks. A total of 30 nt were inserted in the fragment between the forward and reverse priming sites to allow for product discrimination on an agarose gel (amplicon lengths of the synthetic standard (105 nt) and *B. burgdorferi* strain B31 (75 nt) differ by 30 nucleotides). A *BamHI* restriction enzyme cut site was included in the 30-nucleotide insert so that a restriction digest would cleave the synthetic standard, but not a copy of the real *23S rRNA* gene. The gblock was initially suspended in Buffer AE (Qiagen DNEasy kit) with 0.1 mg/mL tRNA (Sigma-Aldrich: 10109517001). This was done so that the standard was in the same suspension buffer as all the experimental samples. The tRNA was added to reduce the impact of DNA adsorption to the walls of the qPCR tubes in dilutions with a low concentration of gblock *23S rRNA*.

Table S2. The sequences used in creating the *23S rRNA* synthetic standard as well as the primer and probe sequences for the *23S rRNA* qPCR. All sequences are reported in 5'-3' direction. The *23S rRNA* forward primer and the *23S rRNA* reverse primer are highlighted in yellow and green, respectively. The 30-nucleotide insert sequence and the *BamHI* cut site are shown in red and purple, respectively.

Identity	Sequence (5'-3')
23S rRNA forward primer	CGAGTCTTAAAAGGGCGATTTAGT
23S rRNA reverse primer	GCTTCAGCCTGGCCATAAATAG
23S rRNA probe	AGATGTGGTAGACCCGAAGCCGAGTG
B. burgdorferi B31 original sequence	TTATCATGTCTAGCAAGATTAAAGCATAGAAGTGCTGGAGTC GAAGCGAAAGCGAGTCTTAAAAGGGCGATTTAGTTAGATGTG GTAGACCCGAAGCCGAGTGATCTATTTATGGCCAGGCTGAAG CTTGGGTAAAACCAAGTGGAGGGCC
gBlock synthetic standard	TTATCATGTCTAGCAAGATTAAAGCATAGAAGTGCTGGAGT CGAAGCGAAAGCGAGTCTTAAAAGGGCGATTTAGTGCGGA TCCTATCATGTAGATGTGGTAGACCCGAAGCCGAGTGAGCG CTGATTGCATAATCTATTTATGGCCAGGCTGAAGCTTGGGTA AAACCAAGTGGAGGGCC

Synthetic mouse *Beta-actin* gene standard: The abundance of the mouse genome (*M. musculus*) in the mouse tissues was estimated using a *Beta-actin* qPCR that was previously described (Dai et al., 2009). A synthetic gblock standard was created for the *Beta-actin* gene of *M. musculus* mice following the same rationale as above. This was based on the reference sequence (Genbank Accession number: NC_000071.7) to encompass the region targeted by the *Beta-actin* primers (Table S3). The total sequence length of the synthetic mouse *Beta-actin* gene is 197 nt. Like the *23S rRNA* standard, the internal gene sequence was modified by adding a 33-nucleotide insert that contained a *BamHI* cut site. This 33-nt insert will allow for differentiation from a natural sample. The *Beta-actin* standard was suspended in the same manner as the *23S rRNA* standard.

Table S3. The sequences used in creating the mouse *Beta-actin* synthetic standard as well as the primer and probe sequences for the mouse *Beta-actin* qPCR. All sequences are reported in 5'-3' direction. The *Beta-actin* forward primer and the *Beta-actin* reverse primer are highlighted in yellow and green, respectively. The 33-nucleotide insert sequence and the *BamHI* cut site are shown in red and purple, respectively.

Identity	Sequence (5'-3')

Beta-actin forward primer	AGAGGGAAATCGTGCGTGAC
Beta-actin reverse primer	CAATAGTGATGACCTGGCCGT
Beta-actin probe	CACTGCCGCATCCTCTTCCTCCC
M. musculus Beta-actin original sequence	TACCTCATGAAGATCCTGACCGAGCGTGGCTACAGCTTCACCA CCACAGCTGAGAGGGAAATCGTGCGTGACATCAAAGAGAAGC TGTGCTATGTTGCTCTAGACTTCGAGCAGGAGATGGCCACTGC CGCATCCTCTTCCTCCCTGGAGAAGAGCTATGAGCTGCCTGAC GGCCAGGTCATCACTATTGGCAACGAGCGGTTCCGATGC
gBlock synthetic standard	TTCACCACCACAGCTGAGAGGGAAATCGTGCGTGACATCAATC CAGGATCCTTCACAGAGAAGCTGTGCTATGTTGCTCTAGACTTC GAGCAGGAGATGGCCACTGCCGCATCCTCTTCCTCCCTGGAGCT TCAACACCCCAGCCAGAGCTATGAGCTGCCTGACGGCCAGGTCA TCACTATTGGCAACGAGCGGTT

Section 4 – Comparison of methods of standardizing abundance of *B. burgdorferi* in mouse tissues

The abundance of *B. burgdorferi* in the mouse tissues was standardized relative to 3 different estimates of the amount of host tissue: (1) mass of host tissue, (2) DNA concentration of the DNA extraction, and (3) number of mouse *Beta-actin* gene copies. For standardization method 1, each sample was weighed prior to DNA extraction. For standardization method 2, following DNA extraction, each sample had their DNA concentration measured via Nanodrop. For standardization method 3, a qPCR targeting the mouse *Beta-actin* gene was performed for all DNA extractions. These 3 methods of standardizing the abundance of *B. burgdorferi* have the following units: (1) number of *23S rRNA* copies per mg of tissue, (2) number of *23S rRNA* copies per mg of DNA, and (3) number of *23S rRNA* copies per 10^6 *Beta-actin* copies. These three response variables were all log10-transformed to normalize the residuals. Three identical linear mixed effect models (LMMs) were run for each method of standardization with the fixed factors of sex, tissue, strain, and temporal block. Mouse identity was included as a random factor. The significance of the fixed factors increased as the method of standardization became more sophisticated (Table S4). In general, the three methods were all significantly positively correlated (Table S5).

Table S4. The results of the LMMs for the 3 different methods of standardizing the abundance of *B. burgdorferi* in the mouse tissues. In methods 1, 2, and 3, the number of *23S rRNA* copies was standardized relative to mg of tissue, ng of DNA, and number of mouse *Beta-actin* gene copies, respectively. Each LMM contained the fixed factors of strain, sex, tissue, and temporal block and mouse was treated as a random factor. The p-values (P) show that strain and sex are both significant for the standardization method that uses the number of mouse *Beta-actin* gene copies as an estimate of host tissue abundance.

Method	Denominator	Factor	P
1	mg of tissue	Strain	0.004
1	mg of tissue	Sex	0.840
1	mg of tissue	Tissue	$2.2*10^{-16}$
1	mg of tissue	Temporal block	$7.292*10^{-10}$
2	ng of DNA	Strain	$4.16*10^{-4}$
2	ng of DNA	Sex	0.625
2	ng of DNA	Tissue	$2.2*10^{-16}$
2	ng of DNA	Temporal block	0.034
3	*Beta-actin*	Strain	0.002
3	*Beta-actin*	Sex	0.0020
3	*Beta-actin*	Tissue	$2.2*10^{-16}$
3	*Beta-actin*	Temporal block	0.153

Table S5. The three methods of standardizing the abundance of *B. burgdorferi* in the mouse tissues were strongly correlated. For each pairwise correlation, the Pearson correlation coefficient (r) and the associated p-value are shown.

Comparison	r	P
Beta-actin versus mg of tissue	0.945	$1.177*10^{-5}$
Beta-actin versus ng of DNA	0.959	$3.008*10^{-6}$
mg of tissue versus ng of DNA	0.944	$1.243*10^{-5}$

Standardizing the number of spirochetes relative to a host housekeeping gene gives the best estimate of the abundance of *B. burgdorferi* in the host tissues: Previous studies have shown that the first two methods of standardizing the spirochete load are highly correlated (Genné et al., 2021; Gomez-Chamorro et al., 2019). Our study showed that all three methods of standardizing the tissue spirochete load were highly correlated (Table S5). For all statistical analyses in the main manuscript, the spirochete load was standardized relative to the number of mouse *Beta actin* gene copies, as this was considered the most sophisticated method. Standardizing the spirochete load relative to the tissue mass (method 1) is easy to conceptualize, as it gives the number of spirochetes per unit mass of host tissue, but it does not account for potential differences in DNA extraction success of the differing tissue types. Standardizing the spirochete load relative to the DNA concentration (method 2) is more accurate because it uses a post-extraction estimate of host DNA content and therefore corrects for variation in DNA extraction success among tissue samples. Standardizing the spirochete load relative to the number of mouse *Beta actin* gene copies corrects for additional measurement error if contaminants in the DNA extraction bias both qPCR assays in the same direction. We found that the results were qualitatively the same for the 3 methods of standardizing the spirochete load, but that the statistical significance of the explanatory factors could change among methods. In summary, the most sophisticated method of standardizing spirochete load relative to a host housekeeping gene increased the power of our statistical analyses because it corrected for measurement error introduced during the DNA extraction and the qPCR assay.

The effect of temporal block on the abundance of *B. burgdorferi* in the host tissues depended on the method of standardization: The effect of temporal block on the abundance of *B. burgdorferi* in the host tissues was highly significant for method 1 ($p = 7.292*10^{-10}$), marginally significant for method 2 ($p = 0.034$), and not significant for method 3 ($p = 0.153$; Table S4). Our explanation for this surprising result is as follows. To prepare the mouse tissues for DNA extraction, two different forms of homogenization were used: (1) micropestle and (2) beads and the Qiagen TissueLyser II. Samples from the first temporal block (block A) were all homogenized by micropestle, whereas samples from the second temporal block (block B) were homogenized by bead beating. We observed that bead beating disrupted tissue samples more thoroughly compared to micropestling. Thus, we expect a greater DNA yield from the bead-disrupted samples in block B compared to the micropestle-disrupted samples in block A.

To test this hypothesis, the ratio of the DNA concentration to the mass of tissue was used as an estimate of the efficiency of the tissue homogenization and DNA extraction process for the 784 mouse tissues samples (112 mice x 7 tissues per mouse = 784 tissues). This response variable was analyzed using an LMM with the fixed factors of sex, tissue, and temporal block, and mouse identity as a random factor. All three fixed factors were significant (Table S6). Estimated marginal means (EMMs) for the ng DNA per mg tissue were generated by sex, by necropsy tissue type, and by temporal block (Table S7). The amount of DNA per unit tissue mass was 1.2x higher in female mice compared to male mice (Female: 816 ng DNA per mg tissue; Male: 688 ng DNA per mg tissue) and this difference was significant ($p = 0.003$). Male C3H/HeJ mice have a higher percent body fat than females (Reed et al., 2007), and such a compositional difference could lead to a difference in the density of nuclei (i.e., DNA) in a sample of tissue.

A difference among the DNA per weight of the different tissue types is expected, as different tissues have different cell densities. The amount of DNA extracted per mg of tissue was highest for the ears and bladder, intermediate for the ventral skin, low for the kidney and the right rear tibiotarsal joint, and lowest for the heart (Table S7).

The amount of DNA per unit tissue mass in the tissue samples of block B (homogenized by bead beating; 965 ng DNA per mg tissue) was 1.8x higher compared to the tissue samples of block A (homogenized by micropestle; 539 ng DNA per mg tissue) and this difference was significant ($p = 2.2*10^{-16}$). This result suggests that the yield of whole DNA per unit tissue mass was higher for bead beating homogenization compared to micropestle homogenization. Thus, analyses of spirochete load standardized to tissue mass would be expected to find a significant effect of temporal block on the tissue abundance of *B. burgdorferi*. In contrast, analyses of spirochete load standardized to mouse *Beta-actin* would not be influenced by the differences in tissue homogenization and DNA extraction between blocks A and B. In summary, the differences in tissue homogenization between blocks A and B resulted in a higher yield of DNA per mg of tissue and in better detection of *B. burgdorferi* in block B compared to block A. For this reason, the analysis of spirochete load standardized to the mass of tissue found a significant effect of temporal block, whereas the analysis of spirochete load standardized to a host housekeeping gene did not.

Table S6. Model simplification of the LMM for the ng of DNA per mg of tissue. The interaction between tissue and sex was not significant and was not included in the final model. The three fixed factors were significant in the final simplified model. For each term, the Chi-squared statistic (Chi), change in degrees of freedom (Δ df), and p-value (p) are shown. For the non-

significant interaction, the p-value is for the model from which it was removed. For the significant terms, the p-values are from the final simplified model.

Term	Order removed	Chi	Δ df	p
Tissue:Sex	1	11.039	6	0.087
Tissue	Final model	648.283	6	$2.2*10^{-16}$
Sex	Final model	9.074	1	0.003
Temporal block	Final model	101.266	1	$2.2*10^{-16}$

Table S7. The estimated marginal means (EMMs) of the amount of DNA per amount of tissue for sex, necropsy tissue, and temporal block. The EMMs have units of ng of DNA per mg of tissue. The lower limits (LL) and upper limits (UL) of the 95% confidence interval are shown.

Factor	Term	EMM	LL	UL
Sex	Female	816	757	874
Sex	Male	688	628	748
Tissue	Ventral skin	734	641	826
Tissue	Left ear	1323	1230	1416
Tissue	Right ear	1106	1015	1197
Tissue	Heart	100	9	191
Tissue	Bladder	1194	1103	1285
Tissue	Kidney	420	327	512
Tissue	Tibiotarsal joint	387	294	479
Temporal block	A	539	479	598
Temporal block	B	965	906	1024

Effect of *B. burgdorferi* infection status on the number of mouse *Beta-actin* copies in mouse tissue samples: Infection with *B. burgdorferi* causes the recruitment of immune cells to the tissues of the vertebrate host. This recruitment of nucleated immune cells would increase the number of mouse *Beta-actin* gene copies, which would decrease our estimates of the abundance of *B. burgdorferi* in the mouse tissues. We weighed the mass of the mouse tissues prior to DNA extraction, and we can therefore standardize the number of *Beta-actin* copies per mg of tissue. To determine whether infection with *B. burgdorferi* influences the number of mouse *Beta-actin* copies per mg of tissue, we used an LMM that analyzed this response variable (log10-transformed) as a function of 5 fixed effects including infection status (2 levels: uninfected, infected), strain, sex, tissue, and temporal block. The starting model included the 3-way interaction of infection status, tissue, and sex, as well as each 2-way interaction. Strain and temporal block were not included in the interaction terms. Mouse identity was included as a random factor.

The 3-way interaction and the 2-way interactions between infection status and sex and between infection status and tissue were not significant (Table S8). The *B. burgdorferi* infection status had no effect on the number of mouse *Beta-actin* per mg of mouse tissue (Table S8). As expected, there were significant differences in mouse *Beta-actin* among mouse tissues. We also found a significant effect of temporal block on the mouse *Beta-actin* per mg of mouse tissue; as

explained above, this result was probably caused by the different tissue homogenization methods between the two blocks: pestling in block A versus bead beating in block B.

Table S8. Model simplification of the LMM for the number of mouse *Beta-actin* copies per mg of tissue. Non-significant terms were sequentially removed in order of increasing significance; the model was updated each time a non-significant term was removed. The final simplified model contained the fixed factors and the interaction between tissue type and mouse sex. For each term, the order in which it was removed, the Chi-squared statistic (Chi), change in degrees of freedom (Δ df), and p-value (p) are shown. For the non-significant interactions, the p-values are from the model from which it was removed. The other p-values are from the final simplified model.

Term	Order removed	Chi	Δ df	p
Infection status:Tissue:Sex	1	-	-	-
Infection status:Sex	2	0.345	1	0.557
Infection status:Tissue	3	5.628	6	0.466
Infection status	Final model	0.700	1	0.403
Tissue	Final model	253.101	6	$2.2*10^{-16}$
Sex	Final model	0.358	1	0.550
Strain	Final model	12.430	10	0.257
Temporal block	Final model	44.748	1	$2.242*10^{-11}$
Tissue:Sex	Final model	28.315	6	$8.197*10^{-5}$

Section 5 – Correlation between the strain-specific spirochete loads in the mouse tissues and the observed strain frequencies in nature.

Frequency of *B. burgdorferi* strains in the PubMLST database: To determine the frequencies of our strains in nature, we used the PubMLST database for *Borrelia* (Jolley et al., 2018). Submissions to this database include samples from wildlife, ticks, and human patients (Jolley et al., 2018). For each of our 11 strains, we queried the MLST against the PubMLST database (accessed on June 26, 2022) and recorded the number of counts. Two of our strains have MLST 3; thus, our set of strains contained 10 unique MLSTs. To determine the frequency of each strain in our set of 10 unique MLSTs, we expressed these counts as a proportion of the total number of entries for our strains (n = 450; Table S9).

Frequency of *B. burgdorferi* strains in *I. scapularis* ticks in North America: Two previous studies determined the frequencies of *B. burgdorferi* MLSTs in questing *I. scapularis* ticks collected in the USA and Canada (Ogden et al., 2011; Travinsky et al., 2010). These two studies combined contained 9 of the 11 strains (8 of 10 MLST types) in the present study. Strains 66 and 54, which corresponded to MLSTs 237 and 741, were not detected, and were therefore assigned counts of zero (Table S9). To determine the frequency of each strain in our set of 10 unique MLSTs, we expressed these counts as a proportion of the total number of entries for our strains (n = 251; Table S9).

Table S9. The mean tissue spirochete load for each of the 11 strains of *B. burgdorferi* and their frequencies in nature. The mean tissue spirochete load is the log10-transformed ratio of *23S*

rRNA gene copies per 10^6 mouse *Beta-actin* gene copies and for each strain it was averaged over the subset of infected tissues from both sexes and all tissue types. The lower limit (LL) and the upper limit (UL) for the 95% confidence interval of the mean spirochete load and frequencies are shown. The counts and frequencies of the MLST types were obtained from the *Borrelia* PubMLST database (count1, frequency1) or the combined tick database (count2, frequency2) published by Travinsky et al. (2010) and by Ogden et al. (2011).

Strain	MLST	Mean	LL	UL	Count1	Freq1 (%)	LL (%)	UL (%)	Count2	Freq2 (%)	LL (%)	UL (%)
66	237	2.427	2.323	2.531	5	1.1	0.4	2.7	0	0.0	0.0	1.9
57	29	2.780	2.686	2.873	38	8.4	6.1	11.5	29	11.6	8.0	16.3
150	19	3.041	2.929	3.152	48	10.7	8.0	14.0	24	9.6	6.3	14.1
167	12	2.929	2.835	3.023	43	9.6	7.1	12.7	7	2.8	1.2	5.9
126	43	2.746	2.637	2.855	17	3.8	2.3	6.1	10	4.0	2.0	7.4
22.2	55	2.897	2.814	2.979	22	4.9	3.2	7.4	5	2.0	0.7	4.8
10.2	32	2.981	2.879	3.083	31	6.9	4.8	9.7	65	25.9	20.7	31.9
54	741	2.588	2.499	2.678	4	0.9	0.3	2.4	0	0.0	0.0	1.9
198	3	3.085	2.984	3.187	217	48.2	43.5	53.0	94	37.5	31.5	43.8
174	37	3.059	2.911	3.206	25	5.6	3.7	8.2	17	6.8	4.1	10.8
178	3	3.015	2.919	3.110	217*	48.2*	43.5	53.0	94*	37.5*	31.5	43.8
Total					450				251			

* Strain 198 and 178 are both MLST type 3. The number of reads for MLST 3 was only counted once for the total number of reads.

Estimates of abundance in mouse tissues for strains of *B. burgdorferi*: We used 3 estimates of abundance in the mouse tissues for the 11 strains of *B. burgdorferi*: (1) proportion of infected mouse tissues at necropsy (n = 588), (2) mean spirochete load in subset of infected mouse tissues at necropsy (n = 342), and (3) mean spirochete load in all mouse tissues at necropsy (n = 588). For each strain, these estimates were calculated across the 2 sexes and the 7 tissue types. The spirochete load was measured as the number of *23S rRNA* gene copies per 10^6 mouse *Beta-actin* gene copies; this variable was log10-transformed to normalize the residuals (Table S9).

Relationship between frequency of *B. burgdorferi* strain in nature and estimates of spirochete load in mouse tissues: We used generalized linear models (GLMs) with quasibinomial errors to model each of our two estimates of the strain-specific frequencies (response variable) as a function of each of our three estimates of the presence or abundance of *B. burgdorferi* in the mouse tissues (i.e., total of 6 GLMs). We used quasibinomial errors rather than binomial errors because the strain-specific frequencies exhibited a high degree of overdispersion; the ratio of the residual deviance to the residual degrees of freedom ranged from 26.0 to 107.4. For the proportion of infected mouse tissues at necropsy (estimate 1) and for the mean spirochete load in all mouse tissues at necropsy (estimate 3), we found no significant relationship with either estimate of the strain-specific frequencies in nature (Table S10). For the mean spirochete load in the subset of infected mouse tissues, there was a positive and almost significant relationship with the strain-specific frequencies in the pubMLST database (Figure S1;

Table S10; p = 0.055) and a positive and significant relationship with the strain-specific frequencies in *I. scapularis* ticks (see Figure 2.5 in the main manuscript; Table S10; p = 0.045).

Table S10. GLM with quasibinomial errors of the relationship between the strain-specific frequencies and the strain-specific estimates of the mouse tissue spirochete abundance. The two estimates of the strain-specific frequencies were obtained from PubMLST and from two published studies on *I. scapularis* ticks. The three estimates of the abundance of *B. burgdorferi* included (1) proportion of infected mouse tissues at necropsy (Estimate 1), (2) mean spirochete load in subset of infected mouse tissues at necropsy (Estimate 2), and (3) mean spirochete load in all mouse tissues at necropsy (Estimate 3). For each of the 6 GLM models, the Chi-squared statistic (χ^2), degrees of freedom (df), and p-value are shown for the log-likelihood ratio test. For each of the 6 GLM models, the slope of the relationship, standard error (SE), t-statistic (t), and p-value (p) are shown.

Frequency	*Bb* abundance	χ^2	df	p	Slope	SE	t	p
PubMLST	Estimate 1	2.620	1	0.106	-8.485	6.242	-1.359	0.207
PubMLST	Estimate 2	8.756	1	0.003	7.121	3.238	2.199	0.055
PubMLST	Estimate 3	0.087	1	0.768	-0.545	1.850	-0.294	0.775
Ticks	Estimate 1	2.141	1	0.143	-6.648	5.183	-1.283	0.232
Ticks	Estimate 2	9.604	1	0.002	6.750	2.893	2.334	0.045
Ticks	Estimate 3	0.073	1	0.787	-0.439	1.620	-0.271	0.793

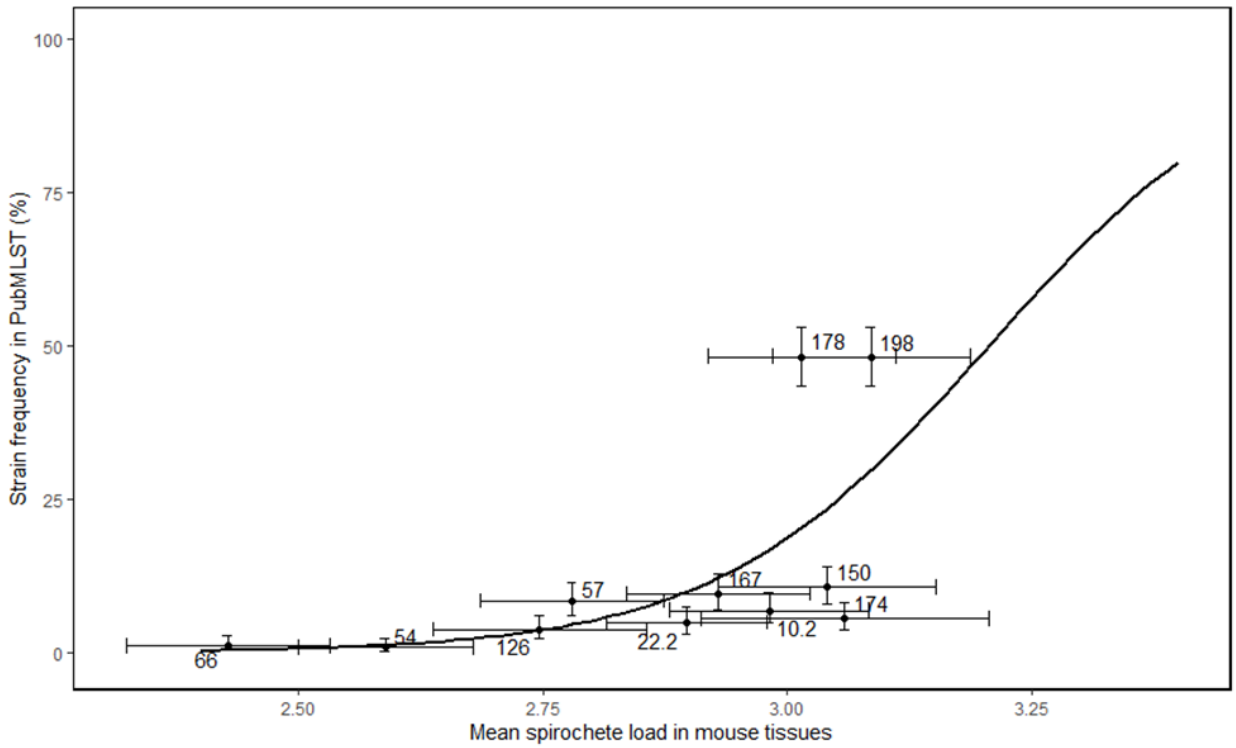

Figure S1. Relationship between the strain-specific estimates of the mean spirochete load in the infected mouse tissues and the strain-specific frequency in the *Borrelia* PubMLST database. The MLST was used to determine how many times each strain appeared in the *Borrelia* PubMLST database. The strain-specific frequencies were calculated by dividing the counts for each strain by the sum of the counts for all 11 strains (n = 450). The mean spirochete load in the mouse tissues was based on the subset of infected mouse tissues tested at necropsy (day 97 PI) and was averaged over the 2 sexes and the 7 tissue types. Spirochete loads were expressed as the log10-transformed ratio of the *B. burgdorferi 23S rRNA* copies/10^6 mouse *Beta-actin* copies. The relationship between the two variables is positive and almost significant (slope = 7.121, SE = 3.238, t = 2.199, p = 0.055). Horizontal and vertical error bars represent the 95% confidence intervals for the two variables.

Section 6 – The mouse IgG antibody response to infection with *B. burgdorferi*

ELISA to measure mouse IgG antibodies against *B. burgdorferi*: Blood samples were allowed to clot for 10 to 15 min at room temperature prior to centrifugation at 1,500 rcf for 15 min. The serum was transferred to sterile microcentrifuge tubes and stored at -80 ºC until use. All ELISA assays were done using the Zeus Scientific *B. burgdorferi* IgG test system (reference number: 3Z9651G). This ELISA is prepared with *B. burgdorferi* whole cell adsorption to detect all strains of *B. burgdorferi*. Modifications were made to the manufacturer's protocol to adapt this test to mice. The kit-supplied secondary antibody was substituted with goat anti-mouse IgG conjugated to horseradish peroxidase (Thermo Scientific, #31430) at a 1:5000 dilution in sterile PBS (0.1 M, pH 7.2). Additionally, 1 µL of mouse serum was used with 104 µL of sample diluent. All TMB reactions were stopped at 12.5 min and the absorbance values were read within 30 min at 450 nm (Varioskan Lux multimode microplate reader). The repeatability of the absorbance measurements was 97.7% based on 135 samples retested using separate plates.

The IgG antibody response to *B. burgdorferi* indicates mouse infection status: To measure the mouse IgG antibody response to infection with *B. burgdorferi*, a commercial ELISA kit (Zeus Scientific: 3Z9651G) was used. To modify this kit for use with mouse serum, a mouse secondary antibody (Thermo Scientific: 31430) was substituted. As a result, the kit-specified cut-off values for determination of a positive or negative response could not be used. While each of the 84 infected mice were confirmed positive by direct detection of *B. burgdorferi* DNA using qPCR, analyses were done to determine whether the IgG antibody responses of infected mice differed significantly from their pre-infection blood samples, and from uninfected control mice. A linear mixed effect model (LMM) was used to analyze the strength of the IgG antibody response as a function of blood draw (three levels: pre-infection, 28 days PI, and terminal at 97 days PI), mouse infection status based on qPCR results (two levels: uninfected and infected), and their interaction. Mouse identity was included as a random factor. Blood draw, mouse infection status, and their interaction were highly significant ($p = 2.2*10^{-16}$; Figure S2). All negative post-infection serum samples and all pre-infection serum samples did not differ in their relative absorbance (Figure S2; Table S11). The relative absorbance of the serum samples from 28 days PI and the terminal serum samples from 97 days PI taken from infected mice were significantly different from all other serum samples.

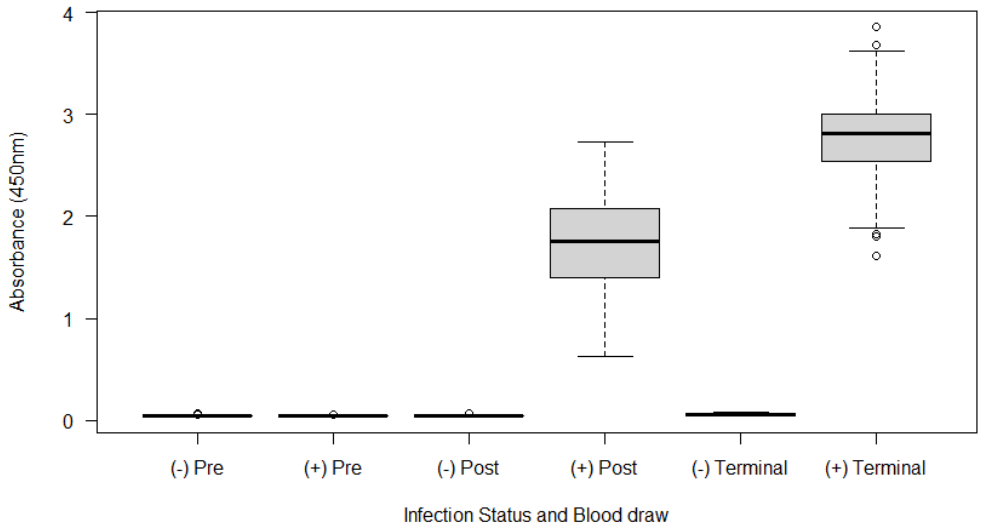

Figure S2. The serum IgG antibody response of the mouse against *B. burgdorferi* depends on mouse infection status. The strength of the IgG antibody response was measured as the absorbance at 450 nm using a commercially available ELISA plate. Only the post-infection serum and the terminal serum from the infected mice differed significantly from all other serum samples. Uninfected and infected mice are indicated with (-) and (+), respectively. Mouse infection status was determined by direct detection of *B. burgdorferi* DNA in mouse tissues using qPCR. The pre-infection, post-infection, and terminal blood samples were taken 1 to 2 weeks prior to infection, 28 days post-infection, and at 97 days post-infection (euthanasia), respectively.

Table S11. The strength of the mouse serum IgG antibody response against *B. burgdorferi* depends on the mouse infection status and the timing of the blood sample. The strength of the mouse IgG antibody response against *B. burgdorferi* was measured as the absorbance at 450 nm in a commercial ELISA. Shown are the number of mice (N), the estimated marginal means (EMM), and the lower limit (LL) and upper limit (UL) of the 95% confidence interval.

Infection status	Sample	N	EMM	LL	UL
Uninfected	Pre-infection	20	0.05	-0.08	0.17
Uninfected	Day 28 PI	20	0.05	-0.08	0.17
Uninfected	Day 97 PI	20	0.06	-0.08	0.19
Infected	Pre-infection	84	0.05	-0.02	0.12
Infected	Day 28 PI	84	1.73	1.66	1.80
Infected	Day 97 PI	84	2.77	2.70	2.85

Section 7 – Comparison of the infectious tick challenge among *B. burgdorferi* strains

Controlling infectious dose: In this study, mice were infected with *B. burgdorferi* via the bite of *I. scapularis* nymphs. Each mouse in the infected group was infested with 3 putatively infected *I. scapularis* nymphs carrying the desired strain; mice in the control group were infested

with 3 uninfected nymphs. During the nymphal infestation, the nymphs were allowed to feed to repletion. The number of engorged nymphs recovered was recorded, and all engorged nymphs were tested for the presence of *B. burgdorferi*. The mice in the infected group were infested with 276 putatively infected nymphs, of which 224 engorged nymphs were recovered. The mice in the control group were infested with 60 uninfected nymphs, of which 45 engorged nymphs were recovered. Of the 224 engorged nymphs recovered from the mice in the infected group, 92.0% (206/224) were infected with *B. burgdorferi*. Of the 45 engorged nymphs recovered from the mice in the control group, 0.0% (0/45) were infected with *B. burgdorferi*.

To determine whether the infectious challenge was similar between the 11 strains of *B. burgdorferi* we analyzed the following 3 binomial response variables, Y1, Y2, and Y3. Y1 is the proportion of recovered engorged nymphs relative to the number of unfed nymphs with which the mouse was infested. Y2 is the proportion of recovered engorged infected nymphs relative to the number of unfed nymphs with which the mouse was infested. Y3 is the proportion of recovered engorged infected nymphs relative to the number of recovered engorged nymphs. Each response variable was modelled as a GLMM with binomial errors with the fixed factors of strain, mouse sex, and temporal block; mouse identity was a random factor. The analyses were restricted to the subset of 84 mice in the infected group. For each of the 3 response variables that measured the efficacy of the infectious challenge, there were no significant effects of strain, sex, or temporal block (Table S12).

Table S12. GLMM of the 3 response variables, Y1, Y2, and Y3, that summarize the infectious tick challenge as a function of 3 fixed factors: strain, mouse sex, and temporal block. For each fixed factor, the Chi-squared statistic (Chi), the change in degrees of freedom (Δ df), and the p-value (p) are shown.

Variable [1]	Factor	Chi	Δ df	p
Y1	Strain	10.150	10	0.427
Y1	Sex	2.373	1	0.123
Y1	Block	0.097	1	0.756
Y2	Strain	7.144	10	0.712
Y2	Sex	3.878	1	0.049
Y2	Block	0.164	1	0.685
Y3	Strain	3.799	10	0.956
Y3	Sex	0.538	1	0.463
Y3	Block	0.000	1	0.984

[1] Y1 = n2/ n1, Y2 = n3/ n1, and Y3 = n3/ n2

n1 = number of unfed nymphs with which the mouse was infested (n1 = 3 for all mice)
n2 = number of engorged nymphs that were recovered for each mouse
n3 = number of engorged nymphs that were recovered for each mouse and that tested positive for *B. burgdorferi* on the *23S rRNA* qPCR

Effect of the number of infected engorged nymphs on the mouse infection phenotype: To further assess whether there was variation in the infectious challenges, the number of infected engorged nymphs (i.e., n3 in Table S12) was included as a covariate in the fixed effects structure in models for the prevalence and abundance of *B. burgdorferi* in the mouse tissues. For both models, the fixed factors of sex, strain, and tissue were included. Mouse identity was included as a random factor. Infectious tick challenge did not significantly affect the prevalence of *B. burgdorferi* in the mouse tissues ($p = 0.187$) or the abundance of *B. burgdorferi* in the mouse tissues ($p = 0.271$).

Effect of the mean spirochete load in the engorged nymphs on the mouse infection phenotype: The quantity of spirochetes left behind in the engorged nymphs after feeding are not indicative of the number of spirochetes inoculated into the mouse (i.e., the infectious dose). Nevertheless, we included the mean spirochete load averaged over the subset of engorged infected nymphs for each mouse (i.e., n3 in Table S12) as a covariate (i.e., as we did above for the number of infected engorged nymphs). For the two response variables of presence and abundance of *B. burgdorferi* in the mouse tissues, the fixed factors of sex, strain, and tissue were included. Mouse identity was included as a random factor. The mean spirochete load averaged over the subset of engorged infected nymphs for each mouse was not a significant predictor of the prevalence of *B. burgdorferi* in mouse tissues ($p = 0.552$) or the abundance of *B. burgdorferi* in mouse tissues ($p = 0.181$).

Section 8 – Analyses of the prevalence and abundance of *B. burgdorferi* in the ear tissue samples

GLMM of presence of *B. burgdorferi* in ear tissue samples: The response variable was the infection status of the right ear tissue samples for the infected mice ($n = 84$) as measured by qPCR. This binomial response variable (0 = absent = uninfected, 1 = present = infected) was modelled using a generalized linear mixed effect model (GLMM) with binomial errors. The fixed factors included strain (11 levels), mouse sex (2 levels: female, male), ear tissue sample or punch (days 29, 59, 89, and 97 PI), and temporal block (2 levels: A and B). The starting model included the 3-way interaction of strain, mouse sex, and punch, and three 2-way interactions. Temporal block was not included in the interaction terms. Mouse identity was included as a random factor. None of the interactions were significant and they were removed sequentially (Table S13). The final simplified model contained no interactions, and all the fixed factors were significant except temporal block (Table S13).

Table S13. Model simplification of the GLMM for the presence of *B. burgdorferi* in the mouse right ear tissue samples. Non-significant terms were sequentially removed in order of increasing significance; the model was updated each time a non-significant term was removed. The final simplified model contained only the fixed factors and no interactions. For each term, the order in which it was removed, the Chi-squared statistic (Chi), change in degrees of freedom (Δ df), and p-value (p) are shown. For the non-significant interactions, the p-values are the ones in the model from which they were removed. For the fixed factors, the p-values are the ones from the final simplified model.

Term	Order removed	Chi	Δ df	p
Strain:Sex:Punch	1	0	30	1.000
Sex:Punch	2	0	3	1.000

Strain:Punch	3	0	30	1.000
Strain:Sex	4	10.588	10	0.391
Strain	Final model	25.817	10	0.004
Sex	Final model	5.493	1	0.019
Punch	Final model	47.298	3	$3.004*10^{-10}$
Temporal block	Final model	0.805	1	0.370

LMM of the abundance of *B. burgdorferi* in the ear tissue samples: The response variable was the log10-transformed abundance of *B. burgdorferi* (spirochete load) in the subset of the infected right ear tissue samples as measured by qPCR. This data set contained 256 infected ear tissue samples from the 84 infected mice. Abundance was expressed as the log10-transformed ratio of the number of *B. burgdorferi 23S rRNA* gene copies per 10^6 copies of the mouse *Beta-actin* gene. The log10-transformed spirochete load was analyzed using an LMM with the same fixed effects and random effects as the previous GLMM of presence of *B. burgdorferi* in ear tissue samples.

As with the previous models, the 3-way interaction was removed first, followed by the 2-way interactions in order of increasing significance. The 2-way interactions between strain and punch, and between mouse sex and punch were significant (Table S14). The final simplified model contained these two significant interactions. In the final simplified model, all the fixed factors were significant except temporal block (Table S14).

Table S14. Model simplification of the LMM for the abundance of *B. burgdorferi* in the mouse right ear tissue samples. Non-significant terms were sequentially removed in order of increasing significance; the model was updated each time a non-significant term was removed. The final simplified model contained the fixed factors and the interactions between strain and punch and between sex and punch. For each term, the order in which it was removed, Chi-squared statistic (Chi), change in degrees of freedom (Δ df), and p-value (p) are shown. For the non-significant interactions, the p-values are the ones in the model from which they were removed. For the significant terms, the p-values are the ones from the final simplified model.

Term	Order removed	Chi	Δ df	p
Strain:Punch:Sex	1	15.093	20	0.771
Strain:Sex	2	10.120	10	0.430
Strain:Punch	Final model	83.971	25	$3.467*10^{-8}$
Sex:Punch	Final model	11.614	3	0.017
Strain	Final model	28.769	10	0.004
Sex	Final model	4.879	1	0.027
Punch	Final model	205.796	3	$2.2*10^{-16}$
Temporal block	Final model	0.578	1	0.447

Separate LMs of the abundance of *B. burgdorferi* for each ear tissue sample: Due to the involvement of ear biopsy (punch) in both interaction terms, separate linear models (LMs) were run for each ear biopsy (days 29, 59, and 89 PI). Each LM had strain and sex as fixed factors. Mouse was not included as a random factor as there was only one sample per mouse for each right ear biopsy. The right ear necropsies on day 97 PI were excluded from this analysis because there were only 12 positive samples (10 male, 2 female, 6 strains represented). Sex was

only significant for the latter two ear biopsies (days 59, and 89 PI) whereas strain was significant for each of the three ear biopsies (Table S15).

Table S15. The 3 separate LMs for each ear biopsy (punch) that model the abundance of *B. burgdorferi* in the ear tissue as a function of *B. burgdorferi* strain and mouse sex. The three ear biopsies were taken on days 29, 59, and 89 PI. For each of the 3 ear biopsies, the results from the ANOVA table are shown for each of the two fixed factors (strain, and sex), which include an F-statistic (F), degrees of freedom (df) and p-value (p).

Ear biopsy	Factor	F	df	p
Day 29 PI	Strain	4.875	10	$2.547*10^{-5}$
Day 29 PI	Sex	0.693	1	0.408
Day 59 PI	Strain	3.149	10	0.002
Day 59 PI	Sex	15.064	1	$2.28*10^{-4}$
Day 89 PI	Strain	2.193	10	0.029
Day 89 PI	Sex	4.953	1	0.030

Estimated marginal means (EMMs) were calculated for each of the 6 combinations of ear biopsy and sex (Table S16) using the final simplified model in Table S14. On day 59 PI, the mean spirochete load in the ear tissue biopsies in the males (1431 *23S rRNA*/10^6 *Beta-actin*) was 1.95x higher compared to the females (732 *23S rRNA*/10^6 *Beta-actin*). On day 89 PI, the mean spirochete load in the ear tissue biopsies in the males (1706 *23S rRNA*/10^6 *Beta-actin*) was 1.48x higher compared to the females (1151 *23S rRNA*/10^6 *Beta-actin*). EMMs were also calculated for each of the 33 combinations of ear biopsies and strain (Table S17) using the final simplified model in Table S14.

Table S16. The EMMs of the abundance of *B. burgdorferi* for each of the 6 combinations of ear biopsy and sex. The EMM1 values are the log10-transformed (*23S rRNA*/10^6 mouse *Beta-actin* gene) and the EMM2 values are the number of *23S rRNA* copies per 10^6 mouse *Beta-actin* copies. Lower and upper (LCL, UCL) 95% confidence limits are reported. The EMMs were calculated using the final simplified model in Table S14.

Punch	Sex	EMM1	LCL1	UCL1	EMM2	LCL2	UCL2
Day 29 PI	Female	3.61	3.48	3.73	4052	3026	5427
Day 29 PI	Male	3.52	3.40	3.64	3309	2493	4392
Day 59 PI	Female	2.86	2.74	2.99	732	549	977
Day 59 PI	Male	3.16	3.03	3.28	1431	1082	1892
Day 89 PI	Female	3.06	2.92	3.20	1151	836	1584
Day 89 PI	Male	3.23	3.10	3.36	1706	1261	2309

Table S17. The EMMs of the abundance of *B. burgdorferi* for each of the 33 combinations of strain and ear biopsy. The EMM1 values are the log10-transformed (*23S rRNA*/10^6 mouse *Beta-actin*) and the EMM2 values are the number of *23S rRNA* copies per 10^6 mouse *Beta-actin* copies. Lower and upper (LCL, UCL) 95% confidence limits are reported. The EMMs were calculated using the final simplified model in Table S14.

Strain	Biopsy	EMM1	LCL1	UCL1	EMM2	LCL2	UCL2
66	Day 29 PI	4.12	3.82	4.42	13201	6608	26373
66	Day 59 PI	2.59	2.29	2.89	391	196	782
66	Day 89 PI	2.61	2.05	3.17	408	111	1493
57	Day 29 PI	4.20	3.92	4.48	15771	8261	30106
57	Day 59 PI	3.17	2.89	3.45	1472	771	2811
57	Day 89 PI	3.04	2.76	3.32	1090	571	2080
150	Day 29 PI	3.16	2.88	3.44	1444	756	2757
150	Day 59 PI	3.11	2.83	3.39	1299	680	2480
150	Day 89 PI	3.34	3.06	3.62	2177	1140	4155
167	Day 29 PI	3.22	2.94	3.50	1650	864	3150
167	Day 59 PI	2.87	2.58	3.15	734	384	1401
167	Day 89 PI	3.12	2.84	3.40	1318	691	2516
126	Day 29 PI	3.31	3.03	3.59	2044	1071	3903
126	Day 59 PI	2.92	2.64	3.20	826	433	1577
126	Day 89 PI	3.38	3.10	3.66	2409	1262	4598
22.2	Day 29 PI	3.06	2.78	3.34	1152	604	2200
22.2	Day 59 PI	2.76	2.48	3.04	579	303	1105
22.2	Day 89 PI	3.06	2.78	3.35	1161	608	2217
10.2	Day 29 PI	3.31	3.03	3.59	2046	1072	3905
10.2	Day 59 PI	3.18	2.90	3.46	1515	794	2892
10.2	Day 89 PI	3.13	2.85	3.41	1340	702	2559
54	Day 29 PI	3.87	3.57	4.17	7489	3748	14961
54	Day 59 PI	2.97	2.69	3.25	925	485	1766
54	Day 89 PI	2.93	2.63	3.23	844	422	1686
198	Day 29 PI	3.61	3.33	3.89	4041	2117	7715
198	Day 59 PI	3.16	2.88	3.44	1441	755	2752
198	Day 89 PI	3.34	3.06	3.62	2188	1146	4177
174	Day 29 PI	3.81	3.45	4.16	6426	2832	14578
174	Day 59 PI	3.02	2.66	3.38	1048	462	2379
174	Day 89 PI	3.46	3.06	3.86	2901	1156	7282
178	Day 29 PI	3.53	3.23	3.83	3414	1709	6821
178	Day 59 PI	3.37	3.08	3.65	2320	1215	4428
178	Day 89 PI	3.20	2.92	3.48	1597	837	3050

Section 9 – Analyses of the prevalence and abundance of *B. burgdorferi* in the mouse necropsy tissues

GLMM of presence of *B. burgdorferi* in mouse necropsy tissues: The presence of *B. burgdorferi* was assessed in 7 mouse necropsy tissues collected at euthanasia (97 days PI): kidney, left ear, right ear, ventral skin, right rear tibiotarsal joint, heart, and bladder. The response variable was the infection status of the mouse necropsy tissues for the infected mice (n = 84) as measured by qPCR. This binomial response variable (0 = absent = uninfected, 1 = present = infected) was modelled using a generalized linear mixed effect model (GLMM) with binomial errors. The fixed factors included strain (11 levels), mouse sex (2 levels: female, male), mouse necropsy tissue (7 levels: kidney, left ear, right ear, ventral skin, tibiotarsal joint, heart, and bladder), and temporal block (2 levels: A and B). The starting model included the 3-way interaction of strain, sex, and tissue, as well as each 2-way interaction. Temporal block was not included in the interaction terms. Mouse identity was included as a random factor.

The R software was not able to process the GLMM that included the 3-way interaction between strain, sex, and tissue and so this interaction could not be tested. The R software was not able to process the GLMM that included the three 2-way interactions terms. The statistical significance of each 2-way interaction was therefore tested separately in a main effects model; 2-way interactions with a p-value < 0.10 were included in the final model. The final model included the 2-way interactions between strain and sex, and between sex and tissue (Table S18).

Table S18. Model simplification of the GLMM for the prevalence of *B. burgdorferi* in the mouse necropsy tissues. The R software was unable to estimate the 3-way interaction. Each 2-way interaction was tested in a main effects model that included strain, mouse sex, tissue, and temporal block. The 2-way interactions with a p-value < 0.10 were then added to the final model. For each term, the Chi-squared statistic (Chi), change in degrees of freedom (Δ df), and p-value (p) are shown.

Term	Test	Chi	Δ df	p
Strain:Sex:Tissue	-	-	-	-
Strain:Sex	Main effects	18.148	10	0.053
Strain:Tissue	Main effects	26.940	60	1.000
Sex:Tissue	Main effects	48.609	6	$8.964*10^{-9}$
Temporal block	Main effects	5.843	1	0.016
Strain	Final model	26.120	10	0.004
Sex	Final model	7.032	1	0.008
Tissue	Final model	95.797	6	$2.20*10^{-16}$
Temporal block	Final model	6.125	1	0.013
Strain:Sex	Final model	19.650	10	0.033
Sex:Tissue	Final model	48.993	6	$7.442*10^{-9}$

Percentage of infected tissues for the 14 combinations of sex and tissue and for the 22 combinations of sex and strain: The estimated marginal means (EMMs) were generated for the 14 combinations of sex and tissue using the final simplified model (Table S19), and the 22 combinations of sex and strain (Table S20). For strain and sex, the emmeans() function did not

provide realistic EMMs (see below). For this reason, these EMMs are not used in describing the differences in prevalence as they are not correct (see below).

The percentage of tibiotarsal joints infected with *B. burgdorferi* was 1.7x higher in male mice compared to female mice (Table S19; male: 93.1%; female: 55.6%). Similarly, the percentage of ventral skin samples infected with *B. burgdorferi* was 23.7x higher in male mice compared to female mice (Table S19; male: 94.9%; female: 4.0%). In contrast, the percentage of kidneys infected with *B. burgdorferi* was 2.3x higher in female mice compared to male mice (Table S19; male: 17.6%; female: 40.0%). All strains had a higher infection prevalence in the mouse tissues in male mice compared to female mice, except strain 126 (Table S20).

Table S19. The prevalence of *B. burgdorferi* infection for each of the 14 combinations of sex and tissue. The estimated marginal means (EMMs) were generated from the separate GLMMs for each sex. The EMMs were originally estimated on the logit scale and were back-calculated to the original probability scale and are here expressed as a percent (%). The 95% confidence limits (lower confidence limit; LCL, upper confidence limit; UCL) are given when possible. As EMMs approach 100%, confidence intervals cannot be correctly estimated. The fraction of infected necropsy tissues, and the percentage of infected tissues are given for each combination of tissue and sex.

Tissue	Sex	EMM	LCL	UCL	Infected tissues	Infected tissues (%)
Kidney	Female	40.0	24.1	58.3	25/41	61.0
Kidney	Male	17.6	8.7	32.4	9/43	20.9
Left Ear	Female	40.0	24.1	58.3	16/41	39.0
Left Ear	Male	35.6	21.9	52.2	16/43	37.2
Right Ear	Female	1.3	0.2	9.1	2/41	4.9
Right Ear	Male	20.0	10.3	35.3	10/43	23.3
Ventral Skin	Female	4.0	0.9	15.9	4/41	9.8
Ventral Skin	Male	94.9	84.5	98.4	40/43	93.0
Tibiotarsal Joint	Female	55.6	38.2	71.7	21/41	51.2
Tibiotarsal Joint	Male	93.1	81.9	97.5	39/43	90.7
Heart	Female	95.4	85.8	98.6	38/41	92.7
Heart	Male	94.9	84.5	98.4	40/43	93.0
Bladder	Female	97.0	88.1	99.3	39/41	95.1
Bladder	Male	100.0	-	-	43/43	100.0
Total	Female				145/287	50.5
Total	Male				197/301	65.4

Table S20. The percentage of necropsy tissues infected with *B. burgdorferi* for each of the 22 combinations of strain and sex. The estimated marginal means (EMMs) and their 95% confidence intervals are not reliable as explained in Table S19. The number of mice, the fraction of infected necropsy tissues, and the percentage of infected tissues are given for each combination of strain and sex. Each mouse had 7 necropsy tissues tested.

Strain	Sex	Number of mice	EMM	LCL	UCL	Infected tissues	Infected tissues (%)
66	Female	3	26.0	8.3	57.8	8/21	38.1
66	Male	4	96.5	-	-	15/28	53.6
57	Female	4	63.5	35.6	84.6	16/28	57.1
57	Male	4	99.6	-	-	21/28	75.0
150	Female	4	34.8	14.3	63.1	12/28	42.9
150	Male	4	97.6	-	-	16/28	57.1
167	Female	4	34.8	14.3	63.1	12/28	42.9
167	Male	4	98.3	-	-	17/28	60.7
126	Female	4	97.5	88.3	99.5	24/28	85.7
126	Male	4	99.4	-	-	20/28	71.4
22.2	Female	4	49.1	23.6	75.0	14/28	50.0
22.2	Male	4	99.8	-	-	23/28	82.1
10.2	Female	4	34.8	14.3	63.1	12/28	42.9
10.2	Male	4	98.3	-	-	17/28	60.7
54	Female	4	49.1	23.6	75.0	14/28	50.0
54	Male	4	97.6	-	-	16/28	57.1
198	Female	4	21.9	7.7	48.8	10/28	35.7
198	Male	4	98.8	-	-	18/28	64.3
174	Female	2	21.9	5.0	60.0	5/14	31.2
174	Male	3	99.6	-	-	16/21	76.2
178	Female	4	16.5	5.3	41.0	9/28	32.1
178	Male	4	98.8	-	-	18/28	64.3

Using an LMM to generate EMMs and confidence intervals for graphing: In this study, the prevalence of *B. burgdorferi* in the 7 necropsy tissues was assessed using a GLMM. The parameter estimates from this GLMM were used to estimate the EMMs and their 95% CIs (see Tables S19 and S20). For the 22 combinations of strain and sex, there was a poor correspondence between the EMMs and the mean percentage of infected tissues (see Table S20). We inspected the parameter estimates on the logit scale for the final model in Table S18 and found that there were 2 parameters where the standard error was an order of magnitude larger than the estimate (bladder: estimate = 21.172, SE = 130.048; bladder:female: estimate = -17.286, SE = 130.049), which explains why the EMMs based on these parameter estimates were not accurate. This problem occurred because 100.0% (43/43) of the bladders in the male mice were infected with *B. burgdorferi*. GLMMs with logit links cannot estimate parameters for groups with an infection prevalence of 0.0% or 100.0% because the estimate approaches negative infinity or positive infinity, respectively. When we arbitrarily changed the infection status of 1 of the 43 male bladders to uninfected, all 35 parameters had reasonable estimates and SEs. In

summary, the GLMM of the prevalence of *B. burgdorferi* in the 7 necropsy tissues gave parameter estimates and EMMs that were not reliable.

The problem remained of how to graph the mean infection prevalence and their 95% CIs for each of the 22 combinations of strain and sex and for each of the 14 combinations of sex and tissue. To obtain means and 95% CIs, we compared two different approaches. In the first approach, we used the prop.test() function in R to calculate the mean infection prevalence and 95% CI for each group. The problem with this approach is that by separately analyzing each group, the resultant 95% CI is larger (i.e., less precise) than if all the data were analyzed together. In the second approach, we re-analyzed the tissue infection status data using an LMM with normal errors and using the same fixed factors and interactions that we had identified as being significant in the GLMM (Figures 2.2A and 2.3A in the main manuscript). The disadvantage of this approach is that binomial data (0, 1) violate the assumptions of normality and equal variances, and that the resultant 95% CIs sometimes go below 0 or above 1. The two approaches gave similar means (as expected) and the 95% CIs were smaller for the second approach because it considered all the data together (again, as expected). For this reason, we used the means and 95% CIs estimated from the second method to visualize the data.

LMM of the abundance of *B. burgdorferi* in mouse necropsy tissues: The abundance of *B. burgdorferi* was assessed for the subset of infected necropsy tissues (n = 333) from the 84 infected mice. The response variable was the log10-transformed ratio of the number of *B. burgdorferi 23S rRNA* gene copies per 10^6 copies of the mouse *Beta-actin* gene. This response variable was modelled using LMMs. The fixed factors included strain, sex, tissue, and temporal block. The starting model included the 3-way interaction of strain, sex, and tissue, and the three 2-way interactions. Temporal block was not included in the interaction terms. Mouse identity was included as a random factor.

Non-significant interactions included the 3-way interaction and the 2-way interaction between strain and sex (Table S21). The main effects of strain, sex, and tissue as well as the 2-way interactions between strain and tissue, and between sex and tissue were significant (Table S21).

Table S21. Model simplification of the LMM for the abundance of *B. burgdorferi* in the mouse tissues. Non-significant terms were sequentially removed in order of increasing significance; the model was updated each time a non-significant term was removed. The final simplified model contained the fixed factors and the interactions between strain and tissue and between sex and tissue. For each term, the order in which it was removed, the Chi-squared statistic (Chi), change in degrees of freedom (Δ df), and p-value (p) are shown. For the non-significant interactions, the p-values are the ones in the model from which they were removed. For the significant terms, the p-values are the ones from the final simplified model.

Term	Order removed	Chi	Δ df	p
Strain:Sex:Tissue	1	18.532	29	0.933
Strain:Sex	2	10.015	10	0.439
Strain:Tissue	Final model	81.215	54	0.010
Sex:Tissue	Final model	18.234	6	0.006
Strain	Final model	28.562	10	0.001
Sex	Final model	7.851	1	0.005
Tissue	Final model	231.554	6	$2.2*10^{-16}$
Temporal block	Final model	2.388	1	0.122

Separate LMs for each necropsy tissue to analyse the effect of strain and sex on the abundance of *B. burgdorferi* in the necropsy tissues: In the previous analysis, the 2-way interactions with tissue, strain:tissue and sex:tissue, were both significant (Table S21). For this reason, separate linear models (LMs) were run for each of the 7 necropsy tissues to remove these interactions (Table S22). Each LM had the fixed factors of strain and sex. Mouse identity was not included as a random factor since the analysis for each tissue contained only a single sample per mouse.

Males had a significantly higher abundance in their skin and joint samples (Table S22). Strain specific differences were found in the heart and bladder, with the ventral skin and tibiotarsal joint samples approaching significance (Table S22). EMMs for the abundance of *B. burgdorferi* in the mouse tissues were generated using the final simplified model for each of the 14 combinations of sex and tissue (Table S23) and the 77 combinations of strain and tissue (Table S24).

Table S22. The 7 separate LMs for each mouse necropsy tissue that modelled the abundance of *B. burgdorferi* in the mouse tissue as a function of *B. burgdorferi* strain and mouse sex. For each necropsy tissue, the results of the LM are shown including the F-statistic (F), degrees of freedom (df), and p-value (p) for the two fixed factors (strain and sex). The degrees of freedom for strain differ among the LMs as not every strain has a representative positive for each tissue type.

Tissue	Factor	F	df	p
Kidney	Strain	1.498	9	0.240
Kidney	Sex	0.193	1	0.667
Left Ear	Strain	1.190	10	0.353
Left Ear	Sex	0.116	1	0.737
Right Ear	Strain	0.275	5	0.908

Right Ear	Sex	0.430	1	0.541
Ventral Skin	Strain	1.870	10	0.087
Ventral Skin	**Sex**	**7.051**	**1**	**0.012**
Tibiotarsal Joint	Strain	1.783	10	0.090
Tibiotarsal Joint	**Sex**	**14.197**	**1**	**$4.50*10^{-4}$**
Heart	**Strain**	**2.529**	**10**	**0.012**
Heart	Sex	2.534	1	0.116
Bladder	**Strain**	**2.150**	**10**	**0.031**
Bladder	Sex	0.389	1	0.535

Table S23. The EMMs of the abundance of *B. burgdorferi* for each of the 14 combinations of mouse sex and mouse tissue. The EMM1 values are the log10-transformed (*23S rRNA*/10^6 *Beta-actin*) and the EMM2 values are the number of *23S rRNA* copies per10^6 mouse *Beta-actin* copies. Lower and upper (LCL, UCL) 95% confidence limits are reported. Blank spaces are where an EMM could not be estimated.

Tissue	Sex	EMM1	LCL1	UCL1	EMM2	LCL2	UCL2
Kidney	Female	-	-	-	-	-	-
Kidney	Male	-	-	-	-	-	-
Left Ear	Female	2.24	1.92	2.56	174	83	363
Left Ear	Male	2.16	1.83	2.48	144	68	305
Right Ear	Female	-	-	-	-	-	-
Right Ear	Male	-	-	-	-	-	-
Ventral Skin	Female	1.92	1.25	2.59	83	18	387
Ventral Skin	Male	3.10	2.93	3.28	1266	851	1885
Tibiotarsal Joint	Female	2.20	1.93	2.48	160	85	301
Tibiotarsal Joint	Male	2.78	2.61	2.96	604	404	903
Heart	Female	3.26	3.07	3.44	1800	1184	2736
Heart	Male	3.40	3.23	3.58	2541	1703	3790
Bladder	Female	3.06	2.89	3.24	1160	771	1746
Bladder	Male	3.15	2.98	3.31	1404	959	2055

Table S24. The EMMs of the abundance of *B. burgdorferi* for each of the 77 combinations of *B. burgdorferi* strain and mouse tissue. Lower and upper (LCL, UCL) 95% confidence limits are reported. All values are in log10-transformed *23S rRNA*/10^6 mouse *Beta-actin* gene copies. Blank spaces are where an EMM could not be estimated.

	Kidney			L_ear			R_ear			Skin			Joint			Heart			Bladder		
Strain	EMM	LCL	UCL	EMM	LCL	UCL	EMM	LCL	UCL	EMM	LCL	UCL	EMM	LCL	UCL	EMM	LCL	UCL	EMM	LCL	UCL
66	1.56	0.79	2.32	1.56	0.80	2.33	-	-	-	1.61	0.97	2.25	2.76	2.27	3.24	2.95	2.33	3.58	2.51	2.10	2.92
57	2.00	1.19	2.82	2.52	2.03	3.01	1.97	1.14	2.79	2.87	2.15	3.58	2.54	2.15	2.92	3.03	2.65	3.42	3.23	2.84	3.61
150	1.75	1.19	2.31	2.24	1.13	3.34	-	-	-	2.68	2.04	3.32	2.15	1.50	2.79	3.54	3.15	3.92	3.38	3.00	3.76
167	1.62	0.81	2.44	2.62	1.86	3.39	-	-	-	2.38	1.74	3.02	2.35	1.86	2.84	3.41	3.02	3.79	3.06	2.68	3.45
126	1.79	1.24	2.35	2.32	1.82	2.82	1.70	1.16	2.25	3.08	2.66	3.49	2.72	2.34	3.11	3.57	3.19	3.95	2.81	2.43	3.19
22.2	1.55	0.43	2.67	2.54	2.09	2.99	2.29	1.36	3.23	2.70	2.06	3.34	3.08	2.69	3.46	3.05	2.67	3.43	3.02	2.64	3.40
10.2	1.33	0.51	2.14	1.97	1.21	2.74	-	-	-	2.33	1.69	2.97	2.77	2.28	3.27	3.52	3.14	3.91	3.16	2.78	3.54
54	-	-	-	2.55	2.06	3.03	2.08	0.87	3.30	1.75	1.18	2.32	2.64	2.23	3.05	2.94	2.50	3.38	2.63	2.22	3.04
198	2.05	1.42	2.68	1.31	0.20	2.41	-	-	-	2.79	2.14	3.43	2.07	1.51	2.64	3.51	3.13	3.89	3.48	3.10	3.86
174	2.28	1.64	2.91	2.85	1.74	3.96	2.45	1.24	3.66	2.73	2.02	3.44	2.35	1.80	2.89	3.68	3.20	4.17	3.47	2.93	4.02
178	2.32	1.55	3.09	1.71	0.91	2.50	2.30	1.09	3.51	2.71	2.00	3.43	2.00	1.35	2.64	3.43	3.04	3.81	3.40	3.02	3.79

Section 10 – Analysis of geographic region

In this study, four different response variables were analyzed: (1) presence of *B. burgdorferi* in ear biopsies, (2) abundance of *B. burgdorferi* in ear biopsies, (3) presence of *B. burgdorferi* in mouse necropsy tissues, and (4) abundance of *B. burgdorferi* in mouse necropsy tissues. In the initial selection of *B. burgdorferi* strains for this study, strains were chosen from two distinct geographic regions, eastern (East) and midwestern (West) Canada. As strain was nested inside geographic region, models that contained both of these factors in the fixed effects structure were not able to converge. However, geographic region can be tested as a fixed factor if strain is included in the random effects structure. For each of the 4 response variables, a GLMM or LMM was run with the fixed factors of geographic region, mouse sex, the sample type (e.g., mouse ear biopsy, mouse necropsy tissue). Strain and mouse were treated as random factors (Table S25). The geographic regions were not statistically significant for any of the 4 response variables, except for the abundance of *B. burgdorferi* in the mouse necropsy tissues ($p = 0.046$; Table S25). The mean spirochete load in the mouse necropsy tissues in the eastern strains was 1.55x higher compared to the western strains (EMM = 490 versus 316 *23S rRNA* copies per 10^6 mouse *Beta-actin* copies, respectively).

Table S25. Models run to assess the effect of geographic region on the four response variables in this study. The type of model (GLMMs for prevalence versus LMMs for abundance), the fixed factors, and the statistical significance for geographic region (p) are shown for each of the 4 response variables. Each model contained the random factors of strain and mouse identity.

Response variable	Model type	Fixed factors	p
Ear tissue prevalence	GLMM	Region, sex, punch, block	0.814
Ear tissue abundance	LMM	Region, sex, punch, block	0.480
Necropsy tissue prevalence	GLMM	Region, sex, tissue, block	0.079
Necropsy tissue abundance	LMM	Region, sex, tissue, block	0.046

Section 11 – Correlations among the *B. burgdorferi* infection phenotypes in the mouse tissues

Correlation between the infection prevalence in the mouse necropsy tissues and the abundance of *B. burgdorferi* in the mouse necropsy tissues across 117 combinations of strain, sex, and necropsy tissue: Our analysis found that both the prevalence and abundance of *B. burgdorferi* in the necropsy tissues were significantly affected by strain, mouse sex, and necropsy tissue (Tables S18 and S21). For this reason, the correlation between prevalence and abundance was investigated using the group means of each combination of strain, mouse sex, and necropsy tissue; 11 strains x 2 sexes x 7 tissues = 154 combinations. Of these 154 combinations, 37 combinations had no positive values; thus, there were 154 – 137 = 117 realized combinations. There was a significant positive correlation between prevalence and abundance of *B. burgdorferi* across the 117 combinations ($r = 0.676$, $df = 115$, $t = 9.83$, $p = 2.2*10^{-16}$; Figure S3).

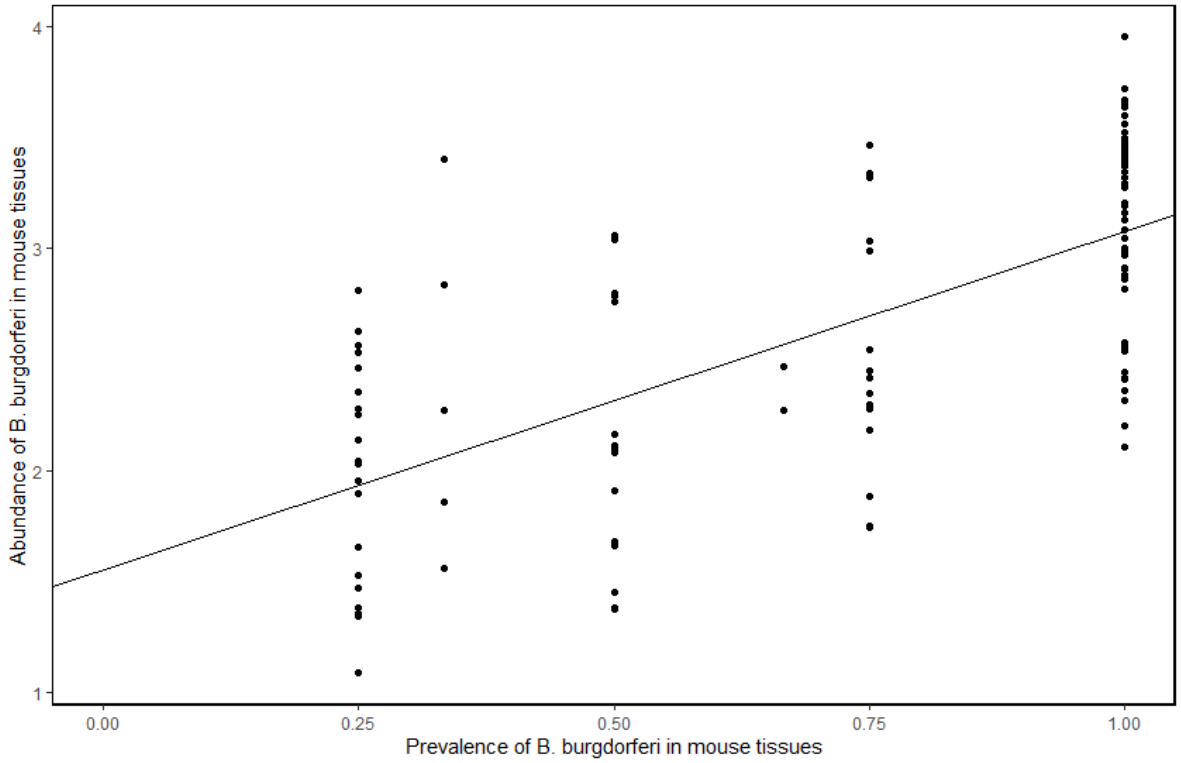

Figure S3. Correlation between the abundance of *B. burgdorferi* in mouse necropsy tissues versus the prevalence of *B. burgdorferi* in mouse necropsy tissues across the 117 realized combinations of strain, mouse sex, and necropsy tissue. The mouse necropsy tissues were harvested at euthanasia (day 97 PI). For each of the 117 data points, the prevalence of *B. burgdorferi* in mouse tissues is based on the detection of *B. burgdorferi* in 4 mice using qPCR. For each the of the 117 data points, the abundance of *B. burgdorferi* in mouse tissues is based on the subset of infected mice (maximum n = 4).

Correlation between the abundance of *B. burgdorferi* in the third ear biopsy and the abundance of *B. burgdorferi* in the mouse necropsy tissues across the 11 strains of *B. burgdorferi*: Our analysis in the main manuscript found that the prevalence of *B. burgdorferi* infection in the right ear was 91.7% (77/84) in the third ear tissue biopsy on day 89 PI and 14.3% (12/84) in the necropsy at euthanasia on day 97 PI. Thus, the prevalence of *B. burgdorferi* infection decreased 6.4-fold over a time interval of 8 days. We suspect that this dramatic decrease in the detection of *B. burgdorferi* in the right ear was caused by the third larval infestation that occurred between the third biopsy (day 89 PI) and euthanasia (day 97 PI).

A correlation analysis was done between the strain-specific spirochete load in the third ear biopsy (day 89 PI) and the strain-specific spirochete load in the mouse necropsy tissues at euthanasia (day 97 PI). The EMMs for the spirochete load of the third ear tissue biopsy were generated from an LM with the fixed factors of strain, sex, and block. The EMMs for the spirochete load of the mouse necropsy tissues were generated from an LMM with the fixed factors of strain, sex, tissue, and block and with mouse identity as a random factor. For the 11 *B. burgdorferi* strains, the spirochete loads in the third ear tissue biopsy and the mouse necropsy tissues were strongly positively correlated ($r = 0.913$, $df = 9$, $t = 6.724$, $p = 8.617*10^{-5}$). For the

22 combinations of mouse sex and *B. burgdorferi* strain, there was also a strong positive correlation between the spirochete load in the third biopsy of the right ear on day 89 PI versus the spirochete load in the necropsy tissues on day 97 PI ($r = 0.923$, $df = 20$, $t = 10.73$, $p = 9.551*10^{-10}$; see Figure 2.4 in the main manuscript). This strong positive correlation suggests that any reduction of spirochete abundance caused by the larval infestation was consistent across strains.

Correlation of infection prevalence among the seven necropsy tissues: Among the 84 infected mice, a correlation analysis was done to determine whether the presence of infection covaried among pairs of necropsy tissues. All 21 pairwise correlations were positive, and 14 were significant at an $\alpha = 0.01$ (Table S26, Figure S4A).

Table S26. The correlation matrix of *B. burgdorferi* infection presence among the 21 pairs of mouse tissues. Each of the 21 pairwise correlations were calculated across the subset of 84 infected mice. The Pearson correlation coefficients and their p-values are shown above and below the diagonal, respectively. Significant correlation coefficients and their p-values are shown in boldface type.

	Ventral skin	Left ear	Right ear	Heart	Bladder	Kidney	Tt joint
Ventral skin	NA	**0.220**	**0.253**	**0.452**	**0.487**	0.052	**0.639**
Left ear	**0.020**	NA	**0.420**	**0.332**	**0.383**	**0.231**	**0.391**
Right ear	**0.007**	**0.000**	NA	**0.229**	**0.210**	0.092	**0.265**
Heart	**0.000**	**0.000**	**0.015**	NA	**0.828**	**0.307**	**0.515**
Bladder	**0.000**	**0.000**	**0.027**	**0.000**	NA	**0.276**	**0.569**
Kidney	0.588	**0.014**	0.337	**0.001**	**0.003**	NA	0.155
Tt joint	**0.000**	**0.000**	**0.005**	**0.000**	**0.000**	0.103	NA

Correlation of spirochete abundance among the seven necropsy tissues: Among the 84 infected mice, a correlation analysis was done to determine whether the spirochete abundance covaried among pairs of necropsy tissues. The mouse tissue spirochete loads were calculated as log10 [(*23S rRNA* + 1) / 10^6 *Beta-actin*], which includes the uninfected tissues. All 21 pairwise correlations were positive, and all 21 correlations were significant at an $\alpha = 0.01$ (Table S27, Figure S4B).

Table S27. The correlation matrix of *B. burgdorferi* abundance among the 21 pairs of mouse tissues. The abundance of *B. burgdorferi* in each mouse tissue was calculated as log10 [(*23s rRNA* + 1) / 10^6 *Beta-actin*]. Each of the 21 pairwise correlations was calculated across the subset of 84 infected mice. The Pearson correlation coefficients and their p-values are shown above and below the diagonal, respectively. Significant correlation coefficients and their p-values are shown in boldface type.

	Ventral skin	Left ear	Right ear	Heart	Bladder	Kidney	Tt joint
Ventral skin	NA	**0.723**	**0.487**	**0.862**	**0.842**	**0.513**	**0.850**
Left ear	**0.000**	NA	**0.671**	**0.851**	**0.889**	**0.634**	**0.891**

Right ear	**0.000**	**0.000**	NA	**0.754**	**0.743**	**0.315**	**0.725**
Heart	**0.000**	**0.000**	**0.000**	NA	**0.918**	**0.787**	**0.916**
Bladder	**0.000**	**0.000**	**0.000**	**0.000**	NA	**0.794**	**0.911**
Kidney	**0.000**	**0.000**	**0.004**	**0.000**	**0.000**	NA	**0.757**
Tt joint	**0.000**	**0.000**	**0.000**	**0.000**	**0.000**	**0.000**	NA

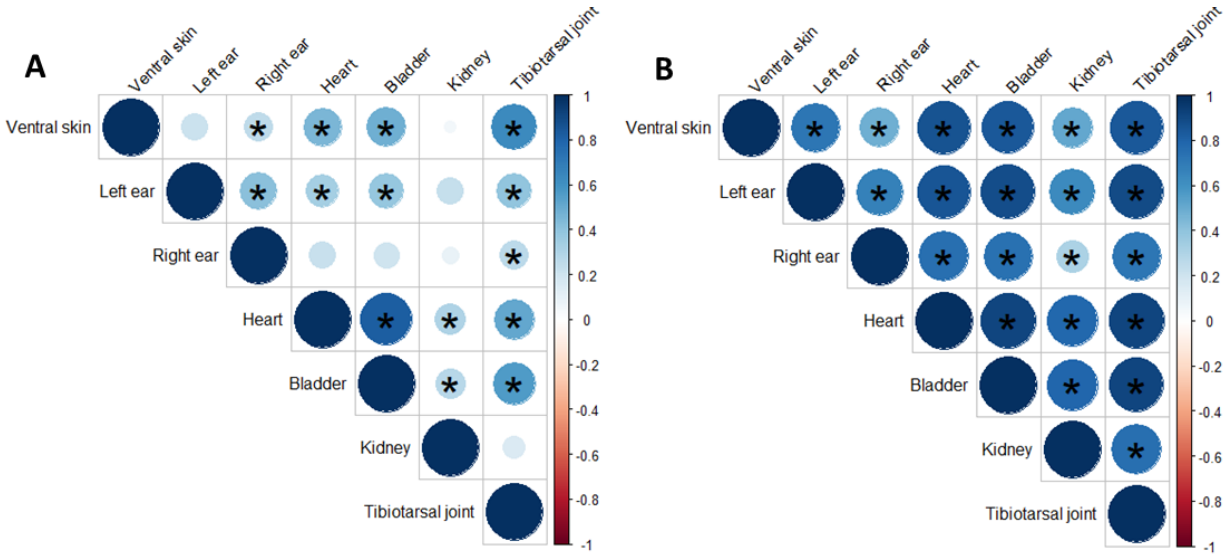

Figure S4. Correlation plots for the 21 pairs of mouse necropsy tissues of (A) *B. burgdorferi* infection presence and (B) abundance of *B. burgdorferi*. (A) The *B. burgdorferi* infection presence was based on the presence or absence of *B. burgdorferi* in the mouse necropsy tissue. (B) The abundance of *B. burgdorferi* in the mouse necropsy tissues was estimated using the log10[(*23s rRNA* + 1) / 10^6 *Beta-actin*] to include the uninfected tissues. All 42 correlations were positive as indicated by the blue colours and the size of the circles. Of the 42 correlations, 35 correlations were statistically significant at an $\alpha = 0.01$ as indicated by the asterisks.

Section 12 – Literature search for sex-specific differences in *B. burgdorferi* infection of mice

In our study we found that male mice had a higher infection prevalence and abundance of *B. burgdorferi* in their tissues than females, independent of strain. We conducted a literature search to determine whether such sex-specific differences were previously reported in rodent hosts. We restricted this search to experimental infections of rodent hosts (e.g., *M. musculus*, *P. leucopus*, and the European bank vole, *Myodes glareolus*) with *B. burgdorferi* sensu lato (sl) pathogens (e.g., *B. burgdorferi* ss, *B. afzelii*, and *B. garinii*). The selected studies investigated a variety of infection phenotypes such as the host antibody response, pathology, and the prevalence and abundance of *B. burgdorferi* in host tissues. In total, 27 studies were found meeting these criteria (Table S28). For each study, we determined whether they used male mice and/or female mice, and whether sex was included in the statistical analyses. Of the 27 studies, 9 used both male and female mice, but only one study (Yang et al., 1994) included sex in their statistical analyses (Table 2, main manuscript).

Table S28. A literature search for sex-specific differences in *B. burgdorferi* sensu lato infection in rodent hosts. The included studies all experimentally infected rodent hosts with *B. burgdorferi* sensu lato. The sex of mouse used is shown if this information was indicated in the study. The mouse species and *Borrelia* genospecies used in the study are listed. One study (2) used sex in their statistical analyses and found no difference in tissue spirochete loads.

Number	Study	Sex of mice	Mouse species [1]	*Borrelia* species [2]
1	(Barthold et al., 1990)	N/A	MM	*burg*
2	(Yang et al., 1994)	M+F	MM	*burg*
3	(Ma et al., 1998)	F	MM	*burg*
4	(Zeidner et al., 2001)	N/A	MM	*burg*
5	(Wang et al., 2001)	M + F	MM	*burg*
6	(Wang et al., 2002)	M + F	MM	*burg*
7	(Dolan et al., 2004)	F	MM	*burg*
8	(Derdáková et al., 2004)	N/A	PL	*burg*
9	(Liang et al., 2004)	N/A	MM	*burg*
10	(Lima et al., 2005)	N/A	MM	*burg*
11	(Hanincová et al., 2008)	M+F	PL, MM	*burg*
12	(Craig-Mylius et al., 2009)	N/A	MM	*burg*
13	(Schwanz et al., 2011)	M	PL	*burg*
14	(Baum et al., 2012)	F	PL, MM	*burg*
15	(Golovchenko et al., 2014)	F	MM	*burg*
16	(Kern et al., 2015)	N/A	MM	*burg*
17	(Tonetti et al., 2015)	M	MM	*afz*
18	(Elsner et al., 2015)	M + F	MM	*burg*
18	(Devevey et al., 2015)	F	MM	*burg*
20	(Jacquet et al., 2015)	F	MM	*afz*
21	(Belli et al., 2017)	F	MM	*afz*
22	(Grillon et al., 2017)	M + F	MM	*burg, afz, gar*
23	(Rynkiewicz et al., 2017)	M + F	PL	*burg*
24	(Sertour et al., 2018)	F	MM	*burg, afz, bav*
25	(Genné et al., 2018)	F	MM	*afz*
26	(Gomez-Chamorro et al., 2019a)*	M+F	MG	*afz*
27	(Gomez-Chamorro, et al., 2019b)	M+F	MG	*afz*

[1] Mouse species: MG = *Myodes glareolus*, MM = *Mus musculus*, PL = *Peromyscus leucopus*

[2] *Borrelia burgdorferi* sensu lato genospecies abbreviations: *Borrelia afzelii* (*afz*), *Borrelia bavariensis* (*bav*), *Borrelia burgdorferi* sensu stricto (*burg*), *Borrelia garinii* (*gar*)

*This study investigated whether host sex impacted susceptibility to infection with *B. afzelii* and found it did not, which agrees with our results. This is not included as this search was restricted to differences in infection, not susceptibility to infection.

Section 13 – Estimating the reduction in spirochete abundance from a larval infestation

We suspect that the third infestation with *I. scapularis* larvae prior to euthanasia resulted in a significant reduction in spirochete abundance in the tissues of the mice, and that this would have primarily affected the external tissues. We estimated that an infestation of 100 larvae could remove 316,200 spirochetes per mouse, which represents ~26.2% of the spirochetes present in the skin. We got this value using the following assumptions:

- The average mouse weighed 28,030 mg at 1 week prior to the third larval infestation
- Mouse skin represents 17% of the total weight of a mouse (Blackburn et al., 1997). Thus, the average weight of the skin of our mice was 4,765.1 mg.
- The average spirochete load per mg tissue (253 spirochetes per mg tissue) of the 7 tissues can represent the expected quantity of spirochetes in the skin without a larval feeding
- Thus, the mouse skin contains 4,765 mg x 253 spirochetes/mg = 1,205,570 spirochetes
- Each mouse was fed on by 100 larvae
- A single larvae will take 3,162 spirochetes when feeding (Soares et al., 2006). Thus, 100 larvae will remove 316,200 spirochetes from the skin of the mouse
- The percentage of spirochetes removed from the skin = 100 x (316,200)/ (1,205,570) = 26.2%

A second estimation of the reduction of spirochetes was done using the average spirochete abundance for the final ear biopsy (day 89 PI) taken immediately prior to the infestation (830 spirochetes/mg). Using this average, the expected quantity of spirochetes in the mouse skin prior to feeding is 3,947,480 (4,765 mg x 830 spirochetes/mg = 3,947,480 spirochetes). With this estimate, an infestation with 100 larvae would remove ~8.0% of the spirochetes found in the skin 100 x (316,200 spirochetes / 3,947,480 spirochetes = 8.0%).

Section 14 – References

Barthold, S. W., Beck, D. S., Hansen, G. M., Terwilliger, G. A., & Moody, K. D. (1990). Lyme borreliosis in selected strains and ages of laboratory mice. *The Journal of Infectious Diseases*, *162*(1), 133–138. https://doi.org/10.1093/infdis/162.1.133

Bates, D., Mächler, M., Bolker, B., & Walker, S. (2015). Fitting linear mixed-effects models using lme4. *Journal of Statistical Software*, *67*, 1–48. https://doi.org/10.18637/jss.v067.i01

Baum, E., Hue, F., & Barbour, A. G. (2012). Experimental infections of the reservoir species *Peromyscus leucopus* with diverse strains of *Borrelia burgdorferi*, a Lyme disease agent. *MBio*, *3*(6), e00434-12. https://doi.org/10.1128/mBio.00434-12

Belli, A., Sarr, A., Rais, O., Rego, R. O. M., & Voordouw, M. J. (2017). Ticks infected via co-feeding transmission can transmit Lyme borreliosis to vertebrate hosts. *Scientific Reports*, *7*(1), 5006. https://doi.org/10.1038/s41598-017-05231-1

Blackburn, A., Schmitt, A., Schmidt, P., Wanke, R., Hermanns, W., Brem, G., & Wolf, E. (1997). Actions and interactions of growth hormone and insulin-like growth factor-II: Body and organ growth of transgenic mice. *Transgenic Research*, *6*(3), 213–222. https://doi.org/10.1023/A:1018494108654

Courtney, J. W., Kostelnik, L. M., Zeidner, N. S., & Massung, R. F. (2004). Multiplex real-time PCR for detection of *Anaplasma phagocytophilum* and *Borrelia burgdorferi*. *Journal of Clinical Microbiology*, *42*(7), 3164–3168. https://doi.org/10.1128/JCM.42.7.3164-3168.2004

Craig-Mylius, K. A., Lee, M., Jones, K. L., & Glickstein, L. J. (2009). Arthritogenicity of *Borrelia burgdorferi* and *Borrelia garinii*: Comparison of infection in mice. In *Am. J. Trop. Med. Hyg* (Vol. 80, Issue 2, pp. 252–258).

Dai, J., Wang, P., Adusumilli, S., Booth, C. J., Narasimhan, S., Anguita, J., & Fikrig, E. (2009). Antibodies against a tick protein, Salp15, protect mice from the Lyme disease agent. *Cell Host and Microbe*, *6*(5), 482–492. https://doi.org/10.1016/j.chom.2009.10.006

Derdáková, M., Dudiò, V., Brei, B., Brownstein, J. S., Schwartz, I., & Fish, D. (2004). Interaction and transmission of two *Borrelia burgdorferi* sensu stricto strains in a tick-rodent maintenance system. *Applied and Environmental Microbiology*, *70*(11), 6783–6788. https://doi.org/10.1128/AEM.70.11.6783-6788.2004

Devevey, G., Dang, T., Graves, C. J., Murray, S., & Brisson, D. (2015). First arrived takes all: Inhibitory priority effects dominate competition between co-infecting *Borrelia burgdorferi* strains. *BMC Microbiology*, *15*(1), 61. https://doi.org/10.1186/s12866-015-0381-0

Dolan, M. C., Piesman, J., Schneider, B. S., Schriefer, M., Brandt, K., & Zeidner, N. S. (2004). Comparison of disseminated and nondisseminated strains of *Borrelia burgdorferi* sensu

stricto in mice naturally infected by tick bite. *Infection and Immunity*, *72*(9), 5262–5266. https://doi.org/10.1128/IAI.72.9.5262-5266.2004

Dulebohn, D. P., Bestor, A., Rego, R. O. M., Stewart, P. E., & Rosa, P. A. (2011). *Borrelia burgdorferi* linear plasmid 38 is dispensable for completion of the mouse-tick infectious cycle. *Infection and Immunity*, *79*(9), 3510–3517. https://doi.org/10.1128/IAI.05014-11

Elias, A. F., Stewart, P. E., Grimm, D., Caimano, M. J., Eggers, C. H., Tilly, K., Bono, J. L., Akins, D. R., Radolf, J. D., Schwan, T. G., & Rosa, P. (2002). Clonal polymorphism of *Borrelia burgdorferi* strain B31 MI: implications for mutagenesis in an infectious strain background. *Infection and Immunity*, *70*(4), 2139–2150. https://doi.org/10.1128/IAI.70.4.2139-2150.2002

Elsner, R. A., Hastey, C. J., Olsen, K. J., & Baumgarth, N. (2015). Suppression of long-lived humoral immunity following *Borrelia burgdorferi* infection. *PLOS Pathogens*, *11*(7), e1004976. https://doi.org/10.1371/journal.ppat.1004976

Fox, J., & Weisberg, S. (2019). *An R companion to applied regression, third edition*. Sage.

Genné, D., Rossel, M., Sarr, A., Battilotti, F., Rais, O., Rego, R. O. M., & Voordouw, M. J. (2021). Competition between strains of *Borrelia afzelii* in the host tissues and consequences for transmission to ticks. *The ISME Journal*, *15*(8), 2390–2400. https://doi.org/10.1038/s41396-021-00939-5

Genné, D., Sarr, A., Gomez-Chamorro, A., Durand, J., Cayol, C., Rais, O., & Voordouw, M. J. (2018). Competition between strains of *Borrelia afzelii* inside the rodent host and the tick vector. *Proceedings of the Royal Society B: Biological Sciences*, *285*(1890), 17–20. https://doi.org/10.1098/rspb.2018.1804

Golovchenko, M., Sima, R., Hajdusek, O., Grubhoffer, L., Oliver, J. H., & Rudenko, N. (2014). Invasive potential of *Borrelia burgdorferi* sensu stricto *ospC* type L strains increases the possible disease risk to humans in the regions of their distribution. *Parasites & Vectors*, *7*(1), 538. https://doi.org/10.1186/s13071-014-0538-y

Gomez-Chamorro, A., Battilotti, F., Cayol, C., Mappes, T., Koskela, E., Boulanger, N., Genné, D., Sarr, A., & Voordouw, M. J. (2019). Susceptibility to infection with *Borrelia afzelii* and TLR2 polymorphism in a wild reservoir host. *Scientific Reports*, *9*(1), 6711. https://doi.org/10.1038/s41598-019-43160-3

Gomez-Chamorro, A., Heinrich, V., Sarr, A., Roethlisberger, O., Genné, D., Bregnard, C., Jacquet, M., & Voordouw, M. J. (2019). Maternal antibodies provide bank voles with strain-specific protection against infection by the Lyme disease pathogen. *Applied and Environmental Microbiology*, *85*(23), e01887-19. https://doi.org/10.1128/AEM.01887-19

Grillon, A., Westermann, B., Cantero, P., Jaulhac, B., Voordouw, M. J., Kapps, D., Collin, E., Barthel, C., Ehret-Sabatier, L., & Boulanger, N. (2017). Identification of *Borrelia* protein candidates in mouse skin for potential diagnosis of disseminated Lyme borreliosis. *Scientific Reports*, *7*(1), 1–13. https://doi.org/10.1038/s41598-017-16749-9

Hanincová, K., Ogden, N. H., Diuk-Wasser, M., Pappas, C. J., Iyer, R., Fish, D., Schwartz, I., & Kurtenbach, K. (2008). Fitness variation of *Borrelia burgdorferi* sensu stricto strains in mice. *Applied and Environmental Microbiology*, *74*(1), 153–157. https://doi.org/10.1128/AEM.01567-07

Harrell Jr., F. E. (2021). *Hmisc: Harrell miscellaneous. R package version 4.5-0*. https://CRAN.R-project.org/package=Hmisc

Jacquet, M., Durand, J., Rais, O., & Voordouw, M. J. (2015). Cross-reactive acquired immunity influences transmission success of the Lyme disease pathogen, *Borrelia afzelii*. *Infection, Genetics and Evolution*, *36*, 131–140. https://doi.org/10.1016/j.meegid.2015.09.012

Jolley, K. A., Bray, J. E., & Maiden, M. C. J. (2018). Open-access bacterial population genomics: BIGSdb software, the PubMLST.org website and their applications. *Wellcome Open Research*, *3*, 124. https://doi.org/10.12688/wellcomeopenres.14826.1

Kern, A., Schnell, G., Bernard, Q., Bœuf, A., Jaulhac, B., Collin, E., Barthel, C., Ehret-Sabatier, L., & Boulanger, N. (2015). Heterogeneity of *Borrelia burgdorferi* sensu stricto population and its involvement in *Borrelia* pathogenicity: Study on murine model with specific emphasis on the skin interface. *PLOS ONE*, *10*(7), e0133195. https://doi.org/10.1371/journal.pone.0133195

Lenth, R. V. (2021). *Emmeans: Estimated marginal means, aka least-squares means. R package version 1.5-2.1*. https://CRAN.R-project.org/package=emmeans

Liang, F. T., Yan, J., Mbow, M. L., Sviat, S. L., Gilmore, R. D., Mamula, M., & Fikrig, E. (2004). *Borrelia burgdorferi* changes its surface antigenic expression in response to host immune responses. *Infection and Immunity*, *72*(10), 5759–5767. https://doi.org/10.1128/iai.72.10.5759-5767.2004

Lima, C. M. R., Zeidner, N. S., Beard, C. B., Soares, C. A. G., Dolan, M. C., Dietrich, G., & Piesman, J. (2005). Differential infectivity of the Lyme disease spirochete *Borrelia burgdorferi* derived from *Ixodes scapularis* salivary glands and midgut. *Journal of Medical Entomology*, *42*(3), 506–510. https://doi.org/10.1603/0022-2585(2005)042[0506:diotld]2.0.co;2

Lüdecke, D. (2018). *ggeffects: Tidy data frames of marginal effects from regression models*. *Journal of Open Source Software*, *3*(26), 772. https://doi.org/10.21105/joss.00772

Ma, Y., Seiler, K. P., Eichwald, E. J., Weis, J. H., Teuscher, C., & Weis, J. J. (1998). Distinct characteristics of resistance to *Borrelia burgdorferi*- induced arthritis in C57BL / 6N mice. *Infection and Immunity*, *66*(1), 161–168.

Ogden, N. H., Margos, G., Aanensen, D. M., Drebot, M. A., Feil, E. J., Hanincová, K., Schwartz, I., Tyler, S., & Lindsay, L. R. (2011). Investigation of genotypes of *Borrelia burgdorferi* in *Ixodes scapularis* ticks collected during surveillance in Canada. *Applied and Environmental Microbiology*, *77*(10), 3244–3254. https://doi.org/10.1128/aem.02636-10

Purser, J. E., & Norris, S. J. (2000). Correlation between plasmid content and infectivity in *Borrelia burgdorferi*. *Proceedings of the National Academy of Sciences, 97*(25), 13865–13870. https://doi.org/10.1073/pnas.97.25.13865

R Core Team. (2021). *R: A language and environment for statistical computing*. R Foundation for Statistical Computing. https://www.R-project.org/

Reed, D. R., Bachmanov, A. A., & Tordoff, M. G. (2007). Forty mouse strain survey of body composition. *Physiology & Behavior*, *91*(5), 593–600. https://doi.org/10.1016/j.physbeh.2007.03.026

Roehrig, J. T., Piesman, J., Hunt, A. R., Keen, M. G., Happ, C. M., & Johnson, B. J. B. (1992). The hamster immune response to tick-transmitted *Borrelia burgdorferi* differs from the response to needle-inoculated, cultured organisms. *Journal of Immunology*, *149*(11), 3648–36453.

Rynkiewicz, E. C., Brown, J., Tufts, D. M., Huang, C.-I., Kampen, H., Bent, S. J., Fish, D., & Diuk-Wasser, M. A. (2017). Closely-related *Borrelia burgdorferi* (sensu stricto) strains exhibit similar fitness in single infections and asymmetric competition in multiple infections. *Parasites & Vectors*, *10*(1), 64. https://doi.org/10.1186/s13071-016-1964-9

Schwan, T. G., & Piesman, J. (2000). Temporal changes in outer surface proteins A and C of the Lyme disease- associated spirochete, *Borrelia burgdorferi*, during the chain of infection in ticks and mice. *Journal of Clinical Microbiology*, *38*(1), 382–388. https://doi.org/10.1128/jcm.38.1.382-388.2000

Schwanz, L. E., Voordouw, M. J., Brisson, D., & Ostfeld, R. S. (2011). *Borrelia burgdorferi* has minimal impact on the Lyme disease reservoir host *Peromyscus leucopus*. *Vector-Borne and Zoonotic Diseases*, *11*(2), 117–124. https://doi.org/10.1089/vbz.2009.0215

Sertour, N., Cotté, V., Garnier, M., Malandrin, L., Ferquel, E., & Choumet, V. (2018). Infection kinetics and tropism of *Borrelia burgdorferi* sensu lato in mouse after natural (via ticks) or artificial (needle) infection depends on the bacterial strain. *Frontiers in Microbiology*, *9*, 1722. https://doi.org/10.3389/fmicb.2018.01722

Soares, C. A. G., Zeidner, N. S., Beard, C. B., Dolan, M. C., Dietrich, G., & Piesman, J. (2006). Kinetics of *Borrelia burgdorferi* infection in larvae of refractory and competent tick vectors. *Journal of Medical Entomology*, *43*(1), 61–67. https://doi.org/10.1093/jmedent/43.1.61

Tonetti, N., Voordouw, M. J., Durand, J., Monnier, S., & Gern, L. (2015). Genetic variation in transmission success of the Lyme borreliosis pathogen *Borrelia afzelii*. *Ticks and Tick-Borne Diseases*, *6*(3), 334–343. https://doi.org/10.1016/j.ttbdis.2015.02.007

Travinsky, B., Bunikis, J., & Barbour, A. G. (2010). Geographic differences in genetic locus linkages for *Borrelia burgdorferi*. *Emerging Infectious Diseases*, *16*(7), 1147–1150. https://doi.org/10.3201/eid1607.091452

Wang, G., Ojaimi, C., Wu, H., Saksenberg, V., Iyer, R., Liveris, D., McClain, S. A., Wormser, G. P., & Schwartz, I. (2002). Disease severity in a murine model of Lyme borreliosis is associated with the genotype of the infecting *Borrelia burgdorferi* sensu stricto strain. *The Journal of Infectious Diseases*, *186*(6), 782–791. https://doi.org/10.1086/343043

Wang, G., Ojaimi, C., Wu, H., Saksenberg, V., Iyer, R., McClain, S. A., Wormser, G. P., & Schwartz, I. (2001). Impact of genotypic variation of *Borrelia burgdorferi* sensu stricto on kinetics of dissemination and severity of disease in C3H/HeJ mice. *Abstracts of the General Meeting of the American Society for Microbiology*, *101*(7), 294–295. https://doi.org/10.1128/IAI.69.7.4303

Yang, L., Weis, J. H., Eichwald, E., Kolbert, C. P., Persing, D. H., & Weis, J. J. (1994). Heritable susceptibility to severe *Borrelia burgdorferi*-induced arthritis is dominant and is associated with persistence of large numbers of spirochetes in tissues. *Infection and Immunity*, *62*(2), 492–500. https://doi.org/10.1128/iai.62.2.492-500.1994

Zeidner, N. S., Schneider, B. S., Dolan, M. C., & Piesman, J. (2001). An analysis of spirochete load, strain, and pathology in a model of tick-transmitted Lyme borreliosis. *Vector-Borne and Zoonotic Diseases*, *1*(1), 35–44. https://doi.org/10.1089/153036601750137642

Appendix B – Supplementary material for Ch. 3

This appendix is currently in submission to the journal PLOS pathogens as the supplementary material for a manuscript. Currently full copyright remains with the author, C. B. Zinck

Zinck, C.B., Thanpy, P. R., Uhlemann, E.E., Wachter, J., Suchan, D., Cameron, A. D. S., Rego, R. O. M., Brisson, D., Bouchard, C., Ogden, N. H., & Voordouw, M. (2023). Variation among strains of *Borrelia burgdorferi* in host tissue abundance and lifetime transmission determine the population strain structure in nature. (submitted, April 7, 2023)

Section 1 – Additional Methods

Larval infestation of mice: Specific pathogen-free *I. scapularis* larval ticks were purchased from the National Tick Research and Education Resource at Oklahoma State University. At days 30, 60, and 90 post-infection (PI), mice were infested with 50-100 *I. scapularis* larvae. All mice were anaesthetized for ~20 min with ketamine and xylazine for each infestation, where larvae were brushed onto their fur. During each infestation, mice were housed in their mouse cage with the plastic top removed and placed on risers within a rat cage containing a shallow moat of water. As a precaution, a 1-inch-tall strip of petroleum jelly was put around the inner wall of each rat cage. Engorged larvae climbed out of the mouse cage and fell into the water moat of the rat cage where they were easily recovered. At 5 days post-infestation, most larvae were in the water moat, and no larvae were found in the bedding by 7 days post-infestation. At 7-8 days post-infestation, the mice were housed under normal conditions. For each mouse and infestation, 5 engorged larvae were frozen immediately at -80 ºC following recovery (this was not done for the first infestation in block 1; it was done for infestations 2 and 3 in block 1 and for infestations 1, 2, and 3 in block 2). The remaining engorged larvae were placed into 50 mL Falcon tubes where they were allowed to moult into nymphs. These tubes had perforated lids and a double layer of nylon stocking to allow air exchange. The centrifuge tubes were placed in sealed clear plastic containers that had a layer of standing ultrapure water (Milli-Q) to ensure a high relative humidity (~100%). Four weeks after the engorged larvae moulted into nymphs, a sample of 10 nymphs per mouse per infestation were frozen at -80 ºC for later DNA extraction.

DNA extraction of whole *Ixodes scapularis* ticks: For each mouse, there were 45 ticks (3 infestations * (5 larvae + 10 nymphs) per infestation) for a total of 5,040 tick DNA extractions (112 mice x 45 ticks per mouse = 5,040 ticks). Ticks were homogenized using bead beating with the Qiagen TissueLyser II. First, ticks were placed into 5 µL of nuclease free water at the bottom of a 2.0 mL MP BIO disruption tube. These were then frozen for 1-2 hrs at -80 ºC before adding a 1.6 mm stainless steel bead, and refreezing inverted at -80 ºC for a minimum of 24 hours. This allows the tick to freeze in place at the center of the tube bottom but keeps the bead from freezing to the tick. The ticks were then disrupted with the TissueLyser II with two runs at 30 Hz for 45 seconds, flipping the two racks of tubes in between runs. DNA was extracted from the homogenized ticks using the Qiagen DNEasy 96-well plate extraction kit and following the manufacturer's instructions. The disrupted ticks were extracted following the kit guidelines with some modifications. The plate extraction was done in batches of 192 samples per run. Each run included 8 no sample controls (i.e., with no DNA substrate added), and experimental controls (ticks from uninfected control mice). The proteinase K digestion step was done overnight in the MP BIO tubes without removing the disruption bead in a shaking incubator (56 ºC, 400 rpm). Samples were then moved into the Qiagen kit plates for the remainder of the extraction. All extractions were eluted into a final volume of 65 µL and stored at -80 ºC prior to use in qPCR.

Statistical software: We used R version 4.0.4 with RStudio version 1.4.1103 for all statistical analyses (R Development Core Team, 2021; RStudio Team, 2020). We used the *lmer()* function in the lme4 package to run the LMMs, and *glmer()* to run the GLMMs (Bates et al., 2015). The *Anova()* function in the car package was used to run the Wald tests of statistical

significance (Fox & Weisberg, 2019). Post-hoc analysis and calculation of estimated marginal means were done using *emmeans(), pairs(), pwpm()* functions in the emmeans package (Lenth, 2021) and *ggemmeans()* and *ggpredict()* in the ggeffects package (Lüdecke, 2018). Correlations were calculated using the *cor.test()* function in the base package. Correlation matrices and correlation plots were calculated using the *rcorr()* function in the Hmisc package (Harrell & Dupont, 2020).

Section 2 – Synthetic standards used in qPCR

Synthetic *23S rRNA* gene standard: The presence and abundance of *B. burgdorferi* in the *I. scapularis* ticks was estimated using real-time PCR that targeted the *23S rRNA* gene of *B. burgdorferi* and was previously described (Courtney et al., 2004). To translate the quantification cycle (Cq) values produced by the *23S rRNA* qPCR to estimates of the abundance of *B. burgdorferi* requires a standard curve. We created this standard curve by repeatedly performing the *23S rRNA* qPCR on a dilution series of a synthetic *23S rRNA* gene of known concentrations. The synthetic standard was purchased as a gblock from IDTDNA. The standard was based on the *B. burgdorferi* B31 reference sequence (Genbank Accession number: AE000783.1) to encompass the region targeted by the *23S rRNA* primers (Table S1). A total sequence length of 181 nucleotides (nt) was used to ensure that the forward and reverse primer sites were not at the ends of the gblock where degradation could impact binding. To be able to check for contamination, the *23S rRNA* gene sequence was modified from the reference genome to allow for two methods of differentiation between the *23S rRNA* gene of *B. burgdorferi* and the synthetic standard. A total of 30 nt were inserted in the synthetic fragment between the forward and reverse priming sites to allow for product discrimination on an agarose gel; the amplicon lengths of the synthetic standard (105 nt) and the *23S rRNA* gene of *B. burgdorferi* strain B31 (75 nt) differ by 30 nucleotides. A *BamHI* restriction enzyme cut site was included in the 30-nucleotide insert so that a restriction digest would cleave the synthetic standard, but not a copy of the real *23S rRNA* gene. The gblock was initially suspended in Buffer AE (Qiagen DNEasy kit) with 0.1 mg/mL tRNA (Sigma-Aldrich: 10109517001). This was done so that the standard was in the same suspension buffer as all the experimental samples. The tRNA was added to reduce the impact of DNA adsorption to the walls of the qPCR tubes in dilutions with a low concentration of gblock *23S rRNA*.

Table S1. The sequences used in creating the *23S rRNA* synthetic standard as well as the primer and probe sequences for the *23S rRNA* qPCR. All sequences are reported in the 5'-3' direction. The *23S rRNA* forward primer and the *23S rRNA* reverse primer are highlighted in yellow and green, respectively. The 30-nucleotide insert sequence and the *BamHI* cut site are shown in red and purple, respectively.

Identity	Sequence (5'-3')
23S rRNA forward primer	CGAGTCTTAAAAGGGCGATTTAGT

23S rRNA reverse primer	GCTTCAGCCTGGCCATAAATAG
23S rRNA probe	AGATGTGGTAGACCCGAAGCCGAGTG
B. burgdorferi B31 original sequence	TTATCATGTCTAGCAAGATTAAAGCATAGAAGTGCTGGAGTC GAAGCGAAAGCGAGTCTTAAAAGGGCGATTTAGTTAGATGTG GTAGACCCGAAGCCGAGTGATCTATTTATGGCCAGGCTGAAG CTTGGGTAAAACCAAGTGGAGGGCC
gBlock synthetic standard	TTATCATGTCTAGCAAGATTAAAGCATAGAAGTGCTGGAGT CGAAGCGAAAGCGAGTCTTAAAAGGGCGATTTAGTGCGGA TCCTATCATGTAGATGTGGTAGACCCGAAGCCGAGTGAGCG CTGATTGCATAATCTATTTATGGCCAGGCTGAAGCTTGGGTA AAACCAAGTGGAGGGCC

Synthetic tick *calreticulin* gene standard: The abundance of the tick genome in the tick DNA extractions was estimated using a real-time PCR that targeted the *calreticulin* gene of *I. scapularis*. A synthetic gblock standard was created for the *calreticulin* gene of *I. scapularis* ticks following the same rationale as above. This standard was based on the reference sequence (Genbank Accession number: AY690335.1) to encompass the region targeted by the *calreticulin* primers (Table S2). The total sequence length of the synthetic tick *calreticulin* gene is 177 nt. Like the *23S rRNA* standard, the internal sequence of the *calreticulin* standard was modified by adding a 33-nucleotide insert that contained a *BamHI* cut site. This 33-nt insert will allow us to differentiate the standard from a real copy of the *calreticulin* gene. The *calreticulin* standard was suspended in the same manner as the *23S rRNA* standard.

Table S2. The sequences used in creating the synthetic tick *calreticulin* standard as well as the primer and probe sequences for the tick *calreticulin* qPCR. All sequences are reported in the 5'-3' direction. The *calreticulin* forward primer and the *calreticulin* reverse primer are highlighted in yellow and green, respectively. The 33-nucleotide insert sequence and the *BamHI* cut site are shown in red and purple, respectively.

Identity	Sequence (5'-3')
Calreticulin forward primer	AAGCGAGCAGGGAACTTTCA
Calreticulin reverse primer	GAACTTGGTGGACAGTCCGT
Calreticulin probe	CACTGCCGCATCCTCTTCCTCCC
I. scapularis	CTCCACGAAGAAGGGAAGCGAGCAGGGAACTTTCAAGCTGTCCGCCG GCAAGTTCCACGGCGACCCGGAGAAGGACCTCGGCATCCAGACCTCT

Calreticulin original sequence	GAAGATGCCCGCTTTTACGGACTGTCCACCAAGTTCGAGCCGTTCTCGAAC
gBlock synthetic standard	CTCCACGAAGAAGGGAAGCGAGCAGGGAACTTTCAAGCTGTTCCAGGATCCTTCACCGCCGGCAAGTTCCACGGCGACCCGGAGAAGGACCTCGGCATCCAGACCTCTGAAGATGCCCGCCTTCAACACCCCAGCCATTTTACGGACTGTCCACCAAGTTCGAGCCGTTCTCGAAC

Section 3 – Analyses of the larval infection prevalence (LIP)

GLMM of LIP: The larval infection prevalence (LIP) is the proportion of engorged larvae infected with *B. burgdorferi*. The analysis of the LIP was performed on all the engorged larvae (n = 950 engorged larvae) that fed on the subset of infected mice (n = 84 mice). The response variable was the infection status for each engorged larva as measured by *23S rRNA* qPCR. This binomial response variable (0 = uninfected, 1 = infected) was modelled using a generalized linear mixed effect model (GLMM) with binomial errors. The fixed factors were strain (11 levels), mouse sex (2 levels: male, female), infestation (3 levels: infestation 1, infestation 2, infestation 3), and temporal block (2 levels: A and B). Tick *calreticulin* gene copy number was not included in the model. The full model included all the two-way and the three-way interactions between strain, sex, and infestation. Temporal block was included as a main effect only. Mouse identity was included as a random factor. Non-significant interaction terms (at $\alpha = 0.05$) were removed sequentially (Table S3). The final simplified model included no interactions (Table S3).

Strain ($p = 1.346*10^{-15}$), infestation ($p = 3.359*10^{-5}$), and temporal block ($p = 8.088*10^{-10}$) but not mouse sex ($p = 0.085$) had significant effects on the LIP (Table S3). The parameter estimates for the final simplified model are shown in Table S4. The mean LIP for the levels of a given factor were calculated from the raw data by averaging over the levels of the other factors (Table S5). Estimated marginal means (EMMs) of the LIP and post-hoc tests were generated using the ggemmeans() function and the final simplified model (Table S5). The means from the raw data and the EMMs were similar (Table S5). The Pearson correlation between the means and the EMMs of the LIP across the 18 levels was positive and significant (Mean vs EMM in Table S5; r = 0.977, t = 18.36, df = 16, p = 3.563e-12). In what follows, we present the EMMs of the LIP and their post-hoc tests (Table S5).

Among strains of *B. burgdorferi* and averaged across mouse sex, infestation, and block, the mean LIP ranged from 32.89% for strain 54 to 97.10% for strain 178-1. All strains, except strain 54, had a significantly higher LIP compared to the reference strain 66 (Table S4). Averaged across *B. burgdorferi* strains, infestation, and block, the EMM LIP for male mice (79.72%) was higher compared to female mice (73.56%), but this difference was not significant ($p = 0.085$). Averaged across *B. burgdorferi* strains, mouse sex, and block, the EMM LIP for infestation 1 (88.96%) was significantly higher compared to infestation 2 (65.88%; $p < 0.0001$) and infestation 3 (69.94%; $p = 0.0002$). The EMM LIP for block B (86.48%) was significantly higher compared to block A (63.10%; $p < 0.0001$). The decision to freeze engorged larvae was made after the first infestation for block A and for this reason we do not have any engorged

larvae for this infestation. Thus, the difference in LIP between blocks is driven by the fact that we did not collect engorged larvae for the first infestation in block A.

Table S3. Model simplification of the GLMM of LIP. Non-significant interactions were sequentially removed in order of increasing significance; the model was updated each time a non-significant term was removed. The final simplified model contained the fixed factors only. For each term, the order in which it was removed, the Chi-squared statistic (Chi), degrees of freedom, and p-value (p) are shown. For the non-significant interactions, the p-values are the ones in the model from which they were removed. For the included terms, the p-values are from the final simplified model.

Term	Order removed	Chi	df	p	Signif [a]
Strain:Sex:Infestation	1	8.738	19	0.978	
Strain:Infestation	2	12.306	20	0.905	
Sex:Infestation	3	3.184	2	0.203	
Strain:Sex	4	14.660	10	0.145	
Strain	Final model	93.020	10	$1.346*10^{-15}$	***
Sex	Final model	2.965	1	0.085	
Infestation	Final model	20.603	2	$3.359*10^{-5}$	***
Temporal block	Final model	37.739	1	$8.088*10^{-10}$	***

[a] Categories of significance are as follows: * 0.05 > p > 0.01, ** 0.01 > p > 0.001, *** p < 0.001.

Table S4. Parameter estimates of the GLMM of LIP. Factors include strain (11 levels), mouse sex (2 levels: male, female), infestation (3 levels: infestation 1, infestation 2, infestation 3), and temporal block (2 levels: A and B). For each parameter in the GLMM, the type, description, estimate, standard error (SE), and p-value (p) are shown.

Parameter type	Parameter description	Estimate	SE	p	Signif [a]
Intercept	Reference [b]	-0.188	0.454	0.679	
Contrast	Strain 57 – Strain 66	2.149	0.468	$4.443*10^{-6}$	***
Contrast	Strain 150 – Strain 66	1.497	0.447	$8.163*10^{-4}$	***
Contrast	Strain 167 – Strain 66	1.666	0.436	$1.316*10^{-4}$	***
Contrast	Strain 126 – Strain 66	1.536	0.447	$5.888*10^{-4}$	***
Contrast	Strain 22-2 – Strain 66	1.289	0.451	0.004	**
Contrast	Strain 10-2 – Strain 66	2.015	0.480	$2.666*10^{-5}$	***
Contrast	Strain 54 – Strain 66	-0.122	0.448	0.785	
Contrast	Strain 198 – Strain	2.924	0.498	$4.379*10^{-9}$	***
Contrast	Strain 174 – Strain 66	2.604	0.542	$1.538*10^{-6}$	***
Contrast	Strain 178-1 – Strain 66	4.103	0.649	$2.564*10^{-10}$	***
Contrast	Female – Male	-0.346	0.201	0.085	
Contrast	Inf 2 – Inf 1	-1.428	0.315	$5.988*10^{-6}$	***
Contrast	Inf 3 – Inf 1	-1.242	0.311	$6.581*10^{-5}$	***

Contrast	Block B – Block A	1.319	0.215	$8.088*10^{-10}$	***

[a] Categories of significance are as follows: * 0.05 > p > 0.01, ** 0.01 > p > 0.001, *** p < 0.001.

[b] Reference condition refers to engorged larvae from infestation 1 that fed on a male mouse in block A that was infected with *B. burgdorferi* strain 66.

Table S5. The means and EMMs of the LIP for each of the levels of the factors of interest. The LIP is the percentage of engorged larvae infected with *B. burgdorferi*. The means are from the raw data, whereas the EMMs were calculated using the final simplified model in Table S3. The mean or EMM of a given level was averaged over the levels of the other factors. Lower and upper (LCL, UCL) 95% confidence limits for the EMM are reported.

Factor	Level	Mean (%)	EMM (%)	LCL (%)	UCL (%)
Strain	66	35.06	35.64	22.33	51.60
Strain	57	77.78	82.61	70.97	90.23
Strain	150	64.89	71.21	57.41	81.95
Strain	167	69.81	74.55	62.34	83.83
Strain	126	64.44	72.01	58.33	82.54
Strain	22-2	63.86	66.77	52.04	78.81
Strain	10-2	72.97	80.59	67.50	89.25
Strain	54	35.48	32.89	21.14	47.24
Strain	198	86.46	91.15	83.11	95.57
Strain	174	81.03	88.21	76.20	94.59
Strain	178-1	95.51	97.10	91.76	99.02
Sex	Male	71.40	79.72	73.97	84.47
Sex	Female	64.00	73.56	66.79	79.38
Infestation	Inf 1	89.67	88.96	81.88	93.49
Infestation	Inf 2	60.54	65.88	59.33	71.88
Infestation	Inf 3	64.65	69.94	63.73	75.49
Block	A	51.28	63.10	54.94	70.57
Block	B	79.57	86.48	82.17	89.88

Section 4 – Analyses of the larval spirochete load (LSL)

LMM of the LSL: The larval spirochete load (LSL) is the number of *23S rRNA* copies per infected engorged larvae. The analysis of the LSL was performed on the subset of engorged larvae that were infected with *B. burgdorferi* (n = 645 infected engorged larvae) that fed on the subset of infected mice (n = 84 mice). The LSL was log10-transformed to normalize the residuals. The $\log_{10}$ *23S rRNA* copies per engorged larva was modelled using a linear mixed effect model (LMM). The fixed factors were strain (11 levels), mouse sex (2 levels: male,

female), infestation (3 levels: infestation 1, infestation 2, infestation 3), and temporal block (2 levels: A and B). The $\log_{10}$ *calreticulin* copies per tick was included as a covariate. The full model included all the two-way and three-way interactions between strain, sex, and infestation. Temporal block was included as a main effect only. Mouse identity was included as a random factor. The three-way interaction between strain, sex, and infestation was significant ($p = 0.010$), but none of the two-way interactions were significant (Table S6). A comparison of the AIC values found that the main effects model had an AIC value (1633.779) that was 36.4 units lower compared to the full interaction model (1670.186). For this reason, the parameter estimates and EMMs are presented for the more parsimonious main effects model (i.e., does not include any interactions; Table S7).

Strain ($p = 5.968*10^{-12}$), infestation ($p = 4.773*10^{-11}$), temporal block ($p = 6.236*10^{-05}$), and log10 *calreticulin* ($p = 2.2*10^{-16}$), but not mouse sex ($p = 0.317$) had significant effects on the LSL (Table S6). The parameter estimates for this final simplified model and their significance are shown in Table S7. Means and EMMs (using the final model) were generated for each factor level (Table S8). The means from the raw data and the EMMs were similar (Table S8). The Pearson correlation between the means and the EMMs of the LSL across the 18 levels was positive and significant (Mean1 vs EMM1 in Table S8; $r = 0.944$, $t = 11.494$, $df = 16$, $p = 3.829*10^{-9}$). The units of the LSL are the number of *23S rRNA* gene copies per infected engorged larva. In what follows, we present the EMMs of the LSL and their post-hoc tests (EMM2 in Table S8).

The EMM LSL varied 11.8-fold among strains from 728.5 units for strain 54 to 15635.5 units for strain 178-1. Larvae that fed on female mice had an EMM LSL (4094.7 units) that was 23.3% higher compared to larvae that fed on male mice (3320.7 units), but this difference was not significant ($p = 0.322$). The EMM LSL of infestation 1 (8502.2 units) was significantly higher compared to infestation 2 (2142.2 units; $p < 0.0001$) and infestation 3 (2752.9 units; $p < 0.0001$). Finally, the EMM LSL of larvae in block B (5808.5 units) was 2.5x higher compared to block A (2340.9 units; $p = 0.0001$).

The LSL had a positive and significant relationship with the number of *calreticulin* gene copies in the tick (Table S7: slope = 0.735, SE = 0.058, $p < 2.2*10^{-16}$). Thus, DNA extractions from engorged larvae that had higher levels of *calreticulin* also had higher levels of *23S rRNA* (Figure S1). This relationship suggests that larger larvae (as estimated by a higher abundance of *calreticulin*) may also have higher spirochete loads. A separate analysis of the ratio of the *23S rRNA* gene copy number to the tick *calreticulin* copy number provided very similar results (see below).

Table S6. Model simplification of the LMM of the LSL. Non-significant interactions were sequentially removed in order of increasing significance; the model was updated each time a term was removed. The final simplified model contained the fixed factors only. For each term, the order in which it was removed, the Chi-squared statistic (Chi), degrees of freedom (df), and p-value (p) are shown. For the non-significant interactions, the p-values are the ones in the model from which they were removed. For the included terms, the p-values are from the final simplified model.

Term	Order removed	Chi	df	p	Signif [a]
Strain:Sex:Infestation	1	36.180	19	0.010	*
Sex:Infestation	2	0.052	2	0.974	
Strain:Sex	3	7.160	10	0.710	
Strain:Infestation	4	27.011	20	0.135	
Strain	Final model	74.494	10	$5.968*10^{-12}$	***
Sex	Final model	1.002	1	0.317	
Infestation	Final model	47.531	2	$4.773*10^{-11}$	***
Temporal block	Final model	16.030	1	$6.236*10^{-5}$	***
log10(*calreticulin*)	Final model	162.05	1	$2.2*10^{-16}$	***

[a] Categories of significance are as follows: * 0.05 > p > 0.01, ** 0.01 > p > 0.001, *** p < 0.001.

Table S7. Parameter estimates of the LMM of the LSL. Factors include strain (11 levels), mouse sex (2 levels: male, female), and infestation (3 levels: infestation 1, infestation 2, infestation 3), temporal block (2 levels: A and B). Covariates included $\log_{10}$ *calreticulin* copies per tick. For each parameter in the LMM, the type, description, estimate, standard error (SE), and p-value (p) are shown.

Parameter type	Parameter description	Estimate	SE	p	Signif [a]
Intercept	Reference [b]	0.362	0.324	0.676	
Contrast	Strain 57 – Strain 66	0.286	0.242	0.241	
Contrast	Strain 150 – Strain 66	-0.443	0.247	0.077	
Contrast	Strain 167 – Strain 66	0.092	0.237	0.701	
Contrast	Strain 126 – Strain 66	0.126	0.246	0.609	
Contrast	Strain 22-2 – Strain 66	0.151	0.248	0.544	
Contrast	Strain 10-2 – Strain 66	0.277	0.250	0.270	
Contrast	Strain 54 – Strain 66	-0.518	0.266	0.054	
Contrast	Strain 198 – Strain 66	0.591	0.237	0.015	*
Contrast	Strain 174 – Strain 66	0.671	0.261	0.012	*
Contrast	Strain 178-1 – Strain 66	0.813	0.237	0.001	**
Contrast	Female – Male	0.091	0.091	0.321	
Contrast	Inf 2 – Inf 1	-0.599	0.089	$4.118*10^{-11}$	***
Contrast	Inf 3 – Inf 1	-0.490	0.090	$8.939*10^{-8}$	***
Contrast	Block B – Block A	0.395	0.099	$1.349*10^{-4}$	***
Slope	log10(*calreticulin*)	0.735	0.058	$2.2*10^{-16}$	***

[a] Categories of significance are as follows: * 0.05 > p > 0.01, ** 0.01 > p > 0.001, *** p < 0.001.

[b] Reference condition refers to engorged larvae from infestation 1 that fed on a male mouse in block A that was infected with *B. burgdorferi* strain 66. The value of the covariate log10(*calreticulin*) was set to 0.

Table S8. The means and EMMs of the LSL for each of the levels of the factors of interest. The LSL is the number of *23S rRNA* gene copies per infected engorged larva (i.e., uninfected larvae are excluded). The means are from the raw data, whereas the EMMs were calculated using the final simplified model in Table S6. The mean or EMM of a given level was averaged over the levels of the other factors. For each EMM, the values of log10 *calreticulin* copies per tick were set to 4.57. Mean 1, EMM1, are on the log10-transformed scale, whereas Mean 2 and EMM2 are on the original scale. LCL and UCL refer to the 95% lower and upper confidence limits reported on the same scale.

Factor	Level	Mean1	Mean 2	EMM1	LCL1	UCL1	EMM2	LCL2	UCL2
Strain	66	3.572	3731.1	3.381	2.992	3.769	2402.6	982.5	5875.0
Strain	57	3.698	4986.9	3.667	3.389	3.945	4644.0	2449.4	8804.9
Strain	150	3.107	1280.1	2.937	2.642	3.233	865.6	438.1	1710.3
Strain	167	3.565	3672.5	3.472	3.213	3.731	2966.2	1634.7	5382.2
Strain	126	3.571	3727.2	3.507	3.216	3.799	3214.3	1642.8	6289.3
Strain	22-2	3.522	3323.1	3.532	3.234	3.829	3403.3	1715.2	6753.0
Strain	10-2	3.532	3402.1	3.658	3.356	3.960	4548.9	2270.8	9112.2
Strain	54	3.120	1317.4	2.862	2.511	3.213	728.5	324.7	1634.5
Strain	198	3.924	8402.2	3.972	3.714	4.230	9379.0	5174.1	17001.1
Strain	174	4.008	10189.2	4.051	3.717	4.385	11254.3	5213.9	24292.8
Strain	178-1	4.194	15635.5	4.194	3.937	4.451	15635.5	8645.3	28277.6
Sex	Male	3.633	4293.4	3.521	3.395	3.647	3320.7	2483.0	4441.1
Sex	Female	3.715	5182.3	3.612	3.476	3.748	4094.7	2995.6	5597.0
Infestation	Inf 1	4.021	10501	3.930	3.771	4.088	8502.2	5906.7	12238.2
Infestation	Inf 2	3.325	2115.3	3.331	3.205	3.457	2142.2	1603.1	2862.5
Infestation	Inf 3	3.743	5538.3	3.440	3.317	3.563	2752.9	2073.8	3654.2
Block	A	3.271	1867.1	3.369	3.215	3.524	2340.9	1640.9	3339.6
Block	B	3.850	7071.7	3.764	3.649	3.880	5808.5	4451.9	7578.5

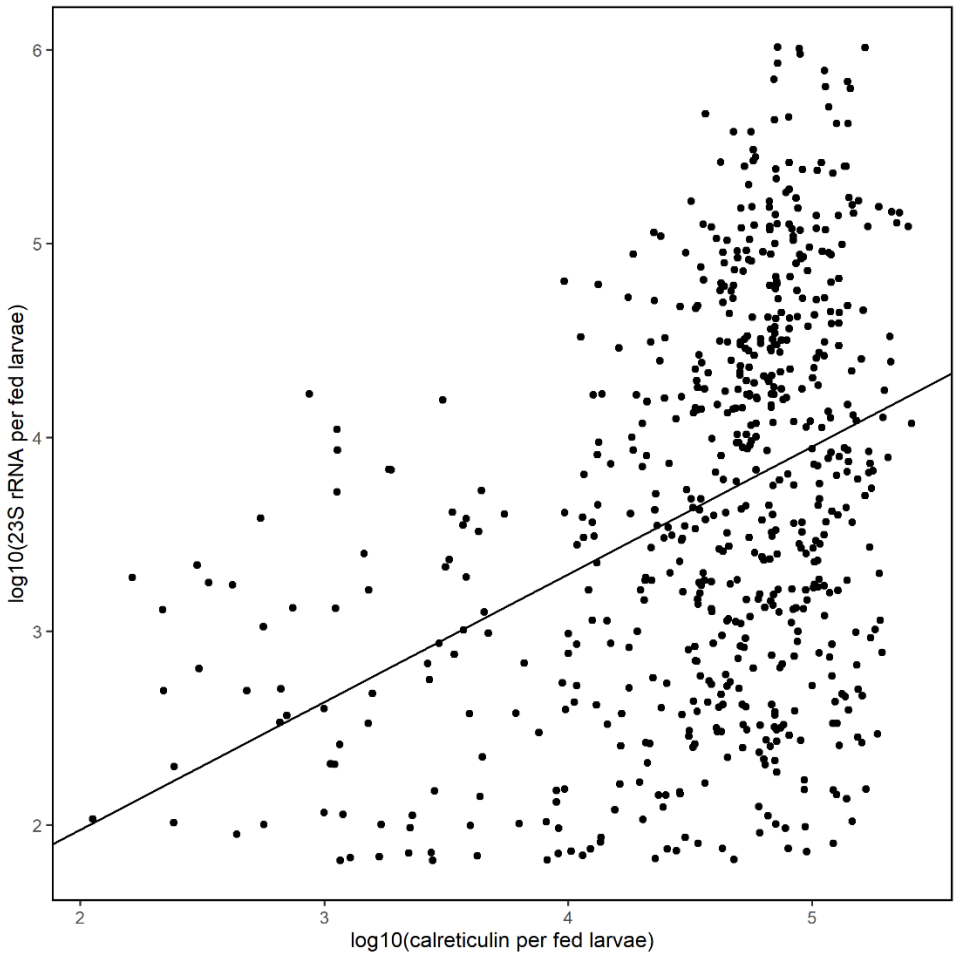

Figure S1. The larval spirochete load (LSL) in engorged larvae increased with the tick *calreticulin* load. The LSL was measured as the $\log_{10}$ *23S rRNA* copies per tick. The *calreticulin* load was measured as the $\log_{10}$ *calreticulin* copies per tick. Each point represents an individual infected engorged larva (n = 645). The line represents the simple linear regression (slope = 0.657, r = 0.38, p = $2.2*10^{-16}$).

Analysis of LSL standardized to *calreticulin*: In the previous analysis of LSL, the tick *calreticulin* gene copy number was included as a covariate. In the present analysis, the response variable was the ratio of *23S rRNA* gene copies per million tick *calreticulin* gene copies per tick (LSLCAL). This ratio was log10 transformed to standardize the residuals. As before, this analysis was performed on the subset of engorged larvae that were infected with *B. burgdorferi* (n = 645 engorged larvae) that fed on the subset of infected mice (n = 84 mice). The LSLCAL was modelled using an LMM. The fixed factors were strain (11 levels), mouse sex (2 levels: male, female), infestation (3 levels: infestation 1, infestation 2, infestation 3), and temporal block (2 levels: A and B). The full model included all the two-way and three-way interactions between strain, sex, and infestation. Temporal block was included as a main effect only. Mouse identity was included as a random factor. As before, the three-way interaction between strain, sex, and infestation was significant (p = 0.013), but none of the two-way interactions were significant

(Table S9). For simplicity, we interpreted the parameter estimates for the main effects model (i.e., all interactions were removed).

Strain ($p = 1.462*10^{-12}$), infestation ($p = 1.229*10^{-13}$), and temporal block ($p = 6.565*10^{-04}$), but not mouse sex ($p = 0.406$) had significant effects on the LSLCAL (Table S9). The parameter estimates for this final simplified model and their significance are shown in Table S10. The correlation in the parameter estimates of the 14 contrasts between Table S7 and Table S10 is positive and highly significant (r = 0.996, df = 12, t = 36.703, p = 1.073E-13). Thus, the results from these two analyses are very similar regardless of whether tick *calreticulin* gene copy number is included as an explanatory covariate in the analysis of the LSL (Table S6, S7) or in the denominator of the LSLCAL response variable (Table S9, Table S10).

Table S9. Model simplification of the LMM of the LSLCAL. Non-significant interactions were sequentially removed in order of increasing significance; the model was updated each time a term was removed. The final simplified model contained the fixed factors only. For each term, the order in which it was removed, the Chi-squared statistic (Chi), degrees of freedom (df), and p-value (p) are shown. For the non-significant interactions, the p-values are the ones in the model from which they were removed. For the included terms, the p-values are from the final simplified model.

Term	Order removed	Chi	df	p	Signif [a]
Strain:Sex:Infestation	1	35.141	19	0.013	*
Sex:Infestation	2	0.145	2	0.930	
Strain:Sex	3	8.022	10	0.627	
Strain:Infestation	4	26.595	20	0.147	
Strain	Final model	77.628	10	$1.462*10^{-12}$	***
Sex	Final model	0.692	1	0.406	
Infestation	Final model	59.454	2	$1.229*10^{-13}$	***
Temporal block	Final model	11.608	1	$6.565*10^{-4}$	***

[a] Categories of significance are as follows: * 0.05 > p > 0.01, ** 0.01 > p > 0.001, *** p < 0.001.

Table S10. Parameter estimates of the LMM of the LSLCAL. Factors include strain (11 levels), mouse sex (2 levels: male, female), and infestation (3 levels: infestation 1, infestation 2, infestation 3), temporal block (2 levels: A and B). For each parameter in the LMM, the type, description, estimate, standard error (SE), and p-value (p) are shown.

Parameter type	Parameter description	Estimate	SE	p	Signif [a]
Intercept	Reference [b]	4.986	0.229	$2.2*10^{-16}$	***
Contrast	Strain 57 – Strain 66	0.329	0.248	0.188	
Contrast	Strain 150 – Strain 66	-0.439	0.253	0.087	
Contrast	Strain 167 – Strain 66	0.141	0.242	0.563	
Contrast	Strain 126 – Strain 66	0.176	0.251	0.486	
Contrast	Strain 22-2 – Strain 66	0.203	0.254	0.426	

Contrast	Strain 10-2 – Strain 66	0.341	0.255	0.184	
Contrast	Strain 54 – Strain 66	-0.498	0.272	0.070	
Contrast	Strain 198 – Strain 66	0.662	0.242	0.008	**
Contrast	Strain 174 – Strain 66	0.724	0.266	0.008	**
Contrast	Strain 178-1 – Strain 66	0.872	0.242	0.001	**
Contrast	Female – Male	0.077	0.093	0.409	
Contrast	Inf 2 – Inf 1	-0.622	0.090	$1.418*10^{-11}$	***
Contrast	Inf 3 – Inf 1	-0.619	0.087	$3.836*10^{-12}$	***
Contrast	Block B – Block A	0.341	0.100	0.001	**

[a] Categories of significance are as follows: * 0.05 > p > 0.01, ** 0.01 > p > 0.001, *** p < 0.001.

[b] Reference condition refers to engorged larvae from infestation 1 that fed on a male mouse in block A that was infected with *B. burgdorferi* strain 66.

Section 5 – Analyses of the nymphal infection prevalence (NIP)

GLMM of NIP: The nymphal infection prevalence (NIP) is the proportion of unfed nymphs infected with *B. burgdorferi*. The analysis of the NIP was performed on all the unfed nymphs (n = 2471 unfed nymphs) that fed as larvae on the subset of infected mice (n = 84 mice). The response variable was the infection status for each nymph as measured by *23S rRNA* qPCR. This binomial response variable (0 = uninfected, 1 = infected) was modelled using a GLMM with binomial errors. The fixed factors were strain (11 levels), mouse sex (2 levels: male, female), infestation (3 levels: infestation 1, infestation 2, infestation 3), and temporal block (2 levels: A and B). The full model included all the two-way and the three-way interactions between strain, sex, and infestation. Temporal block was included as a main effect only. Mouse identity was included as a random factor. Non-significant, or non-functional interaction terms were removed sequentially (Table S11). Significant interactions were removed if they had standard errors that were orders of magnitude greater than the parameter estimates. Such problem interactions usually have marginally significant p-values (i.e., 0.01 < p < 0.05). Retention of such problem interactions in the model results in biased estimates of the EMMs.

The interaction between strain and sex (p = 0.022) and between strain and infestation (p = 0.017) were examples of problem interactions. Although these interactions were both statistically significant according to the Wald chi-square tests, inspection of the parameter estimates found that the contrasts for some strains had standard errors that were an order of magnitude larger than the parameter estimates. For this reason, these interactions were removed from the model. The final simplified model included the main effects and the interaction between sex and infestation (Table S11). The interaction between sex and infestation had a significant effect on the NIP ($p = 1.57*10^{-4}$). Strain ($p = 1.835*10^{-14}$), mouse sex ($p = 9.76*10^{-4}$), infestation ($p = 2.2*10^{-16}$), but not temporal block (p = 0.568) had significant effects on the NIP (Table S11).

The parameter estimates for the final simplified model and their significance are shown in Table S12. The mean NIP for the levels of a given factor were calculated from the raw data by averaging over the other levels (Table S13). Estimated marginal means (EMMs) of NIP were

generated for each factor level using the ggemmeans() function and the final simplified model (Table S13). The means from the raw data and the EMMs were similar (Table S13). The Pearson correlation between the means and the EMMs of the NIP across the 24 levels was positive and significant (Mean vs EMM in Table S13; r = 0.953, t = 14.806, df = 22, p = $6.379*10^{-13}$). In what follows, we present the EMMs of the NIP and their post-hoc tests (Table S13).

Among strains of *B. burgdorferi* and averaged across mouse sex, infestation, and block, the EMM NIP ranged from 57.53% for strain 66 to 99.46% for strain 178-1. All strains, except strain 54, had a significantly higher NIP compared to reference strain 66 (Table S12). Averaged across *B. burgdorferi* strains, infestation, and block, the EMM NIP for male mice (95.30%) was higher compared to female mice (93.19%), but this difference was not significant (p = 0.157). Averaged across *B. burgdorferi* strains, mouse sex, and block, the EMM NIP for infestation 1 (98.85%) was significantly higher compared to infestation 2 (90.18%; p < 0.0001) and infestation 3 (85.40%; p < 0.0001). The EMM NIP for block B (94.71%) was similar to block A (93.94%; p = 0.565).

The interaction between sex and infestation refers to the fact that the difference in NIP between males and females changes over the successive infestations (Figure 2 in the main manuscript). For infestation 1, males have a lower EMM NIP compared to females (98.29% vs 99.23%, p = 0.095) but the difference is not significant. Males have a significantly higher NIP compared to females for infestation 2 (93.22% vs 86.00%, p = 0.008) and infestation 3 (91.33% vs 76.45%, p < 0.0001).

The relationship between NIP and infestation is shown for each of the 11 *B. burgdorferi* strains in Figure 3.1 in the main manuscript and in Figure S2. In this study, the NIP is synonymous with host-to-tick transmission (HTT), but the latter term has as stronger connotation of being a pathogen life history trait. For this reason, the NIP is labelled as host-to-tick transmission (HTT) in Figure S2. Figure S2 shows the estimated marginal means and their 95% confidence intervals that were calculated for the 33 combinations of strain and infestation using the final simplified model and the ggemmeans() function.

Table S11. Model simplification of the GLMM of the NIP. Non-significant interactions were sequentially removed in order of increasing significance; the model was updated each time a term was removed. Significant interactions were removed if they had standard errors that were orders of magnitude greater than the parameter estimates. The final simplified model contained the fixed factors and the interaction of sex and infestation. For each term, the order in which it was removed, the Chi-squared statistic (Chi), degrees of freedom (df), and p-value (p) are shown. For the non-significant interactions, the p-values are the ones in the model from which they were removed. For the included terms, the p-values are from the final simplified model.

Term	Order removed	Chi	df	p	Signif [a]
Strain:Sex:Infestation	1	17.386	20	0.628	
Strain:Sex	2	20.847	10	0.022	*
Strain:Infestation	3	35.616	20	0.017	*
Sex:Infestation	Final model	17.520	2	$1.57*10^{-4}$	***
Strain	Final model	87.300	10	$1.835*10^{-14}$	***

Sex	Final model	10.873	1	$9.76*10^{-4}$	***
Infestation	Final model	111.972	2	$2.2*10^{-16}$	***
Temporal block	Final model	0.326	1	0.568	

[a] Categories of significance are as follows: * 0.05 > p > 0.01, ** 0.01 > p > 0.001, *** p < 0.001.

Table S12. Parameter estimates of the GLMM of the NIP. Factors include strain (11 levels), mouse sex (2 levels: male, female), infestation (3 levels: infestation 1, infestation 2, infestation 3), and temporal block (2 levels: A and B). For each parameter in the GLMM, the type, description, estimate, standard error (SE), and p-value (p) are shown.

Parameter type	Parameter description	Estimate	SE	p	Signif [a]
Intercept	Reference [b]	1.471	0.449	0.001	**
Contrast	Strain 57 – Strain 66	2.826	0.559	$4.336*10^{-7}$	***
Contrast	Strain 150 – Strain 66	2.252	0.537	$2.783*10^{-5}$	***
Contrast	Strain 167 – Strain 66	2.059	0.529	$9.906*10^{-5}$	***
Contrast	Strain 126 – Strain 66	2.508	0.541	$3.485*10^{-6}$	***
Contrast	Strain 22-2 – Strain 66	1.641	0.535	0.002	**
Contrast	Strain 10-2 – Strain 66	2.185	0.532	$4.041*10^{-5}$	***
Contrast	Strain 54 – Strain 66	0.741	0.508	0.144	
Contrast	Strain 198 – Strain 66	3.585	0.602	$2.666*10^{-9}$	***
Contrast	Strain 174 – Strain 66	4.902	0.945	$2.104*10^{-7}$	***
Contrast	Strain 178-1 – Strain 66	4.906	0.779	$3.043*10^{-10}$	***
Contrast	Female – Male	0.805	0.483	0.095	
Contrast	Inf 2 – Inf 1	-1.432	0.291	$8.405*10^{-7}$	***
Contrast	Inf 3 – Inf 1	-1.698	0.286	$2.902*10^{-9}$	***
Contrast	Block B – Block A	0.145	0.253	0.565	
Contrast	Female Inf 2 – Male Inf 1	-1.611	0.477	0.001	**
Contrast	Female Inf 3 – Male Inf 1	-1.982	0.475	$2.950*10^{-5}$	***

[a] Categories of significance are as follows: * 0.05 > p > 0.01, ** 0.01 > p > 0.001, *** p < 0.001.

[b] Reference condition refers to engorged larvae from infestation 1 that fed on a male mouse in block A that was infected with *B. burgdorferi* strain 66.

Table S13. The means and EMMs of the NIP for each of the levels of the factors of interest. The NIP is the percentage of unfed nymphs infected with *B. burgdorferi* (these nymphs took their larval blood meal from the experimentally infected mice). The means are from the raw data, whereas the EMMs were calculated using the final simplified model in Table S11. The mean or EMM of a given level was averaged over the levels of the other factors. Lower and upper (LCL, UCL) 95% confidence limits for the EMM are reported. For factors with significant interactions, the means and EMMs are reported for the relevant combinations of factors.

Factor	Level	Mean (%)	EMM (%)	LCL (%)	UCL (%)
Strain	66	54.29	57.53	39.63	73.65
Strain	57	92.17	95.81	90.86	98.13
Strain	150	85.77	92.79	85.58	96.54
Strain	167	83.40	91.39	83.31	95.76
Strain	126	88.98	94.33	88.37	97.33
Strain	22-2	77.88	87.49	76.47	93.76
Strain	10-2	86.27	92.33	84.92	96.26
Strain	54	67.39	73.98	58.77	85.00
Strain	198	95.42	97.99	95.02	99.21
Strain	174	98.67	99.45	97.05	99.90
Strain	178-1	98.73	99.46	97.93	99.86
Sex	Male	87.78	95.30	93.00	96.87
Sex	Female	80.71	93.19	89.96	95.44
Infestation	Inf 1	96.28	98.85	98.09	99.31
Infestation	Inf 2	81.30	90.18	86.71	92.82
Infestation	Inf 3	75.15	85.40	80.81	89.04
Block	A	83.68	93.94	91.25	95.84
Block	B	85.01	94.71	92.17	96.47
Sex:Inf	Male & Inf 1	94.85	98.29	96.90	99.06
Sex:Inf	Male & Inf 2	85.75	93.22	89.50	95.68
Sex:Inf	Male & Inf 3	82.62	91.33	86.93	94.34
Sex:Inf	Female & Inf 1	97.78	99.23	98.34	99.65
Sex:Inf	Female & Inf 2	76.72	86.00	80.05	90.38
Sex:Inf	Female & Inf 3	67.10	76.45	68.30	83.03

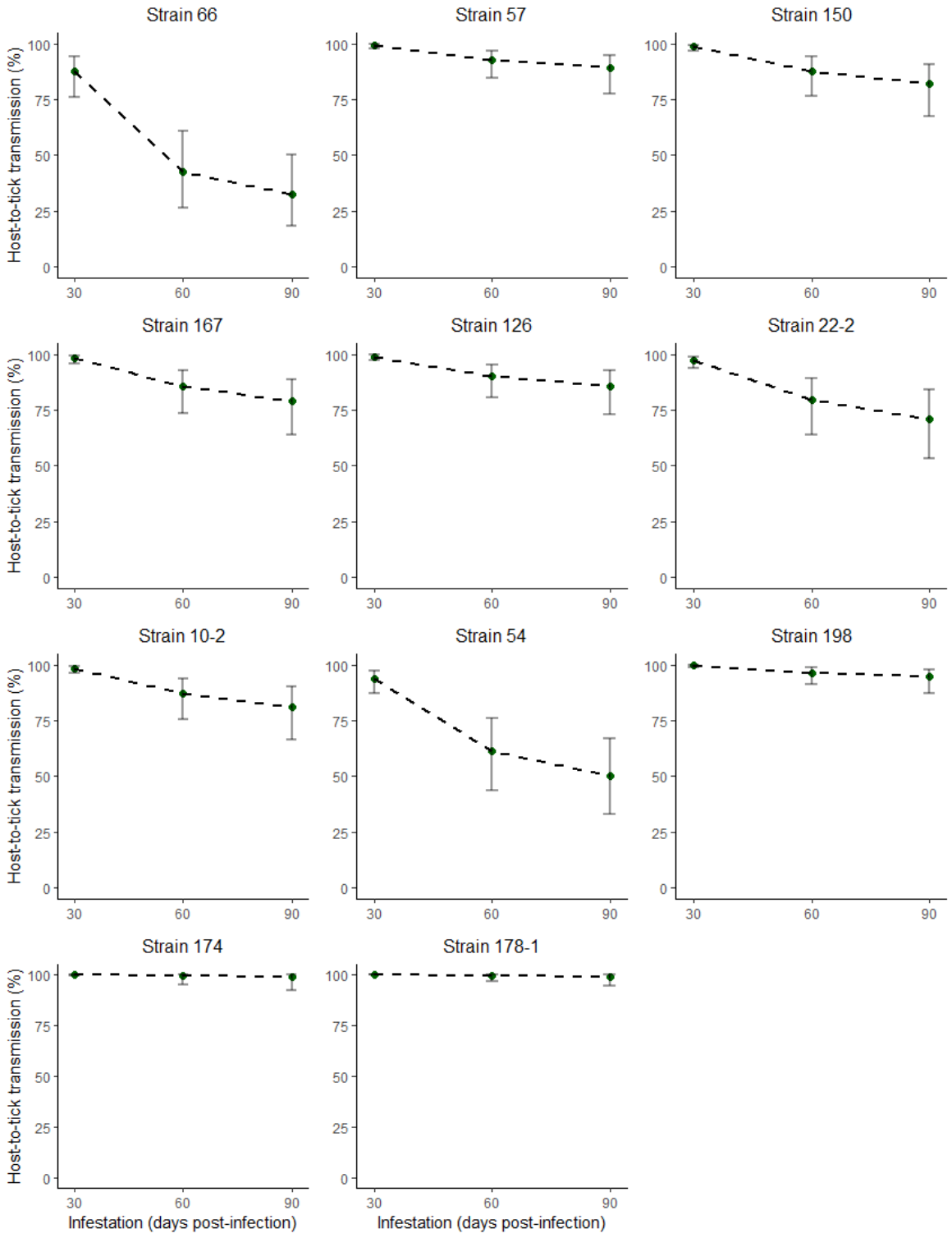

Figure S2. The lifetime host-to-tick transmission (HTT) of *B. burgdorferi* from infected mice to immature *I. scapularis* ticks decreased over the 3 successive larval infestations for some strains but remained constant over time for other strains. For this reason, the 2-way interaction between strain and infestation was significant (p = 0.017). Lifetime HTT was measured by infesting mice

with *I. scapularis* larvae on 3 occasions (days 30, 60, and 90 post-infection), allowing the engorged larvae to moult into nymphs, and testing the nymphs for infection with *B. burgdorferi*. The mean values (green circles) for each infestation are the EMMs from the GLMM for the HTT of each strain over time. Error bars are the 95% confidence intervals for the EMMs.

Section 6 – Analyses of the nymphal spirochete load (NSL)

LMM of the NSL: The nymphal spirochete load (NSL) is the number of *23S rRNA* copies per infected unfed nymph. The analysis of the NSL was performed on the subset of unfed nymphs that were infected with *B. burgdorferi* (n = 2,084 infected unfed nymphs) and that fed on the subset of infected mice (n = 84 mice). The NSL was log10-transformed to normalize the residuals. The $\log_{10}$ *23S rRNA* copies per unfed nymph was modelled using an LMM. The fixed factors were strain (11 levels), mouse sex (2 levels: male, female), infestation (3 levels: infestation 1, infestation 2, infestation 3), and temporal block (2 levels: A and B). The full model included all the two-way and the three-way interactions between strain, sex, and infestation. Temporal block was included as a main effect only. Mouse identity was included as a random factor. Non-significant interactions ($p > 0.05$) were removed sequentially (Table S14).

The final simplified model included the main effects and the interactions between strain and infestation, and sex and infestation (Table S14). The interaction between strain and infestation ($p = 0.0001$) and the interaction between sex and infestation ($p = 0.026$) both had significant effect on the NSL. Strain ($p = 2.2*10^{-16}$) and infestation ($p = 1.01*10^{-11}$), but not mouse sex ($p = 0.988$) and temporal block ($p = 0.182$), had significant effects on the NSL (Table S14).

The parameter estimates for this final simplified model and their significance are shown in Table S15. Means and EMMs (using the final model and the ggemmeans() function) of the NSL were generated for each factor level (Table S16). As there were significant interactions between strain and infestation, and sex and infestation, EMMs for the combinations of these factors were also estimated (Table S16). The means from the raw data and the EMMs were similar (Table S16). The Pearson correlation between the means and the EMMs of the NSL across the 57 levels was positive and significant (Mean1 vs EMM1 in Table S16; $r = 0.997$, $t = 102.32$, $df = 55$, $p < 2.2*10^{-16}$). The units of the NSL are the number of *23S rRNA* gene copies per infected unfed nymph. In what follows, we present the EMMs of the NSL and their post-hoc tests (EMM2 in Table S16).

The EMM NSL varied 8.9-fold among strains from 7665.2 units for strain 66 to 68086.7 units for strain 174. All the strains had a higher NSL compared to reference strain 66 (Table S15). The EMM NSL of infestation 1 (29631.2 units) was 59.5% higher compared to infestation 2 (18580.3 units; $p < 0.0001$) and 86.0% higher compared to infestation 3 (15934.6 units; $p < 0.0001$). The interaction between strain and infestation indicated that the NSL changed over the three infestations for some strains, but not for others (Figure S3).

Nymphs that had fed as larvae on male mice had an EMM NSL (20936.3 units) that was 3.0% higher compared to nymphs that had fed as larvae on female mice (20317.1 units), but this difference was not significant ($p = 0.768$). The interaction between sex and infestation refers to the fact that the difference in NSL between males and females changes over the successive

infestations. For infestation 1, males have a lower EMM NSL compared to females (26270.5 vs 33421.9), but males have a higher EMM NSL compared to females for infestation 2 (19525.2 vs 17681.1) and infestation 3 (17891.0 vs 14192.1). Finally, the EMM NSL of larvae in block B (22017.2 units) was similar compared to block A (19319.7 units; p = 0.198).

Table S14. Model simplification of the LMM of the NSL. Non-significant interactions were sequentially removed in order of increasing significance; the model was updated each time a term was removed. For each term, the order in which it was removed, the Chi-squared statistic (Chi), degrees of freedom (df), and p-value (p) are shown. For the non-significant interactions, the p-values are the ones in the model from which they were removed. For the included terms, the p-values are from the final simplified model.

Term	Order removed	Chi	df	p	Signif [a]
Strain:Sex:Infestation	1	23.840	20	0.249	
Strain:Sex	2	4.014	10	0.947	
Sex:Infestation	Final model	7.318	2	0.026	*
Strain:Infestation	Final model	53.213	20	$7.561*10^{-5}$	***
Strain	Final model	215.753	10	$2.2*10^{-16}$	***
Sex	Final model	$1.0*10^{-4}$	1	0.992	
Infestation	Final model	50.887	2	$8.914*10^{-12}$	***
Temporal block	Final model	1.692	1	0.193	

[a] Categories of significance are as follows: * 0.05 > p > 0.01, ** 0.01 > p > 0.001, *** p < 0.001.

Table S15. Parameter estimates of the LMM of the NSL. Factors include strain (11 levels), mouse sex (2 levels: male, female), infestation (3 levels: infestation 1, infestation 2, infestation 3), and temporal block (2 levels: A and B). For each parameter in the LMM, the type, description, estimate, standard error (SE), and p-value (p) are shown.

Parameter type	Parameter description	Estimate	SE	p	Signif [a]
Intercept	Reference [b]	3.831	0.114	$2.2*10^{-16}$	***
Contrast	Strain 57 – Strain 66	0.236	0.145	0.104	
Contrast	Strain 150 – Strain 66	0.333	0.144	0.021	
Contrast	Strain 167 – Strain 66	0.440	0.144	0.002	
Contrast	Strain 126 – Strain 66	0.522	0.145	$3.812*10^{-4}$	***
Contrast	Strain 22-2 – Strain 66	0.665	0.143	$5.723*10^{-6}$	***
Contrast	Strain 10-2 – Strain 66	0.660	0.144	$7.061*10^{-6}$	***
Contrast	Strain 54 – Strain 66	0.656	0.145	$9.412*10^{-6}$	***
Contrast	Strain 198 – Strain 66	0.815	0.144	$4.130*10^{-8}$	***
Contrast	Strain 174 – Strain 66	1.012	0.161	$1.645*10^{-9}$	***
Contrast	Strain 178-1 – Strain 66	0.823	0.144	$3.186*10^{-8}$	***
Contrast	Female – Male	0.105	0.059	0.079	
Contrast	Inf 2 – Inf 1	-0.122	0.162	0.451	

Contrast	Inf 3 – Inf 1	0.217	0.191	0.256	
Contrast	Block B – Block A	0.057	0.044	0.198	
Contrast	57 Inf 2 - 66 Inf 1	0.009	0.199	0.965	
Contrast	150 Inf 2 - 66 Inf 1	-0.316	0.199	0.112	
Contrast	167 Inf 2 - 66 Inf 1	-0.101	0.203	0.618	
Contrast	126 Inf 2 - 66 Inf 1	0.115	0.200	0.566	
Contrast	22-2 Inf 2 - 66 Inf 1	-0.230	0.202	0.255	
Contrast	10-2 Inf 2 - 66 Inf 1	-0.157	0.201	0.436	
Contrast	54 Inf 2 - 66 Inf 1	-0.039	0.214	0.854	
Contrast	198 Inf 2 - 66 Inf 1	0.287	0.198	0.148	
Contrast	174 Inf 2 - 66 Inf 1	0.202	0.217	0.350	
Contrast	178-1 Inf 2 - 66 Inf 1	0.157	0.197	0.427	
Contrast	57 Inf 3 - 66 Inf 1	-0.254	0.226	0.261	
Contrast	150 Inf 3 - 66 Inf 1	-0.635	0.228	0.005	**
Contrast	167 Inf 3 - 66 Inf 1	-0.532	0.226	0.019	*
Contrast	126 Inf 3 - 66 Inf 1	-0.558	0.226	0.014	*
Contrast	22-2 Inf 3 - 66 Inf 1	-0.610	0.241	0.011	*
Contrast	10-2 Inf 3 - 66 Inf 1	-0.390	0.226	0.085	
Contrast	54 Inf 3 - 66 Inf 1	-0.746	0.237	0.002	**
Contrast	198 Inf 3 - 66 Inf 1	-0.015	0.222	0.947	
Contrast	174 Inf 3 - 66 Inf 1	-0.393	0.239	0.099	
Contrast	178-1 Inf 3 - 66 Inf 1	-0.093	0.222	0.674	
Contrast	Female Inf 2 – Male Inf 1	-0.148	0.077	0.055	
Contrast	Female Inf 3 – Male Inf 1	-0.205	0.080	0.011	*

[a] Categories of significance are as follows: * 0.05 > p > 0.01, ** 0.01 > p > 0.001, *** p < 0.001.

[b] Reference condition refers to engorged larvae from infestation 1 that fed on a male mouse in block A that was infected with *B. burgdorferi* strain 66.

Table S16. The means and EMMs of the NSL for each of the levels of the factors of interest. The NSL is the number of *23S rRNA* gene copies per infected unfed nymph (i.e., uninfected nymphs are excluded). The means are from the raw data, whereas the EMMs were calculated using the final simplified model in Table S14. The mean or EMM of a given level was averaged over the levels of the other factors. Mean 1 and EMM1 are on the log10-transformed scale, whereas Mean 2 and EMM2 are on the original scale. For factors with significant interactions, the means and EMMs are reported for the relevant combinations of factors. LCL and UCL represent the lower and upper 95% confidence intervals reported on the same scale.

Factor	Level	Mean1	Mean2	EMM1	LCL1	UCL1	EMM2	LCL2	UCL2
Strain	66	3.887	7707.3	3.885	3.706	4.063	7665.2	5077.9	11570.8

Strain	57	4.041	10997.7	4.038	3.903	4.173	10922.1	8002.4	14907.1
Strain	150	3.951	8929.6	3.901	3.764	4.038	7960.8	5801.5	10923.7
Strain	167	4.141	13843.4	4.113	3.975	4.251	12976.4	9448.0	17822.5
Strain	126	4.274	18795.0	4.259	4.123	4.394	18136.8	13285.0	24760.6
Strain	22-2	4.342	21994.3	4.269	4.120	4.418	18580.4	13180.9	26191.6
Strain	10-2	4.382	24110.7	4.363	4.225	4.500	23041.9	16801.2	31600.8
Strain	54	4.346	22162.0	4.279	4.128	4.430	19010.0	13414.6	26939.2
Strain	198	4.790	61632.0	4.790	4.658	4.922	61645.9	45500.1	83521.1
Strain	174	4.827	67141.7	4.833	4.667	4.999	68086.7	46477.6	99742.5
Strain	178-1	4.730	53671.0	4.729	4.598	4.860	53600.9	39619.3	72516.6
Sex	Male	4.344	22083.3	4.321	4.262	4.380	20936.3	18265.1	23998.2
Sex	Female	4.364	23105.4	4.308	4.244	4.372	20317.1	17535.0	23540.7
Inf	Inf 1	4.468	29370.4	4.472	4.413	4.530	29631.2	25896.7	33904.4
Inf	Inf 2	4.293	19617.5	4.269	4.205	4.333	18580.3	16028.6	21538.3
Inf	Inf 3	4.269	18578.1	4.202	4.132	4.272	15934.6	13566.0	18716.7
Block	A	4.337	21702.8	4.286	4.225	4.347	19319.7	16790.1	22230.3
Block	B	4.370	23444.7	4.343	4.281	4.405	22017.2	19099.0	25381.4
Sex:Inf	Male & Inf 1	4.424	26525.1	4.419	4.338	4.501	26270.5	21774.6	31694.7
Sex:Inf	Male & Inf 2	4.316	20693.1	4.291	4.204	4.377	19525.2	16004.5	23820.5
Sex:Inf	Male & Inf 3	4.280	19075.1	4.253	4.164	4.341	17891.0	14582.1	21950.8
Sex:Inf	Female & Inf 1	4.513	32587.7	4.524	4.441	4.607	33421.9	27592.6	40482.7
Sex:Inf	Female & Inf 2	4.266	18449.4	4.248	4.154	4.341	17681.1	14268.1	21910.6
Sex:Inf	Female & Inf 3	4.254	17937.3	4.152	4.048	4.256	14192.1	11163.7	18041.9
Strain:Inf	Strain 66 & Inf 1	3.908	8083.4	3.912	3.699	4.124	8157.9	5006.1	13294.2
Strain:Inf	Strain 66 & Inf 2	3.748	5600.5	3.716	3.449	3.983	5194.5	2808.8	9606.7
Strain:Inf	Strain 66 & Inf 3	4.054	11331.2	4.026	3.693	4.360	10627.8	4935.1	22887.1
Strain:Inf	Strain 57 & Inf 1	4.147	14015.1	4.147	3.959	4.335	14033.0	9106.7	21624.3
Strain:Inf	Strain 57 & Inf 2	3.953	8964.9	3.960	3.768	4.152	9116.1	5860.7	14179.8
Strain:Inf	Strain 57 & Inf 3	4.016	10378.1	4.008	3.805	4.211	10185.0	6379.5	16260.4
Strain:Inf	Strain 150 & Inf 1	4.247	17669.5	4.245	4.060	4.430	17575.2	11478.6	26909.9
Strain:Inf	Strain 150 & Inf 2	3.755	5687.4	3.733	3.540	3.926	5411.8	3470.0	8440.3
Strain:Inf	Strain 150 & Inf 3	3.778	5998.2	3.725	3.508	3.941	5304.2	3220.9	8735.1
Strain:Inf	Strain 167 & Inf 1	4.356	22724.6	4.351	4.166	4.537	22449.8	14652.0	34397.7
Strain:Inf	Strain 167 & Inf 2	4.062	11541.3	4.054	3.846	4.262	11321.8	7016.3	18269.2
Strain:Inf	Strain 167 & Inf 3	3.950	8911.9	3.934	3.730	4.139	8596.7	5369.1	13764.6
Strain:Inf	Strain 126 & Inf 1	4.425	26617.8	4.433	4.244	4.622	27124.0	17556.0	41906.4
Strain:Inf	Strain 126 & Inf 2	4.352	22472.0	4.352	4.160	4.544	22487.6	14450.7	34994.2
Strain:Inf	Strain 126 & Inf 3	4.005	10126.0	3.990	3.788	4.193	9781.1	6133.5	15598.1
Strain:Inf	Strain 22-2 & Inf 1	4.576	37690.0	4.576	4.392	4.760	37690.0	24666.1	57590.7
Strain:Inf	Strain 22-2 & Inf 2	4.153	14214.6	4.150	3.942	4.358	14125.7	8748.7	22807.5

Strain:Inf	Strain 22-2 & Inf 3	4.138	13754.8	4.081	3.815	4.347	12048.3	6527.3	22239.1
Strain:Inf	Strain 10-2 & Inf 1	4.572	37294.8	4.572	4.386	4.758	37306.2	24316.2	57235.6
Strain:Inf	Strain 10-2 & Inf 2	4.227	16868.5	4.219	4.016	4.421	16556.3	10386.8	26390.1
Strain:Inf	Strain 10-2 & Inf 3	4.299	19898.9	4.297	4.090	4.503	19806.7	12314.8	31856.3
Strain:Inf	Strain 54 & Inf 1	4.566	36841.7	4.568	4.378	4.758	36982.2	23889.2	57251.2
Strain:Inf	Strain 54 & Inf 2	4.342	21953.8	4.333	4.088	4.577	21506.9	12237.5	37797.4
Strain:Inf	Strain 54 & Inf 3	3.941	8739.1	3.936	3.692	4.181	8637.2	4918.1	15168.8
Strain:Inf	Strain 198 & Inf 1	4.725	53032.8	4.726	4.540	4.912	53232.7	34695.1	81675.0
Strain:Inf	Strain 198 & Inf 2	4.821	66169.0	4.817	4.626	5.008	65664.9	42314.5	101900.6
Strain:Inf	Strain 198 & Inf 3	4.826	67018.9	4.826	4.640	5.012	67019.5	43677.0	102836.8
Strain:Inf	Strain 174 & Inf 1	4.906	80629.1	4.924	4.689	5.159	83907.0	48819.6	144212.1
Strain:Inf	Strain 174 & Inf 2	4.929	84823.0	4.930	4.695	5.165	85148.7	49534.1	146369.6
Strain:Inf	Strain 174 & Inf 3	4.650	44626.5	4.645	4.412	4.879	44178.4	25807.7	75626.1
Strain:Inf	Strain 178-1 & Inf 1	4.737	54541.9	4.735	4.548	4.922	54334.2	35335.2	83548.5
Strain:Inf	Strain 178-1 & Inf 2	4.697	49820.3	4.696	4.510	4.882	49655.4	32363.3	76187.0
Strain:Inf	Strain 178-1 & Inf 3	4.755	56907.9	4.756	4.571	4.942	57078.9	37201.5	87577.1

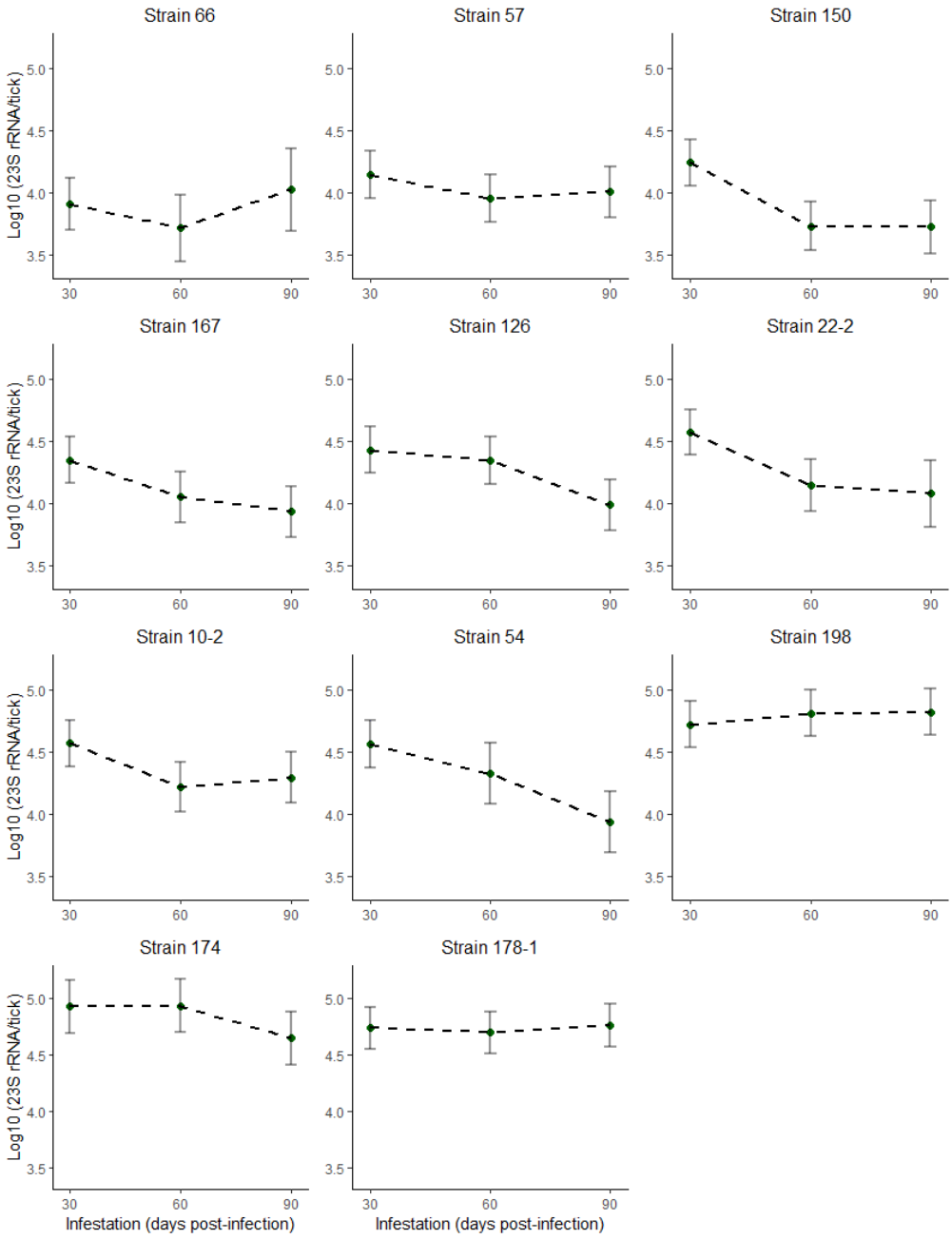

Figure S3. The nymphal spirochete load (NSL) of *B. burgdorferi* from infected mice to immature *I. scapularis* ticks decreased over the 3 successive larval infestations for some strains but remained constant or increased over time for other strains. For this reason, the 2-way interaction between strain and infestation was significant ($p = 7.561*10^{-5}$). NSL was measured by infesting mice with *I. scapularis* larvae on 3 occasions (days 30, 60, and 90 post-infection), allowing the engorged larvae to moult into nymphs, and testing the nymphs for infection with *B. burgdorferi* and measuring the abundance of the *B. burgdorferi 23S rRNA* gene in each tick. The mean values (green circles) for each infestation are the EMMs from the LMM for the NSL of each strain over time. Error bars are the 95% confidence intervals for the EMMs.

Section 7 – Relationship between laboratory estimates of HTT and strain frequencies observed in nature.

Frequency of *B. burgdorferi* strains in *I. scapularis* ticks in North America: The estimates of the frequencies of the *B. burgdorferi* strains in *I. scapularis* tick populations were described previously (Zinck et al., 2022). Briefly, two previous studies determined the frequencies of *B. burgdorferi* MLSTs in questing *I. scapularis* ticks collected in the USA and Canada (Ogden et al., 2011; Travinsky et al., 2010). These two studies combined contained 9 of the 11 strains (8 of 10 MLST types) in the present study. Strains 66 and 54, which corresponded to MLSTs 237 and 741, were not detected, and were therefore assigned counts of zero. To determine the frequency of each strain in our set of 10 unique MLSTs, we expressed these counts as a proportion of the total number of entries for our strains (Table S17).

Estimate of abundance of *B. burgdorferi* in mouse tissues for strains of *B. burgdorferi*: We previously generated 3 estimates for abundance in the mouse tissues for the 11 strains of *B. burgdorferi* (Zinck et al., 2022). The estimate used in these analyses was the mean spirochete load in the subset of infected mouse tissues at necropsy (n = 333). For each strain, these estimates were calculated across the 2 sexes and the 7 tissue types. The spirochete load was measured as the number of *23S rRNA* gene copies per 10^6 mouse *Beta-actin* gene copies; this variable was log10-transformed to normalize the residuals (Table S17).

Estimates of LIP and NIP: For both the larval infection prevalence (LIP) and the nymphal infection prevalence (NIP), mean values were weighted by infestation to account for the significant differences in infection prevalence between infestation times (Table S5, Table S13). Mean infection prevalence was calculated using all ticks that had fed on infected mice (infected mice: n = 84, engorged larvae: n = 950, unfed nymphs: n = 2,471) by first averaging by infestation, and then taking the average of these values (Table S17).

Estimates of abundance of *B. burgdorferi* in larvae and nymphs: For both measures of abundance, mean values for each strain were generated by averaging the abundance of *B. burgdorferi* in the subset of positively infected ticks (*23S rRNA* copies/tick; engorged larvae: n = 645, unfed nymphs: n = 2,084). The spirochete loads were log10-transformed to normalize the residuals (Table S17).

Table S17. Six variables for the 11 strains of *B. burgdorferi*. The 11 *B. burgdorferi* strains and their multi-locus sequence types (MLST) are shown. The number of mice, larvae, and nymphs over which the strain-specific variables were calculated are also shown. The six variables include mouse tissue spirochete load (MTSL), larval infection prevalence (LIP), larval spirochete load (LSL), nymphal infection prevalence (NIP), nymphal spirochete load (NSL), and the frequencies of the strains in *I. scapularis* populations in Canada and the USA (Nat Freq). The standard error for each estimate is given in brackets.

Strain	MLST	Mice	Larvae	Nymphs	MTSL	LIP (%)	LSL	NIP (%)	NSL	Nat Freq (%)
66	237	7	77	210	2.427 (0.104)	38.77 (10.09)	3.572 (0.107)	54.29 (5.32)	3.887 (0.057)	0.00 (0.00)
57	29	8	90	230	2.78 (0.094)	78.78 (7.56)	3.698 (0.104)	92.14 (3.05)	4.041 (0.046)	11.55 (2.02)
150	19	8	94	239	3.041 (0.112)	71.71 (5.25)	3.107 (0.077)	85.71 (3.32)	3.951 (0.051)	9.56 (1.86)
167	12	8	106	241	2.929 (0.094)	72.92 (6.92)	3.565 (0.095)	83.35 (3.84)	4.141 (0.054)	2.79 (1.04)
126	43	8	90	236	2.746 (0.109)	70.64 (7.86)	3.571 (0.104)	89.14 (3.08)	4.274 (0.049)	3.98 (1.23)
22-2	55	8	83	226	2.897 (0.082)	66.57 (8.62)	3.522 (0.106)	76.52 (3.66)	4.342 (0.054)	1.99 (0.88)
10-2	32	8	74	233	2.981 (0.102)	76.8 (8.04)	3.532 (0.118)	86.19 (3.46)	4.382 (0.048)	25.9 (2.77)
54	741	8	93	230	2.588 (0.089)	43.08 (7.26)	3.12 (0.096)	67.14 (4.73)	4.346 (0.05)	0.00 (0.00)
198	3	8	96	240	3.085 (0.101)	88.52 (4.08)	3.924 (0.103)	95.42 (2.22)	4.79 (0.043)	37.45 (3.05)
174	37	5	58	150	3.059 (0.148)	84.52 (5.64)	4.008 (0.14)	98.67 (1.32)	4.827 (0.052)	6.77 (1.59)
178-1	3	8	89	236	3.015 (0.096)	96.11 (2.67)	4.194 (0.119)	98.74 (1.01)	4.73 (0.05)	37.45 (3.05)
		84	950	2471						

Relationships between the six strain-specific variables: There were a total of 6 strain-specific variables: (1) mouse tissue spirochete load (MTSL), (2) larval spirochete load (LSL), (3) larval infection prevalence (LIP), (4) nymphal spirochete load (NSL), (5) nymphal infection prevalence (NIP), and (6) frequency in nature. The relationship was investigated for each of the 15 pairs of variables. For many pairs of variables, the sequence of events in the study allowed us to specify a relationship of functional dependence. For example, the ticks fed on the mice, and we therefore assume that the tick phenotypes (LSL, LIP, NSL, and NIP) depend on the mouse tissue spirochete loads. Similarly, the larvae moulted into nymphs, and we therefore assume that the nymphal phenotypes (NSL and NIP) depend on the larval phenotypes (LSL and LIP). As we wanted to test whether our laboratory estimates of strain performance could predict the frequencies of strains in nature, the latter are dependent on the former. If the dependent variable (or response variable) was normally distributed (e.g., LSL, NSL), a simple linear regression was used. If the dependent variable (or response variable) was binomially distributed (e.g., LIP, NIP, natural frequency), a generalized linear model with quasibinomial errors was used. For the pairwise relationships between LSL and LIP and between NSL and NIP there is no clear independent and dependent variable. To maximize the statistical power, we treated the tick infection prevalence (LIP and NIP) as the dependent variable so that we could use GLMs with binomial errors as the statistical test. Ten of the 15 pairs of phenotypes were significant at an α value of 0.05 (Table S18).

Of the 15 pairwise relationships, 10 were positive and statistically significant (Table S18). Remarkably, all 5 laboratory estimates of the strain-specific performance (MTSL, LIP, LSL, NIP, and NSL) were positively related to the frequencies of the strains in *I. scapularis* populations in Canada and the USA and 4 of these 5 relationships were statistically significant (LSL had a p-value of 0.056). Interestingly, the LIP and the NIP ($p = 0.003$ and 0.033) were more significant predictors of the strain-specific frequencies in nature compared to the LSL and NSL ($p = 0.056$ and 0.048). These pairwise relationships suggest the following scenario. Strains that establish high spirochete loads in the tissues of the mouse host (MTSL) cause a higher proportion of engorged larval ticks to acquire the infection (LIP). These larvae subsequently moult into unfed nymphs that carry a higher spirochete load (NSL) and that are more likely to be infected with *B. burgdorferi* (NIP). The NIP over the duration of the infection is the lifetime host-to-tick transmission (HTT). Strains that have higher HTT in the lab have higher frequency in *I. scapularis* populations in Canada and the USA.

Table S18. Pairwise relationships between the 6 variables across the 11 strains of *B. burgdorferi*. The predictor and response variables are shown for each of the 15 pairwise relationships. The test refers to whether simple linear regression (SLR) or generalized linear models with quasibinomial errors were used to analyze the relationship. Also shown are the slope of the relationship, standard error (SE), and p-value (p). All 15 pairwise relationships are positive and 9 are statistically significant.

Predictor	Response	Test	Slope	SE	p	Signif[a]
MTSL	LSL	SLR	0.625	0.484	0.228	
MTSL	LIP	GLM	3.445	0.751	0.001	**
MTSL	NSL	SLR	0.907	0.422	0.060	
MTSL	NIP	GLM	3.551	0.902	0.003	**
MTSL	Nat Freq	GLM	6.750	2.893	0.045	*
LSL	LIP	GLM	1.925	0.691	0.021	*
LSL	NSL	SLR	0.676	0.239	0.020	*
LSL	NIP	GLM	1.918	0.942	0.072	
LSL	Nat Freq	GLM	2.530	1.157	0.056	
LIP	NSL	SLR	1.179	0.490	0.039	*
LIP	NIP	GLM	5.188	0.668	< 0.001	***
LIP	Nat Freq	GLM	9.479	2.327	0.003	**
NSL	NIP	GLM	2.129	0.976	0.057	
NSL	Nat Freq	GLM	2.456	1.075	0.048	*
NIP	Nat Freq	GLM	10.750	4.287	0.033	*

[a] Categories of significance are as follows: * $0.05 > p > 0.01$, ** $0.01 > p > 0.001$, *** $p < 0.001$.

Correlation matrix of strain-specific life history traits: The pattern of pairwise Pearson correlations was investigated among 13 variables that included 3 estimates of mouse tissue spirochete load, 8 estimates of host-to-tick transmission, and 2 estimates of the frequencies of the strains in nature. The 13 variables are defined in Table S19. The correlation matrices among these 13 variables are shown in Figure S4 and Figure S5. As expected, the results of the simple linear regression and GLM in the previous section are similar to the correlation results in the present section. A difference is that for binomial variables, the GLM approach has more statistical power because it includes the sample size on which the proportions (or percentages) are based.

Interestingly, mouse tissue spirochete load 2 (MTSL2), which was based on the subset of infected tissues, was significantly correlated with 6 of the 8 transmission variables (the exceptions were LSL1 and NSL1). In contrast, mouse tissue spirochete loads 1 and 3 (MTSL1 and MTSL3), which also included the uninfected tissues were significantly correlated with each other but not with any of the other variables. Of the 28 pairwise correlations between the 8 transmission variables, 26 were statistically significant; the exception was LSL1, which was not significantly correlated with NIP1 or NIP2. The frequencies of the strains were significantly

correlated between the PubMLST database and the literature (r = 0.889, t = 5.835, df = 9, p = 0.0002). Six of the 8 transmission variables were significantly correlated with the strain-specific frequencies in wild *I. scapularis* tick populations (the exceptions are LSL1 and NSL1). Five of the 8 transmission variables were significantly correlated with the strain-specific frequencies in in the PubMLST database (the exceptions are NIP1, NIP2, and NSL1).

Table S19. List of variables and their definitions included in the correlation matrix

Variable	Definition
MTSL1	Mouse tissue spirochete load 1 is the proportion of mouse tissues that tested positive for *B. burgdorferi* for each of the 11 strains. Calculated over all 588 mouse tissues (84 mice x 7 tissues per mouse = 588 mouse tissues)
MTSL2	Mouse tissue spirochete load 2 is the mean tissue spirochete load [log10(*23S rRNA*/million *Beta actin*)] for each of the 11 strains. Calculated for the subset of 333 infected mouse necropsies (i.e., uninfected necropsies were excluded).
MTSL3	Mouse tissue spirochete load 3 is the mean tissue spirochete load [log10((*23S rRNA*/million *Beta actin*) + 1)] for each of the 11 strains. Calculated for all 588 mouse necropsies. All negative tissues were assigned a value of 0 (i.e., log10(1) = 0).
LIP1	Larval infection prevalence 1 is the proportion of infected larvae averaged across each infestation (i.e., infestation is not accounted for)
LIP2	Larval infection prevalence 2 is [LIP inf1 + LIP inf2 + LIP inf3]/3. In other words, the LIPs for each infestation are weighted equally.
LSL1	Larval spirochete load 1 [log10(*23S rRNA* per larva)] for each of the 11 strains. Calculated for subset of infected larvae (n=645); uninfected larvae excluded.
LSL2	Larval spirochete load 2 [log10((*23S rRNA* per larva) + 1)] for each of the 11 strains. Calculated for all the larvae from infected mice (n=950). All negative larvae were assigned a value of 0 (i.e., log10(1) = 0).
NIP1	Nymphal infection prevalence 1 is the proportion of infected nymphs averaged across each infestation (i.e., infestation is not accounted for)
NIP2	Nymphal infection prevalence 2 is [NIP inf1 + NIP inf2 + NIP inf3]/3. In other words, the NIPs for each infestation are weighted equally.
NSL1	Nymphal spirochete load 1 [log10(*23S rRNA* per nymph)] for each of the 11 strains. Calculated for subset of infected nymphs (n=2084); uninfected nymphs excluded.
NSL2	Nymphal spirochete load 2 [log10((*23S rRNA* per nymph) + 1)] for each of the 11 strains. Calculated for all the nymphs from infected mice (n=2471). All negative nymphs were assigned a value of 0 (i.e., log10(1) = 0).
Freq1	Frequency (%) of the MLSTs in the Borrelia MLST database; total N = 450.
Freq2	Frequency of the MLSTs in the combined database by Travinsky et al. (2010) and by Ogden et al. (2011); total N = 251.

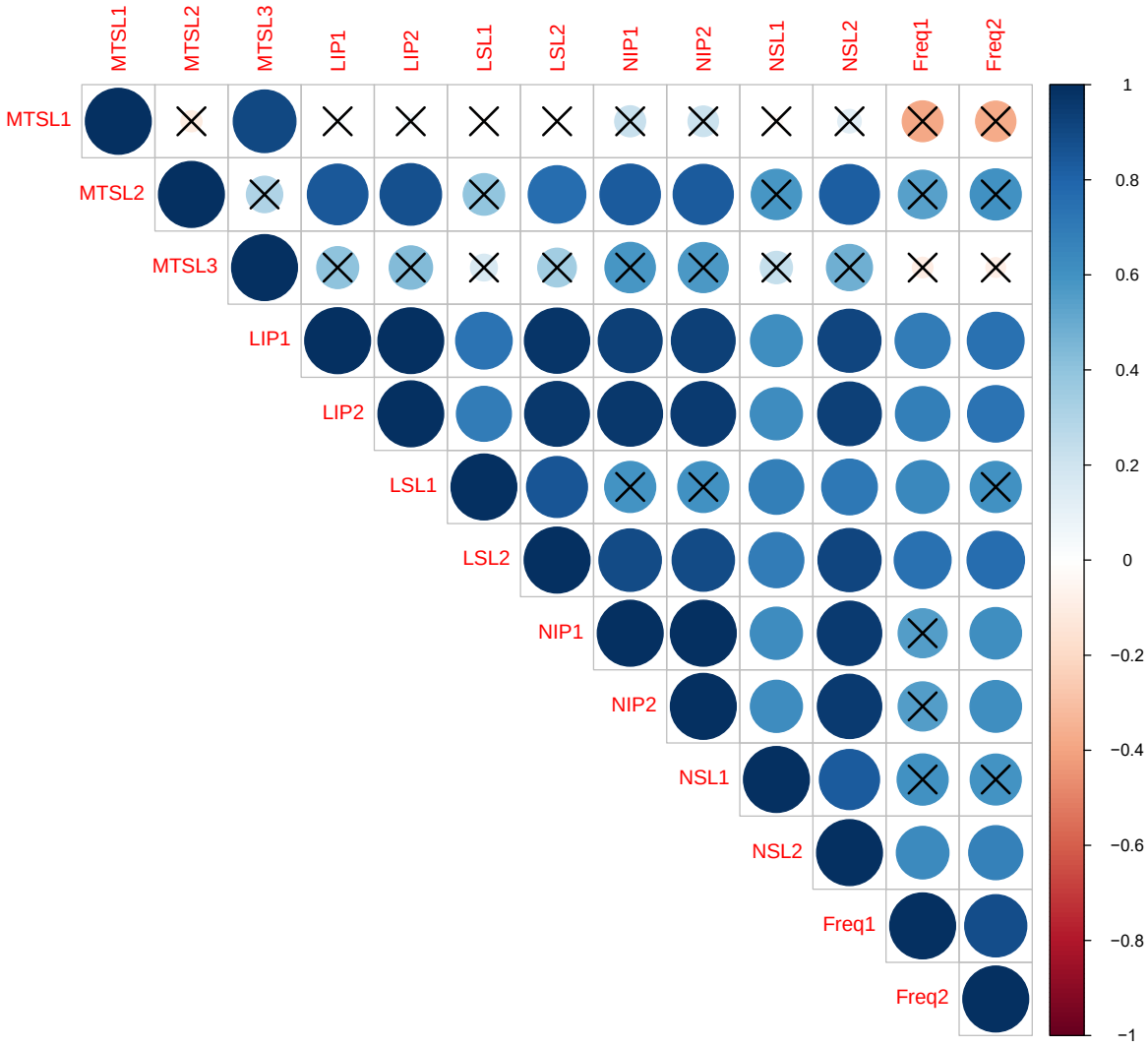

Figure S4. Correlation matrix between the 13 variables defined in Table S19. Pairwise correlations that are positive and negative are shown in blue and red, respectively. Non-significant pairwise correlations are indicated with an 'X'.

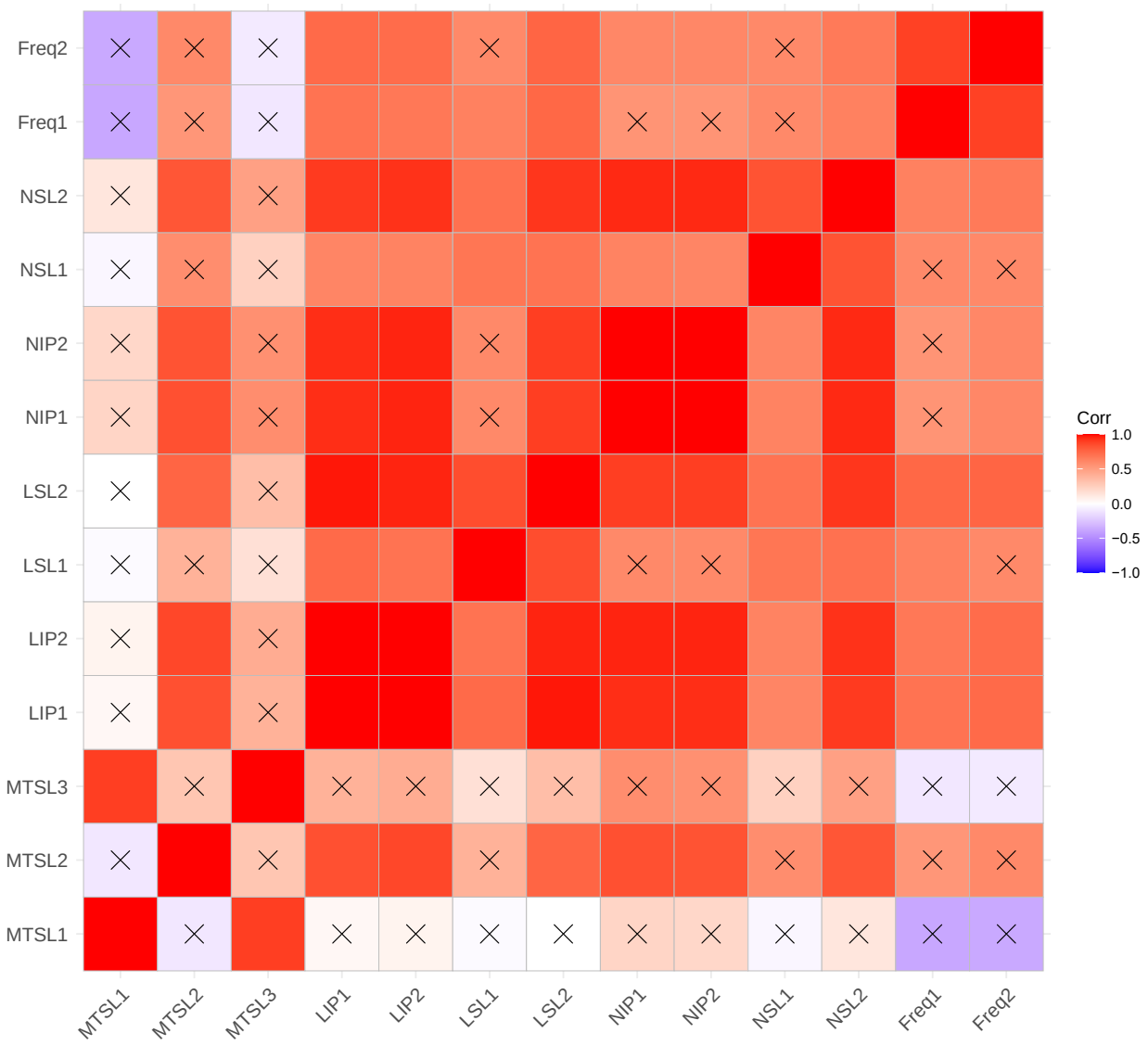

Figure S5. Correlation matrix between the 13 variables defined in Table S19. Pairwise correlations that are positive and negative are shown in red and purple, respectively. Non-significant pairwise correlations are indicated with an 'X'.

Section 8 - References

Bates, D., Machler, M., Bolker, B. M., & Walker, S. C. (2015). Fitting Linear Mixed-Effects Models Using lme4. *Journal of Statistical Software*, *67*(1), 1-48. https://doi.org/10.18637/jss.v067.i01

Courtney, J. W., Kostelnik, L. M., Zeidner, N. S., & Massung, R. F. (2004). Multiplex real-time PCR for detection of *Anaplasma phagocytophilum* and *Borrelia burgdorferi*. *Journal of Clinical Microbiology*, *42*(7), 3164-3168. https://doi.org/10.1128/jcm.42.7.3164-3168.2004

Fox, J., & Weisberg, S. (2019). *An R Companion to Applied Regression* (Third edition ed.). Sage.

Harrell, F. E. J., & Dupont, C. (2020). *Hmisc: Harrell Miscellaneous*. In (Version R package version 4.4-2) https://CRAN.R-project.org/package=Hmisc

Lenth, R. V. (2021). *Emmeans: Estimated marginal means, aka least-squares means. R package version 1.5-2.1.* In https://CRAN.R-project.org/package=emmeans

Lüdecke, D. (2018). ggeffects: Tidy Data Frames of Marginal Effects from Regression Models. *Journal of Open Source Software*, *3*(26). https://doi.org/https://doi.org/10.21105/joss.00772

Ogden, N. H., Margos, G., Aanensen, D. M., Drebot, M. A., Feil, E. J., Hanincová, K., Schwartz, I., Tyler, S., & Lindsay, L. R. (2011). Investigation of genotypes of *Borrelia burgdorferi* in *Ixodes scapularis* ticks collected during surveillance in Canada. *Applied and Environmental Microbiology*, *77*(10), 3244-3254. https://doi.org/10.1128/aem.02636-10

R Development Core Team. (2021). *R: A language and environment for statistical computing*. In R Foundation for Statistical Computing. URL http://www.R-project.org/

RStudio Team. (2020). *RStudio: Integrated Development for R*. In RStudio, PBC.

Travinsky, B., Bunikis, J., & Barbour, A. G. (2010). Geographic Differences in Genetic Locus Linkages for Borrelia burgdorferi. *Emerging Infectious Diseases*, *16*(7), 1147-1150. https://doi.org/10.3201/eid1607.091452

Zinck, C. B., Thampy, P. R., Rego, R. O. M., Brisson, D., Ogden, N. H., & Voordouw, M. (2022). *Borrelia burgdorferi* strain and host sex influence pathogen prevalence and abundance in the tissues of a laboratory rodent host. *Molecular Ecology*. https://doi.org/https://doi.org/10.1111/mec.16694

Appendix C – Supplementary material for Ch. 4

Section 1 – Statistical software used in analyses

We used R version 4.0.4 for all statistical analyses (R Core Team, 2021). We used the *lmer()* function in the lme4 package to run the LMMs (Bates et al., 2015) and the *Anova()* function in the car package to run the Wald tests of statistical significance (Fox & Weisberg, 2019). Post-hoc analysis and calculation of estimated marginal means were done using *emmeans(), pairs(), pwpm()* functions in the emmeans package (Lenth, 2021) and *ggemmeans()* function in the ggeffects package (Lüdecke, 2018). Correlations were calculated using the *cor.test()* function in the base package. Correlation matrices and correlation plots were calculated using the *rcorr()* function in the Hmisc package (Harrell Jr., 2021). Generalized additive models were run with the functions *bam()* and *gam()* in the mgcv package (Wood, 2017). Ordinal logistic regressions were done with the function *polr()* in the package MASS (Venables & Ripley, 2002).

Section 2 – Analysis of mouse antibody response

LMM of ELISA absorbance: The ELISA absorbance value (Abs) is based on the fluorescence reading of the corresponding mouse serum sample where a higher value is a greater concentration of antibodies. The analysis of Abs was performed on all infected mice (n = 84) using both the post-infection (day 28 PI) and terminal (day 97 PI) blood samples. The response was Abs modelled using a linear mixed effect model (LMM). The fixed factors were strain (11 levels), mouse sex (2 levels: male, female), blood draw (2 levels: day 28 PI, 97 PI), and temporal block (2 levels: A and B). The full model included all the two-way and the three-way interactions between strain, sex, and blood draw. Temporal block was included as a main effect only. Mouse identity was included as a random factor. Non-significant interaction terms (at $\alpha = 0.05$) were removed sequentially (Table S1). The final simplified model included no interactions (Table S1).

The parameter estimates for this final simplified model and their significance are shown in Table S2. Means and EMMs (using the final model and the ggemmeans() function) of the Abs were generated for each factor level (Table S3). The means from the raw data and the EMMs were similar (Table S3). The Pearson correlation between the means and the EMMs of the Abs across the 17 levels was positive and significant (Mean vs EMM in Table S3; $r = 0.999$, $t = 92.32$, $df = 15$, $p < 2.2*10^{-16}$). In what follows, we present the EMMs of the Abs with block as a factor and their post-hoc tests (EMM in Table S3).

The host antibody response measured by ELISA absorbance varied 1.7-fold among strains from 1.656 for strain 174 to 2.823 for strain 22-2. Females had a significantly higher Abs across strains than males (2.328 vs. 2.183, $p = 0.012$). For all strains, there was a slight increase in Abs comparing block B to block A, and a significant increase in the response from day 28 PI to day 97 PI (Table S2). The difference among blocks is consistent (i.e., no interactions) and could be attributed to differences among batches of mice, ELISA kits, and/or ticks used to

generate the infection. The difference between blood draws taken at day 28 PI and 97 PI shows that the mouse antibody response to *B. burgdorferi* increased over the duration of the experiment.

Table S1. Model simplification of the LMM of Abs. Non-significant interactions were sequentially removed in order of increasing significance; the model was updated each time a non-significant term was removed. The final simplified model contained the fixed factors only. For each term, the order in which it was removed, the Chi-squared statistic (Chi), degrees of freedom, and p-value (p) are shown. For the non-significant interactions, the p-values are the ones in the model from which they were removed. For the included terms, the p-values are from the final simplified model.

Term	Order removed	Chi	df	p	Signif [a]
Strain:Sex:Blood draw	1	9.845	10	0.454	
Strain:Sex	2	5.352	10	0.866	
Blood draw:Sex	3	0.183	1	0.669	
Strain:Blood draw	4	14.332	10	0.158	
Strain	Final model	96.894	10	$2.276*10^{-16}$	***
Sex	Final model	6.384	1	0.012	*
Blood draw	Final model	419.886	1	$2.2*10^{-16}$	***
Temporal block	Final model	10.930	1	$9.465*10^{-4}$	***

[a] Categories of significance are as follows: * 0.05 > p > 0.01, ** 0.01 > p > 0.001, *** p < 0.001.

Table S2. Parameter estimates of the Abs measured by ELISA. Factors include strain (11 levels), mouse sex (2 levels: male, female), blood draw (2 levels: day 28 PI, 97 PI), and temporal block (2 levels: A and B). For each parameter in the LMM, the type, description, estimate, standard error (SE), and p-value (p) are shown.

Parameter type	Parameter description	Estimate	SE	p	Signif [a]
Intercept	Reference [b]	1.953	0.111	$2.2*10^{-16}$	***
Contrast	Strain 57 – Strain 66	-0.330	0.138	0.019	*
Contrast	Strain 150 – Strain 66	-0.250	0.138	0.073	
Contrast	Strain 167 – Strain 66	-0.684	0.138	$4.452*10^{-6}$	***
Contrast	Strain 126 – Strain 66	-0.282	0.138	0.044	*
Contrast	Strain 22-2 – Strain 66	0.327	0.138	0.020	*
Contrast	Strain 10-2 – Strain 66	-0.105	0.138	0.449	
Contrast	Strain 54 – Strain 66	-0.420	0.138	0.003	**
Contrast	Strain 198 – Strain 66	-0.149	0.138	0.283	
Contrast	Strain 174 – Strain 66	-0.807	0.156	$1.921*10^{-6}$	***
Contrast	Strain 178-1 – Strain 66	-0.112	0.138	0.419	
Contrast	Day 97 PI – Day 28 PI	1.042	0.051	$2.2*10^{-16}$	***

Contrast	Female – Male	-0.147	0.058	0.014	*
Contrast	Block B – Block A	0.192	0.058	0.001	**

[a] Categories of significance are as follows: * 0.05 > p > 0.01, ** 0.01 > p > 0.001, *** p < 0.001.

[b] Reference condition refers to an Abs value taken on day 28 PI from a male mouse in block A that was infected with *B. burgdorferi* strain 66.

Table S3. The means and EMMs of the Abs for each of the levels of the factors of interest. The means are from the raw data, whereas the EMMs were calculated using the final simplified model in Table S1. The mean or EMM of a given level was averaged over the levels of the other factors. Lower and upper (LCL, UCL) 95% confidence limits for the EMM are reported.

Factor	Level	Mean	EMM	LCL	UCL
Strain	66	2.473	2.497	2.296	2.698
Strain	57	2.167	2.167	1.980	2.354
Strain	150	2.247	2.247	2.059	2.434
Strain	167	1.813	1.813	1.625	2.000
Strain	126	2.215	2.215	2.028	2.402
Strain	22-2	2.823	2.823	2.636	3.011
Strain	10-2	2.392	2.392	2.205	2.579
Strain	54	2.077	2.077	1.889	2.264
Strain	198	2.348	2.348	2.161	2.535
Strain	174	1.656	1.690	1.452	1.927
Strain	178-1	2.385	2.385	2.198	2.572
Sex	Male	2.183	2.168	2.087	2.249
Sex	Female	2.328	2.315	2.231	2.398
Blood draw	28 PI	1.733	1.720	1.644	1.797
Blood draw	97 PI	2.775	2.762	2.685	2.839
Block	A	2.160	2.145	2.064	2.226
Block	B	2.353	2.337	2.254	2.421

Section 3 – Mouse body mass

A two-way ANOVA was used to test whether sex and *B. burgdorferi* infection status influenced the mouse body mass on day 84 (Figure S1). The interaction between sex and *B. burgdorferi* infection status was not significant ($F_{1, 100} = 0.115$, $p = 0.736$). The effect of sex was highly significant ($F_{1, 100} = 187.299$, $p < 2.2*10^{-16}$), but the effect of *B. burgdorferi* infection status was not ($F_{1, 100} = 2.221$, $p = 0.139$). The mean body size on day 84 for males (n = 53 male mice; mean ± SE = 31.03 g ± 0.381 g) was 25.4% heavier compared to the females (n = 51

female mice; mean ± SE = 24.74 ± 0.356 g), and this difference was highly significant (t = 13.746, df = 101, $p < 2.2*10^{-16}$). In summary, there was no evidence that infection with *B. burgdorferi* influenced the body mass of C3H/HeJ mice.

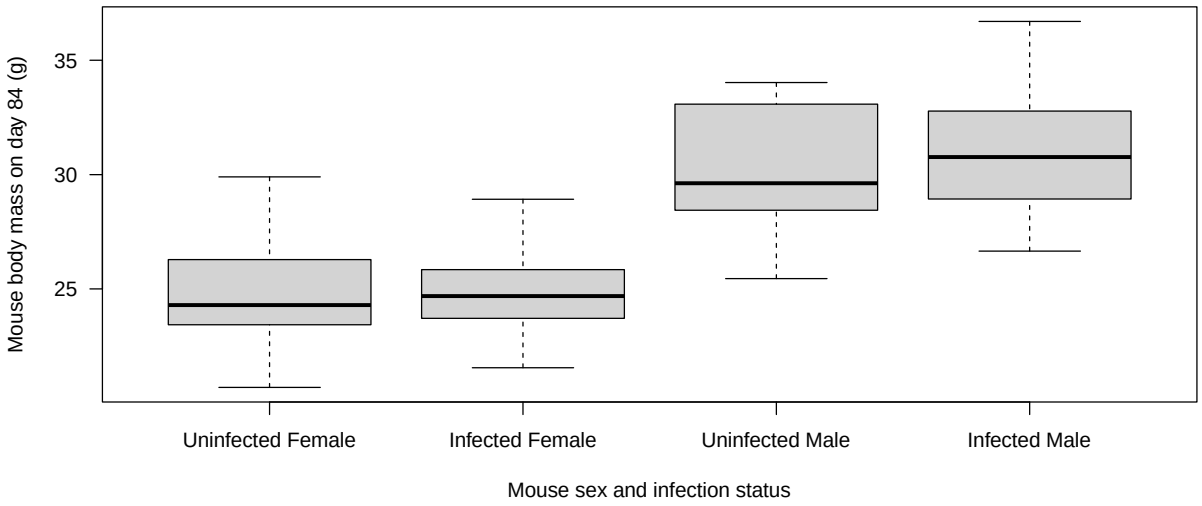

Figure S1. Mouse body mass (grams) on day 84 post-infection via nymphal tick bite versus sex and infection status of the mice. The four groups and their samples sizes include uninfected females (n = 12), infected females (n = 46), uninfected males (n = 9), and infected males (n = 46). The boxplots show the median (black line), 25th and 75th percentiles (edges of the box), minimum and maximum values (whiskers), and outliers (open circles).

Section 4 – Mouse ankle swelling

Summary of sample sizes: There were 104 mice in this study: 20 in the uninfected control group and 84 in the infected group. For each mouse, between 9 and 13 measurements were obtained for each of 3 morphological variables: body weight, left rear tibiotarsal joint width, and right rear tibiotarsal joint width (i.e., up to 1352 measurements for each variable). The measurements were taken from days -25 to 96 post-infection.

Correlation in width between left and right rear tibiotarsal joints: There was a strong positive correlation in the ankle width between the left and right rear tibiotarsal joints (Figure S2; r = 0.692, t = 33.832, df = 1247, p-value $< 2.2*10^{-16}$). After log10-transformation of the ankle width, the results remained the same (r = 0.699, t = 34.553, df = 1247, p-value $< 2.2*10^{-16}$).

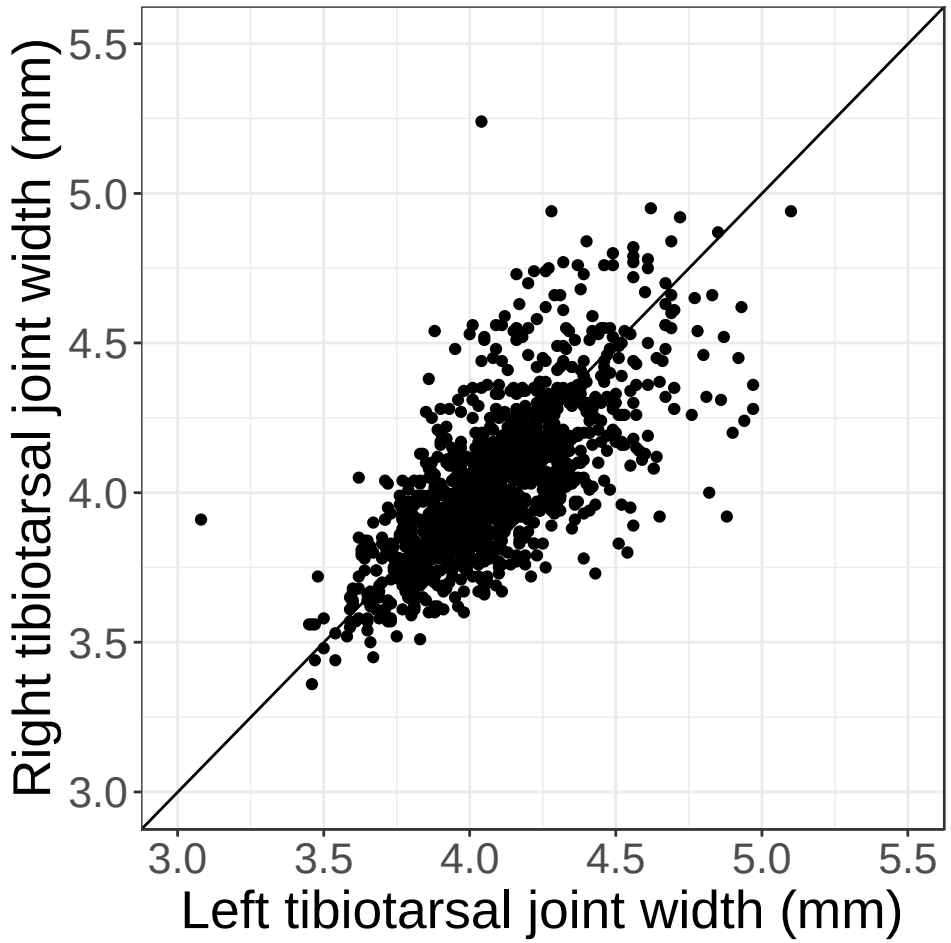

Figure S2. Relationship between the width of the left and right rear tibiotarsal joint. The correlation is positive and highly significant ($r = 0.692$, $t = 33.832$, $df = 1247$, p-value < $2.2*10^{-16}$).

Effect of infection with *B. burgdorferi* on mouse ankle width: For each mouse the ankle widths for the left and right rear tibiotarsal joints were averaged for each occasion. The mean ankle width of the rear tibiotarsal joint was analyzed using a generalized additive model (GAM). This GAM included 3 fixed factors, infection status, mouse sex, and block, a smoother function of days post-infection conditioned on infection status, and mouse identity as a random effect (Table S4). This model had an adjusted r^2 value of 51.7% and the deviance explained was 55.2%.

Infection status ($p = 4.81*10^{-15}$), mouse sex ($p = 8.62*10^{-11}$), and block ($p = 0.004$) had significant effects on the ankle width diameter (Table S4). The smoothed function of the covariate days.PI ($p < 2.2*10^{-16}$) was highly significant for infected mice ($p < 2.2*10^{-16}$), but it was almost not significant for uninfected control mice ($p = 0.044$) indicating that the function of ankle width over days post-infection has different shapes between uninfected and infected mice

(see Figure 4.2; Table S4). The emmeans() function was used to calculate estimated marginal means (EMMs) for the levels of each fixed factor at 28 days post-infection.

Table S4. Fixed effects and smoother functions for the GAM of mouse ankle width. The fixed effects include mouse infection status (uninfected control, infected), mouse sex (female, male), temporal block (block A, block B). The GAM included separate smoother functions of days post infection for uninfected control mice and infected mice and mouse ID was included as a random effect. For the fixed effects, the estimate, standard error (SE), t-statistic (t) and p-value (p) are shown. For the smoother function and random effects, the estimated degrees of freedom (edf), reference degrees of freedom (Ref df), F-statistic (F), and p-value (p) are shown.

Fixed effects	Estimate	SE	t	p	Signif[a]
Intercept[b]	3.914	0.020	192.586	$< 2.2*10^{-16}$	***
Infected - Control	0.158	0.020	7.939	$4.81*10^{-15}$	***
Male - Female	0.114	0.017	6.550	$8.62*10^{-11}$	***
Block B - Block A	-0.051	0.018	-2.877	0.004	**

Smoother	edf	Ref df	F	p	Signif[a]
s(days PI, uninfected)	2.610	3.213	2.658	0.044	*
s(days PI, infected)	8.704	8.974	69.911	$< 2.2*10^{-16}$	***
s(mouse ID)	77.664	109.000	2.575	$< 2.2*10^{-16}$	***

[a] Categories of significance are as follows: * 0.05 > p > 0.01, ** 0.01 > p > 0.001, *** p < 0.001

[b] Intercept refers to the mean ankle width of an uninfected (control) female mouse in block A on day 0 post-infection.

Effect of *B. burgdorferi* strain on mouse ankle width: Mouse ankle width was analyzed using a GAM and the fixed factors included *B. burgdorferi* strain, mouse sex, and block. The smoother function contained the covariate days post infection (PI). In GAM01, this smoother function was not conditioned on any fixed factor. In GAM02 and GAM03, the smoother function of days PI was conditioned on either *B. burgdorferi* strain or mouse infection status. Mouse identity was modelled as a random effect (Table S5).

The model with the smoother function of days PI conditioned on *B. burgdorferi* strain (GAM02) had the highest % deviance explained value (55.6%), whereas the model with the smoother function of days PI conditioned on infection status (GAM03) had the highest adjusted r^2 value (51.7%; Table S5). In all three GAMs, the fixed effects of *B. burgdorferi* strain, mouse sex, and block were highly significant (i.e., the least significant p-values based on F-tests for strain, mouse sex, and block were $1.19*10^{-27}$, $9.05*10^{-15}$, and 0.0008, respectively). The parameter estimates for GAM02 are shown in Table S6. Ten of 11 strains, not strain 167,

induced significant ankle swelling in the mice (Table S6). As before, the mean ankle width was larger in male mice compared to female mice and in block A compared to block B (Table S6).

The emmeans() function with GAM02 was used to calculate the EMMS for the levels of each factor at day 28 PI. To evaluate differences among strains, mouse ankle swelling was expressed as a % increase in ankle width relative to the uninfected control mice on day 28 PI (Table S7). Strain 22-2 increased mouse ankle width by 13.6%, whereas strain Bb16-167 only increased mouse ankle width by 1.6%. The mean ankle width on day 28 PI was 2.7% bigger in male mice compared to female mice. The mean ankle width on day 28 PI was 1.5% bigger in block A compared to block B.

Table S5. Table of GAMs of mouse ankle width with different fixed effects structures. The smoother functions of days post infection are conditioned on strain or infection status. For each model, the adjusted r^2 value and the % deviance explained by the model are shown.

R ID	Model ID	Fixed effects	Smoothers	r^2	% Dev
GAM.13a	GAM01	strain + sex + block1	s(days PI)	0.485	51.4
GAM.14a	GAM02	strain + sex + block1	s(days PI, by strain)	0.507	55.6
GAM.14c	GAM03	strain + sex + block1	s(days PI, by infection)	0.517	54.6

Table S6. Fixed effects and smoother functions for the GAM of mouse ankle width (model 3 in Table S5). The fixed effects include *B. burgdorferi* strain, mouse sex (female, male), and temporal block (block A, block B). The GAM included separate smoother functions of days post infection for each *B. burgdorferi* strain and mouse ID was included as a random effect. For the fixed effects, the estimate, standard error (SE), t-statistic (t) and p-value (p) are shown. For the smoother function and random effects, the estimated degrees of freedom (edf), reference degrees of freedom (Ref df), F-statistic (F), and p-value (p) are shown.

Parameter	Estimate	SE	t	p	Signif[a]
Intercept[b]	3.919	0.015	255.249	$< 2.2*10^{-16}$	***
10-2 - Uninfected	0.177	0.028	6.305	$4.14*10^{-10}$	***
22-2 - Uninfected	0.243	0.028	8.697	$< 2.2*10^{-16}$	***
54 - Uninfected	0.073	0.028	2.625	0.009	**
57 - Uninfected	0.203	0.028	7.332	$4.34*10^{-13}$	***
66 - Uninfected	0.126	0.029	4.313	$1.75*10^{-5}$	***
126 - Uninfected	0.179	0.028	6.397	$2.32*10^{-10}$	***
150 - Uninfected	0.101	0.028	3.621	$3.00*10^{-4}$	***
167 - Uninfected	0.015	0.028	0.529	0.597	
174 - Uninfected	0.222	0.034	6.620	$5.55*10^{-11}$	***
178-1 - Uninfected	0.186	0.028	6.635	$5.05*10^{-11}$	***
198 - Uninfected	0.244	0.028	8.726	$< 2.2*10^{-16}$	***

Male - Female	0.114	0.013	8.647	$< 2.2*10^{-16}$	***
Block B - Block A	-0.064	0.014	-4.659	$3.56*10^{-6}$	***

Smoother	edf	Ref df	F	p	Signif[a]
s(days PI, uninfected)	2.644	3.252	2.918	0.030	*
s(days PI, 10-2)	7.275	8.166	8.205	$< 2.2*10^{-16}$	***
s(days PI, 22-2)	6.824	7.813	13.457	$< 2.2*10^{-16}$	***
s(days PI, 54)	5.113	6.211	4.884	$5.16*10^{-5}$	***
s(days PI, 57)	6.766	7.885	9.444	$< 2.2*10^{-16}$	***
s(days PI, 66)	3.056	3.798	4.932	$9.00*10^{-4}$	***
s(days PI, 26)	5.707	6.781	8.187	$< 2.2*10^{-16}$	***
s(days PI, 150)	4.023	4.879	6.357	$1.37*10^{-5}$	***
s(days PI, 167)	3.225	3.940	5.753	$2.00*10^{-4}$	***
s(days PI, 174)	5.398	6.442	5.867	$5.59*10^{-6}$	***
s(days PI,178-1)	7.148	8.187	10.761	$< 2.2*10^{-16}$	***
s(days PI, 198)	5.628	6.700	11.403	$< 2.2*10^{-16}$	***
s(mouse ID2)	47.670	99.000	0.944	$4.08*10^{-7}$	***

[a] Categories of significance are as follows: * 0.05 > p > 0.01, ** 0.01 > p > 0.001, *** p < 0.001.
[b] Intercept refers to the mean ankle width of an uninfected (control) female mouse in block A on day 0 post-infection.

Table S7. Estimated marginal means (EMMs) for the GAM02 of mouse ankle width for each of the levels of the factors of interest. For the 11 strains of *B. burgdorferi*, the EMMs were averaged over the two sexes and the two blocks. For the 2 sexes, the EMMs were averaged over the 11 strains and the two blocks. For the 2 blocks, the EMMs were averaged over the 11 strains and the two sexes. For each level, the EMM of the mouse ankle width, standard error (SE), degrees of freedom (df), p-value (p), and the lower limit (LL) and upper limit (UL) of the 95% confidence interval are shown. For each level, the % increase is calculated by comparing it to the relevant reference level.

Factor	Levels	EMM	SE	df	LL	UL	% increase
Strain	Negative	3.956	0.017	1124.524	3.906	4.007	---
Strain	10-2	4.338	0.052	1124.524	4.184	4.492	9.6
Strain	22-2	4.494	0.050	1124.524	4.345	4.643	13.6
Strain	54	4.128	0.042	1124.524	4.004	4.252	4.3
Strain	57	4.310	0.048	1124.524	4.167	4.452	8.9
Strain	66	4.121	0.036	1124.524	4.015	4.227	4.2
Strain	126	4.284	0.046	1124.524	4.147	4.421	8.3
Strain	150	4.163	0.039	1124.524	4.048	4.278	5.2

Strain	167	4.020	0.035	1124.524	3.916	4.125	1.6
Strain	174	4.260	0.055	1124.524	4.096	4.425	7.7
Strain	178-1	4.402	0.050	1124.524	4.255	4.549	11.3
Strain	198	4.389	0.046	1124.524	4.253	4.524	10.9
Sex	Female	4.182	0.014	1124.524	4.139	4.224	---
Sex	Male	4.296	0.014	1124.524	4.253	4.338	2.7
Block	A	4.271	0.014	1124.524	4.229	4.313	1.5
Block	B	4.207	0.015	1124.524	4.163	4.251	---

Effect of *B. burgdorferi* strain on mouse ankle width in week 4 post-infection: The mouse ankle width measured in week 4 PI (i.e., days 22 to 28 PI) was analyzed using a linear model with *B. burgdorferi* strain, mouse sex, and block as fixed factors. As each of the 113 mice appeared only once in the analysis, mouse ID did not need to be included as a random effect. The ankle widths were measured on days 23, 24, 25, and 27 PI with sample sizes of 28, 7, 55, and 23, respectively. Strain of *B. burgdorferi* ($F_{11, 99} = 10.428$, $p = 1.94*10^{-12}$) and block ($F_{1, 99} = 5.522$, $p = 0.021$) but not mouse sex ($F_{1, 99} = 0.170$, $p = 0.681$) had significant effects on mouse ankle width in week 4 PI. The parameter estimates for this linear model are shown in Table S8. Like the parameter estimates for GAM 02 in Table S6, all the strains, except Bb16-167, induced significant ankle swelling in week 4 PI. The mean ankle width was significantly greater for block B compared to block A (Table S8), which was the opposite result for GAM02 in Table S6.

Table S8. Parameter estimates for the linear model of mouse ankle width in week 4 post-infection. The fixed effects include *B. burgdorferi* strain, mouse sex (female, male), and block (block A, block B). For the fixed effects, the estimate, standard error (SE), t-statistic (t) and p-value (p) are shown.

Parameter	Estimate	SE	t	p	Signif[a]
Intercept[b]	3.911	0.039	100.423	$1.984*10^{-101}$	***
Bb16-010 - Uninfected	0.380	0.071	5.388	$4.830*10^{-7}$	***
Bb16-022 - Uninfected	0.554	0.071	7.852	$4.979*10^{-12}$	***
Bb16-054 - Uninfected	0.166	0.071	2.357	0.020	*
Bb16-057 - Uninfected	0.374	0.071	5.308	$6.797*10^{-7}$	***
Bb16-066 - Uninfected	0.320	0.075	4.293	$4.114*10^{-5}$	***
Bb16-126 - Uninfected	0.321	0.071	4.555	$1.497*10^{-5}$	***
Bb16-150 - Uninfected	0.264	0.071	3.748	$2.998*10^{-4}$	***
Bb16-167 - Uninfected	0.132	0.071	1.878	0.063	
Bb16-174 - Uninfected	0.356	0.086	4.149	$7.071*10^{-5}$	***

Bb16-178 - Uninfected	0.446	0.071	6.318	$7.592*10^{-9}$	***
Bb16-198 - Uninfected	0.379	0.071	5.370	$5.212*10^{-7}$	***
Male - Female	0.013	0.033	0.388	0.699	
Block B - Block A	0.078	0.033	2.350	0.021	*

[a] Categories of significance are as follows: * 0.05 > p > 0.01, ** 0.01 > p > 0.001, *** p < 0.001

[b] Intercept refers to the mean ankle width of an uninfected (control) female mouse in block A on day 0 post-infection.

Correlation in mouse ankle swelling between blocks: The mice were processed in two temporal blocks (A and B) that were separated by 6 months. If *B. burgdorferi* strain induces a repeatable amount of ankle swelling in C3H/HeJ mice, the mean ankle widths for the 11 strains should be correlated between the two blocks. The mean mouse ankle width measured in week 4 post-infection (i.e., days 22 to 28 PI) was calculated for the 24 combinations of strain (uninfected mice + 11 strains) and block. There was a positive and significant correlation in the mean mouse ankle width in week 4 PI between blocks A and B and across the 11 strains of *B. burgdorferi* (Figure S3; $r = 0.643$, $t = 2.658$, $df = 10$, $p = 0.024$).

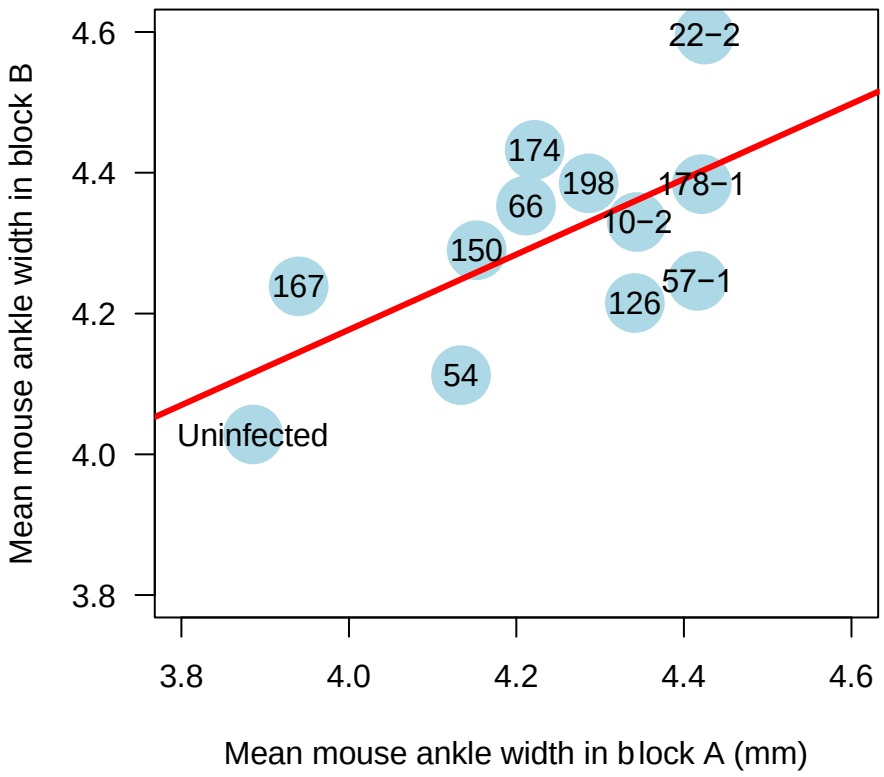

Figure S3. Relationship between the mean mouse ankle width in block A and block B across the 11 strains of *B. burgdorferi* and the uninfected mice. The correlation is positive and significant (r = 0.643, t = 2.658, df = 10, p = 0.024).

Section 6 – Tissue lesion scores

Comparing lesion scores between infected and uninfected mice: for each tissue, an OLR was used to compare lesion scores of infected versus uninfected mice to determine whether the infected mice had significantly higher lesion scores, as would be expected if infection led to increased presence of lesions. Each tissue was analyzed in an OLR with the fixed factors of infection status, mouse sex, and temporal block with no interactions. For each tissue there was a significant effect of infection status with higher lesion scores in the infected mice (Table S9).

Table S9. Parameter contrasts of the tissue lesion scores. Factors include infection status, mouse sex, and temporal block. For each contrast, the factor, estimate, standard error (SE), and p-value (p) are shown.

Tissue	Parameter description	Estimate	SE	p	Signif [a]
Ventral skin	Infected - Uninfected	2.585	0.813	$9.075*10^{-5}$	***
Ventral skin	Female - Male	1.468	0.449	$6.676*10^{-4}$	***
Ventral skin	Block B – Block A	0.088	0.433	0.840	
Kidney	Infected - Uninfected	1.490	0.545	0.004	**
Kidney	Female - Male	0.812	0.387	0.033	*
Kidney	Block B – Block A	-0.855	0.384	0.024	*
Joint	Infected - Uninfected	19.701	0.189	$2.341*10^{-10}$	***
Joint	Female - Male	0.557	0.407	0.169	
Joint	Block B – Block A	-0.442	0.406	0.275	
Heart	Infected - Uninfected	19.575	0.187	$7.655*10^{-10}$	***
Heart	Female - Male	1.343	0.431	0.001	**
Heart	Block B – Block A	-0.404	0.425	0.340	

[a] Categories of significance are as follows: * $0.05 > p > 0.01$, ** $0.01 > p > 0.001$, *** $p < 0.001$.

Analysis of ventral skin tissue lesion scores by OLR: lesions in tissues taken at necropsy (97 days PI) were scored on an ordinal scale of 0 (no lesions), 1 (mild lesions), or 2 (severe lesions). These data are the response variable used in the OLR. Lesion scores for skin were analyzed using a model with the fixed factors of strain (11 levels), mouse sex (2 levels), and temporal block (2 levels). The interaction between sex and strain was included, and the abundance of *B. burgdorferi* in the ventral skin at day 97 PI was included as a covariate. If the interaction was non-significant (at $\alpha = 0.05$) it was removed (Table S10). The final simplified model included no interactions (Table S10).

Means and EMMs (using the final model and the emmeans() function) of the lesion scores were generated for each factor level (Table S11). The function emmeans() recodes ordinal scales starting at 1, so it presents a scale from 1-3 where 3 is severe lesions. The Pearson correlation between the strain means and the EMMs was positive and significant (Mean vs EMM in Table S11; $r = 0.993$, $t = 25.629$, $df = 9$, $p = 1.009*10^{-9}$).

Table S10. Model simplification of the OLR of ventral skin lesions. The non-significant interaction was removed and the model was updated. The final simplified model contained the fixed factors only. For each term, the order in which it was removed, the Chi-squared statistic (Chi), degrees of freedom, and p-value (p) are shown. For the non-significant interaction, the p-value is from the model where they were removed. For the included terms, the p-values are from the final simplified model.

Term	Order removed	Chi	df	p	Signif [a]
Strain:Sex	1	14.592	10	0.148	
Strain	Final model	10.612	10	0.388	

Sex	Final model	2.196	1	0.138
Abundance	Final model	0.002	1	0.961
Temporal block	Final model	0.089	1	0.765

[a] Categories of significance are as follows: * 0.05 > p > 0.01, ** 0.01 > p > 0.001, *** p < 0.001.

Table S11. The means and EMMs of the lesion scores for each of the levels of the factors of interest. The means are from the raw data, whereas the EMMs were calculated using the final simplified model in Table S10. The mean or EMM of a given level was averaged over the levels of the other factors. Lower and upper (LCL, UCL) 95% confidence limits for the EMM are reported. EMMs are greater than average scores as they are calculated on a 1-3 scale, as opposed to a 0-2 scale.

Factor	Level	Mean	EMM	LCL	UCL
Strain	66	0.429	1.396	0.986	1.805
Strain	57	0.250	1.250	0.944	1.555
Strain	150	0.500	1.505	1.170	1.840
Strain	167	0.875	1.872	1.547	2.198
Strain	126	0.750	1.759	1.369	2.148
Strain	22-2	0.500	1.507	1.169	1.844
Strain	10-2	0.375	1.376	1.045	1.707
Strain	54	0.500	1.505	1.158	1.852
Strain	198	0.750	1.763	1.425	2.101
Strain	174	0.600	1.654	1.227	2.080
Strain	178-1	0.625	1.632	1.295	1.970
Sex	Male	0.372	1.383	1.126	1.639
Sex	Female	0.756	1.748	1.475	2.020
Block	A	0.558	1.548	1.394	1.702
Block	B	0.561	1.582	1.428	1.736

Analysis of kidney tissue lesion scores by OLR: lesions in tissues taken at necropsy (97 days PI) were scored on an ordinal scale of 0 (no lesions), 1 (mild lesions), or 2 (severe lesions). These data are the response variable used in the OLR. Lesion scores for kidney were analyzed using a model with the fixed factors of strain (11 levels), mouse sex (2 levels), and temporal block (2 levels). The interaction between sex and strain was included, and the abundance of *B. burgdorferi* in the kidney at day 97 PI was included as a covariate. The interaction was significant (at $\alpha = 0.05$) and was kept in the final model (Table S12).

Means and EMMs (using the final model and the emmeans() function) of the lesion scores were generated for each factor level (Table S13). The function emmeans() recodes ordinal scales starting at 1, so it presents a scale from 1-3 where 3 is severe lesions. The Pearson

correlation between the strain means and the EMMs was positive and significant (Mean vs EMM in Table S13; r = 0.988, t = 19.387, df = 9, p = $1.195*10^{-8}$).

Table S12. The final model of the OLR of kidney lesions. The contained the fixed factors and the interaction of strain and sex. For each term, the Chi-squared statistic (Chi), degrees of freedom, and p-value (p) are shown.

Term	Chi	df	p	Signif [a]
Strain:Sex	21.172	10	0.020	*
Strain	22.871	10	0.011	*
Sex	3.419	1	0.064	
Abundance	0.594	1	0.441	
Temporal block	7.347	1	0.020	*

[a] Categories of significance are as follows: * 0.05 > p > 0.01, ** 0.01 > p > 0.001, *** p < 0.001.

Table S13. The means and EMMs of the lesion scores for each of the levels of the factors of interest. The means are from the raw data, whereas the EMMs were calculated using the model in Table S12. The mean or EMM of a given level was averaged over the levels of the other factors. Lower and upper (LCL, UCL) 95% confidence limits for the EMM are reported. EMMs are greater than average scores as they are calculated on a 1-3 scale, as opposed to a 0-2 scale. For factors with significant interactions, the means and EMMs are reported for the relevant combinations of factors.

Factor	Level	Mean	EMM	LCL	UCL
Strain	66	0.714	1.707	1.292	2.122
Strain	57	0.750	1.735	1.388	2.082
Strain	150	1.000	1.995	1.597	2.394
Strain	167	1.000	2.001	1.601	2.400
Strain	126	1.000	2.043	1.655	2.432
Strain	22-2	1.375	2.341	1.967	2.715
Strain	10-2	0.625	1.590	1.200	1.980
Strain	54	0.625	1.600	1.244	1.955
Strain	198	1.625	2.660	2.371	2.948
Strain	174	0.600	1.557	1.251	1.863
Strain	178-1	1.250	2.266	1.886	2.647
Sex	Male	0.837	1.849	1.692	2.005
Sex	Female	1.122	2.060	1.903	2.216
Block	A	1.116	2.112	1.950	2.275
Block	B	0.829	1.796	1.644	1.948
Strain:Sex	66 & Male	0.500	1.494	0.974	2.014

Strain:Sex	57 & Male	0.250	1.248	0.832	1.665
Strain:Sex	150 & Male	1.000	1.977	1.464	2.491
Strain:Sex	167 & Male	0.750	1.750	1.147	2.354
Strain:Sex	126 & Male	1.000	1.988	1.478	2.499
Strain:Sex	22-2 & Male	1.250	2.218	1.693	2.744
Strain:Sex	10-2 & Male	0.500	1.474	0.960	1.989
Strain:Sex	54 & Male	0.250	1.247	0.828	1.666
Strain:Sex	198 & Male	1.250	2.319	1.742	2.896
Strain:Sex	174 & Male	1.000	2.113	1.501	2.725
Strain:Sex	178-1 & Male	1.500	2.504	2.012	2.996
Strain:Sex	66 & Female	1.000	1.921	1.274	2.568
Strain:Sex	57 & Female	1.250	2.222	1.665	2.778
Strain:Sex	150 & Female	1.000	2.013	1.386	2.641
Strain:Sex	167 & Female	1.250	2.251	1.729	2.772
Strain:Sex	126 & Female	1.000	2.098	1.507	2.690
Strain:Sex	22-2 & Female	1.500	2.464	1.936	2.992
Strain:Sex	10-2 & Female	0.750	1.706	1.123	2.289
Strain:Sex	54 & Female	1.000	1.953	1.386	2.520
Strain:Sex	198 & Female	2.000	3.000	2.998	3.002
Strain:Sex	174 & Female	0.000	1.000	1.000	1.000
Strain:Sex	178-1 & Female	1.000	2.029	1.444	2.614

Analysis of tibiotarsal joint tissue lesion scores by OLR: lesions in tissues taken at necropsy (97 days PI) were scored on an ordinal scale of 0 (no lesions), 1 (mild lesions), or 2 (severe lesions). These data are the response variable used in the OLR. Lesion scores for tibiotarsal joint were analyzed using a model with the fixed factors of strain (11 levels), mouse sex (2 levels), and temporal block (2 levels). The interaction between sex and strain was included. the abundance of *B. burgdorferi* in the tibiotarsal joint at day 97 PI, and the peak joint swelling at day 28 PI were included as covariates. The interaction was not significant (at $\alpha = 0.05$) and was removed from the final model (Table S14).

Means and EMMs (using the final model and the emmeans() function) of the lesion scores were generated for each factor level (Table S15). The function emmeans() recodes ordinal scales starting at 1, so it presents a scale from 1-3 where 3 is severe lesions. The Pearson correlation between the strain means and the EMMs was positive and significant (Mean vs EMM in Table S14; $r = 0.979$, $t = 14.48$, $df = 9$, $p = 1.532*10^{-7}$).

Table S14. Model simplification of the OLR of tibiotarsal joint lesions. The non-significant interaction was removed and the model was updated. The final simplified model contained the fixed factors only. For each term, the order in which it was removed, the Chi-squared statistic (Chi), degrees of freedom, and p-value (p) are shown. For the non-significant interaction, the p-

value is from the model where it was removed. For the included terms, the p-values are from the final simplified model.

Term	Order removed	Chi	df	p	Signif [a]
Strain:Sex	1	9.178	10	0.515	
Strain	Final model	32.842	10	$2.896*10^{-4}$	***
Sex	Final model	0.667	1	0.414	
Abundance	Final model	1.715	1	0.190	
Swelling	Final model	0.097	1	0.755	
Temporal block	Final model	0.808	1	0.369	

[a] Categories of significance are as follows: * 0.05 > p > 0.01, ** 0.01 > p > 0.001, *** p < 0.001.

Table S15. The means and EMMs of the lesion scores for each of the levels of the factors of interest. The means are from the raw data, whereas the EMMs were calculated using the final simplified model in Table S10. The mean or EMM of a given level was averaged over the levels of the other factors. Lower and upper (LCL, UCL) 95% confidence limits for the EMM are reported. EMMs are greater than average scores as they are calculated on a 1-3 scale, as opposed to a 0-2 scale.

Factor	Level	Mean	EMM	LCL	UCL
Strain	66	1.286	2.299	1.794	2.803
Strain	57	1.625	2.710	2.342	3.079
Strain	150	0.250	1.197	0.908	1.486
Strain	167	0.375	1.377	0.938	1.817
Strain	126	0.875	2.008	1.525	2.491
Strain	22-2	1.125	2.252	1.703	2.801
Strain	10-2	0.875	1.898	1.420	2.376
Strain	54	1.125	2.193	1.672	2.714
Strain	198	0.625	1.440	0.952	1.927
Strain	174	1.400	2.418	1.817	3.019
Strain	178-1	1.625	2.532	2.094	2.970
Sex	Male	0.884	1.961	1.749	2.174
Sex	Female	1.122	2.098	1.885	2.311
Block	A	1.093	2.095	1.898	2.291
Block	B	0.902	1.964	1.770	2.159

Analysis of heart tissue lesion scores by OLR: lesions in tissues taken at necropsy (97 days PI) were scored on an ordinal scale of 0 (no lesions), 1 (mild lesions), or 2 (severe lesions). These data are the response variable used in the OLR. Lesion scores for heart were analyzed using a model with the fixed factors of strain (11 levels), mouse sex (2 levels), and temporal

block (2 levels). The interaction between sex and strain was included, and the abundance of *B. burgdorferi* in the kidney at day 97 PI was included as a covariate. The interaction was significant (at $\alpha = 0.05$) and was kept in the final model (Table S16).

Means and EMMs (using the final model and the emmeans() function) of the lesion scores were generated for each factor level (Table S17). The function emmeans() recodes ordinal scales starting at 1, so it presents a scale from 1-3 where 3 is severe lesions. The Pearson correlation between the strain means and the EMMs was positive and significant (Mean vs EMM in Table S16; $r = 0.985$, $t = 16.992$, $df = 9$, $p = 3.802*10^{-8}$).

Table S16. The final model of the OLR of heart lesions. The contained the fixed factors and the interaction of strain and sex. For each term, the Chi-squared statistic (Chi), degrees of freedom, and p-value (p) are shown.

Term	Chi	df	p	Signif [a]
Strain:Sex	28.310	10	0.002	**
Strain	30.431	10	$7.280*10^{-4}$	***
Sex	13.884	1	$1.944*10^{-4}$	***
Abundance	0.520	1	0.471	
Temporal block	0.532	1	0.002	**

[a] Categories of significance are as follows: * $0.05 > p > 0.01$, ** $0.01 > p > 0.001$, *** $p < 0.001$.

Table S17. The means and EMMs of the lesion scores for each of the levels of the factors of interest. The means are from the raw data, whereas the EMMs were calculated using the model in Table S16. The mean or EMM of a given level was averaged over the levels of the other factors. Lower and upper (LCL, UCL) 95% confidence limits for the EMM are reported. EMMs are greater than average scores as they are calculated on a 1-3 scale, as opposed to a 0-2 scale. For factors with significant interactions, the means and EMMs are reported for the relevant combinations of factors.

Factor	Level	Mean	EMM	LCL	UCL
Strain	66	0.714	1.727	1.269	2.185
Strain	57	1.250	2.198	1.687	2.709
Strain	150	1.000	2.113	1.576	2.649
Strain	167	0.250	1.306	0.964	1.648
Strain	126	0.875	1.950	1.311	2.589
Strain	22-2	1.000	1.987	1.479	2.495
Strain	10-2	1.625	2.709	2.310	3.107
Strain	54	1.250	2.160	1.699	2.622
Strain	198	2.000	3.000	3.000	3.000
Strain	174	0.800	2.000	2.000	2.000
Strain	178-1	0.875	1.866	1.621	2.111

Sex	Male	0.767	1.776	1.611	1.942
Sex	Female	1.390	2.408	2.212	2.605
Block	A	1.163	2.143	1.960	2.325
Block	B	0.976	2.042	1.860	2.224
Strain:Sex	66 & Male	0.000	1.000	1.000	1.000
Strain:Sex	57 & Male	1.000	1.986	1.218	2.755
Strain:Sex	150 & Male	0.750	1.876	1.159	2.594
Strain:Sex	167 & Male	0.000	1.000	1.000	1.000
Strain:Sex	126 & Male	0.750	1.899	1.009	2.790
Strain:Sex	22-2 & Male	0.500	1.403	0.709	2.097
Strain:Sex	10-2 & Male	1.500	2.665	2.044	3.286
Strain:Sex	54 & Male	1.750	2.709	2.188	3.230
Strain:Sex	198 & Male	2.000	3.000	3.000	3.000
Strain:Sex	174 & Male	0.000	1.000	1.000	1.000
Strain:Sex	178-1 & Male	0.000	1.000	1.000	1.000
Strain:Sex	66 & Female	1.667	2.455	1.538	3.371
Strain:Sex	57 & Female	1.500	2.409	1.738	3.079
Strain:Sex	150 & Female	1.250	2.349	1.594	3.105
Strain:Sex	167 & Female	0.500	1.612	0.928	2.296
Strain:Sex	126 & Female	1.000	2.000	1.084	2.917
Strain:Sex	22-2 & Female	1.500	2.571	1.832	3.309
Strain:Sex	10-2 & Female	1.750	2.752	2.281	3.224
Strain:Sex	54 & Female	0.750	1.611	0.847	2.376
Strain:Sex	198 & Female	2.000	3.000	3.000	3.000
Strain:Sex	174 & Female	2.000	3.000	3.000	3.000
Strain:Sex	178-1 & Female	1.750	2.732	2.241	3.222

Section 7 – References

Bates, D., Mächler, M., Bolker, B., & Walker, S. (2015). Fitting linear mixed-effects models using lme4. *Journal of Statistical Software, 67*, 1-48. https://doi.org/10.18637/jss.v067.i01

Fox, J., & Weisberg, S. (2019). *An R companion to applied regression, third edition*. Sage.

Harrell Jr., F. E. (2021). *Hmisc: Harrell miscellaneous. R package version 4.5-0*. In

Lenth, R. V. (2021). *emmeans: Estimated marginal means, aka least-squares means. R package version 1.5-2.1*. In

Lüdecke, D. (2018). ggeffects: Tidy data frames of marginal effects from regression models. *Journal of Open Source Software, 3*(26), 772. https://doi.org/10.21105/joss.00772

Venables, W. N., & Ripley, B. D. (2002). *Modern applied statistics with S* (2002 ed.). Springer.

Wood, S. N. (2017). *Generalized Additive Models* (2nd ed.). https://doi.org/10.1201/9781315370279